

Department of Mechanical Engineering

Predictive modelling and reliability analysis of aged, corroded pipelines

Chinedu Ishiodu Ossai

**This thesis is presented for the Degree of
Doctor of Philosophy (PhD)**

of

Curtin University

March 2016

Declaration

To the best of my knowledge and belief, this thesis contains no material previously published by any other person except where due acknowledgement has been made. This thesis contains no material, which has been accepted for the award of any degree or diploma in any university



Signature -----

29/03/2016

Date -----

Abstract

Pipeline corrosion is one of the challenges facing the oil and gas industries today because of the safety and environmental problems associated with corrosion related pipeline failures. Fatigue stress initiation in pipelines has been attributed to corrosion defects whose growth is enhanced by cyclic loading caused by the operating pressure of the transported fluids. In this research, pitting rate and time-dependent pit depth growth models were developed using internal corrosion defect depths and pipeline operational parameters, which included temperature, pH, CO₂ partial pressure, flow rate, water cut, wall shear stress, chloride ion concentration and sulphate ion concentration. This model development, which used ten years of Ultrasonic Thickness Measurement (UTM) data from corroded onshore pipelines, accounted for different categories of maximum pitting rates – low, moderate, high and severe. A Monte Carlo simulation based on the Poisson Square Wave Model (PSWM) was used for the estimation of both time dependent pitting rates, pit depth growth and expected cost of inspection and repair of corrosion degraded pipelines. The reliability of these pipelines was also determined by assuming that the corrosion wastage times followed a Weibull probability function with Akaike Information Criterion (AIC) being used to determine the statistical best-fit distribution of the parameters. A probabilistic-based Markovian process that utilized a continuous time non-homogenous linear growth pure birth Markov model was also used to predict the reliability of the pipeline. Failure probabilities at different lifecycle phases of the corroded pipeline were also determined in consideration of the Remaining Useful Life (RUL) of the pipeline while calculating the corrosion wastage rates at the lifecycle transition phases. Monte Carlo simulation and degradation models were further used for determining future corrosion defect depth growth, in a bid to establish periodic inspection and repair procedures and their costs. Finally, the models developed in this work were tested with field data from Magnetic Flux Leakage (MFL) in-line-inspection (ILI) of API X52, L-80 and N-80 grade offshore well tubing.

Acknowledgements

It is my pleasure to use this opportunity to thank my supervisor and co-supervisor, Dr Brian Boswell and Dr Ian J. Davies, for their patience and advice throughout the period of this research. I am also grateful to my friends and former colleagues – Gift Ojum, Okezie D. Ebirika, Innocent Nwokocha, Francis Odili, Samson Mba, Uche Kalu and Daniel Akano for their numerous contributions in ensuring the success of this research.

The financial supports given to me by the Australian government, Curtin University and Western Australia Energy Research Alliance (WAERA) via the Australia Postgraduate Award (APA) scholarship, Curtin University Postgraduate Scholarship (CUPS) and Postgraduate top-up scholarship respectively are well appreciated.

The support I obtained from the administrative staff of the School of Civil and Mechanical Engineering and the support and courage I received from fellow graduate student – Walter Ikealumba and Feisal Mohammed cannot be overemphasised.

I also wish to thank my wife Angela Ossai and my children - Cherish Ossai, Light Ossai and Chizzy Ossai for their encouragement and care during this research. Finally, I give all the glory to the God of heaven and earth for giving me the ability to complete this academic task.

List of publications included as part of the thesis

1. Chinedu I. Ossai, Brian Boswell, and Ian J. Davies, Pipeline fatigue failures in corrosive environments – A conceptual analysis of trends and effects, *Engineering Failure Analysis* 53 (2015) 36–58.
<http://dx.doi.org/10.1016/j.engfailanal.2015.03.004>
2. Chinedu I. Ossai, Brian Boswell, and Ian J. Davies, Predictive modelling of internal pitting corrosion of aged non-piggable pipelines, *J. Electrochem. Soc.* 2015, 162(6): C251-C259; doi: 10.1149/2.0701506jes
3. Chinedu I. Ossai, Brian Boswell, and Ian J. Davies, Estimation of internal pit depth growth and reliability of aged oil and gas pipelines - A Monte Carlo simulation approach, *Corrosion*: August 2015, Vol. 71, No. 8, pp. 977-99, doi:
<http://dx.doi.org/10.5006/1543>
4. Chinedu I. Ossai, Brian Boswell, and Ian J. Davies, Stochastic modelling of perfect inspection and repair actions for leak–failure prone internal corroded pipelines. *Engineering Failure Analysis*, 2016, 60, 40-56. DOI:
10.1016/j.engfailanal.2015.11.030
5. Chinedu I. Ossai, Brian Boswell, and Ian J. Davies, Markov chain modelling for time evolution of internal pitting corrosion distribution of oil and gas pipelines. *Engineering Failure Analysis*, 2016, 60, 209-228, DOI:
10.1016/j.engfailanal.2015.11.052

List of publications not included as part of the thesis

1. Chinedu I. Ossai, Brian Boswell, and Ian J. Davies, Modelling the effects of production rates and physico-chemical parameters on pitting rate and pit depth growth of onshore oil and gas pipelines, Corrosion Engineering Science and Technology 2016, <http://dx.doi.org/10.1080/1478422X.2015.1110919>
2. Chinedu I. Ossai, Brian Boswell, and Ian J. Davies, 2015, August. Reliability Analysis and Performance Predictions of Aged Pipelines Subjected to Internal Corrosion: A Markov Modelling Technique. In ASME 2015 International Design Engineering Technical Conferences and Computers and Information in Engineering Conference (pp. V010T12A011-V010T12A011). American Society of Mechanical Engineers. doi: 10.1115/DETC2015-46248

Statement of contribution of others

Chapter Two of this thesis is co-authored by Chinedu I. Ossai, Brain Boswell and Ian J. Davies and has been previously published in *Engineering Failure Analysis* 53 (2015) 36–58. <http://dx.doi.org/10.1016/j.engfailanal.2015.03.004>

Chapter Three is co-authored by Chinedu I. Ossai, Brain Boswell and Ian J. Davies and has been previously published in *Journal of Electrochemical Society*, 2015, 162(6): C251-C259; doi: 10.1149/2.0701506jes

Chapter Four is co-authored by Chinedu I. Ossai, Brain Boswell and Ian J. Davies and has been previously published in *Corrosion: August 2015*, Vol. 71, No. 8, pp. 977-99, doi: <http://dx.doi.org/10.5006/1543>

Chapter Five is co-authored by Chinedu I. Ossai, Brain Boswell and Ian J. Davies and has been previously published in *Engineering Failure Analysis*, 2016, 60, 40-56. DOI: 10.1016/j.engfailanal.2015.11.030

Chapter Six is co-authored by Chinedu I. Ossai, Brain Boswell and Ian J. Davies and has been previously published in *Engineering Failure Analysis*, 2016, 60, 209-228, DOI: 10.1016/j.engfailanal.2015.11.052

Table of contents

Declaration	i
Abstract	ii
Acknowledgement	iii
List of publications included as part of the thesis	iv
List of publications not included as part of the thesis	v
Statement of contribution of others	vi
List of Figures	xi
List of Tables	xvii
Chapter 1 - Introduction	
1.0 Background	1
1.1 Objectives and Research significance	7
1.2 Organization of the Thesis	9
References	10
Chapter 2 - Pipeline failures in corrosive environments – A conceptual analysis of trends and effects	
2.0 Introduction	14
2.1 Pipeline corrosion mechanism	16
2.2 Sweet corrosion	20
2.3 Sour corrosion	22
2.4 Microbiologically Induced Corrosion (MIC)	23
2.5 Pipeline integrity optimization framework	25
2.6 Conclusions	31
References	33
Chapter 3 - Predictive modelling of internal pitting corrosion of aged non-piggable pipelines	
3.0 Introduction	43
3.1 Research methodology	47
3.2 Parametric analysis of maximum pit depth	49
3.3 Distribution of maximum pit depth	50
3.4 Maximum pit depth variation with operational parameters	52

3.5	Regression analysis and pit growth modelling	55
3.6	Prediction model validation	61
3.7	Conclusions	65
	References	66
Chapter 4 - Estimation of internal pit depth growth and reliability of aged oil and gas pipelines - A Monte Carlo simulation approach.		
4.0	Introduction	70
4.1	Experimental procedure	73
4.1.1	Field data acquisition	73
4.1.2	Maximum pit depth distribution	74
4.1.3	Regression analysis	74
4.1.4	Model prediction assumptions	76
4.2	Maximum pit depth growth Estimation	77
4.3	Reliability analysis	79
4.4	Monte Carlo simulation framework	82
4.5	Results and discussion	84
4.5.1	Maximum pit depth distribution	84
4.5.2	Correlation of maximum pit depth with operating parameters	87
4.5.3	Time variation of pit depth growth	91
4.5.4	Reliability estimates	93
4.6	Application	98
4.7	Conclusions	102
	References	103
Chapter 5 - Stochastic modelling of inspection and repair actions for leak-failures prone internal corroded pipelines.		
5.0	Introduction	107
5.1	Markov modelling concept	110
5.2	Characterizing pipeline lifecycle phases	113
5.2.1	Remaining useful life and failure probability of corroded pipeline	117
5.3	Modelling corroded pipeline inspection and repair actions	120
5.4	Markovian modelling of inspection and repair of corroded pipeline	121

5.4.1	Transition probabilities of inspection and repair actions	121
5.4.2	Best fit statistical distribution of corroded defect depths	121
5.4.3	Time lapse of corrosion wastage of the pipeline	122
5.4.4	Estimation of the parameters of corrosion wastage time	122
5.4.5	Transition probability at the lifecycle phases	123
5.5	Probability of failure distribution	124
5.6	Holding time over state-action-pair	126
5.7	Inspection and repair cost	126
5.8	Pipeline inspection and repair policy	126
5.9	Strategy for future inspection and repair cost evaluation	128
5.10	A case study of internally corroded X52 pipeline	129
5.11	Estimation of corrosion wastage parameters and transition probabilities	131
5.12	Failure probability analysis	132
5.13	Future cost of inspection and repair	134
5.14	Conclusions	136
	References	137
Chapter 6 - Markov chain modelling for time evolution of internal pitting corrosion distribution of oil and gas pipelines		
6.0	Introduction	141
6.1	Finite Markov chain modelling of internal pitting corrosion of pipelines	145
6.2	Time evolution of pit depth growth	147
6.3	Estimation of the probability distribution of corroded pipeline pit depth	151
6.4	Prediction of the model parameters	152
6.5	Results and discussion	157
6.6	Application of the pitting prediction model	166
6.6.1	Predicting future pitting corrosion distribution of well tubing	167
6.6.2	Modelling pitting distribution of in-line inspected gathering pipeline.	170
6.7	Validation of the Monte Carlo simulated pit depths	172

6.8	Validation of the Markov prediction model	174
6.9	Conclusions	175
	References	176
7.0	Conclusions and recommendations	180
	Appendix	183
	Statement of contributors	183
	Abstracts of published papers not forming part of the thesis	184
	Copyright permission	186
	Bibliography	197

List of Figures

Figure 1.1a: Neutral and alkaline process of pipeline corrosion	2
Figure 1.1b: Acidic process of pipeline corrosion	2
Figure 1.2: Risk-based design and optimization framework	6
Figure 2.1: Some catastrophic pipeline failures	15
Figure 2.2: Causes of pipeline corrosion	17
Figure 2.3: Some defects that enhance fatigue stress failure of corroded pipelines	19
Figure 2.4: Probable mechanism for mackinawite formation in sour corrosion environment	23
Figure 2.5: Epifluorescence micrographs of Iron Oxidizing Bacteria (IOB) inoculated medium containing (a) 1% NaCl and (b) 6% NaCl	24
Figure 2.6: Variation of pipeline lifecycle cost, Operating Expenditure (OPEX) and Capital Expenditure (CAPEX) with pipeline integrity	45
Figure 2.7: Pipeline integrity assurance cycle	46
Figure 2.8: Summary of pipeline integrity management techniques	47
Figure 3.1: Procedure for maximum pit depth estimation using UTM technique.	49
Figure 3.2: Probability density function distribution of all field measured data	52
Figure 3.3: Scatter diagram of the maximum pit depth and operational parameter – temperature, CO ₂ partial pressure, flow rate, chloride ion conc., sulphate ion conc., water cut and pH	53
Figure 3.4: Sensitivity analysis model	55

Figure 3.5: Poisson square wave process for modelling maximum pit depth growth with time	57
Figure 3.6: Framework for Monte Carlo simulation of pitting time of pit depth growth	59
Figure 3.7: Comparison of maximum pit depth distribution for field and Monte Carlo simulated data	60
Figure 3.8: Maximum pit depth growth with exposure time for different pitting corrosion categories	61
Figure 3.9: Comparison of the pipe-wall thickness loss of the predicted model and field data for low pitting corrosion category	63
Figure 3.10: Comparison of the pipe-wall thickness loss of the predicted model and field data for moderate pitting corrosion category	63
Figure 3.11: Comparison of the pipe-wall thickness loss of the predicted model and field data for high pitting corrosion category	64
Figure 3.12: Comparison of the pipe-wall thickness loss of the predicted model and field data for high pitting corrosion category	64
Figure 4.1: Poisson Square Wave Model (PSWM)	81
Figure 4.2: Monte Carlo simulation framework for reliability estimate of internal pit corroded pipeline	83
Figure 4.3: Field data and probability density functions of some of the considered distributions for all-data category	84
Figure 4.4: Field data and probability density functions of some of the considered distributions for severe pitting category	85
Figure 4.5: Field data and probability density functions of some of the considered distributions for high pitting category	85

Figure 4.6: Field data and probability density functions of some of the considered distributions for moderate pitting category	86
Figure 4.7: Field data and probability density functions of some of the considered distributions for low pitting category	86
Figure 4.8: Boxplot analysis of maximum pit depth of the pipelines according to pitting corrosion categories	88
Figure 4.9: Q-Q plot analysis of maximum pit depth as a function of operating parameters for all-data category	88
Figure 4.10: Relative variation of pipeline pit depth due to unit increase of operating parameters	90
Figure 4.11: Time variation of average maximum pit depth growth and cumulative pipeline wall thickness loss	92
Figure 4.12: Goodness of fit test for Weibull probability plot based on Weibull distribution of pitting time	93
Figure 4.13: Goodness of fit test for Weibull probability plot based on Gamma distribution of pitting time	94
Figure 4.14: Goodness of fit test for Weibull probability plot based on lognormal distribution of pitting time	94
Figure 4.15: Goodness of fit test for Weibull probability plot based on exponential distribution of pitting time	95
Figure 4.16: Goodness of fit test for Weibull probability plot based on extreme value distribution of pitting time	95
Figure 4.17: Goodness of fit test for Weibull probability plot based on generalized extreme value distribution of pitting time	96
Figure 4.18: Variation of Weibull function scale parameter with estimated time of pipeline operation	97

Figure 4.19: Variation of Weibull function shape parameter with estimated time of pipeline operation	97
Figure 4.20: Survival probabilities classified according to distribution function types	98
Figure 4.21: PDF of field measured pit depths, GEVD of field and simulated data of API X52 oil and gas transmission pipeline	99
Figure 4.22: Comparison of initial pit depth distribution of MFL ILI-inspected API X52 transmission pipeline after 10 years of ILI-inspection	100
Figure 4.23: Failure and survival probability of MFL ILI-inspected pipeline	101
Figure 4.24: Estimation of the reliability trend of X52 pipeline ILI-inspected in 2012	102
Figure 5.1: State transition & sojourning time of a Markov process	112
Figure 5.2: Variation of corroded pipeline lifecycle phases with the RUL	115
Figure 5.3: Effect of maintenance and repair on the remaining useful life of corrosion defect spots of corroded pipelines	119
Figure 5.4: Impact of pipeline inspection and repairs on failure probability of a corroded defect spot.	120
Figure 5.5: Framework for Monte Carlo simulation of corrosion wastage time of corrosion defect depth.	124
Figure 5.6: Field data and probability density distribution of the corrosion defect data for different probability density functions.	131
Figure 5.7: Failure probability of corroded pipeline managed with different inspection and repair options.	133
Figure 5.8: Long run inspection and repair cost (per km-yr.) for different Inspection and repair options for maintaining a corroded pipeline	133

Figure 5.9: Variation of cost of inspection and repairs for number of corrosion defects per kilometre	134
Figure 5.10: Variation of the cost of managing pipeline integrity based on the inspection and repair actions over a finite planning horizon	135
Figure 5.11: Cost of inspection and repair for different linear predicted and random growth of corrosion defect depth.	136
Figure 6.1: Model of pipeline pitting corrosion	146
Figure 6.2: Graphical representation of Chapman-Kolmogorov equation of three stage Markov process	148
Figure 6.3: Framework for Monte Carlo simulation of pitting initiation time	153
Figure 6. 4: Poisson Square Wave Process (PSWP) for estimating pitting initiation time	156
Figure 6.5: Maximum pit depth plot for Monte Carlo simulated maximum pit depths for studied pipelines	158
Figure 6.6a: GEV distribution of Monte Carlo simulated pit depth for all pitting corrosion data	159
Figure 6.6b: Variation of pitting depth distribution with pipeline exposure time (years)	160
Figure 6.7a: Time evolution of the best fit mean of Monte Carlo simulated pit depth	161
Figure 6.7b: Time evolution of the best fit variance of Monte Carlo simulated pit depth	161
Figure 6.8a: Time evolution of the best fit shape parameter of GEV distribution of the pit depth	162

Figure 6.8b: Time evolution of the best fit scale parameter of GEV distribution of the pit depth	163
Figure 6.8c: Time evolution of the best fit location parameter of GEV distribution of the pit depth	163
Figure 6.9a: Time evolution of the pitting corrosion damage ($\Upsilon(t)$) for GEV distribution of Monte Carlo simulated pit depth for different categories of pitting corrosion	164
Figure 6.9b: Time evolution of probability parameter (Υ_s) for GEV distribution of Monte Carlo simulated pit depth for different categories of pitting corrosion	165
Figure 6.9c: Simulated maximum pit depth growth and pipeline exposure time for different corrosion categories.	166
Figure 6.10: Comparison of Markov model prediction and field measured pit depths distribution for L-80 grade well tubing at 5.8 years from initial field distribution at 5.1 years	168
Figure 6.11a: Comparison of Markov model prediction and field measured pit depths distribution for N-80 grade well tubing at 15.3 years from initial field distribution at 9.1 years	169
Figure 6.11b: Comparison of Markov model prediction and field measured pit depths distribution for N-80 grade well tubing at 18.2 years from initial field distribution at 9.1 years	169
Figure 6.11c: Comparison of Markov model prediction and field measured pit depths distribution for N-80 grade well tubing at 22.8 years from initial field distribution at 9.1 years.	170
Figure 6.12: Monte Carlo simulation framework for estimation of future corroded pit depth distribution of a single in-line inspection	171

Figure 6.13: Comparison of Markov predicted and Monte Carlo simulated pit depth distribution in 2022 from initial pitting distribution in 2012	172
Figure 6.14: Probability density function distribution of field measured data	173
Figure 6.15: Comparison of pit depth distribution for field and Monte Carlo Simulated data.	174

List of Tables

Table 2.1: Summary of the direct cost of corrosion	16
Table 2.2: Summary of bacteria associated with the corrosion of pipelines	25
Table 2.3: Summary of pipeline leakage detection techniques	31
Table 3.1: Description of the field measured data.	48
Table 3.2: Qualitative categorization of carbon steel corrosion rate for oil production systems.	48
Table 3.3: Kolmogorov–Smirnov goodness of fit test for the pitting corrosion data.	51
Table 3.4: Correlation between maximum pit depth and operating variables for all data	52
Table 3.5: Results of regression analysis by pit depth category	58
Table 3.6: Condition of pipelines used to test the proposed model	62
Table 4.1: Qualitative categorization of carbon steel corrosion rate for oil production systems.	74
Table 4.2: Description of the field measured data.	76
Table 4.3: Maximum Likelihood Estimates (MLEs) and Akaike Information Criterion (AIC) for maximum pit depth categories.	87

Table 4.4: Parameter estimate for regression analysis of average pitting rate and operation parameters for all-data category.	89
Table 4.5: Statistical best fit for average operating parameters and average maximum pit depth for all-data category.	91
Table 4.6: Parameter estimate for pit depth growth based on all data category	92
Table 4.7: Summary of Weibull probability scale and shape parameters and failure intensity of different distributions for all-data category.	93
Table 5.1: Cost of magnetic flux leakage in-line inspection of energy pipeline	128
Table 5.2: Akaike Information Criterion (AIC) values for different distributions pit depth.	130
Table 5.3: Parameters of Weibull distribution	131
Table 5.4: Transition probability over a finite horizon	132
Table 5.5: Transition Probability (TP) and Failure Intensity (FI) of the state action pairs for the corroded pipeline.	132
Table 6.1: Qualitative categorization of carbon steel corrosion rate for oil production systems	154
Table 6.2: Variables and coefficients of the predictive for the pitting corrosion.	157
Table 6.3: Summary of the RMSE of the tested field data	174

Chapter 1 Introduction

1.0 Background

Petroleum and natural gas have been transported over long distances in pipelines stretching hundreds of thousands of kilometres around the world. These pipelines, which are either buried under the surface of the earth, underneath the seabed or exposed on the surface, account for the majority of transmission of different oil and gas products from downstream and upstream sectors of these industries. These oil and gas products have different chemical and physical characteristics that result in the degradation of the pipeline asset over time of use in service. Notably, one of the major causes of oil and gas pipeline degradation – internally or externally in service is corrosion (Dewaard, Lotz & Milliams 1991, Netic, Cai & Lee 2005), which is attributed to the presence of different compounds in the oil, gas and their by-products such as oxygen, organic acids such as acetic, formic and propionic acids, CO₂ acid and H₂S (Netic & Lee 2003, Netic 2007).

The act of sustaining the integrity of pipelines has been achieved via mitigation actions by different operators of oil and gas pipelines. These mitigation actions have centred on strategies that include – use of corrosion resistant materials; chemical treatment, vacuum de-aeration, coating and lining and process control (Case 2008, Papavinasam, Doiron & Revie 2010). However, despite the cost associated with the mitigation of pipeline corrosion, corrosion deterioration mechanisms have continued to be the most predominant cause of pipeline failure in the oil and gas industry (Ossai, Boswell & Davies 2015, Bhandari *et al.* 2015).

Pipeline deterioration is a mechanical and electrochemical process that combines the mechanical action of erosion and electrochemical process of corrosion. When pipeline material is exposed to corrosive species passing through it, the electrochemical reaction taking place at the anode and cathode results in corrosion processes (Sun & Netic 2007). This corrosion mechanism, which can take place under acidic, neutral or alkaline conditions (see Figures 1.1a & b) results in the formation of metallic oxides that temporarily seals the surface of the pipeline material (Netic 2007) and stops the corrosion process. The metallic oxide, which is a barrier between the corrosive species and the pipeline material (Biomorgi *et al.* 2012, Bhandari *et al.*

2015) is washed away by the help of subcutaneous substances such as sand and metallic oxide scales flowing through the pipeline (Papavinasam, Doiron & Revie 2010). The loss of the protective film exposes the surface of the pipeline to further corrosion processes. This mechanism, which continuously results in the loss of the pipe-wall thickness eventually brings about failure of the pipeline due to fatigue.

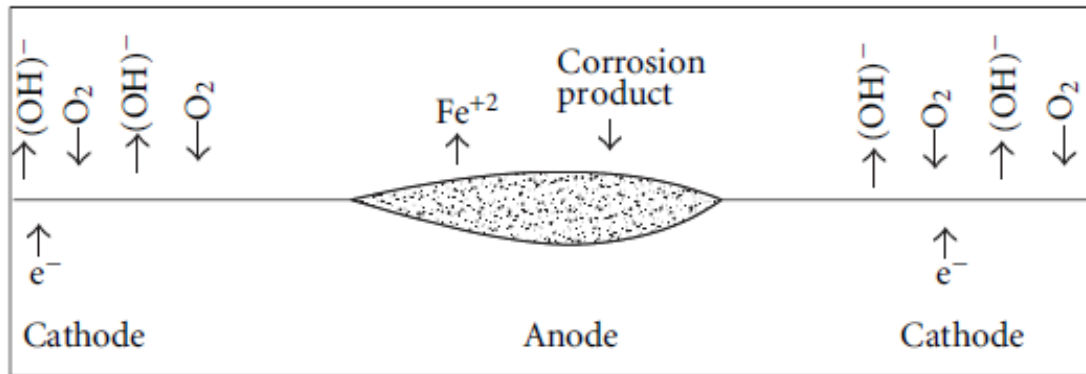


Figure 1.1a: Neutral and alkaline process of pipeline corrosion- adapted from Ossai 2012

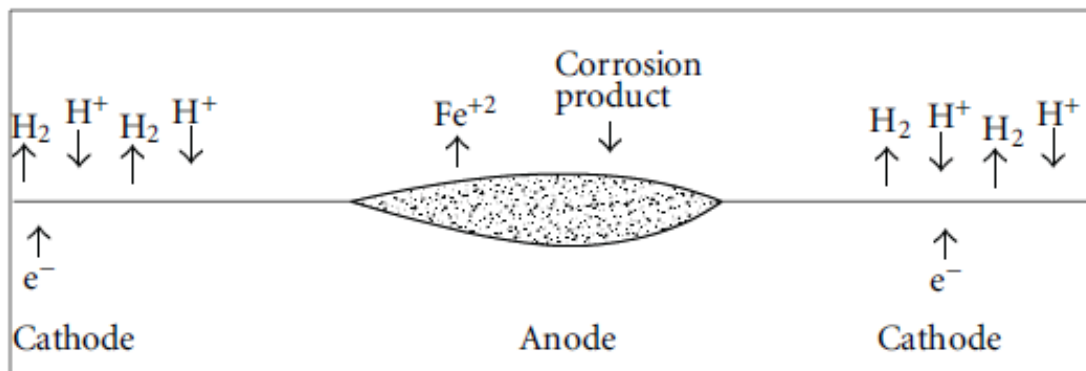


Figure 1.1b: Acidic process of pipeline corrosion- adapted from Ossai 2012.

Seeing that the effect of fluid flow on the corrosion of pipeline is a cardinal problem in the oil and gas sector, it has become a subject of continuous research that is aimed at finding new materials, testing techniques and prediction models for inspection and maintenance management of the pipelines.

Pipeline flow-dependent corrosion can result in serious damage that can result in catastrophic failure of the system from both a safety and economic point of view (Chexal *et al.* 1996). These failures can be in the form of leakage, burst and rupture (Amirat, Mohamed-Chateauneuf & chaoui 2006, Hasan, Khan & Kenny 2012)

with gas, oil, 2-phase flow and condensate contributing 30%, 29%, 19% and 15% of leak failures, respectively (HSE 2001). Most of these failures have been linked to design errors, lack of maintenance, inadequate inspection and monitoring of corroded pipelines (Patel & Rudlin 2000).

The corrosion of pipelines is governed by a complex mechanism that comprises of the interaction of components that include the carbon steel material of the pipeline, water chemistry, flow pattern, oil chemistry, oil wetting and operational conditions (Dugstad *et al.* 2006). The complex relationship between these components has made the prediction of pipeline corrosion mechanisms a difficult task that has left experts without a common ground on the generally acceptable techniques and approaches (Papavinasam, Doiron & Revie 2010). Different, empirical, semi-empirical, mechanistic and hybrid models of pipeline corrosion prediction have been developed by numerous researchers (De-Waard & Milliam 1975, De-Waard, Lotz & Milliam 1991, Dugstad, Lunde & Nestic 1994, Nordsveen *et al.* 2003, Dugstad *et al.* 2006, Sun & Nestic 2007, Paik & Kim 2012,). Gartland, Johnson & Ovstentun (2003) predicted pipeline corrosion based on multiphase flow modelling of water wetting conditions of the pipeline material while considering the pH, CO₂ and H₂S composition of the oil and gas flowing through the pipeline. This research also utilized information concerning the oil and gas production rate and data on chemical injection in the model. Xiao & Nestic (2005) focused on a 2-D stochastic approach in predicting localized CO₂ corrosion, by expounding on the techniques of metal oxide formation and the protective effects it has on the corroding surface. Furthermore, Khajotia, Sormaz & Nestic (2007) described a case-based reasoning approach for CO₂ corrosion prediction. This research, which utilized information on existing corrosion rates to predict future corrosion rates, was based on case-based reasoning and the Taylor series. The authors were able to determine the corrosion rate of fields with similar characteristics to those studied using case retrieval, case ranking and case revision. Similarly, Nestic, Cai & Lee (2005) developed an integrated CO₂/H₂S model of pipeline corrosion for a multiphase flow condition. This model took into account the effects of water entrainment and corrosion inhibitor as well as determining the impact of iron carbonate and iron sulphide scale and morphology on the corrosion rates of carbon steel materials used for pipelines. The authors

calibrated the model with field data after establishing the critical velocity for entraining of free water by the flowing oil phase. To estimate the damaging effect of CO₂ corrosion, Case (2008) applied a corrosion damage distribution methodology to study the production causing failures of oil wells operating in mature oil and gas fields. This mechanistic study was used to develop a methodology for assessing corrosion damage by estimating the failure probability of pipelines.

Despite the enormity of the research work on pipeline corrosion, there is still need for more research in this area due to the need to further understand the emerging trends in pipeline corrosion mechanisms. Furthermore, the fact that much of the research carried out in the area of pipeline corrosion is based on laboratory experiments, underpins the need for more field data-based research work to develop models that will have robust field applications in the oil and gas industry.

In designing pipelines, considerations are always given for the loss of pipe-wall thickness by corrosion. Unfortunately, the nature of the operating environment (Hasan, Khan & Kenny 2012, Bhandari *et al.* 2015) and the complexities associated with the corrosion mechanism makes it difficult for pipe-wall corrosion deterioration to follow the predetermined corrosion allowances. To maintain the integrity of this asset and forestall failure, different reliability models have been used by experts to reasonably predict the probability of failure and the remaining useful life of corroded pipelines at any given time. Although these reliability models are not holistic, they have consistently guided the decisions of corrosion management professionals in the area of inspection, maintenance and repair of corroded pipelines.

By considering the hazards associated with internal corrosion and loss of pressure containment of pipelines due to leakage, burst and rupture, Hasan, Khan & Kenny (2012) predicted the reliability of corroded pipelines. These authors adopted a Monte Carlo simulation and First Order Second Moment (FOSM) technique for estimating the failure probability of the pipelines. This work also understudied different industry standard models and experimental findings associated with corrosion defect geometries and concluded that pipeline designs can be improved by incorporating failure probability information in the design process. The geometry of the pipeline also affects the local distribution of stress and strain (Xu & Cheng 2012), which significantly influences the fatigue failure risk of corroded pipelines. Similarly,

to estimate the future failure probability of corroded pipelines, a software package, which enables experts to estimate the punctual probability of failure, annual probability of failure and annual probability of failure per kilometre of each defect for a pipeline was developed (Lecchi 2011). This software was developed to aid in pipeline integrity management and minimize the cost of corroded pipeline maintenance. This probabilistic study was validated with In-Line-Inspection (ILI) data from transmission pipelines of 125 km and 93 km. The work of many other researchers on the reliability of corroded aged pipelines has been reported in the literature. These researches highlighted techniques for optimizing corroded pipeline performance by determining the failure probabilities, inspection and maintenance trends and procedures for ensuring that imperfect inspection is avoided, and has been summarized in the references shown herein (Moussa 1998, De Leon & Macias 2005, Sun, Ma & Morris 2009, Breton *et al.* 2010, Rimkevicius *et al.* 2012, Bisaggio & Netto 2015).

It is pertinent to note that minimizing the risk associated with internal corrosion of pipelines is essential to maintaining a healthy and safe environment. It therefore follows that investigating the time dependent corrosion failure of pipeline is important for risk-based design and optimization of the system (See Figure 1.2). The application of an imperfect inspection policy to the maintenance of uniform and localized corroded pipelines has been used as a tool for the optimization of cost for corroded pipeline and the estimation of reliability at a given time (Sahraoui, Khelif & Chateauneuf 2013). Through assuming an inspection threshold that depends on the probability of detection, Sahraoui, Khelif & Chateauneuf (2013) were able to determine the error associated with the calculated corrosion defects (depth and width) and its overall effect on the integrity management of corroded pipelines.

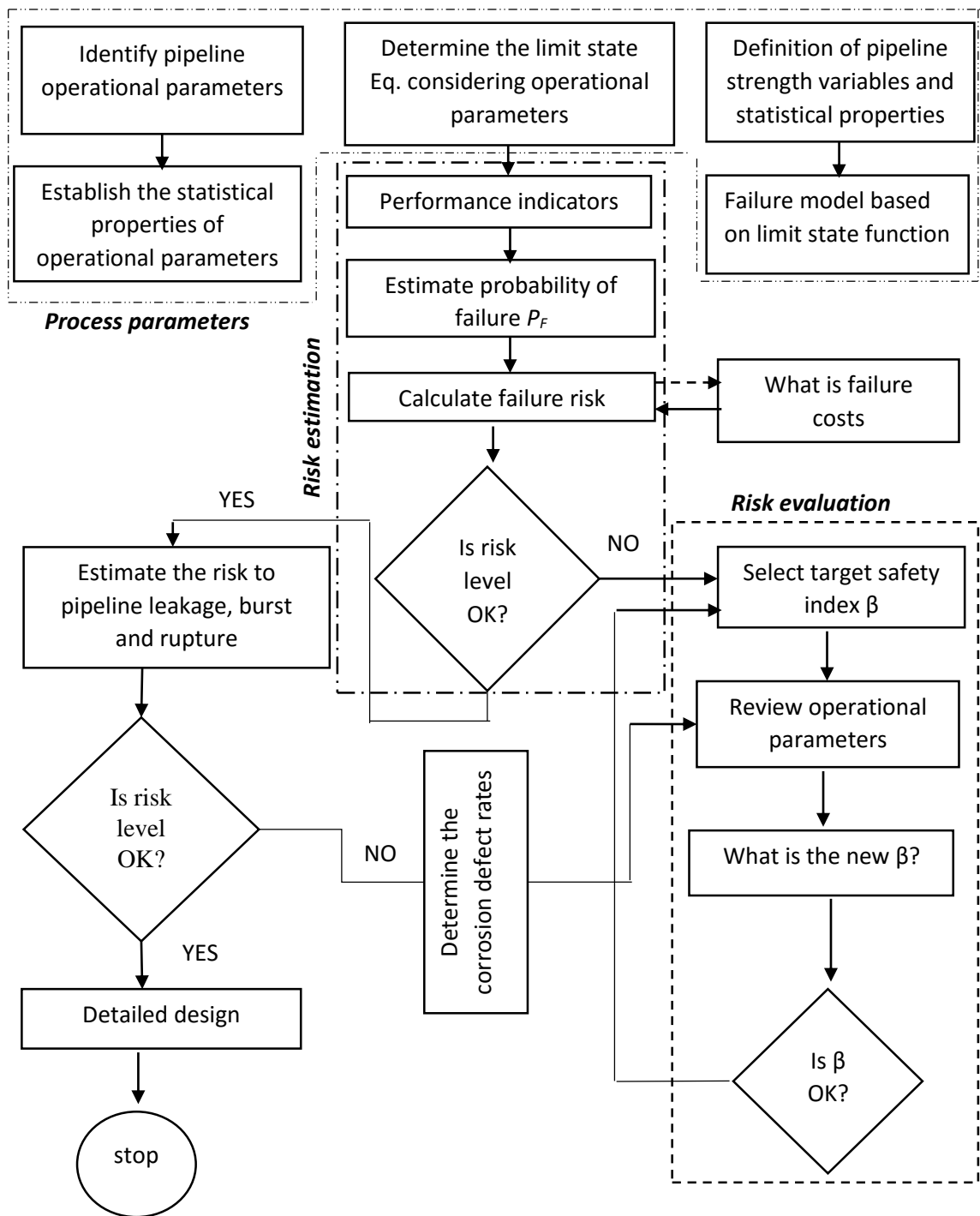


Figure 1.2: Risk-based design and optimization framework- adapted from Hasan, Khan & Kenny (2012).

From the discussion thus far it is clear that significant research has already been carried out with regards to different aspects of pipeline corrosion and reliability analysis. However, it should be pointed out that there is still need for research in this area as there is relatively little information available concerning the prediction of

reliability for corroded pipelines with respect to retained pipe-wall thickness over the lifecycle phases. This has prompted the need for the utilization of Monte Carlo simulation and Markov modelling techniques to reasonably estimate the failure risk and survivability indexes of such pipelines throughout their life cycle. Furthermore, establishing the characterisation of field data for corroded pipelines with respect to different field measured operating parameters will enhance the integrity management of the pipelines as this would be expected to provide a reasonable estimation of the remaining useful life for time-dependent corrosion defect depth growth. Thus, the robustness of field data analysis, which has not been considered by most researchers in the literature, has been addressed in this work. This research also provided an estimation of the future corrosion defect depth growth of pipelines subjected to a single comprehensive ILI by using a Monte Carlo simulation technique. The approach helped to establish the time-dependent corrosion wastage rate while simultaneously establishing a procedure that allowed cost prediction.

In developing new predictive models for corroded pipelines, measurement error coming from tools used for corrosion defects measurement can potentially affect the predicted model. This problem, which can bring about an increased average corrosion rate prediction in areas of increased error distribution can result in an overly optimistic predictive model and reliability estimate. Measurement errors can also cause measured corrosion rates to be less correlated than real corrosion rates and can potentially affect the actual retained strength of the pipeline and the reliability at a given time.

1.1 Objectives and research significance

High reliability is an indispensable requirement for the operation of technical systems and infrastructure such as power plants, oil and gas platforms, aircraft, renewable energy plants and pipelines. Failure of such systems can result in high cost and hazards to people and the environment. In the oil and gas industry, pipelines are pivotal to production but these multi-million-dollar assets undergo continuous deterioration (as a function of utilization rate, age and diverse operational constraints), hence the need for a contingency approach to militating against their failure. Since the failure of a pipeline can result in a major cost blowout due to

production loss, environmental pollution and other ancillary costs, calculating the reliability of pipelines and predicting the remaining useful life at different corrosion wastage rates is vital for efficient and cost effective oil and gas production.

This research is aimed at developing a methodology for predicting the internal corrosion rate and reliability of aged pipelines by:

1. Developing models and algorithms to study the impact of operating parameters such as temperature, pH, operating pressure, flow rate, wall shear stress, chloride ion concentration, sulphate ion concentration, CO₂ partial pressure and water cut on the reliability and corrosion wastage rates of pipelines used for oil and gas transportation. This will involve:
 - i. Utilization of Markov decision process and Monte Carlo simulation techniques in the determination and classification of corroded pipeline reliability using field data.
 - ii. Determining the statistical characteristics of field data comprising of maximum pit depth and operating parameters.
 - iii. Using multivariate regression analysis to establish the relationship between the pitting rate and operating parameters
 - iv. Applying a Monte Carlo simulation to determine the time lapse for the pit depth growth vis-à-vis predicting the remaining useful life of corroded pipelines.
2. Utilize information concerning corrosion wastage times to estimate inspection and repair procedures and cost for internally corroded pipelines subjected to leak-failure and establish the failure probability for leak, burst and rupture prone pipeline failure.
3. Determine the future distribution of pit depths of internally corroded oil and gas pipelines by using a non-homogenous, continuous time linear growth pure birth Markov process.

1.2 Organization of the thesis

This thesis is comprised of five main topic areas that includes fundamental trends associated with the corrosion of pipelines that are exposed to a corrosive environment. This topic illustrates the critical outlook of pipeline corrosion in the oil and gas industries, the principal causes and costs associated with it, together with the steps that are necessary for mitigating the problem.

The second topic area of the thesis concerns the predictive modelling of corroded pipelines and is focused on the use of different stochastic modelling tools for estimating the corrosion wastage rate of corroded pipelines. Multivariate simulation was used for establishing the relationship between corrosive species and the pipeline corrosion wastage throughout the service life using a Poisson Square Wave Model (PSWM) technique. The reliability of the pipelines was determined in the third section by considering the corrosion defect depth growth based on degradation modelling. The corrosion defect depth growth in this scenario was determined via the consideration of Poisson arrival rate, which was following an exponential process while considering different forms of corrosion defect depth distribution.

By determining the lifecycle phases of the pipelines as a function of the retained pipe-wall thickness, the inspection cost for pipelines that are prone to failure by leakage was established in the fourth section. Markov decision process was utilized for the calibration of the cost variability of the pipelines as the lifecycle phases change with the reduction in the pipe-wall thickness. The fifth section of this research involved the use of Markov modelling technique for predicting the corrosion defect depth distribution over a time lapse using a non-homogenous continuous time linear growth pure birth Markov process.

The reliability of the pipelines at different corrosion categories was established by assuming that the corrosion wastage rates and failure followed a Weibull probability distribution. The prediction models developed in this research were tested with field inspection data obtained from the Ultrasonic Thickness Measurement (UTM) and Magnetic Flux Leakage (MFL) In-Line-Inspection (ILI) techniques.

References

- AMIRAT, A., MOHAMED-CHATEAUNEUF, A. & CHAOUI, K. 2006. Reliability assessment of underground pipelines under the combined effect of active corrosion and residual stress. *International Journal of Pressure Vessels and Piping*, 83, 107-117.
- BAZAN, F. A. V. & BECK, A. T. 2013. Stochastic process corrosion growth models for pipeline reliability. *Corrosion Science*, 74, 50-58.
- BIOMORGI, J., HERNANDEZ, S., MARIN, J., RODRIGUEZ, E., LARA, M. & VILORIA, A. 2012. Internal corrosion studies in hydrocarbons production pipelines located at Venezuelan Northeastern. *Chemical Engineering Research and Design*, 90, 1159-1167.
- BHANDARI, J., KHAN, F., ABBASSI, R., GARANIYA, V. & OJEDA, R. 2015. Modelling of pitting corrosion in marine and offshore steel structures – A technical review. *Journal of Loss Prevention in the Process Industries*, 37, 39-62.
- BISAGGIO, H. D. C. & NETTO, T. A. 2015. Predictive analyses of the integrity of corroded pipelines based on concepts of structural reliability and Bayesian inference. *Marine Structures*, 41, 180-199.
- BRETON, T., SANCHEZ-GHENO, J., ALAMILLA, J. & ALVAREZ-RAMIREZ, J. 2010. Identification of failure type in corroded pipelines: A Bayesian probabilistic approach. *Journal of hazardous materials*, 179, 628-634.
- CASE, R., 2008, January. Assessment of CO₂ Corrosion Damage Distribution in Oilwells by Deterministic and Stochastic Modelling. In *CORROSION 2008*. NACE International.
- CHEXAL, B., HOROWITZ, J. & DOOLEY, B. 1998. Flow-accelerated corrosion in power plants. Revision 1. Electric Power Research Inst., Palo Alto, CA (United States).
- DE LEON, D. & MACÍAS, O. F. 2005. Effect of spatial correlation on the failure probability of pipelines under corrosion. *International Journal of Pressure Vessels and Piping*, 82, 123-128.
- DE WAARD, C., LOTZ, U. & MILLIAMS, D. 1991. Predictive model for CO₂ corrosion engineering in wet natural gas pipelines. *Corrosion*, 47, 976-985.

- DE WAARD, C., LOTZ, U. & MILLIAMS, D. 1975. Carbonic acid corrosion of steel. *Corrosion*, 31, 131
- DUGSTAD, A., GULBRANDSEN, E., SEIERSTEN, M., KVAREKVAL, J. & NYBORG, R. Corrosion testing in multiphase flow, challenges and limitations. *CORROSION* 2006, 2006. NACE International.
- DUGSTAD, A., LUNDE, L. & NESIC, S. Control of internal corrosion in multi-phase oil and gas pipelines. *Proceedings of the Conference Prevention of Pipeline Corrosion*, Gulf Publishing Co, 1994.
- GARTLAND, P. O., JOHNSEN, R. & OVSTETUN, I. Application of internal corrosion modeling in the risk assessment of pipelines. *CORROSION* 2003, 2003. NACE International.
- HASAN, S., KHAN, F. & KENNY, S. 2012. Probability assessment of burst limit state due to internal corrosion. *International Journal of Pressure Vessels and Piping*, 89, 48-58.
- HSE. 2001. Review of corrosion management for offshore oil and gas processing, HSE offshore technology report 2001/044. Available from: <<http://www.hse.gov.uk/research/otopdf/2001/oto01044.pdf>>. [22/6/14].
- KHAJOTIA, B., SORMAZ, D. & NESIC, S. Case-based reasoning model of CO₂ corrosion based on field data. *NACE International Conference Series, CORROSION*, 2007.
- LECCHI, M. 2011. Evaluation of predictive assessment reliability on corroded transmission pipelines. *Journal of Natural Gas Science and Engineering*, 3, 633-641.
- MOUSSA, W. A. 1998. Risk-based reliability evaluation of multi-site damage in pipelines. *Computers & Industrial Engineering*, 35, 595-598.
- NESIC, S. 2007. Key issues related to modelling of internal corrosion of oil and gas pipelines—A review. *Corrosion Science*, 49, 4308-4338.

- NESIC, S., CAI, J. & LEE, K.-L. J. 2005. A multiphase flow and internal corrosion prediction model for mild steel pipeline. Paper presented NACE CORROSION/05, Dallas, TX, paper, 5556.
- NESIC, S. & LEE, K.-L. 2003. A mechanistic model for carbon dioxide corrosion of mild steel in the presence of protective iron carbonate films-Part 3: Film growth model. *Corrosion*, 59, 616-628.
- NORDSVEEN, M., NEŠIĆ, S., NYBORG, R. & STANGELAND, A. 2003. A mechanistic model for carbon dioxide corrosion of mild steel in the presence of protective iron carbonate films-Part 1: Theory and verification. *Corrosion*, 59, 443-456.
- OSSAI, C.I. 2012. Advances in asset management techniques: An overview of corrosion mechanisms and mitigation strategies for oil and gas pipelines, ISRN Corrosion, vol. 2012. <http://dx.doi.org/10.5402/2012/570143>, Article ID 570143.
- OSSAI, C. I., BOSWELL, B. & DAVIES, I. J. 2015. Pipeline failures in corrosive environments—A conceptual analysis of trends and effects. *Engineering Failure Analysis*, 53, 36-58.
- PAIK, J. K. & KIM, D. K. 2012. Advanced method for the development of an empirical model to predict time-dependent corrosion wastage. *Corrosion Science*, 63, 51-58.
- PAPAVINASAM, S., DOIRON, A. & REVIE, R. W. 2010. Model to predict internal pitting corrosion of oil and gas pipelines. *Corrosion*, 66, 035006-035006-11.
- PATEL, R. & RUDLIN, J. Analysis of corrosion/erosion incidents in offshore process plant and implications for non-destructive testing. British Institute of Non-Destructive Testing, NDT'99 and UK Corrosion'99 Conference Proceedings (UK), 1999. 5-10.
- RIMKEVICIUS, S., KALIATKA, A., VALINCIUS, M., DUNDULIS, G., JANULIONIS, R., GRYBENAS, A. & ZUTAUTAITE, I. 2012. Development of approach for reliability assessment of pipeline network systems. *Applied Energy*, 94, 22-33.

- SAHRAOUI, Y., KHELIF, R. & CHATEAUNEUF, A. 2013. Maintenance planning under imperfect inspections of corroded pipelines. *International Journal of Pressure Vessels and Piping*, 104, 76-82.
- SUN, W. & NESIC, S. 2007. A mechanistic model of H₂S corrosion of mild steel. Paper No 07655. *Corrosion* 2007.
- SUN, Y., MA, L. & MORRIS, J. 2009. A practical approach for reliability prediction of pipeline systems. *European Journal of Operational Research*, 198, 210-214.
- XIAO, Y. & NEŠIĆ, S. 2005. A stochastic prediction model of localized CO₂ corrosion Paper No. 05507. *CORROSION* 2005.
- XU, L. & CHENG, Y. 2012. Reliability and failure pressure prediction of various grades of pipeline steel in the presence of corrosion defects and pre-strain. *International Journal of Pressure Vessels and Piping*, 89, 75-84.

Chapter 2 - Pipeline failures in corrosive environments – A conceptual analysis of trends and effects

2.0 Introduction

Pipeline failure can be described as the bane of ruined cities due to the destructions that have followed their ruptures. According to the Pipeline and Hazardous Materials Safety Administration (PHMSA) (US DOT 2014) of the US department of transport, 360 fatalities, 1368 injuries and 894 incidences relating to oil, gas and hazardous fluid pipeline failures occurred in US alone between the years 1995 – 2014. Figure 2.1 depicts some notable incidence of pipeline explosion and the ruin they caused to the cities. The figure shows Kaohsiung city in South Taiwan on 1/8/2014 after a gas pipeline explosion which killed 25 people and injured more than 259 others (BBC 2014) and Ghislenghien city, Belgium on 30/7/2004 whose gas pipeline explosion caused 24 fatalities and injured more than 120 people (HInt Dossier 2005).

Fatigue can be described as a structural damage of materials due to stress (Singh & Markeset 2014). Whereas human and natural phenomena can cause fatigue failure in pipelines, research has shown that corrosion plays a pivotal role in fatigue stress initiation (Lambert & Plumtree 1995, Fekete & Varga 2012, Pilkey) whilst cyclic loading has contributed to the growth of this stress and eventual failure of the pipelines (Ossai 2012). Assessment of corrosion induced fatigue failures in pipelines can be done by using stress-life, strain-life, linear elastic fracture mechanics, crack propagation and statistical based techniques (Pandey 1998, Hong 1999, Sinha & Mckim 2007, Breton *et al.* 2010, Singh & Markeset 2014). Fatigue stress analysis is vital for ensuring that the level of safety required for the operation of oil and gas transmission pipelines are maintained (Cumber 2001).

Fatigue stress behaviour of pipelines can be significantly affected by the operating environment, geometry and size of corroded sections, pipe material properties, exposure time and time dependent corrosion propagation (Wang & Zarghamee 2014). Hence, operators of oil and gas industries and numerous experts are concertedly working to ensure that the right operating environments which can reduce the risk of corrosion are created during exploration and production of oil and gas.

Ghislenghien City, Belgium 30/7/04



<http://www.dw.de/belgian-pipeline-explosion-kills-at-least-ten/a-1281229>

Kaohsiung City, Southern Taiwan 1/8/14



<http://www.abc.net.au/news/image/5640024-3x2-700x467.jpg>



<http://www.phmsa.dot.gov>



Kaohsiung City, Southern Taiwan 1/8/14

<http://www.newsmax.com/CMSPages/GetFile.aspx?guid=58794702-bd>

Figure 2.1: Photos of some catastrophic pipeline failures

Corrosion problems have been estimated to cost approximately \$2.2 trillion to the world economy (3.0% of the Gross Domestic Product) with oil, gas and petrochemical industries accounting for a total of \$1 trillion or 45% of this amount (Hays 2010, Elliott 2013). With records showing that over 70% of the current oil and gas fields being developed around the world are highly corrosive (Miller 2013), this cost is bound to increase since it will cost more to manage facilities in corrosive environments.

Based on Bhaskaran *et al.* (2005) estimated global direct cost of corrosion for the year 2004 and inflation factors for years 2005 to June 2014 (Yardeni, Johnson & Quintana 2014), the global direct cost of corrosion for different countries were calculated and the summary shown in Table 2.1. In order to estimate these direct costs of corrosion, It was assumed that they will vary with economic activities based on inflation factor [$F = (1+i)^y$]. The average inflation rate (i) for the durations under review as obtained from reference (Yardeni,

Johnson & Quintana 2014) and the number of years (y) between these periods were used to extrapolate the expected direct corrosion cost for the countries in 2014. This table shows that the world faces an indirect cost of over \$1.4 trillion (approximately 2% of the world Gross Domestic Product) annually in corrosion related problems. United States accounts for over 26% of the world direct cost of corrosion whilst China accounts for about 10%. However, with the increasing infrastructural development and expansion of Chinese economy, the total direct and indirect cost of corrosion in China is sure to increase at a higher rate over the coming years (Lieser & Xu 2002).

Table 2.1: Summary of the direct cost of corrosion (Bhaskaran et al. 2005, Yardeni, Johnson & Quintana 2014)

Country	Average Inflation rate (2005 ~ June 2014)	Inflation factor [$F = (1 + i)^y$]	Direct cost of corrosion 2004 (\$B)	Direct cost of corrosion 2014 (\$B)	Percentage contribution 2014
USA	2.33	1.26	303.76	382.44	26.11%
Japan	0.14	1.01	59.02	59.84	4.08%
Germany	1.62	1.17	49.26	57.86	3.95%
UK	2.74	1.31	8.51	11.15	0.76%
Australia	2.79	1.32	7.32	9.64	0.66%
Canada	1.79	1.19	3.38	4.04	0.28%
South Africa	5.56	1.72	3.18	5.46	0.37%
India	8.37	2.23	3.78	8.45	0.58%
China	6.84	2.36	61.00*	144.23	9.85%
Others				781.77	53.37%
World	4	1.48	990	1464.88	

*Cost of corrosion in 2001

En-Hou Han as cited by Leiser, (2002)

i : inflation rate; y : number of years

2.1 Pipeline corrosion mechanisms

Corrosion is one of the predominant causes of pipeline failures in oil and gas production and accounts for between one quarter to two third of the total downtime in the industry (CAPP 2009, HSE 2001, AER 2013). The most important aspect of pipeline failure consequences is the human safety, property damage and environmental impacts. Every year, enormous amount of money is spent on different forms of corrosion control measures in order to maintain the integrity of pipelines. Unfortunately, the difficulties associated with getting appropriate designs,

predictions, monitoring and mitigation strategies highlight the billions of dollars lost in the economies around the world to corrosion related impairment of pipelines and other structures. Research has shown that over 80% percent of failed pipelines are monitored in one form or another whilst between 20%~65% of the amount spent on corrosion problems could be saved if there was a good knowledge of corrosion inhibitors, protection and control techniques (Hay 2010, Brown 2014). Corrosion of pipelines can be attributed to numerous causes which are related to the physical and chemical factors and includes both environmental conditions and the characteristics of the materials. Figure 2.2 summarizes the causes of pipeline corrosion.

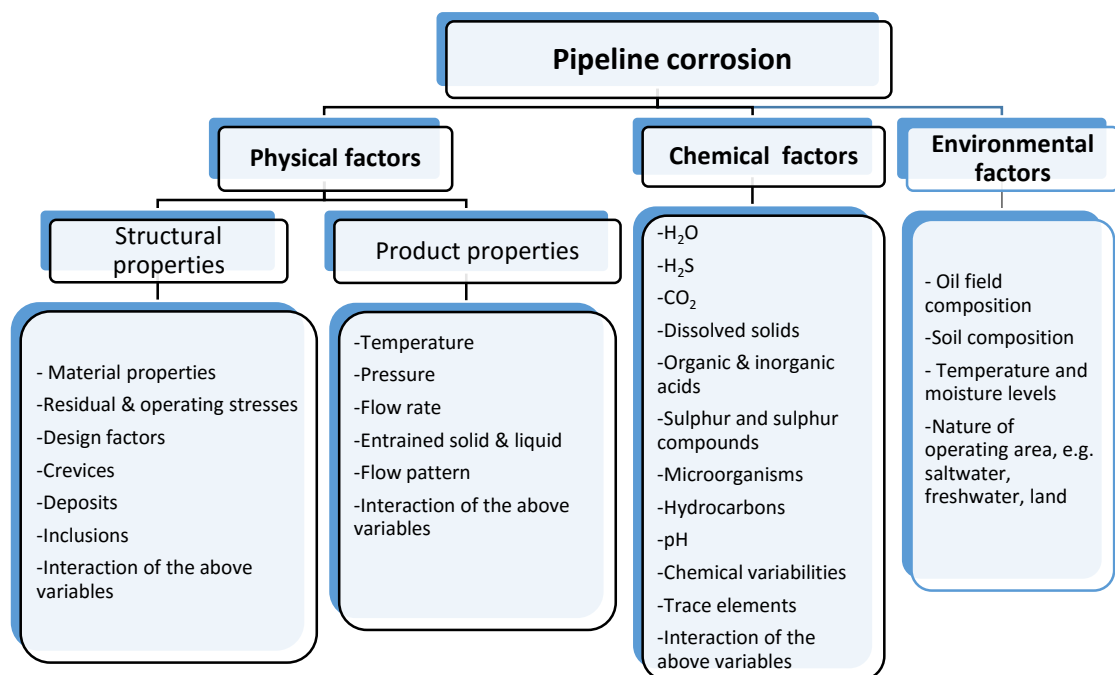


Figure 2.2: Causes of pipeline corrosion (HSE 2001, Nestic, Cai & Lee 2005, Race 2010)

The existence of H₂S, CO₂, organic and inorganic acids in a pipeline operating environment may cause corrosion defects of different sorts (Nestic 2007, Singer *et al.* 2011, Fang, Brown & Nescaronicacute 2011). To this end, Li *et al.* (2014) investigated the effect of H₂S concentration on X60 grade pipe corrosion in an environment of coexistence of H₂S/CO₂. These authors concluded that H₂S concentration below 0.05mmol/l, CO₂ corrosion rate is decreased and at H₂S concentration of between 0.05~2mmol/l corrosion rate of CO₂ corrosion shows no significant changes but increased at concentration above 2mmol/l. This coexistence of H₂S and CO₂ can be

attributed to the formation of sulphide films on steel surfaces with crystal structure forms that includes - mackinawite, pyrrhotite, troilite, pyrite and greigite (Yin *et al.* 2008, Singer *et al.* 2011, Davoodi *et al.* 2011). Water-oil interface and water splashes or slugs contribute to the spread of corrosion on pipelines (Khaksarfard *et al.* 2013).

When fluid in multiphase flow transits from stratified flow to a stable water-in-oil flow regime, dispersion takes places. This only happens if the oil phase turbulence is intense enough to cause the water phase break up into droplets (Nesic, Cai & Lee 2005). This broken droplets migrate to the pipeline walls when it gets beyond a certain critical diameter causing or accelerating corrosion (Nesic, Cai & Lee 2005). Khaksarfard *et al.* (2013) investigated the impact of inclination angles on the internal corrosion of multiphase flow pipelines using computational fluid dynamics (CFD). They found out that, when flow is upwards on the pipeline, the water-wet surface is more than when the flow is downwards. This implies that more surfaces are prone to corrosion with an upward flow than downward flow hence the use of flexible pipes made of Corrosion Resistance Alloys (CRAs) for some critical oil and gas operations such as well tubing, gas lift lines and subsea risers due to the high corrosion resistance ability (Guo *et al.* 2014). When a pipelines has no defect and is uniformly corroded, it may be relatively straightforward to predict the expected corrosion wastage using linear and non-linear models (Ahammed 1998, Caleyó *et al.* 2002, Velazquez *et al.* 2009, Bazan & Becks 2013). However, the existence of defects such as dents, cracks, out-of-roundness, gouges and buckles (see Figure 2.3) around the corroded areas of the pipelines make the estimation more complex.



Figure 2.3: Some defects that enhance fatigue stress failure of corroded pipelines

This is because the effects of these defects will contribute to more stress load on the pipeline and ultimately affect the burst pressures at such corroded sections. One of such defects that is attracting attention to researchers is crack-in-corrosion defect which can be described as a hybrid defect that has cracks which are coincident in a corroded area and has claimed more than 10% of the pipe wall thickness (Bedairi *et al.* 2012). To show the effects of these hybrid defects, Bedairi *et al.* (2012) evaluated cracking, corrosion and crack-in-corrosion defects of pipelines using Finite Element Analysis (FEA) based on elastic-plastic fracture mechanics. These authors experimentally validated this work, which was on a 508 mm diameter and 5.7 mm thick pipe. Their conclusion after analysing 200mm long defect with different percentages of the corroded depths and cracked wall thicknesses is that the corrosion defect had the best prediction result with 3.2% variation existing between the experimental corrosion rate and that obtained from FEA. This was followed by

crack only defect and crack-in-corrosion defects, which had 12.4% and 17.4% variations between the FEA and experimental corrosion rates respectively. This finding shows that the accuracy of prediction of crack-in-corrosion defect may need to be improved in order to effectively manage the integrity of ageing pipelines.

It is also evident from different researches that flow pattern influences pipeline corrosion [Hernandez-Rodriguez *et al.* 2007, Ilman & Kusmono 2014) hence Biomorgi *et al.* (2014) practically measured the effects of variation of operating conditions on the corrosion of oil and gas pipelines. After four months of observation, these researchers concluded that in addition to the influence of flow pattern, sand, iron carbonate and sulphide scales predominately caused under deposits in the studied 102 mm and 154 mm diameter pipelines. They further stated that slug patterned flow contributed to more corrosion than bubbles on the pipelines whereas the pitting corrosion rates was also influenced by the internal diameter of the pipelines. Similarly, Papavinasam, Doiron & Revie (2010) ascertained that subcutaneous substances such as sand contributed to the increased rate of pitting corrosion in oil and gas pipelines. The authors showed that the pitting corrosion rates varied from position to position due to flow type and velocities whilst Mazumder *et al.* (2008) attributed this variation to particle-to-particle, particle-to-fluid and particle-to-wall interactions at such positions.

Increased hydrostatic pressures used for testing of pipes resulted in loss of corrosion resistance of the materials. This was evident in the increased pit generation, pit growth rates and the enlargement of metastable pits into cavities (Zhang *et al.* (2009). Some manufacturing process such as welding have also been found to contribute to the susceptibility of pipelines to corrosion attack due to the differentiation in the microstructure of the material at such welded points (Contreras *et al* 2005).

2.2 Sweet corrosion

When oil and gas flow through pipelines, the wall of the pipeline can be wet with oil or water depending on the fluid that is in the continuous phase. Oil-wet-surface occurs if water is trapped in the oil which is in continuous phase and in direct contact with the wall of the pipeline (water-in-oil phase) whereas water-wet-surface occurs

when oil is trapped in the water which is in direct contact with the pipeline wall and also in continuous phase (oil-in-water phase) (Papavinasam *et al.* 2007). Oil-wet-surface may not readily cause pipeline corrosion since oil may not form an electrolyte for redox reaction. Water-wet-surface is caused by oil-in-water phase flow, wet gas and condensation in gas transmission pipelines are potential sources of water (Wang *et al.* 2000, Park *et al.* 2007) which may result in CO₂ absorption (Nesic 2007, Cole *et al.* 2011), cathodic and anodic reactions (Ossai 2012) and oxide films formation (Nesic 2007). The acidification of CO₂ gas via reaction with water can increase corrosion rate of pipelines (Cole *et al.* 2011) as the system tends to balance the chemical equilibrium by creating more anodic and cathodic reactions. The electrochemical reaction at the water-wet surface for CO₂ induced corrosion is shown below:

- Absorption of CO₂



- Cathodic reaction may occur either by hydrogen reduction or carbonate reduction (Papavinasam *et al.* 2007).



- The anodic reaction follows an oxidation process for iron:



- Oxide films formation can follow any of the following steps:





Numerous experts have commented on different aspects of sweet corrosion of pipelines using empirical and experimental approaches. Nestic (2007) reviewed the physico-chemical modelling of CO₂ corrosion in carbon steel and stated that the corrosion mechanism centres on the anodic dissolution of iron and the cathodic evolution of hydrogen. This involves a direct electrochemical reactions of reduction of carbonic acid and water. The iron carbonate produced during the electrochemical reaction of CO₂ corrosion forms a protective Layer which prevents more corrosion from taking place by covering the carbon steel surface from the corrosive species (Fekete & Varga 2012). However, erosion and turbulence in pipelines mechanically remove them giving room for more corrosion (Bedairi *et al.* 2012, Ilman & Kusmono 2014) or else dissolution of the scale due to chemical reactions necessitated by microorganisms (Ferris *et al.* 1992) or operating condition of the flowing oil and gas (Wang *et al.* 2000, Choi & Al-Ajwad 2008).

2.3 Sour corrosion

This is a sulphide ion induced corrosion in which hydrogen reacts with iron to form iron sulphide that may act as a protective scale depending on the concentration of the hydrogen sulphide and the prevalent environmental condition. The general equation for this reaction is shown in Equation (2.11) below (Popoola *et al.* 2013).



Sour corrosion has resulted in fatigue failure of pipelines by causing hydrogen embrittlement (Beidokhti, Dolati & Koukabi 2009), pitting corrosion (Papavinasam, Doiron & Revie 2010), lamination (Martínez *et al.* 2009) and Stress Oriented Hydrogen Induced Cracking (SOHIC) which could be a manifestation of Sulphide Stress Corrosion (SSC) (Park *et al.* 2007, Kapusta 2008). Elemental sulphur has been reported by some researchers as being responsible for the localized pitting corrosion attack on carbon steel material however, Song *et al.* [(2012) suggested that other substances such as SO₄²⁻, SO₃²⁻, S₂O₃²⁻ and H⁺ may have contributed to the localized attack in a sour environment. The probable mechanism of mackinawite film

formation in sour environment according to Sun (2006) as reported by Popoola *et al.* (2013) is shown in Figure 2.4.

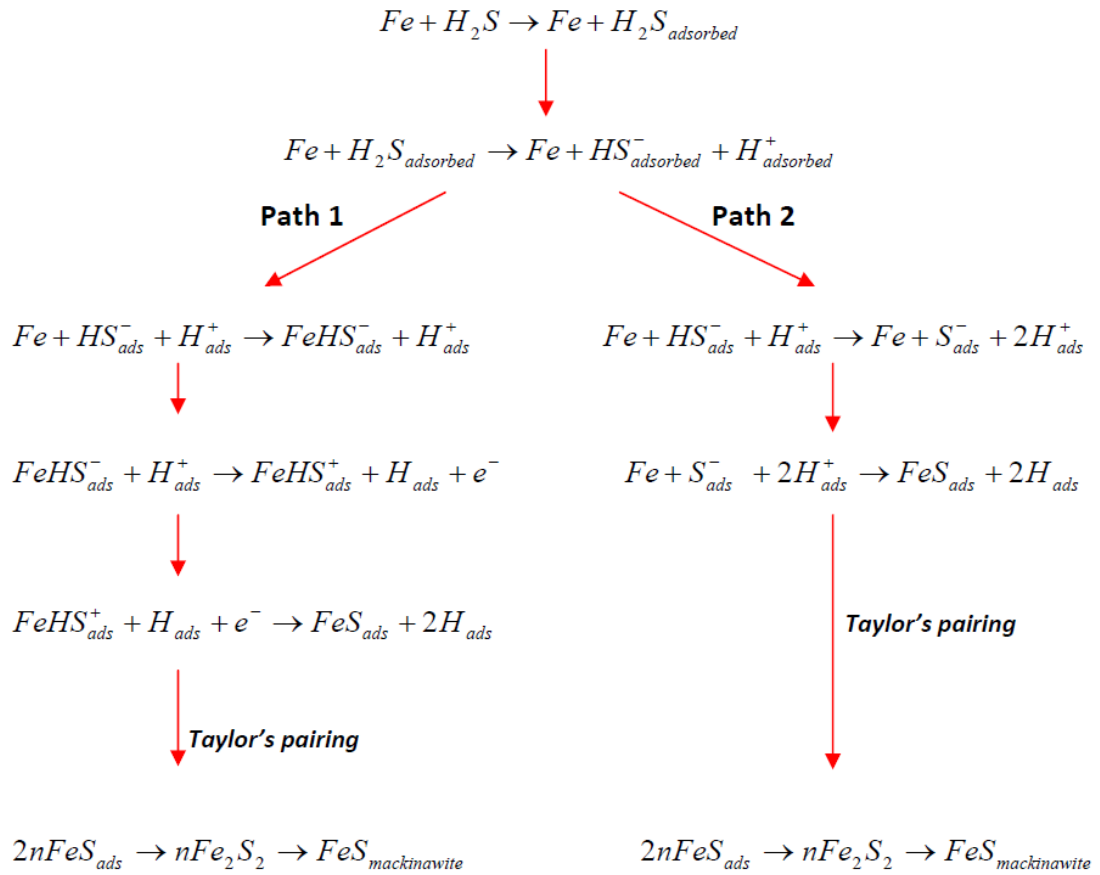


Figure 2.4: Probable mechanism for mackinawite formation in sour corrosion environment (Sun 2006)

2.4 Microbiological Induced Corrosion (MIC)

This type of corrosion is induced by microorganisms in the pipelines. These microorganisms initiate different chemical activities that could include - production of organic and inorganic acids (Muthukumar *et al.* 2003), oxidation and reduction of some elements (Chandrasatheesh *et al.* 2014). The activities of these microorganisms on pipelines are found to be most predominate at pH of 4~9 and temperature of 10°C~50°C (Chandrasatheesh *et al.* 2014). In general, microorganisms produce biofilms which form a good site for both aerobic and anaerobic activities that enhance the corrosion of carbon steel materials. This is done by physical deposition of toxic substances, production of corrosive acidic by-products and depolarization of

the corrosion cell through increased utilization of hydrogen, oxygen or iron compound in the environment (Muthukumar *et al.* 2003). These secreted metabolites can enhance pitting corrosion (Chen *et al.* 2014, Melchers 2008), de-alloying of metals (Sana, Nazirb & Donmezc 2012), galvanic corrosion (Wang *et al.* 2000, Chen *et al.* 2014), stress corrosion cracking and hydrogen induced cracking (Raman *et al.* 2005, Javaherdashti 2011). Research has shown that at a linear velocity of 3.5m/s, the biofilm formed by Sulphur Reducing Bacteria (SRB) could not adhere to the wall of a pipelines (Wen, Gu & Nesic 2007) hence, SRB may not be actively enhancing internal pipeline corrosion for fluids under turbulent flow regime.

Experimental observation has shown that microorganisms that induce corrosion in steel materials are more active at lower concentration of the corrosive environment than at higher concentrations (see Figure 2.5) (Chandrasatheesh *et al.* 2014). It is evident from this figure that at 1% NaCl concentration, the activities of Iron Oxidizing bacteria (IOB) were higher as the microorganism attacked the carbon steel material by more oxidation than it did at 6% NaCl concentration.

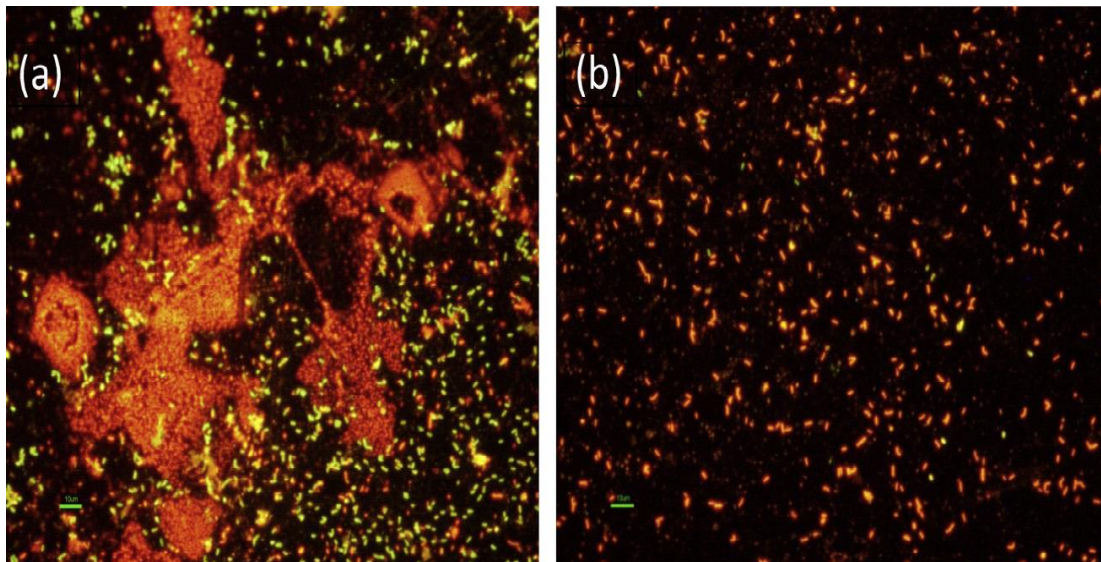


Figure 2.5: Epifluorescence micrographs of Iron Oxidizing Bacteria (IOB) inoculated medium containing (a) 1% NaCl and (b) 6% NaCl, adapted from Chandrasatheesh *et al.* (2014)

Microorganisms such sulphur reducing bacteria can be introduced into the pipelines through formation water injection (Ferris, Jack & Bramhill 1992, Wen *et al.* 2007) and can enhance external corrosion of underground buried pipelines (with disbonded

coating) from the soil (Maruthamuthu 2008). Sulphur reducing bacteria can also exist in high and low temperatures, deep in subsurface reservoirs and can be introduced into oilfield during drilling operation (Gieg, Jack & Foght 2011). Table 2.2 summaries different kinds of bacteria that may cause corrosion of pipelines.

Table 2.2: Summary of bacteria associated with the corrosion of pipelines

Bacteria	Mode of corrosion attack	Remarks
Sulphur Reducing Bacteria (SRB)	Respire sulphate and produce sulphide while oxidizing diverse electron donors (Greg, Jack & Foght 2011)	Increase of anodic reaction to establish a chemical equilibrium results in more corrosion of the material.
Acid Producing Bacteria (APB)	Produce acidic compounds such as acetic and sulphuric acids that may chemically attack the protective surface in pipelines.	Can be introduced by injecting water from seas and rivers into oil and gas fields (Ferris, Jack & Bramhill 1992).
Iron Reducing Bacteria (IRB)	Attack iron compounds by reducing Fe ³⁺ to Fe ²⁺ (Chandrasatheesh 2014).	Promotes corrosion by dissolving the protective film layers on material surfaces.
Iron Oxidizing Bacteria (IOB)	Oxidizes Fe ²⁺ to Fe ³⁺ by depositing metabolites (Chen <i>et al.</i> 2014).	Can produce low pH that enhances Fe ³⁺ dissolution.
Manganese oxidizing bacteria	Deposits MnO ₂ that favours the growth of sulphur reducing bacteria (Muthukumar 2003).	Sulphur reducing bacteria simulates depolarization which brings about increase in the corrosion process.

2.5 Pipeline integrity optimization framework

The increased need for energy and the attendant pressure on oil and gas pipelines entails that the integrity of this asset should be maintained to minimize non-productive time (Nicholson *et al.* 2010), increase the efficiency of oil and gas transportation and protect the environment. Kishawy & Gabbar (2010) summarized pipeline integrity management to involve - identification of process for understanding pipeline failure mode, assessment plan for the failure modes, integrity analysis procedure for failure and consequences, setting criteria for repair action and

information analysis, continuous process of assessment to keep maintaining integrity, mitigation and preventative actions to forestall downtime, effectiveness measure and review techniques. Integrity management involves deciding the type of material to use in laying a pipeline at the design stage (Papavinasam 2014b). This is vital in risk management and cost optimal operation seeing that pipeline failure accounts for more than 50% of the total downtime in oil and gas industry (HSE 2001). If Carbon steel material is used for a pipeline, there may be high operational expenditure (OPEX) involved in running the pipeline due to the high corrosion susceptibility of the material whilst the use of Corrosion Resistance Alloys (CRAs) may bring about high capital expenditure (CAPEX) as the initial cost of investment on the material is very high but it has high corrosion resistance qualities (Papavinasam 2014b). It is therefore imperative that decision makers should strike a balance between these two costs (OPEX and CAPEX) in material selection in order to maintain the appropriate reliability of the pipeline and reduce risk whilst optimizing profit through minimal lifecycle cost of the pipeline. Figure 2.6 shows a trade-off between operating expenditure and capital expenditure in determining the appropriate material for pipeline design.

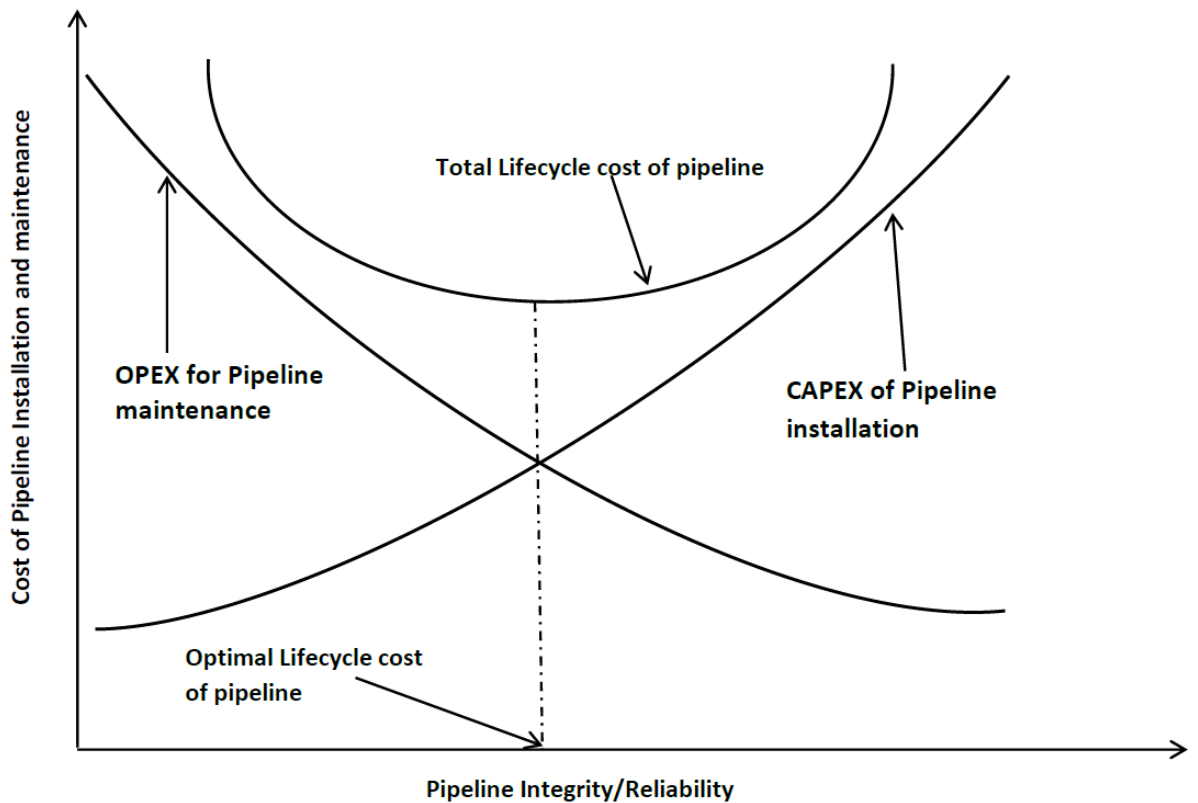


Figure 2.6: Variation of Pipeline Lifecycle cost, operating expenditure (OPEX) and capital expenditure (CAPEX) with pipeline integrity

This figure indicates that very low capital expenditure on pipeline material may result in very high operating expenditure which may include- cost of chemical injection, inspection, maintenance and repair and environmental damage penalties should pollution occur whilst high capital expenditure may bring about minimal operating cost since the material is expected to be highly resistant to corrosion and very low risk. Both extremes of the costs may not be to the advantage of any company since there is very high risk in adopting low capital expenditure and high operating expenditure whereas there may be problem of profitability in adopting high capital expenditure and low operating cost. This is why the balance between these two costs is vital for the management of pipeline integrity and enhancing profitability of an organization since risk and cost will be optimized.

Different frameworks for corroded pipelines integrity management and fitness-for-service testing have been established by different regulatory agencies and they include API 579-1/ASME FFS-1 [(API 2000), Canadian association of petroleum Producers (CAPP) 5-M approach (CAPP 2009), BS 7910 (ASME 2004) and ASME B31.8S

(ASME 2004). Figure 2.7 shows a typical pipeline integrity optimization framework that may be used for managing pipeline against corrosion induced fatigue failures.

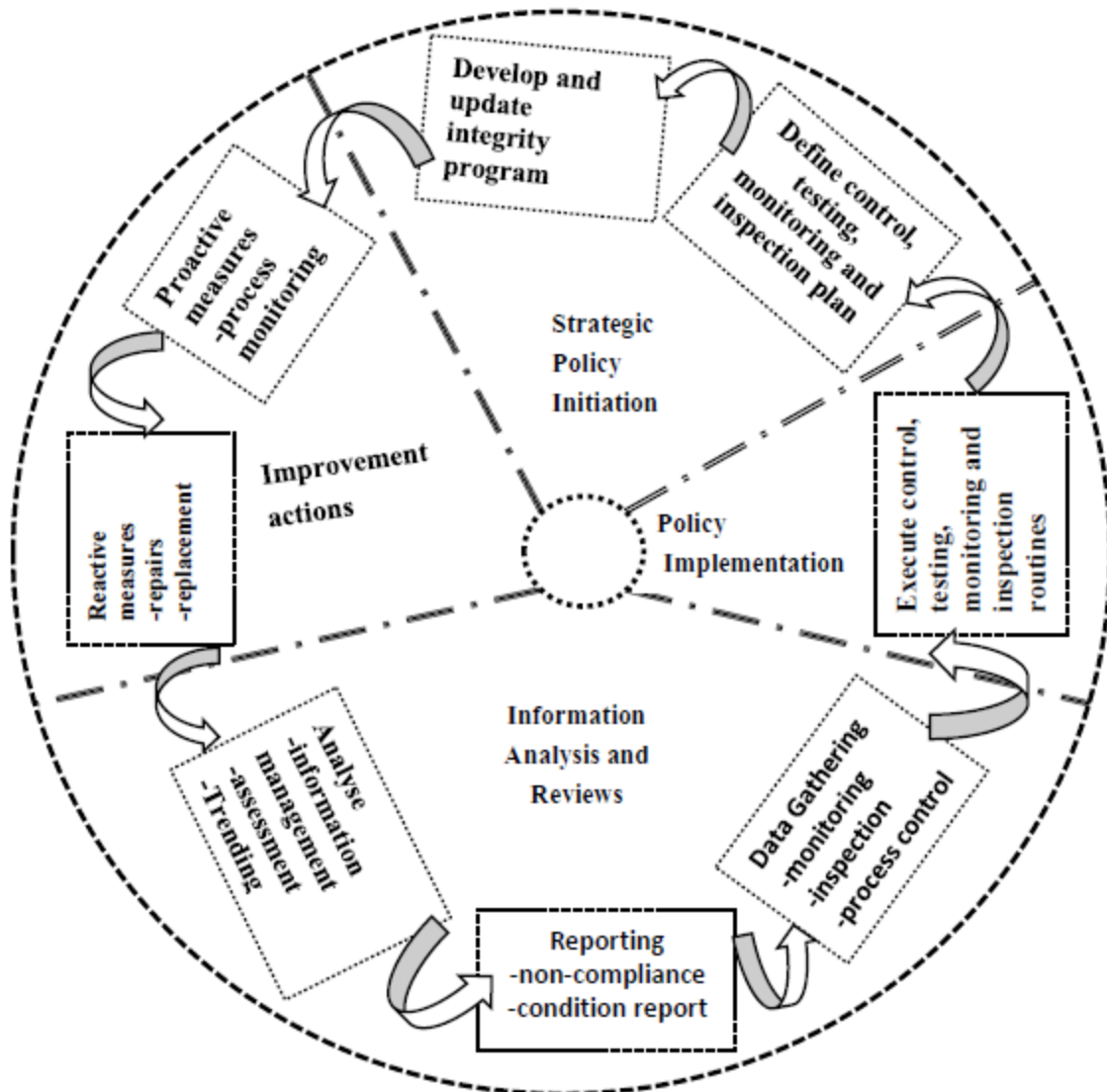


Figure 2.7: Pipeline Integrity assurance cycle

According to this figure, to strategically manage pipeline deterioration and fatigue failures may entail addressing health, safety and environmental risks (Cumber 2001, Han & Weng 2010), threats and barriers for risk escalation (Jo & Crowl 2008), risk based inspection activities (HSE 2001), proactive and reactive actions for integrity control (HSE 2001, Kisawy & Gabbar 2010) and assurance activities for performance standards (Cosham, Hopkins & Macdonald 2007). Corrosion risk assessment which aid in identification, removal and mitigation of corrosion through monitoring and inspection programs (Ossai 2012, Venkatesh & Farinha 2006) is also vital for mapping

the expected risk level of the pipeline under different operating environments. Probabilistic approach has been applied to risk level assessment of corroded pipelines (Sahraoui, Khelif & Chateaufneuf 2013) in order to ensure that the pipeline is fit-for-purpose (Race 2010). This can be achieved if total quality management is adopted at design, manufacture, installation and operation (Kisawy & Gabbar 2010) by testing, monitoring and inspection to stipulated standards. The techniques for control, monitoring and inspection of pipeline against corrosion related defects are shown in Figure 2.8.

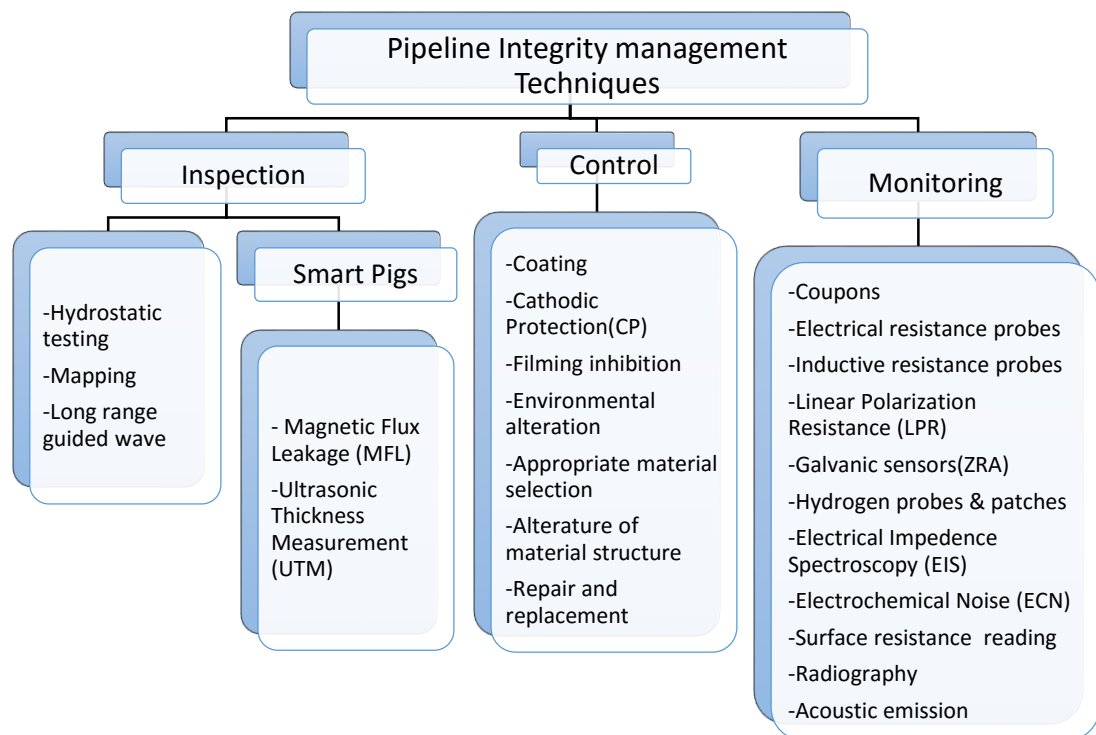


Figure 2.8: Summary of Pipeline Integrity Management techniques

Data used for pipeline integrity management have been collated by in-line-inspections, risk based inspection and process monitoring. Unfortunately, imperfection in the collected data has been identified to be caused by variability and uncertainty (Singh & Markeset 2014) and poor knowledge transfer through inadequate communication (Elliot 2013). Singh & Markeset (2014) attributed variability to lack of uniformity of diameter, corroded pit, corroded length, pipe wall thickness whilst uncertainty could be caused by equipment calibration and mal-functionality, personnel skill, and variability in operating characteristics of pipeline across different zones of the pipeline.

Since changes in operating conditions may potentially influence the integrity of pipelines, process control of key operating parameters such as pH, water chemistry, pressure, CO₂ and H₂S partial pressures, oxygen, carbonates, bicarbonates and bacteria (Ossai 2012a, Ossai 2012b, Brown 2014) is vital for monitoring the level of corrosion on pipelines. Comparing the measured values of these parameters against established key performance indicators will aid in predicting the integrity of the pipeline at any point in time. Other corrective and proactive actions that may be useful in pipeline integrity management includes procedural changes to chemicals applications (Meng, Ogea & King 2011), inspection strategies (Geary & Hobbs 2013) and in some extreme cases repair or replacement of portions of the pipelines (Fazzini & Otegui 2006). Although the use of corrosion inhibitors has been attributed to internal corrosion reduction in pipelines, the right concentration of the inhibitor is needed to achieve this. Martinez *et al.* (2009) showed that 50ppm of amine type inhibitor gave the best corrosion inhibition in X52 pipeline whereas 100 ppm increased the corrosion rate at static condition. The concern about environmental pollution in use of corrosion inhibitors led to the testing of Lanthanum-4 hydroxyl cinnamate compound for their corrosion inhibitive ability (Blin *et al.* 2007). The work showed that this compound inhibited both the anodic and cathodic reactions at 0.01M NaCl solution exposure of carbon steel after using linear polarisation resistance and cyclic potentiodynamic polarisation measurements to check the rate of corrosion of the material. Other environmental friendly inhibitors that are in predominant use in controlling pipeline corrosion in the oil and gas industry includes imidazoline and nitrogen-based inhibitors (Hu *et al.* 2011). Because monitoring is essential for pipeline integrity monitoring, Huang & Dawei (2008) experimentally tested the use of Cu-Zn galvanic sensor to monitor internal corrosion of pipeline in seawater environment by measuring the difference between dissolved oxygen entrant and exit. After comparing the corrosion rates monitored with this sensor and corrosion coupon, the authors affirmed that the sensors can be used to reasonably predict internal corrosion of pipelines despite the need for reliable sensor design and data-base accumulation for the corrosive environment. Although repair of a pipeline by repeated welding operation has been shown not to affect the integrity of X52 pipelines (Vega *et al.* 2008), Fazzini & Otegui (2006) after hydrostatically testing

several rectangular, elliptical and other geometry type welded sections of X52 gas transmission pipeline at 200% of Maximum Allowable Operating pressure (MAOP) concluded that repaired patches that pose most risks to pipeline integrity are those with poor quality of welds, placed with the pipeline at less than half the MAOP, rectangular and roughly twice longer than the width and repairs that have large dimensions with the corrosion defect more than 40% of the nominal wall thickness.

To effectively manage pipelines against fatigue induced failures, leakage may be monitored with some of the techniques listed in Table 2.3 (Nayak 2014).

Table 2.3: Summary of pipeline leakage detection techniques

SN	Methodology	Principle	Remarks
1	Mass balance technique	Uses law of mass transfer	Identifies leakage by balancing the difference between input volume and output volume
2	System rate of change	Uses change in pressure or flow rate	After accounting for frictional losses, decreases in pressure and flow rate may be attributed to leakage.
3	Pressure point analysis	Uses statistical analysis of pressure and flow rate	May require a number of transient runs to detect leakage of various magnitude from pipelines
4	Wave alert system	uses wavelength variation	Detects leakage through bidirectional arrival of negative pressure wavelength from ruptured pipeline.
5	Supervisory control and data acquisition (SCADA)	Uses system data monitoring	Can pick-up information about blocked pipes at metering points and valve sites.
6	Fibre optics	Uses fibre optics sensors such as - clustered sensor system, discrete sensor system, continuous distributed sensor systems.	uses the change in temperature, mechanical stress, surface coating or material absorption of the fibre optics material
7	Chemical detection	Uses chemical sensors such as- discrete sensors, distributed chemical sensors, distributed fibre optics sensors	Chemical probes and sensors can detect the accurate point of pipeline leakage
8	Acoustic method	uses turbulent velocity fluctuation	Fluid leakage may result in the change of turbulent characteristics of such a pipeline.

2.6 Conclusions

Safe operation of oil and gas transmission pipelines requires mitigation of fatigue stress caused by corrosion defects in operating environments. These corrosion defects are caused by the electrochemical reaction of water and iron content of the pipeline material in the presence of CO₂ (sweet corrosion), H₂S (sour corrosion) and/or microorganisms (microbiologically induced corrosion) such as bacteria. The corrosion reaction produces protective scales such as FeCO₃, CaCO₃ and Fe_xS_x which can temporarily prevent corrosion however, hydrodynamic force in the fluid flow removes the scales exposing the pipeline surfaces to more corrosion. The microorganisms introduced into the pipeline via injection water pumping, drilling operations or those surrounding buried pipelines secrete metabolites whose activities accelerate anodic/cathodic reactions which accelerates corrosion rate.

Localized corrosion sites on pipelines are points of initiation of stress corrosion cracking due to the cyclic loads induced on the pipelines by the operating pressures. Stress corrosion cracking occurs in both low and high pH environments and potentially caused fatigue failures of 20% ~ 25% depending on the age of the pipeline. Stress corrosion cracking have been found to be majorly caused by disbonded coatings, manufacturing defects, electrochemical reaction, flow assisted corrosion and ingress of corrosive species such as hydrogen into carbon steel materials.

Pipelines exposed to external and internal cyclic stress in sour environment have hydrogen diffused to the carbon steel surface of the pipeline. This ingress which can happen at a pressure as low as 2 MPa can potentially cause distortion of the microstructure of the carbon steel at defective metallic matrix in the microstructure hence the need for improved quality of manufactured pipes.

Since pipeline corrosion may not be eliminated in its entirety in oil and gas transmission pipelines, it is imperative that optimal performance of pipelines be achieved based on integrity assurance cycle. Hence, core activities that includes strategic policy initiation, policy implementation, information analysis and reviews and implementation actions are vital for fatigue stress minimization. This integrity programme applies corrosion controls, monitoring and inspections strategies to

ensure that the fatigue failure is minimized by carrying out fitness-for-service testing at design, manufacture, installation and operation. Furthermore, there should be enhanced manufacturing processes for pipes in order to reduce defects such as cracks, dents, buckles, bulges and out-of-roundness which increase the stress load on corroded pipelines. Again, when pipelines are produced to high quality – free from inclusions and other microstructural defects, the risk of hydrogen induced cracking is reduced and the chances of fatigue stress failures minimized.

Finally, it is recommended that more research work need to be done on -

- Stress corrosion cracking measurement techniques of pipelines since the present techniques have not adequately provided enough help for in-situ prediction of stress corrosion cracking.
- The effect of manufacturing processes such as welding and hydrostatic testing on the susceptibility of pipelines to corrosion, stress corrosion cracking and hydrogen induced cracking need to be investigated more especially with respect to a safe testing pressure that may not increase the risk of fatigue stress on pipelines.
- There is need for more experimental analysis on the correlation of pipeline burst pressure and toughness of ageing pipelines.

References

- AHAMMED, M. 1998. Probabilistic estimation of remaining life of a pipeline in the presence of active corrosion defects. *International Journal of Pressure Vessels and Piping*, 75, 321-329.
- ALBERTA ENERGY REGULATOR (AER). 2013. Report 2013 - B: Pipeline performance in Alberta, 1990–2012. Available from: <<http://www.aer.ca/documents/reports/R2013-B.pdf>>. [17/09/13].
- ALIZADEH, A.H., KHISHVAND, M., IOANNIDIS, M.A. & PIRI, M. 2014. Multi-scale experimental study of carbonated water injection: An effective process for mobilization and recovery of trapped oil, *Fuel* 132, 219–235.
- AMERICAN PETROLEUM INSTITUTE (API). 2000. Fitness-for-service, API Recommended Practice 579. API Publication 579, USA.

- AMERICAN SOCIETY OF MECHANICAL ENGINEERS, ASME B31.8S. 2004. Managing system integrity of gas pipelines, American Society of Mechanical engineers, New York, USA.
- BAZÁN, F. A. V. & BECK, A. T. 2013. Stochastic process corrosion growth models for pipeline reliability. *Corrosion Science*, 74, 50-58.
- BBC. 2014. Taiwan gas blasts in Kaohsiung kill at least 25. Available from: <<http://www.bbc.com/news/world-asia-28594693>>. [7/2/15].
- BEDAIRI, B., CRONIN, D., HOSSEINI, A. & PLUMTREE, A. 2012. Failure prediction for Crack-in-Corrosion defects in natural gas transmission pipelines. *International Journal of Pressure Vessels and Piping*, 96–97, 90-99.
- BEIDOKHTI, B., DOLATI, A. & KOUKABI, A. H. 2009. Effects of alloying elements and microstructure on the susceptibility of the welded HSLA steel to hydrogen-induced cracking and sulfide stress cracking, *Materials Science and Engineering: A*, 507, 167-73.
- BHASKARAN, R., PALANISWAMY, N., RENGASWAMY, N.S. & JAYACHANDRAN, M. 2005. Global cost of corrosion—A historical review, *ASM Handbook, Volume 13B: Corrosion: Materials*, S.D. Cramer, B.S. Covino, Jr., editors, 2005, p621-628, DOI: 10.1361/asmhba0003968.
- BIOMORGI, J., HERNÁNDEZ, S., MARÍN, J., RODRIGUEZ, E., LARA, M. & VILORIA, A. 2012. Internal corrosion studies in hydrocarbons production pipelines located at Venezuelan Northeastern. *Chemical Engineering Research and Design*, 90, 1159-1167.
- BLIN, F., KOUTSOUKOS, P., KLEPETSANIS, P. & FORSYTH, M. 2007. The Corrosion inhibition mechanism of new rare earth cinnamate compounds — Electrochemical studies, *Electrochimica Acta*, 52, 6212-20.
- BRITISH STANDARDS INSTITUTION (BSI). 2005. Guide on methods for assessing the acceptability of flaws in fusion welded structures BS 7910. London (UK), 2005.
- BROWN, G. K. 2014. Appendix - Internal Corrosion Monitoring techniques for pipeline systems, in *Pipeline Integrity Handbook*, ed. by Ramesh Singh (Boston: Gulf Professional Publishing, 2014), pp. 255-92.

- BRETON, T., SANCHEZ-GHENO, J. C., ALAMILLAC, J.L. & ALVAREZ-RAMIREZ, J. 2010. Identification of failure type in corroded pipelines: A Bayesian probabilistic approach, *Journal of hazardous materials* 179, 628–634.
- CALEYO, F., GONZÁLEZ, J.L. & HALLEN, J.M. 2002. A study on the reliability assessment methodology for pipelines with active corrosion defects, *International Journal of Pressure Vessels and Piping*, 79(1), 77-86.
- CAPP.2009. Best Management Practices: Mitigation of internal corrosion in oil effluent pipeline systems, 2009, Calgary Canada. Available from: <<http://www.capp.ca/getdoc.aspx?DocId=155641&DT=PDF>>. [19/6/14].
- CHANDRASATHEESH, C., JAYAPRIYA, J., GEORGE, R. P., & MUDALI, U. K. 2014. Detection and analysis of microbiologically influenced corrosion of 316 L stainless steel with electrochemical noise technique. *Engineering Failure Analysis*, 42, 133-142.
- CHEN, Y., HOWDYSHELL, R., HOWDYSHELL, S. & JU, L. 2014. Characterizing pitting corrosion caused by a long-term starving sulfate-reducing bacterium surviving on carbon steel and effects of surface roughness, *Corrosion*, 70 (8), 767-780.
- CHOI, H. J. & AL-AJWAD, H. 2008. Flow-dependency of sweet and sour corrosion of carbon steel downhole production tubing in khuff-gas wells. *CORROSION* 2008, 2008. NACE International.
- CHOI, J. B., GOO, B. K., KIM, J. C., KIM, Y. J., & KIM, W. S. 2003. Development of limit load solutions for corroded gas pipelines. *International Journal of Pressure Vessels and Piping*, 80(2), 121-128.
- COLE, I. S., CORRIGAN, P., SIM, S., & BIRBILIS, N. 2011. Corrosion of pipelines used for CO₂ transport in CCS: Is it a real problem? *International Journal of Greenhouse Gas Control*, 5(4), 749-756.
- CONTRERAS, A., ALBITER, A., SALAZAR, M. AND PÉREZ, R., 2005, Slow Strain Rate Corrosion and Fracture Characteristics of X-52 and X-70 Pipeline Steels, *Materials Science and Engineering: A*, 407 (2005), 45-52
- COSHAM, A., HOPKINS, P. & MACDONALD, K.A. 2007. Best practice for the assessment of defects in pipelines—Corrosion. *Engineering Failure Analysis*, 14 (7), 1245-1265.

- CUMBER, P. S. 2001. Predicting outflow from high pressure vessels, *Process Safety and Environmental Protection*, 79, 13-22.
- DAVOODI, A., PAKSHIR, M., BABAIEE, M. & EBRAHIMI, G.R. 2011. A comparative H₂S corrosion study of 304L and 316L stainless steels in acidic media, *Corrosion Sci.*, 53(1), 399-408.
- ELLIOTT, P. 2013. Corrosion-When you see the signs, which way do you go, *Materials performance*, NACE International 52(6), 30-34.
- FAZZINI, P. G. & OTEGUI, J. L. 2007. Experimental determination of stress corrosion crack rates and service lives in a buried ERW pipeline, *International Journal of Pressure Vessels and Piping*, 84, 739-48.
- FAZZINI, P. G. & OTEGUI, J.L. 2006. Influence of old rectangular repair patches on the burst pressure of a gas pipeline, *International Journal of Pressure Vessels and Piping*, 83, 27-34.
- FEKETE, G. & VARGA, L. 2012. The effect of the width to length ratios of corrosion defects on the burst pressures of transmission pipelines, *Engineering Failure Analysis*, 21, 21-30.
- FANG, H., BROWN, B. & NESCARONICACUTE, S. 2011. Effects of sodium chloride concentration on mild steel corrosion in slightly sour environments, *Corrosion*, 67(1), 015001-1.
- FERRIS, F. G., JACK, T. R. & BRAMHILL, B. J. 1992. Corrosion products associated with attached bacteria at an oil field water injection plant, *Canadian Journal of Microbiology*, 38, 1320-24.
- GEARY, W. & HOBBS, J. 2013. Catastrophic failure of a carbon steel storage tank due to internal corrosion, *Case Studies in Engineering Failure Analysis*, 1, 257-64.
- GIEG, L. M., JACK, T. R. & FOGHT, J. M. 2011. Biological souring and mitigation in oil reservoirs. *Applied Microbiology and Biotechnology*, 92(2), 263-82. doi: <http://dx.doi.org/10.1007/s00253-011-3542-6>.
- GUO, B., SONG, S., GHALAMBOR, A. & LIN, T.R. 2014. Chapter 10 - Introduction to flexible pipelines. *Offshore pipelines (Second Edition)*. Gulf professional publishing, Boston, 2014, Pages 125-132, *Offshore pipelines (Second Edition)*. ISBN 9780123979490. <http://dx.doi.org/10.1016/B978-0-12-397949-0.00010-8>.

- HAN, Z. Y. & WENG, W. G. 2010. An integrated quantitative risk analysis method for natural gas pipeline network, *Journal of Loss Prevention in the Process Industries*, 23, 428-36.
- HAYS, G. F. 2010. Now is the time. Available from: <<http://corrosion.org/wp-content/themes/twentyten/images/nowisthetime.pdf>>. [30/6/14].
- HERNÁNDEZ-RODRÍGUEZ, M. A. L., MARTÍNEZ-DELGADO, D., GONZÁLEZ, R., PÉREZ UNZUETA, A., MERCADO-SOLÍS, R. D. & RODRÍGUEZ, J. 2007. Corrosive wear failure analysis in a natural gas pipeline. *Wear*, 263, 567-571.
- HInt Dossier. 2005. Gas Pipeline Explosion at Ghislenghien, Belgium. Available from: <<http://www.iab-atex.nl/publicaties/database/Ghislenghien%20Dossier.pdf>>. [7/2/15].
- HONG, H.P.1999. Inspection and maintenance planning of pipeline under external corrosion considering generation of new defects, *Structural safety* 21, 203-222.
- HSE. 2001. Review of corrosion management for offshore oil and gas processing, HSE offshore technology report 2001/044. Available from: <<http://www.hse.gov.uk/research/otopdf/2001/oto01044.pdf>>. [22/6/14].
- HU, X., BARKER, R., NEVILLE, A. & GNANAVELU, A. 2011. Case study on erosion–corrosion degradation of pipework located on an offshore oil and gas Facility. *Wear* 271, 1295– 1301.
- HUANG, Y. & JI, D. 2008. Experimental Study on seawater-pipeline internal corrosion monitoring system, *Sensors and Actuators B: Chemical*, 135, 375-80.
- ILMAN, M. N. & KUSMONO 2014. Analysis of internal corrosion in subsea oil pipeline. *Case Studies in Engineering Failure Analysis*, 2, 1-8.
- JAVAHERDASHTI, R. 2011. Impact of sulphate-reducing bacteria on the performance of engineering materials. *Applied Microbiology and Biotechnology*, 91(6), 1507-1517.
- JO, Y. & CROWL, D. A. 2008. Individual Risk analysis of high-pressure natural gas pipelines, *Journal of Loss Prevention in the Process Industries* 21, 589-95.
- KAPUSTA, S. 2008. Managing Corrosion in Sour Gas System: Testing, design, implementation and field experience, *CORROSION/2008*, paper no. 08641.

- KHAKSARFARD, R., PARASCHIVOIU, M., ZHU, Z., TAJALLIPOUR, N. & TEEVENS, P. J. 2013. CFD based analysis of multiphase flows in bends of large diameter pipelines, *CORROSION*/2013.
- KISHAWY, H. A. & GABBAR, H. A. 2010. Review of pipeline integrity management practices, *International Journal of Pressure Vessels and Piping*, 87, 373-80.
- LEIS, N. & STEPHENS, D.R. 1997. An alternative approach to assess the integrity of corroded line pipe-part I: current status. *Proceedings of the 7th International Offshore and Polar Engineering Conference, Part I, Honolulu, USA, 1997*, ASME International, New York, 624-641.
- LI, D., ZHANG, L., YANG, J., LU, M., DING, J. & LIU, M. 2014. Effect of H₂S concentration on the corrosion behavior of pipeline steel under the coexistence of H₂S and CO₂, *International Journal of Minerals, Metallurgy, and Materials*, 21, 388-94.
- LIESER, M. J. & XU, J. 2002. Composites and the future of society: Preventing a legacy of costly corrosion with modern materials. Available from: <http://www.ocvreinforcements.com/pdf/library/CSB_Corrosion_White_Paper_Sept_10_10_English.pdf>. [1/7/14].
- LU, G., & KAXIRAS, E. 2005. Hydrogen embrittlement of aluminium: the crucial role of vacancies. *Physical review letters*, 94(15), 155501.
- MACHUCA, L. L., MURRAY, L., GUBNER, R. & BAILEY, S. I. 2014. Evaluation of the effects of seawater ingress into 316L lined pipes on corrosion performance. *Material Corrosion* 65(2014)8–17.
- MA, B., SHUAI, J., LIU, D. & XU, K. 2013. Assessment on failure pressure of high strength pipeline with corrosion defects, *Engineering Failure Analysis*, 32, 209-19.
- MARTÍNEZ, D., GONZALEZ, R., MONTEMAYOR, K., JUAREZ-HERNANDEZ, A., FAJARDO, G. & HERNANDEZ-RODRIGUEZ, M. A. L. 2009. Amine type inhibitor effect on corrosion–erosion wear in oil gas pipes, *Wear*, 267, 255-58.
- MARUTHAMUTHU, S., MUTHUKUMAR, N., NATESAN, M., & PALANISWAMY, N. 2008. Role of air microbes on atmospheric corrosion. *Current Science*, 94(3), 359-363.

- MAZUMDER, Q. H., SHIRAZI, S. A. & MCLAURY, B. 2008. Experimental investigation of the location of maximum erosive wear damage in elbows. *Journal of Pressure Vessel Technology*, 130, 011303-011303.
- MELCHERS, R.E. 2008. Extreme value statistics and long-term marine pitting corrosion of steel, *Probabilistic Engineering Mechanics*, 23(4), 482-488.
- MENG, W., P. OGEA & KING, M. 2011. Changes of operating procedures and chemical application of a mature deepwater tie-back - Aspen field case study, *Offshore Technology Conference, Proceedings*, 2, 881-892
- MILLER, R. 2013. Why pipes matter: The importance of clad pipes in the oil and gas industry. Available from: <<http://breakingenergy.com/2013/03/15/why-pipes-matter-the-importance-of-clad-pipe-in-the-oil-and-gas/>>. [1/7/14].
- MUTHUKUMAR, N., RAJASEKAR, A., PONMARIAPPAN, S., MOHANAN, S., MARUTHAMUTHU, S., MURALIDHARAN, S., ... & RAGHAVAN, M. 2003. Microbiologically influenced corrosion in petroleum product pipelines-a review. *Indian journal of experimental biology*, 41(9), 1012-1022.
- NAYAK, C. 2014. Fault detection in fluid flowing pipes using acoustic method, *International Journal of Applied Engineering Research*, 9 (1), 23-28.
- NESIC, S. 2007. Key issues related to modelling of internal corrosion of oil and gas pipelines – A review, *Corrosion Science*, 49, 4308-38.
- NESIC, S., CAI, J. & LEE, K. J. 2005. A multiphase flow and internal corrosion prediction model for mild steel pipelines. *Corrosion/2005*. Paper no 05556.
- NICHOLSON, R., FEBLOWITZ, J., MADDEN, C., & BIGLIANI, R. 2010. The role of predictive analytics in asset optimization for the oil and gas industry. IDC Energy Insights, White Paper. Available from: <<http://tessella.com/documents/role-predictive-analytics-asset-optimization-oil-gas-industry/>>. [29/6/14].
- OSSAI, C.I. 2012a. Advances in asset management techniques: An overview of corrosion mechanisms and mitigation strategies for oil and gas pipelines, *ISRN Corrosion*, vol. 2012. <http://dx.doi.org/10.5402/2012/570143>, Article ID 570143.

- OSSAI, C. I. 2012b. Predictive modelling of wellhead corrosion due to operating conditions: A field data approach, *ISRN Corrosion*, vol. 2012, Article ID 237025, 2012. doi:10.5402/2012/237025.
- PANDEY, M.D. 1998. Probabilistic models for condition assessment of oil and gas pipelines, *NDT&E International*, 31(5), 349-358.
- PAPAVINASAM, S. 2014a. Chapter 6 - Modelling – Internal corrosion, in *Corrosion Control in the Oil and Gas Industry*, ed. by Sankara Papavinasam (Boston: Gulf Professional Publishing, 2014), pp. 301-60.
- PAPAVINASAM, S. 2014b. Chapter 7 - Mitigation – Internal corrosion', in *Corrosion Control in the Oil and Gas Industry*, ed. by Sankara Papavinasam (Boston: Gulf Professional Publishing, 2014), pp. 361-424.
- PAPAVINASAM, S., DOIRON, A. & REVIE, R. W. 2010. Model to predict internal pitting corrosion of oil and gas pipelines. *Corrosion*, 66(3), 035006-035006-11.
- PAPAVINASAM, S., DOIRON, A., PANNEERSELVAM, T. & Revie, R. W. 2007. Effect of hydrocarbons on the internal corrosion of oil and gas pipelines. *Corrosion*, 63(7), 704-712.
- PARK, G. T., KOH, S. U., JUNG, H. G., & KIM, K. Y. 2008. Effect of microstructure on the hydrogen trapping efficiency and hydrogen induced cracking of linepipe steel. *Corrosion science*, 50(7), 1865-1871.
- PARK, N. G., MORELLO, L., WONG, J. E., & MAKSOUD, S. A. 2007. The Effect of oxygenated methanol on corrosion of carbon steel in sour wet gas environments. In *CORROSION 2007*. NACE International.
- POPOOLA, L. T., GREMA, A. S., LATINWO, G. K., GUTTI, B., & BALOGUN, A. S. 2013. Corrosion problems during oil and gas production and its mitigation. *International Journal of Industrial Chemistry*, 4(1), 1-15.
- RACE, J. M. 2010. 4.42 - Management of corrosion of onshore pipelines, In: Editor-in-Chief: Tony J.A. Richardson, Editor(s)-in-Chief, *Shreir's Corrosion*, Elsevier, Oxford, 2010, Pages 3270-3306, ISBN 9780444527875, <http://dx.doi.org/10.1016/B978-044452787-5.00169-4>.
- RAMAN, R. K. S., AVAHERDASHTI, R., PANTER, J. C. & PERELOMA, E. V. 2005. Hydrogen embrittlement of a low carbon steel during slow strain testing in

- chloride solutions containing sulphate reducing bacteria, *Materials Science and Technology* 21(9), 1094-1098.
- SAHRAOUI, Y., KHELIF, R. & CHATEAUNEUF, A. 2013. Maintenance planning under imperfect inspections of corroded pipelines. *International journal of pressure vessels and piping* 104, 76-82.
- SANA, N. O., NAZIRB, H., DONMEZC, G. 2012. Microbiologically influenced corrosion failure analysis of nickel–copper alloy coatings by *Aeromonas salmonicida* and *Delftia acidovorans* bacterium isolated from pipe system. *Engineering Failure Analysis* 25, 63–70.
- SINGH, M. & MARKESET, T. 2014. Simultaneous handling of variability and uncertainty in probabilistic and possibilistic failure analysis of corroded pipes, *International Journal of System Assurance Engineering and Management*, 5, 43-54.
- SINGER, M., BROWN, B., CAMACHO, A. & NESIC, S. 2011. Combined effect of carbon dioxide, hydrogen sulfide, and acetic acid on bottom-of-the-line corrosion, *Corrosion*, 67(1), 015004-1.
- SINHA, S.K. & MCKIM, R. A. 2007. Probabilistic based integrated pipeline management system, *Tunnelling and underground space technology* 22, 543–552.
- SONG, Y., PALENCŚÁR, A., SVENNINGSEN, G., KVAREKVÅL, J., & HEMMINGSEN, T. 2012. Effect of O₂ and temperature on sour corrosion. *Corrosion*, 68(7), 662-671.
- UNITED STATES DEPARTMENT OF TRANSPORT, US DOT. 2014. Pipeline and Hazardous Materials Safety Administration (PHMSA). Available from: <<https://hip.phmsa.dot.gov/analyticsSOAP/saw.dll?Portalpages>>. [7/02/15].
- VEGA, O. E., HALLEN, J. M., VILLAGOMEZ, A. & CONTRERAS, A. 2008. Effect of multiple repairs in girth welds of pipelines on the mechanical properties, *Materials Characterization*, 59, 1498-507.
- VELAZQUEZ, J. C., VALOR, A. CALEYO, F., VENEGAS, V., ESPINA-HERNANDEZ, J. H., HALLEN J. M., & LOPEZ, M. R. Pitting corrosion models improve integrity management, reliability, *Oil and Gas Journal*, 107(28), 56-62.

- VENKATESH, C. D. & FARINHA, P. A. 2006. Corrosion Risk Assessment (CRA) in the oil and gas industry-An overview and its holistic approach. Available from: <<http://members.iinet.net.au/~extrin/ConferencePapers/CAP04~Paper06.pdf>>. [18/10/13].
- WANG, H., JEPSON, P.W., CAI, J.Y. & GOPAL, M. 2000. Effect of bubbles on mass transfer in multiphase flow, In: NACE Int. Conference series, Corrosion/2000, paper no. 00050.
- WANG, N. & ZARGHAMEE, M. 2014. Evaluating fitness-for-service of corroded metal pipelines: Structural Reliability Bases, Journal of Pipeline Systems Engineering and Practice, 5, 04013012.
- WANG, W., SMITH, M. Q., POPELAR, C. H., & MAPLE, J. A. 1998. New rupture prediction model for corroded pipelines under combined loadings. In The 1998 International Pipeline Conference, IPC. Part 1(of 2) (pp. 563-572).
- WANG, X. & REINHARDT, W. 2003. On the assessment of through-wall circumferential cracks in steam generator tubes with tube supports, Journal of Pressure Vessel Technology 125, 85-90.
- WEN, J., GU, T. & NESIC, S. 2007. Investigation of the effects of fluid flow on SRB biofilm, In: NACE Int. Conference series, Corrosion/2007, paper no. 07516.
- YARDENI, E., JOHNSON, D. & QUINTANA, M. 2014. Global economic briefing: Global inflation, Available from: <http://www.yardeni.com/pub/infltrglb_bb.pdf>. [1/7/14].
- YIN, Z.F., ZHAO, W.Z. BAI, Z.Q., FENG, Y.R. & ZHOU, W.J. 2008. Corrosion behaviour of SM 80SS tube steel in stimulant solution containing H₂S and CO₂, Electrochim. Acta, 53(10), 3690.
- ZHANG, C., ZHANG, Q., CHEN, W., LIU, D., OU, T., HUANG, X., ... & CHEN, C. 2013. Assessment of corrosion and mechanical properties degradation of pipeline steel after long term service in high sour gas-field environments. In IPTC 2013: International Petroleum Technology Conference.
- ZHANG, T., YANG, Y., SHAO, Y., MENG, G. & WANG, F. 2009. A stochastic analysis of the effect of hydrostatic pressure on the pit corrosion of Fe-20Cr alloy. Electrochimica Acta, 54, 3915-3922.

Chapter 3 - Predictive modelling of internal pitting corrosion of aged non-piggable pipelines

3.0 Introduction

It is well known that pipelines used for oil and gas production degrade due to corrosion caused by operation. This corrosion, which can be internally induced by the interaction of the flowing fluid and carbon steel material from, which the pipeline is made has caused huge downtimes as a result of pipeline failures (Nesic, Cai & Lee 2005, Chokshi, Sun & Nesic 2005, Nesic 2007). The fluid inside a pipeline can be in multiphase flow regime, in which oil, gas and water flow together from the reservoir (Nesic, Cai & Lee 2005, Papavinasam *et al.* 2007). The water in this flow regime may cause corrosion when it is in contact with the pipeline wall due to the affinity between iron and carbonic acid formed when CO₂ dissolves in water (Nesic, Cai & Lee 2005, Renpu 2011). Water introduced from different sources into the pipeline such as - when hydrostatically tested pipe is not properly dried or else due to formation water from oil wells and moisture content of gas (Renpu 2011) provide a medium for internal corrosion of pipelines.

The ionic nature of oil and gas affects their solubility in water however, they can form an emulsion at low concentrations of water (Papavinasam, Doiron & Revie 2010). This emulsion can be an oil-in-water (o/w) phase with water being the continuous phase or else water-in-oil (w/o) phase with oil being the continuous phase (Papavinasam *et al.* 2007, Papavinasam, Doiron & Revie 2010). Research has shown that o/w phases possess conductive characteristics, which may result in corrosion of the pipeline whilst w/o phases may generally not cause corrosion due to the presence of an oil-wet-surface, which does not allow the pipeline wall to be in direct contact with water (Papavinasam, Doiron & Revie 2010). The o/w phase has a water-wet-surface which allows water to be in direct contact with the pipeline wall. This contact facilitates anodic/cathodic reactions that lead to different types of internal corrosion (Renpu 2011, Ossai 2012).

In sweet corrosion, CO₂ present in the oil and gas dissolves in formation water to produce carbonic acid which reacts with iron from the carbon steel material of the pipeline as follows (Song 2010, Xian & Nesic 2005, Fajardo *et al.* 2007):



Although carbonic acid is a weak acid with approximately 0.2% of the dissolved molecules being hydrated (Fajardo *et al* 2007, Biomorgi *et al.* 2012), it is still very corrosive towards carbon steel. The iron carbonate formed in Equation (3.2) acts as a protective film on the pipeline wall to prevent more corrosion (Choi & Al-Ajwad 2007). However, the combined effects of erosion-corrosion and other chemical processes result in the dissolution according to Equation (3.3) [Chokshi, Sun & Nesic 2005, Renpu 2011, Hu *et al.* 2011a):



The stability of iron carbonate protective film formed in the corrosion process helps to reduce the rate of uniform corrosion and prevent localized corrosion such as pitting corrosion, preferential weld corrosion and flow-induced localized corrosion (Race 2010). Again, multi-layer species have been shown to have more stability and hence have a better protective ability than single layer species whilst extraneous materials such as sand are known to increase the pitting rate of pipelines (Demoz *et al.* 2009, Hu *et al.* 2011b, Biomorgi *et al.* 2012). The rate of corrosion wastage of pipelines can also be attributed to the steel composition and microstructure at the areas of localized corrosion. This was evident in the work of some researchers who determined that pitting was more pronounced in heat affected zone of pipelines than other areas after a long time exposure of the material to a corrosive environment (Chaves & Melchers 2011).

Management of internal corrosion is an important process of containing the risk of pipeline failure within the oil and gas industry since approximately half of pipeline failures are known to be associated with internal corrosion problems (CAPP 2009). Since the ageing of pipelines result in decreased integrity (and increased risk of failure), the maintenance of safety in operation relies on managing the remaining strength of the corroded pipelines. Understanding the remaining strength, which is dependent on the longitudinal length and depth of the corrosion defects (Choi &

Bomba 2003, Hasan, Khan & Kenny 2012, DNV 2010) is imperative for establishing the remaining useful life, risk mitigation and reliability estimation (Mohd & Paik 2013). It therefore follows that, if the radial, axial and circumferential distributed defects that reduce the tensile strength at the corroded areas in a pipeline is determined on time, the risk of failure, which can be in the form of leakage, burst or rupture (ASME 2009) may be minimized.

Papavinasam *et al.* (2007) experimentally predicted the internal pitting corrosion of oil and gas pipelines by using the physical characteristics of the pipeline - diameter, thickness, inclination angle and operation parameters such as production rate, partial pressure of CO₂ and H₂S and concentration of sulphate, bicarbonate and chloride ions. However, the model was tested against limited field data. Nestic, Cai & Lee (2007) used a mass transfer model for a mechanistic prediction of corrosivity in pipelines by showing the effect of multiphase flow on water entrainment and separation in the o/w phase. The authors developed a model for the critical droplet diameter above which the droplet-diameter of water in multiphase flow deforms. This deformed droplet migrates to the pipeline wall causing or accelerating corrosion as the mass transfer rates of the corrosive species such as H⁺ increases (Nestic 2012). Similarly, water cut, which is the quantity of water in crude oil and hydrocarbons flowing through the pipeline plays a definitive role in internal corrosion of pipelines, since it provides oxygen and hydrogen molecules for corrosion reaction when in contact with carbon steel. Papavinasam *et al.* (2007) showed in their work that related to wettability and the Emulsion Inversion Point (EIP) of hydrocarbons that, at 0%-40% water cut, w/o emulsion converts to o/w emulsion and causes corrosion. Because crude oil transported through pipelines have water cut of the range described by these authors, internal corrosion of pipelines will always take place. This view was shared by other authors who worked on different aspects of internal corrosion of oil and gas pipelines (Nestic, Cai & Lee 2005, Demoz *et al.* 2009, Papavinasam, Doiron & Revie 2010, Biomorgi *et al.* 2012). Although Papavinasam *et al.* (2007) further showed that some hydrocarbons can retard the rate of internal corrosion of pipelines, an effective approach for mitigating against pipeline internal corrosion is the use of corrosion inhibitors, which retard the precipitation of FeCO₃ (Chokshi, Sun & Nestic 2005).

Biomorgi *et al.* (2012) concluded from their field based experimental study of flow related internal corrosion that the nature of internal corrosion damage is a function of the flow pattern and temperature variation in the pipelines. The work of these authors further confirmed that temperature and flow rate have significant influences on internal corrosion of pipelines as shown by other researchers (Choi & Al-Ajwad 2008, Papavinasam, Doiron & Revie 2010). Although Mohd and Paik (2013) used historic database information to develop a time-dependent corrosion wastage model of offshore well tubing, their work focused more on the characterization of the distribution of the pit depths and time dependent distribution of the distribution parameters with little emphasis on a predictive model of pitting corrosion. The work of Bazan and Beck (2013) on pitting corrosion growth was a comparison of non-linear random growth and linear random growth models using previously published data in literature. The authors showed that a random linear growth model conservatively predicted the long run corrosion growth of few selected field data but may not be optimal for inspection interval. This work was also validated with limited field data without consideration of operating conditions. Finally, Song *et al.* (2011) focused on determining the operating condition that has the least likelihood of causing internal corrosion of pipelines by statistically analysing field data from four oil and gas companies, in order to establish the effects of water content, temperature and operating pressure. The work concluded that the threshold of water content in the gas studied is small and may not cause internal corrosion of the pipelines.

The works reviewed above are vital prediction models of internal corrosion of pipelines and proffered mitigation advice, which could include modifying the environmental conditions when necessary (Papavinasam 2014). However, there is still need for more field studies on internal pitting corrosion of pipelines in consideration of operating parameters. The work of some authors in this area are either hampered due to lack of data or else the duration of their study was limited as shown in the review of literature above. This work will enhance practical integrity management of internal corroded pipelines by using data of maximum pit depths obtained from the field and some operating parameters - pH, flow rate, temperature, water cut, sulphate ion, chloride ion and CO₂ partial pressure to estimate the time-dependent pit depth growth.

The authors therefore aim to develop a model for predicting pit depth growth by statistically analysing the maximum pit depths and the aforementioned operational parameters in order to establish the trend of internal pit depth growth of oil and gas pipelines. The model will help in the integrity management of pipelines undergoing low, moderate, high and severe corrosion.

3.1 Research methodology.

Historic records of pit depths, CO₂ partial pressure, sulphate ion and chloride ion concentration, pH, water cut, temperature and production rates of onshore oil and gas pipelines from oil and gas fields in Nigerian Niger Delta region were obtained from the database of the company operating the fields. Ten years' data from 1999 to 2008 from sixty operating pipelines collected from this company were used for this work. To ensure that errors were limited in the data acquisition, pipelines with incomplete data due to certain operational constraints were left out prior to analysing 600 samples (see Table 3.1 for the summarized results of the field data). The maximum pit depth measurements were determined using the pulse-echo technique of Ultrasonic Thickness Measurement (UTM) whilst the other parameters were measured as part of the routine operating condition monitoring procedure of the pipelines. The flow rates were calculated using information from the daily production rates, which were also routinely collected by the organization. The operating parameters used in this work represent the average operational conditions in the pipelines for the duration of the maximum pit depth measurement. The procedure for measuring the internal corrosion wastage and estimation of the maximum pit depth of the pipelines is shown in Figure 3.1.

The maximum pit depths of the inspected pipelines were classified into four categories - low, moderate, high and severe pitting corrosions according to NACE standard RP0775 (see Table 3.2) (NACE 2005). According to this categorization, 80, 70, 150 and 300 of the samples fell into low, moderate, high and severe pitting corrosion rates respectively.

Table 3.1: Description of the field measured data.

	D_{max} (mm)	Θ (°C)	P_{CO_2} (MPa)	V (m/s)	p_H	W_C (%)	S_{O_4} (mg/L)	C_L (mg/L)	No of samples
Low pitting rate									
Min	0.049	24.0	0.01	0.07	6.2	1	2.00	117.00	80
Max	0.118	40.0	0.14	0.23	8.2	88	70.00	4431.00	
Mean	0.087	30.6	0.06	0.13	7.6	35	30.13	1291.34	
SD	0.027	5.9	0.04	0.05	0.8	38	22.38	1474.22	
Moderate pitting rate									
Min	0.132	21.0	0.01	0.04	6.8	6	6.00	66.00	70
Max	0.183	32.0	0.16	0.30	8.3	84	67.00	2729.00	
Mean	0.159	28.0	0.06	0.15	7.8	34	39.14	1273.00	
SD	0.018	3.5	0.05	0.09	0.5	30	23.81	841.73	
High pitting rate									
Min	0.204	27.0	0.02	0.05	6.2	3	7.00	404.60	150
Max	0.371	70.0	0.31	1.39	8.2	83	69.00	7621.00	
Mean	0.263	49.4	0.15	0.24	7.6	32	32.53	3513.73	
SD	0.044	17.2	0.10	0.34	0.7	29	20.79	2520.07	
Severe pitting rate									
Min	0.396	21.0	0.03	0.07	6.7	1	4.00	602.40	300
Max	1.309	74.0	0.61	2.01	8.6	90	66.00	7571.10	
Mean	0.654	50.7	0.19	0.41	7.7	42	36.33	4353.08	
SD	0.248	17.0	0.14	0.40	0.6	36	19.63	2285.35	
All data									
Min	0.049	21.000	0.01	0.04	6.2	1	2.00	66.00	600
Max	1.309	74.000	0.61	2.01	8.6	90	70.00	7621.00	
Mean	0.423	45.050	0.15	0.30	7.7	37	35.97	3482.07	
SD	0.297	17.350	0.12	0.35	0.6	33	19.93	2402.62	
D_{max}	: Maximum pitting rate (mm)								
θ	: Temperature (°C)								
P_{CO_2}	: CO2 partial pressure (MPa)								
V	: Fluid flow rate (ms ⁻¹)								
p_H	: pH of the fluid								
S_{O_4}	: Sulphate ion (mg/L)								
C_L	: Chloride ion (mg/L)								
W_C	: Water cut (%)								

Table 3.2: Qualitative categorization of carbon steel corrosion rate for oil production systems.

Pitting categories	Maximum Pitting Rate (mmyr ⁻¹)
Low	<0.13
Moderate	0.13-0.20
High	0.21-0.38
Severe	>0.38

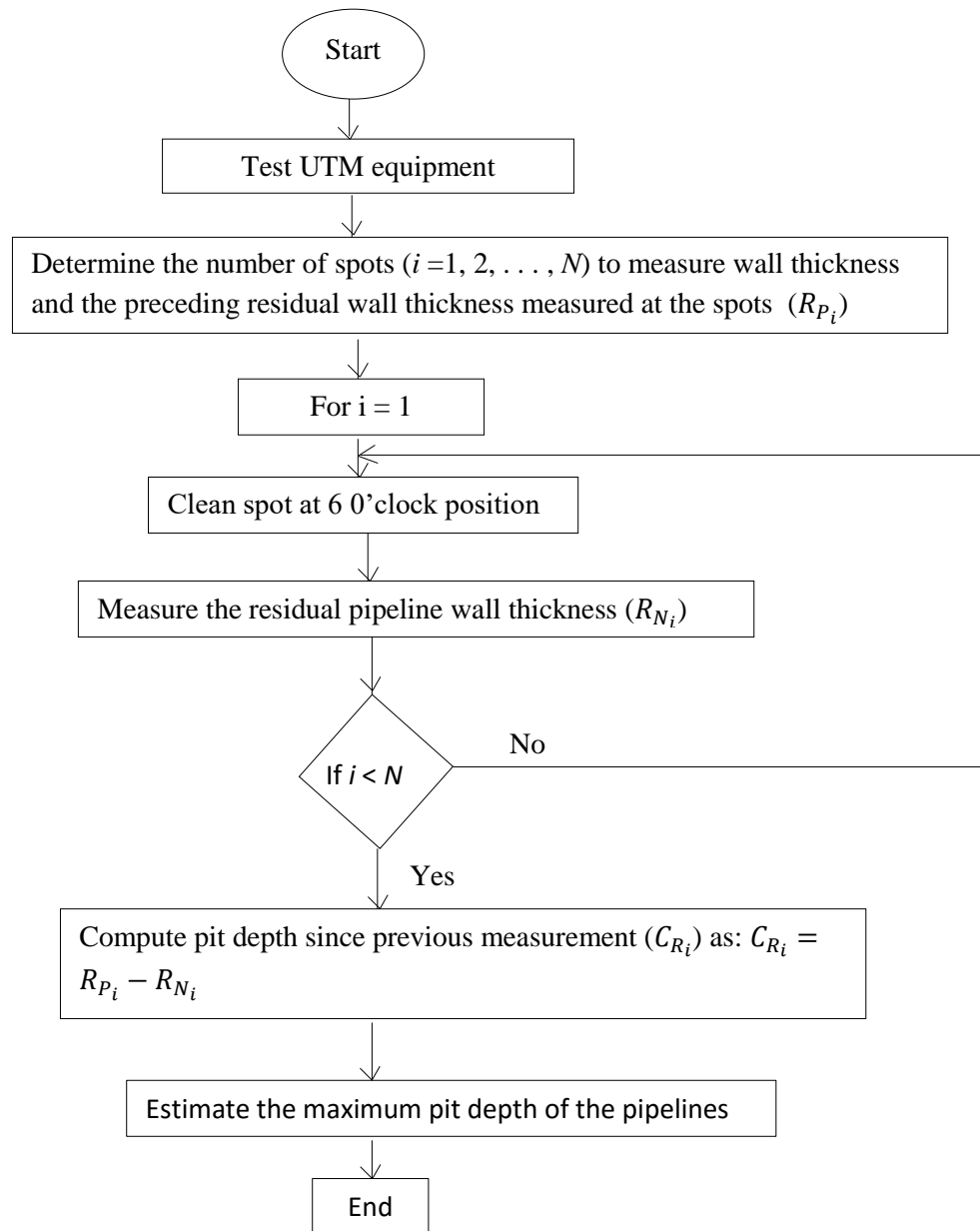


Figure 3.1: Procedure for maximum pit depth estimation using UTM technique.

3.2 Parametric analysis of maximum pit depth

The data were analysed for the four pitting corrosion categories and a generic category, which included all the collected data for this work. Information about the data used in this research and its classification is shown in Table 3.1. This table shows the minimum and maximum values of the variables respectively as:

- i. Maximum pit depth: 0.049 ~ 1.309 mm
- ii. Temperature: 21 ~ 74°C
- iii. pH: 6.21 ~ 8.57

- iv. Flow rate: 0.04 ~ 2.01 ms⁻¹
- v. CO₂ partial pressure: 0.01~0.61 MPa
- vi. Water cut:1~90%
- vii. Sulphate ion:2~70 mg/L
- viii. Chloride ion: 66~7621 mg/L

It is pertinent to note that despite the usual experimental errors associated with data collection, the variability of the operating conditions in the pipelines due to the changing nature of the fields may have resulted in the large uncertainty of the obtained data. This fluctuation of the fields conditions might play a role in the covariance that may exist between fields measured data and laboratory experimental data. It has been assumed that the operating conditions studied in this work are responsible for the pitting corrosion in the pipelines and remains the same for the operating life of the pipelines.

3.3 Distribution of maximum pit depth

The probability density function of the sampled data (all data category) is shown in Figure 3.2. To determine the best fitting curve for this data, the probability density functions shown below were tested using the Kolmogorov-Smirnov (KS) goodness of fit:

Generalized extreme value (GEV) distribution:

$$f(x) = \text{Exp} \left[- \left(1 + \tau \frac{x - \beta}{\alpha} \right)^{-\frac{1}{\tau}} \right] \text{ for } \left(1 + \tau \frac{x - \beta}{\alpha} \right) > 0 \quad (3.4)$$

Weibull distribution:

$$f(x) = \frac{\tau}{\alpha} \left(\frac{x - \beta}{\alpha} \right)^{(\tau-1)} \cdot \left(\text{Exp} \left(- \left(\frac{x - \beta}{\alpha} \right)^\tau \right) \right), x \geq \beta; \tau, \alpha > 0, \quad (3.5)$$

If $\beta = 0$ and $\alpha = 1$, a standard 2-parameter Weibull distribution shown in Equation (3.6) will be obtained.

$$f(x) = \tau x^{(\tau-1)} \cdot \left(\text{Exp}(-x^\tau) \right), x \geq 0, \tau > 0 \quad (3.6)$$

Lognormal distribution:

$$f(x) = \frac{1}{\sqrt{2\pi\delta x}} \cdot \text{Exp}\left(-\frac{(\ln(x) - \mu)^2}{2\delta^2}\right), x > 0 \quad (3.7)$$

Extreme value distribution:

$$f(x) = \frac{1}{\alpha} \cdot \text{Exp}\left(\frac{x - \beta}{\alpha}\right) \cdot \left(\text{Exp}\left(-\text{Exp}\left(\frac{x - \beta}{\alpha}\right)\right)\right) \quad (3.8)$$

If $\beta = 0$ and $\alpha = 1$, a standard Gumbel distribution extreme value equation shown in Equation (3.9) will be obtained.

$$f(x) = \text{Exp}(x) \cdot \left(\text{Exp}(-\text{Exp}(x))\right) \quad (3.9)$$

where $f(x)$ represents the probability density function of variable x , τ represents the shape parameter, α represents the scale parameter, β represents the location parameter, μ represents the mean and δ represents the standard deviation.

The result of the KS one tail goodness of fit tests for the above probability density functions is shown in Table 3.3.

Table 3.3: Kolmogorov–Smirnov goodness of fit test for the pitting corrosion data.

Extreme value value	Weibull	Lognormal	Generalized Extreme value
0.244	0.034	0.000	0.408

This table indicates that lognormal distribution with mean ($\mu = -1.1266$) and standard deviation ($\delta = 0.7847$) is the best fit distribution for the data. Lognormal distribution has also been reported by other authors (Mohd & Paik 2013, Bazan & Beck 2013) as the fitting curve for pitting corrosion of pipelines.

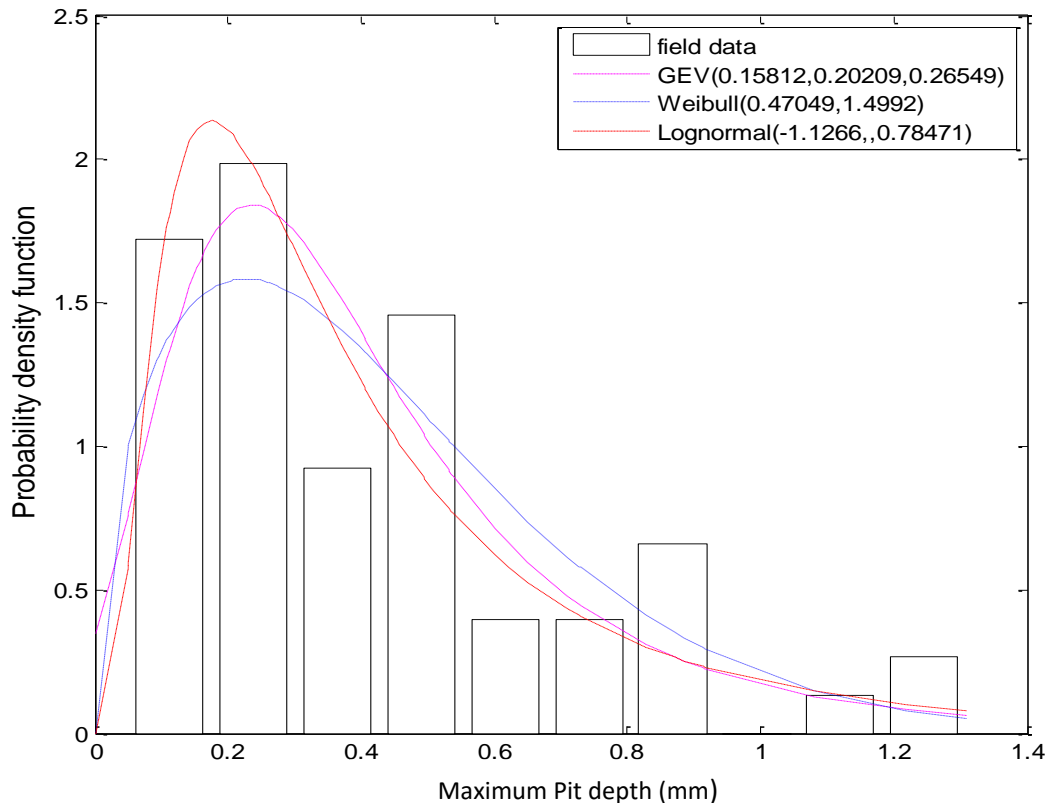


Figure 3.2: Probability density function distribution of all field measured data

3.4 Maximum Pit Depth Variation with Operational Parameters

The scatter diagram of the maximum pit depth variation with the field measured operational parameters are shown in Figure 3.3a-3.3g whereas their correlation is shown in Table 3.4.

Table 3.4: Correlation between maximum pit depth and operating variables for all data

Operating Parameters	Correlation with maximum pit depth
Temperature	0.429
CO ₂ Partial pressure	0.601
Flow rate	0.377
pH	0.018
Sulphate ion	0.087
Chloride ion	0.462
Water cut	0.225

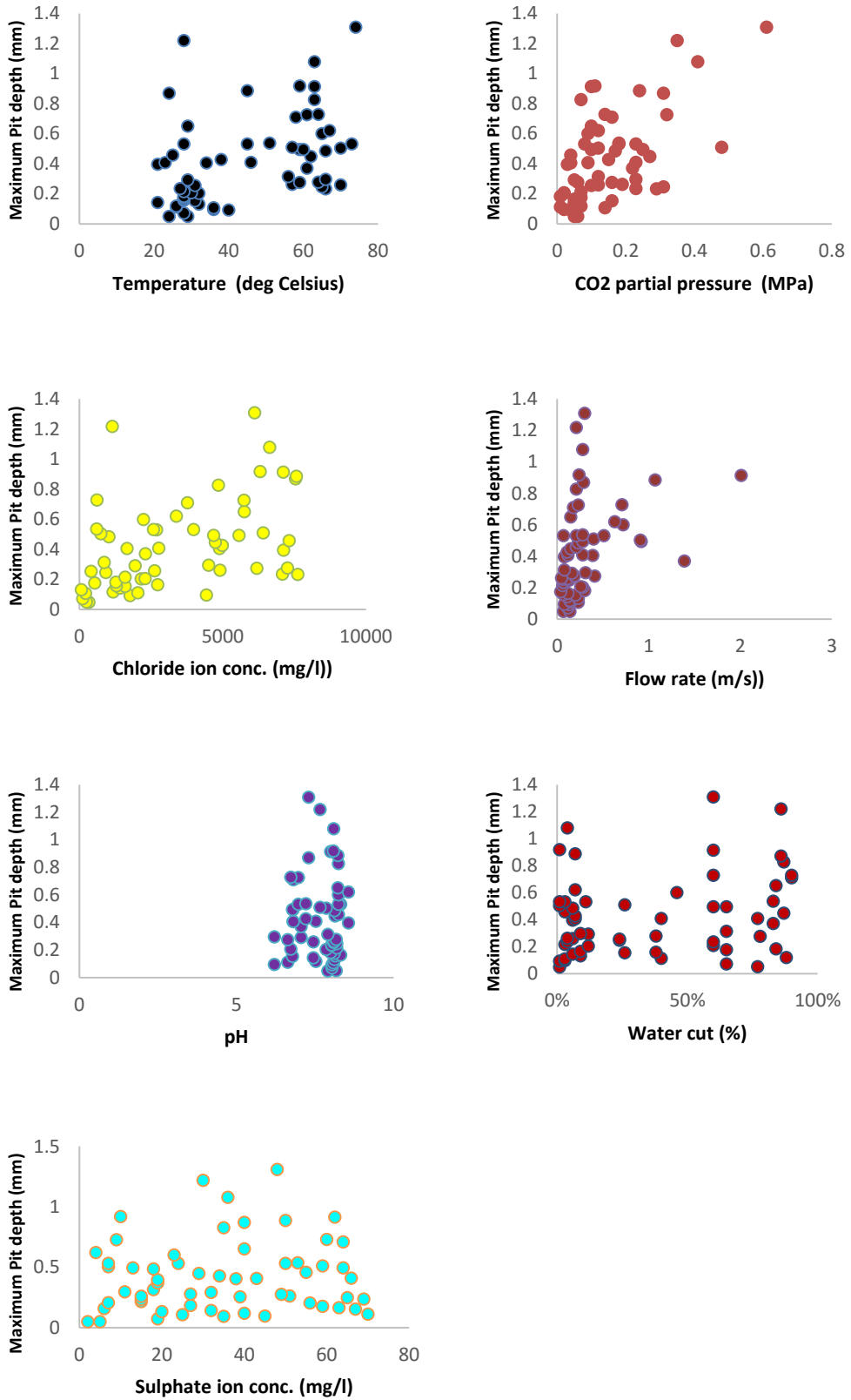


Figure 3.3: Scatter diagram of the maximum pit depth and operational parameter – temperature, CO₂ partial pressure, flow rate, chloride ion conc., pH, water cut and sulphate ion conc.

The scatter pattern noticed in the relationship between the maximum pit depth and the operational parameters may be attributed to the variability of the operating conditions of the studied pipelines. Since there was no control of the field operating conditions, there is a tendency that the interactions of the operating variables may have affected their variation with the maximum pit depth.

Table 3.4 shows the amount of influence the operating variables have on the maximum pit depth of the pipelines. Except for sulphate ion, other variables have significant impact on the pit depth of pipelines. This is consistent with some of the notable research in this area of study (Song 2010, Xian & Nescic 2005, Papavinasam, Doiron & Revie 2010, Song *et al.* 2011, Papavinasam 2014). Figure 3.4 shows the sensitivity analysis graph of the operational parameters on the maximum pit depth. The sensitivity analysis is vital for dictating the influence of operational parameters on the pit depth growth. Based on the acquired data, the model developed in this work indicates that CO₂ partial pressure, flow rate, chloride ion, pH, water cut and temperature influenced the increase of maximum pit depth in the order listed. This inference is similar to the experimental findings of Zhou and Jepson (1993), Jepson & Menezes (1995) and Jepson *et al.* (1996) (as reported by Zhang, Gopal & Jepson (1997) and that of Biomorgi *et al.* (2012), which shows that increase in temperature and flow rate resulted in pitting corrosion increase. The result also shows that sulphate ion increase resulted in limited decrease of the maximum pit depth growth. This is not surprising seeing that sulphate ion will significantly affect pit depth in the presence of H₂S (Papavinasam, Doiron & Revie 2010) however, H₂S was not significantly present in the studied fields. Although water cut predominately influences the pitting rate of oil and gas pipelines at 0~40% (Papavinasam, Doiron & Revie 2010), inhibitors may retard the rate of water wetting of the pipeline surface (McMahon 1991) as they block the active sites of corrosion due to the presence of heterocyclic compounds (containing nitrogen, oxygen and sulphur atoms) being adsorb to the pipe-wall (Wang *et al.* 2005). Despite the fact that Papavinasam, Doiron & Revie (2010) reported that pitting rate decreased with increase in CO₂ partial pressure in the range 0.17~0.69MPa, other researchers have shown that increase in CO₂ partial pressure resulted in increased pitting rate (Wang, George & Nescic 2004, Zhang *et al.* 2011) as was found in this work. Flow rate also increases the pitting rate

of pipelines (Hernandez-Rodriguez *et al.* 2007, Papavinasam, Doiron & Revie 2010) especially in multiphase flow due to turbulent gas flow. The fact that increase in temperature may result in higher electrochemical reaction is one of the reasons why pitting rate may increase as seen in this work, however, pitting corrosion rate may reduce in some instances when precipitation of FeCO_3 at a higher temperature brings about scale formation on the surface of the carbon steel material of the pipeline.

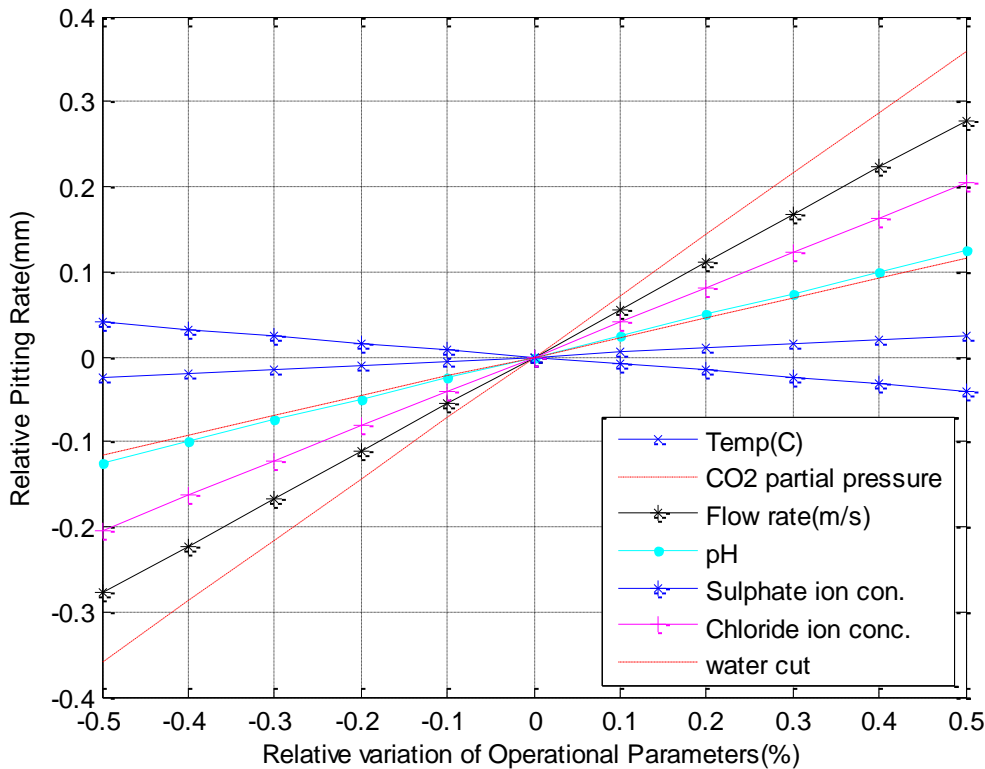


Figure 3.4: sensitivity analysis model

3.5 Regression analysis and pit growth modelling

The maximum pit depth (D_{max}) of the sampled pipelines were used to model the pitting rate of the pipelines according to the expression in Equation (3.10):

$$D_{max} = f(\theta, P_{CO_2}, V, p_H, S_{O_4}, C_L, W_C, t) \quad (3.10)$$

where t is the time of exposure of the pipeline.

A multivariate regression analysis was conducted in order to solve Equation (3.10) by assuming that the pit depth growth follows a power model as shown below:

$$D_{max} = \left(\gamma_0 + \sum_{j=1}^k \gamma_j y_j \right) * (t - t_0)^\rho \quad (3.11)$$

If Equation (3.11) is linearized and t_0 (time of initiation of pitting) is assumed to be zero, then the equations below will be necessary for estimating maximum pit depth growth with time.

$$\log D_{max} = \gamma_0 + \gamma_1 y_1 + \gamma_2 y_2 + \dots + \gamma_p y_p + \rho \log t \quad (3.12)$$

$$D_{max} = \left(e^{(\gamma_0 + \sum_{j=1}^k (\gamma_j y_j))} \right) * t^\rho \quad (3.13)$$

where y_j represents j^{th} operational parameter and γ_j represents the regression coefficient for the operational parameter, γ_0 represents the intercept and k represents the number of operational parameters.

To predict this time dependent pit depth growth for the categories of pitting corrosion considered in this research, a Monte Carlo simulation experiment was carried out using the maximum pit depths and operational parameters of each category of the pitting corrosion as the boundary condition. Poisson Square Wave Process (PSWP) was utilized for estimating the variability of time, maximum pit depth and operational parameters. The PSWP was adopted for this study because the technique can describe the damage model of stochastic processes that follow random failure pattern. Since the internal pit depth growth of pipelines over time is a stochastic process that follows a random walk technique (Ossai 2013), the PSWP was suitable for the modelling. This technique has also been utilized by different researchers for predicting corrosion defect depth growth of pipelines (Bazan & Beck 2013, Zhang & Zhou 2013). Although any positive random distribution can be used for realizing the pulse heights in a Poisson square wave process (Bazan & Beck 2013), Bazan and Beck (2013) and Pandey, Yuan & van Noortwijk (2009) used gamma distribution whilst Zheng and Zhou (2013) used Gumbel distribution, however, lognormal distribution is used in this work because it is the best fit distribution of the field data. With the knowledge of the prediction parameters - Poisson arrival rate (λ) and the growth parameters of the lognormal distribution mean (μ_{log}) and standard

deviation (δ_{log}), the random pit depth growth over time was modelled. In this research, the magnitude and duration of the generated pulses from Poisson square wave process are random variables with the magnitude following a lognormal distribution and the duration of individual pulses being independently exponentially distributed. The use of Poisson Square Wave Process (PSWP) to construct the stochastic process of maximum pit depth growth with time is exemplified in Figure 3.5 whereas the relationship between predicted maximum pit depth and time of generation of the wave pulses is shown in Equation (3.14). The total number of pulses of the maximum pit depth is represented by m . A schematic of the simulation framework adopted for this study is shown in Figure 3.6.

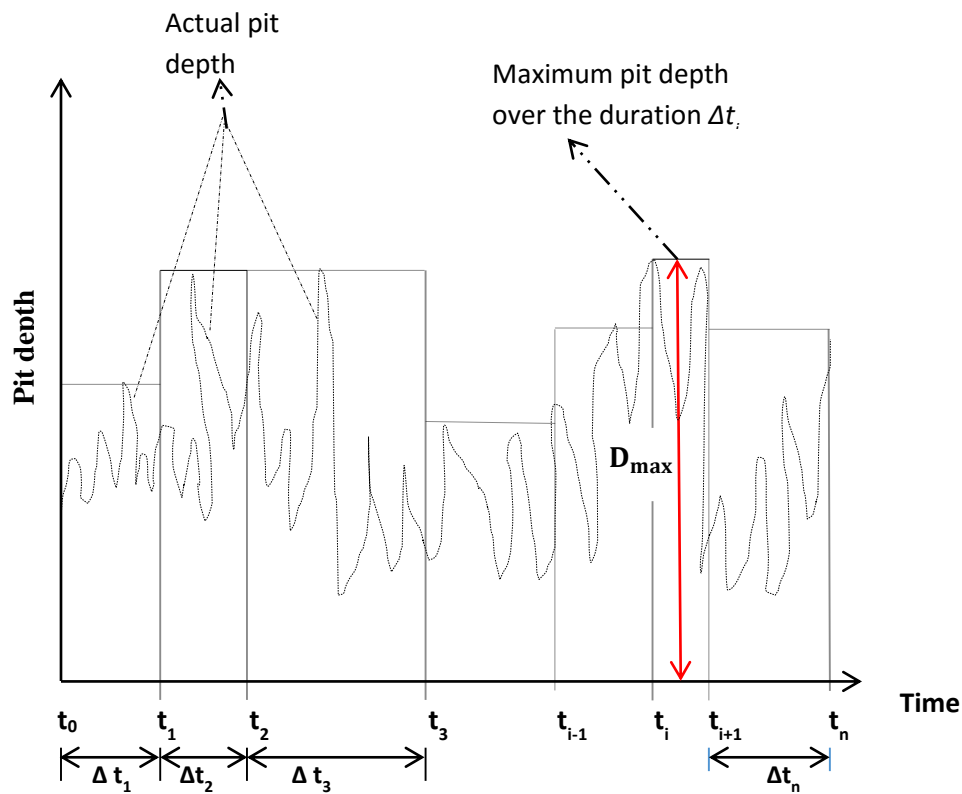


Figure 3.5: Poisson Square wave process for modelling maximum pit depth growth with time

$$D_{max}(t_{i+1}) = \{D_{max}(t_i) + D_{max}(t_{i+1} - t_i)\}, \quad \text{for } i = 0, 1, \dots, m \quad (3.14)$$

Table 3.5: Results of regression analysis by pit depth category

Variable		Pit depth Category				
		Low	Moderate	High	Severe	All data
θ	Coefficient	3.87E-03	1.55E-03	-4.29E-04	-2.72E-03	-6.90E-04
	Standard Error	2.18E-03	3.00E-03	8.52E-04	1.26E-03	8.75E-04
P_{CO_2}	Coefficient	-4.87E-01	2.04E-01	-5.47E-02	1.45E-01	4.05E-03
	Standard Error	2.56E-01	2.30E-01	1.28E-01	1.33E-01	1.19E-01
V	Coefficient	2.69E-01	-1.80E-01	3.55E-02	6.11E-02	-4.11E-02
	Standard Error	2.09E-01	1.27E-01	2.44E-02	3.61E-02	3.81E-02
P_H	Coefficient	-2.04E-02	1.56E-02	-2.74E-03	1.18E-02	1.26E-02
	Standard Error	1.70E-02	2.13E-02	1.56E-02	3.52E-02	1.88E-02
S_{O_4}	Coefficient	7.16E-04	-9.28E-04	-3.94E-04	3.67E-05	4.26E-04
	Standard Error	5.54E-04	5.91E-04	4.76E-04	1.11E-03	5.99E-04
C_L	Coefficient	2.35E-06	2.77E-06	-3.51E-06	6.69E-06	2.52E-06
	Standard Error	7.75E-06	1.20E-05	4.58E-06	8.64E-06	5.59E-06
W_C	Coefficient	1.79E-02	3.82E-02	-1.53E-02	-2.27E-02	1.98E-02
	Standard Error	4.80E-02	4.10E-02	3.74E-02	6.85E-02	3.65E-02
ρ		0.771	0.7408	0.7879	0.8657	0.7639
ξ		0.1200	0.2687	0.3887	0.6508	0.695

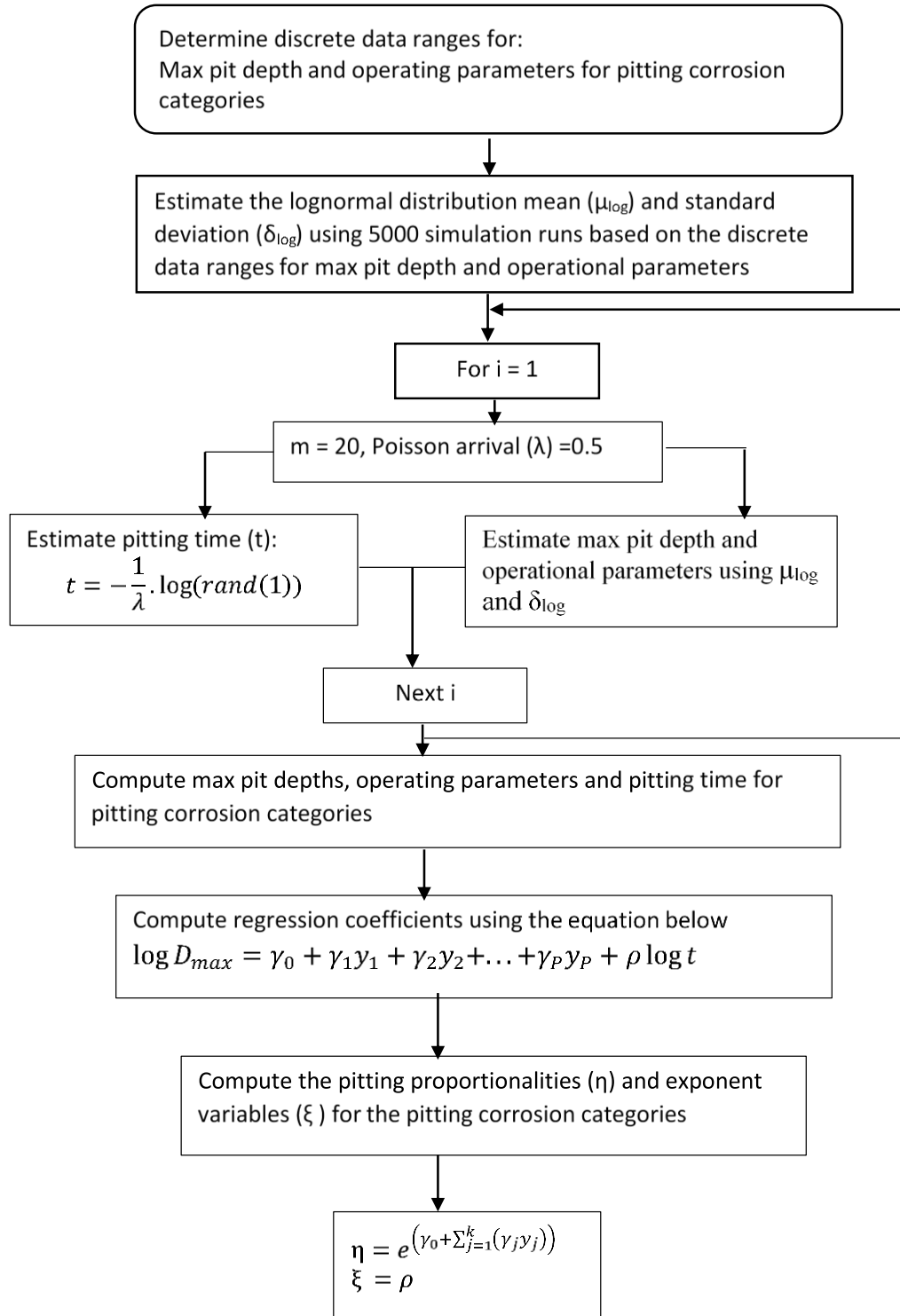


Figure 3.6: Framework for Monte Carlo simulation of pitting time of pit depth growth

The predicted maximum pit depth was compared with the field data and the hypothesis that Monte Carlo simulated pit depth is similar to those obtained in the field was tested with a two-sample Kolmogorov Smirnov goodness of fit test and the result showed that a p-value of 0.995 is enough to accept the hypothesis that both Monte Carlo simulated and field observed distributions are similar. Figure 3.7 shows the lognormal distribution comparison of the field measured maximum pit depth and those predicted with Monte Carlo simulation.

Table 3.5 shows the result of the time variation of the pit depth growth and the proportionality and exponent variables for all the categories of pitting corrosion and all data category. Figure 3.8 showed the evolution of maximum pit depth growth predicted from Monte Carlo simulation. As expected, the severity of corrosion rates is shown in descending order according to the listing of the corrosion categories - severe, high, moderate and low. This result indicated that the more the corrosion severity, the faster the loss of the pipe-wall thickness and eventual failure of the pipeline. Hence, more cost is directed towards pipelines integrity management via application of corrosion inhibitors (McMahon & Paisley 1997) and increased rate of monitoring (HSE 2001).

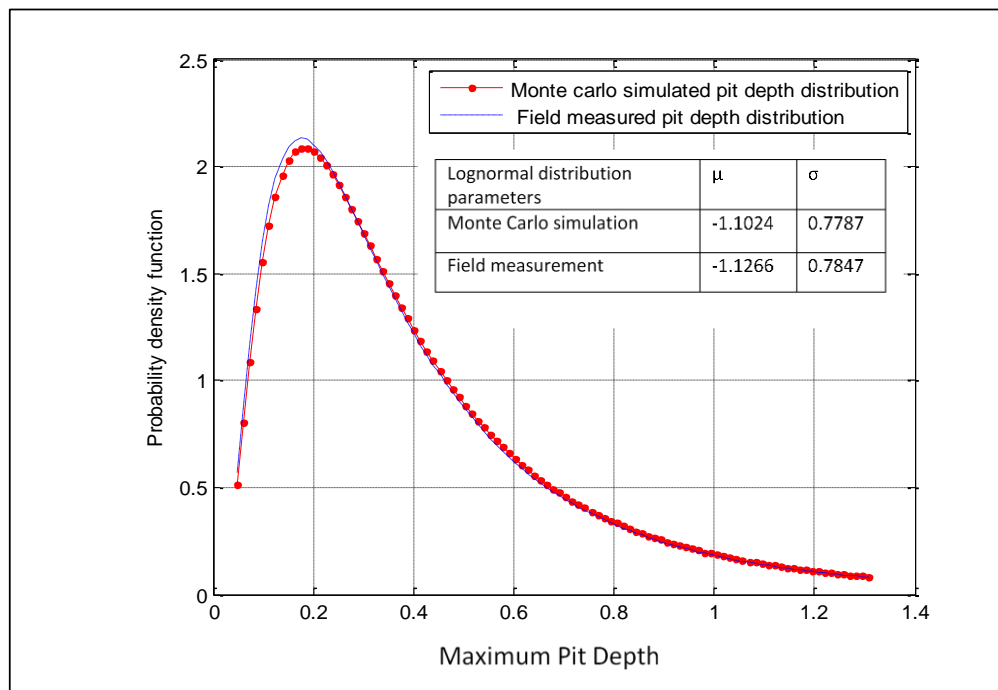


Figure 3.7: Comparison of maximum pit depth distribution for field and Monte Carlo simulated data

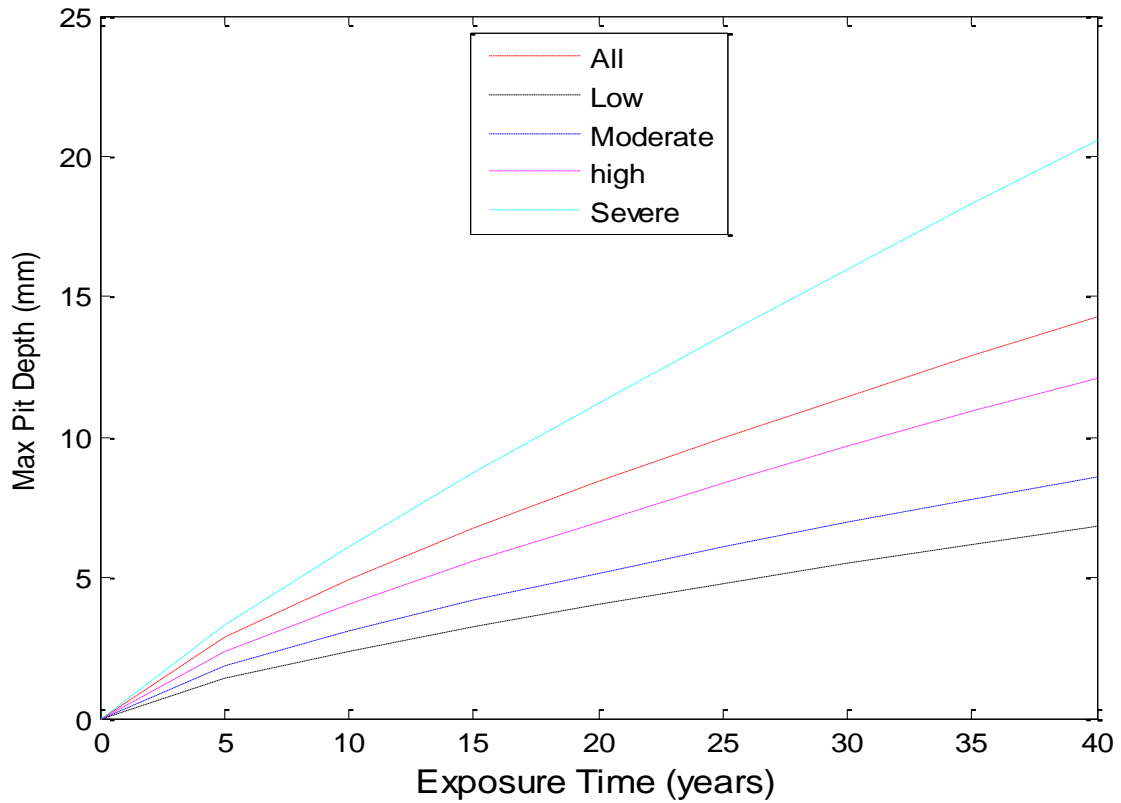


Figure 3.8: Maximum pit depth growth with exposure time for different pitting corrosion categories

3.6 Predictive model validation

The proposed model was tested on API X52 onshore oil and gas transmission pipelines inspected with Ultrasonic Thickness Measurement (UTM) technique. These pipelines, which transported oil and gas from oil fields to the flow stations in Niger Delta region of Nigeria have nominal external diameter of 114 mm, internal diameter of 97.18 mm and length in the range 2300 m to 5750 m. Table 3.6 shows the characteristics of the fluid in the pipelines used to test the proposed model in this research.

Table 3 6: Condition of pipelines used to test the proposed model

S/N	Max Pit depth (mm)	Temp (°C)	P _{CO2} (MPa)	V(m/s)	pH	SO ₄ ²⁻ (mg/l)	CL ⁻ (mg/l)	W _c (%)
Low Pitting								
Pipeline #1	0.013~0.083	36	0.02	0.08	6.21	45	4431	3%
Pipeline#2	0.05~0.108	36	0.14	0.23	8.09	25	211	3%
Pipeline#3	0.033~0.111	26	0.01	0.15	6.63	70	2038	40%
Moderate Pitting								
Pipeline #1	0.01~0.143	21	0.05	0.11	7.45	32	1418	6%
Pipeline#2	0.037~0.154	31	0.16	0.2	6.78	67	1595	26%
Pipeline#3	0.073~0.158	28	0.06	0.07	8.14	6	1295	38%
High Pitting								
Pipeline #1	0.123~0.236	27	0.23	0.07	8.03	69	7090	4%
Pipeline#2	0.098~0.247	65	0.31	0.13	8.19	65	927.8	24%
Pipeline#3	0.018~0.255	31	0.1	0.06	8.1	39	404.6	24%
Severe Pitting								
Pipeline #1	0.151~0.427	38	0.15	0.11	7.21	34	4984.5	7%
Pipeline#2	0.059~0.448	62	0.27	0.15	8.14	29	4742.8	87%
Pipeline#3	0.22~0.458	25	0.04	0.21	8.25	55	7317.1	3%

The prediction model for the categories of pitting corrosion which was developed from the data obtained from Monte Carlo simulation described previous (see Equation (3.15)) was used to estimate the percentage of pipe-wall thickness loss over a ten-year period for the categories of pitting corrosion. The results were compared with the field data shown in Table 3.6. The result of the comparison of the predicted and actual percentage pipe-wall thickness for these pitting corrosion categories is shown in Figures 3.9 – 3.12.

$$D_{\max}(t) = \begin{cases} 0.12t^{0.771} & \text{for low} \\ 0.2687t^{0.7408} & \text{for moderate} \\ 0.3887t^{0.7879} & \text{for high} \\ 0.6508t^{0.8657} & \text{for severe} \\ 0.695t^{0.7639} & \text{for all data} \end{cases} \quad (3.15)$$

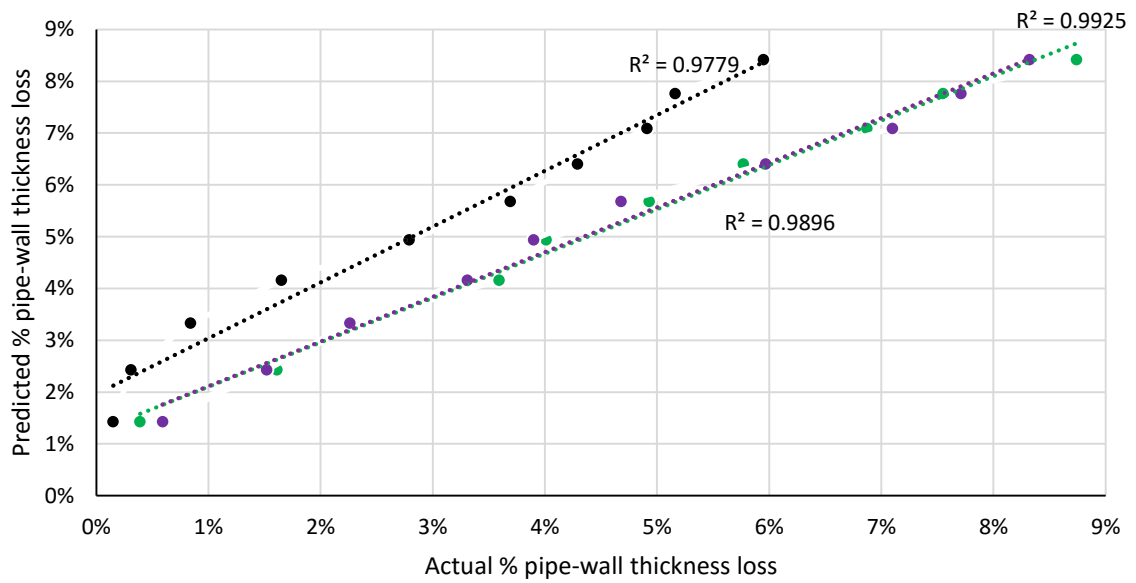


Figure 3.9: Comparison of the pipe-wall thickness loss of the predicted model and field data for low pitting corrosion category.

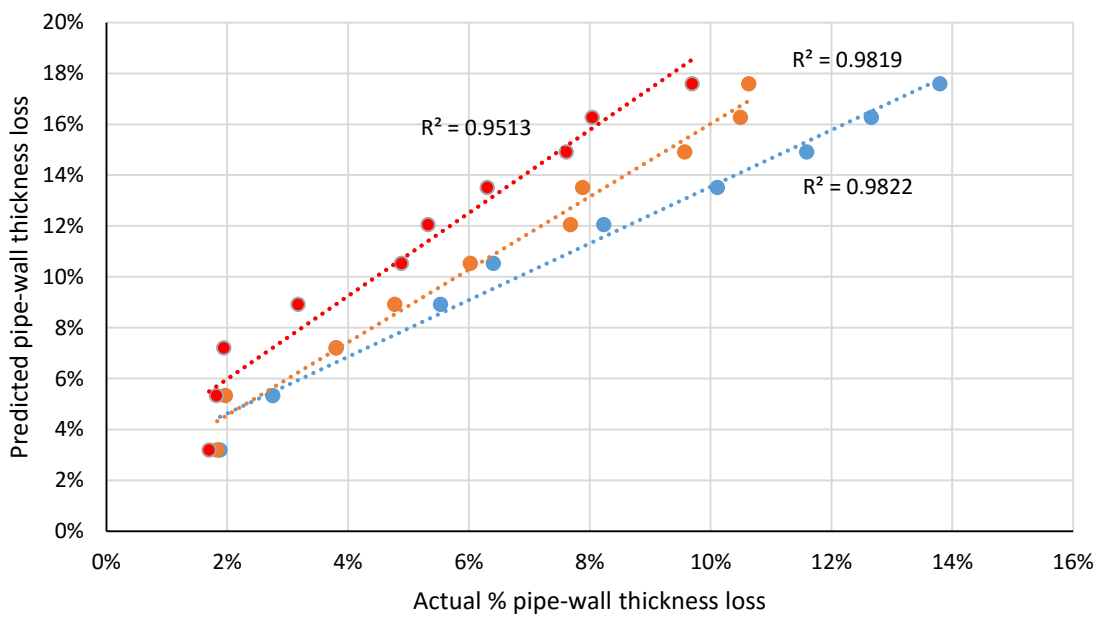


Figure 3.10: Comparison of the pipe-wall thickness loss of the predicted model and field data for moderate pitting corrosion category

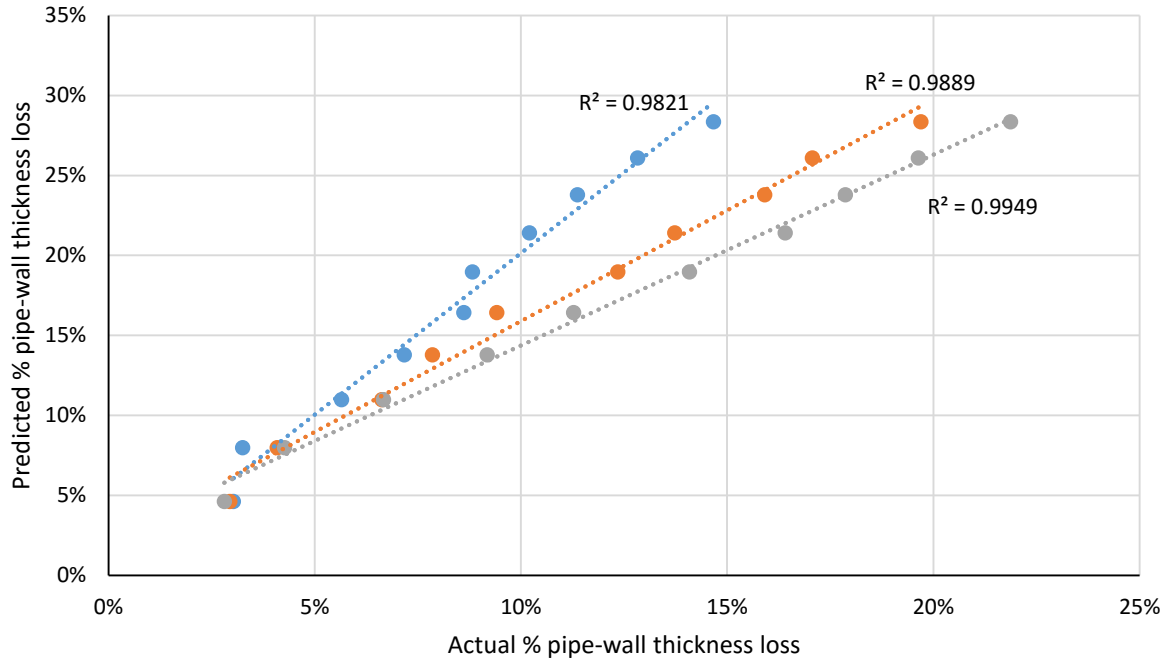


Figure 3.11: Comparison of the pipe-wall thickness loss of the predicted model and field data for high pitting corrosion category.

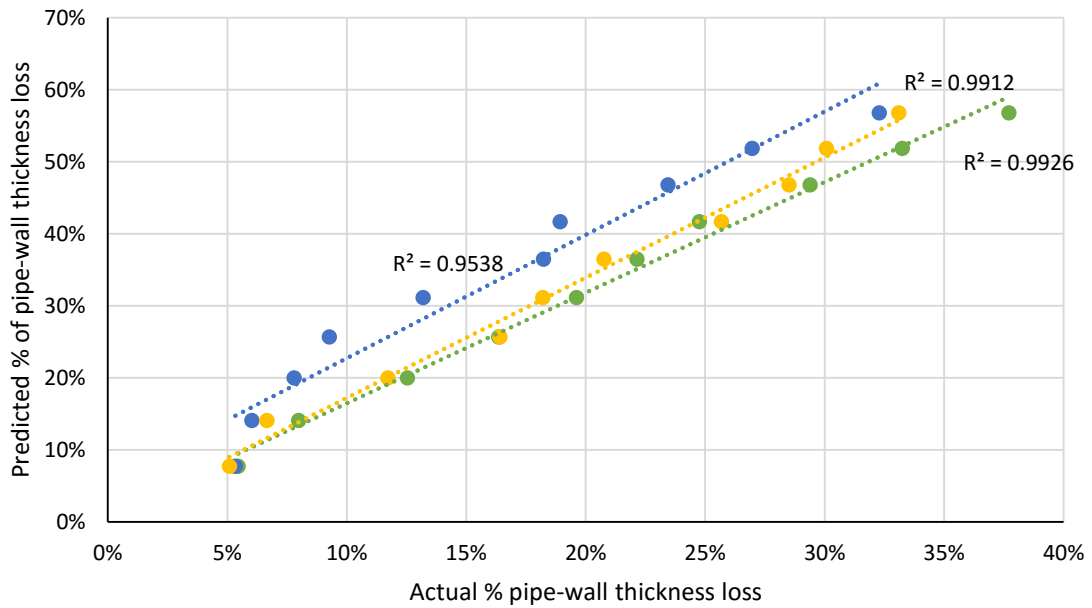


Figure 3.12: Comparison of the pipe-wall thickness loss of the predicted model and field data for severe pitting corrosion category.

These figures show that the predicted model agrees well with the field data. To establish the variation of the maximum pit depth from the field measured data (ω)

and the predicted one from the model (ℓ), Root Mean Square Percentage Error (RMSPE) shown in Equation (3.16) was used.

$$RMSPE = \sqrt{\frac{\sum_{i=1}^h \left(\frac{\omega_i - \ell_i}{\omega_i}\right)^2}{h}} \quad (3.16)$$

where h represents the number of years of measured data.

Based on the RMSPE values calculation, low pitting corrosion category shows percentage error of 0.52 ~ 3.54 whereas moderate, high and severe pitting categories show error percentages in the range 0.59~7.26, 0.51~1.03 and 0.60~1.20 respectively. This result is an indication of the level of accuracy of the prediction model for pipelines with characteristics that fall within the range of field data used for this study.

3.7 Conclusions

This work modelled internal pitting corrosion using operational parameters that included CO₂ partial pressure, temperature, flow rate, pH, sulphate ion concentration, chloride iron concentration and water cut. To estimate the time lapse for low, moderate, high and severe pitting corrosion, a Monte Carlo simulation was carried out based on Poisson square wave process using the field measured maximum pit depths and operational parameters as the boundary conditions. The model was predicted for pit depth growth of low, moderate, high and severe pitting corrosion categories using field data from sixty oil fields. The model was validated with three field data for each of the pitting corrosion categories and the results agreed well. Although the predicted model shows a good agreement with field data, it should be noted that for fields with a wide range of pH outside the range considered in this work (6.21~8.6), the result may vary considerably. This limitation makes the model predicted in this work not to be most suitable for pipelines operating in more acidic condition with pH lower than 6.21.

It is therefore pertinent to note that a future study in this area will include the influence of sulphate Reducing Bacteria (SRB), which is one of the major

contributors to internal pitting corrosion of oil and gas pipelines. Although this work did not consider H₂S because of the trace quantity in the fields, the study of fields with significant quantity of H₂S in subsequent studies will be vital for more understanding of the growth trend of maximum pit depths in pipelines whereas the consideration of fields with pH outside the studied range will be vital.

References

- ASME, 2009, Manual for determining the remaining strength of corroded pipelines. American Society of Mechanical Engineers, B31G, New York.
- BAZÁN, F. A. V. & BECK, A. T. 2013. Stochastic process corrosion growth models for pipeline reliability. *Corrosion Science*, 74, 50-58.
- BIOMORGI, J., HERNÁNDEZ, S., MARÍN, J., RODRIGUEZ, E., LARA, M. & VILORIA, A. 2012. Internal corrosion studies in hydrocarbons production pipelines located at Venezuelan Northeastern. *Chemical Engineering Research and Design*, 90, 1159-1167.
- CAPP, Best Management Practices: Mitigation of internal corrosion in oil effluent pipeline systems. Calgary Canada, 2009. Available from: <http://www.capp.ca/getdoc.aspx?DocId=155641&DT=PDF>. [19/6/15].
- CHAVES, I. A. & MELCHERS, R. E. 2011. Pitting corrosion in pipeline steel welds zones, *Corrosion Science* 53, 4026-4032
- CHOKSHI, K., SUN, W. & NESIC, S. 2005. Iron carbonate scale growth and the effect of inhibition in CO₂ corrosion of mild steel. *Corrosion/2005*, paper no 05285.
- CHOI, H. J. & AL-AJWAD, H. 2008. Flow-dependency of sweet and sour corrosion of carbon steel downhole production tubing in Khuff-gas wells. *Corrosion* 2008, 2008. NACE International.
- CHOI, H.S. & BOMBA, J.G. 2003. Acceptance criteria of defects in undersea pipeline using internal inspection. *Ocean engineering*, 30, 1613–1624.
- DEMOZ, A., PAPA VINASAM, S., OMOTOSO, O., MICHAELIAN, K., & REVIE, R. W. 2009. Effect of field operational variables on internal pitting corrosion of oil and gas pipelines, *Corrosion*, 65(11), 741-747.
- DET NORSKE VERITAS (DNV), Recommended Practice - RP-F101 Corroded Pipelines, 2010.

- FAJARDO, V., CANTO, C., BROWN, B. & NESIC, S. 2007. Effect of organic acids in CO₂ corrosion. In proceedings of the NACE international conference and exposition Corrosion/2007, paper no. 07319,
- HASAN, S., KHAN, F. & KENNY, S. 2012. Probability assessment of burst limit state due to internal corrosion. International Journal of Pressure Vessels and Piping, 89, 48-58.
- HERNANDEZ-RODRIGUEZ, M., MARTINEZ-DELGADO, D., GONZALEZ, R., UNZUETA, A. P., MERCADO-SOLIS, R. & RODRIGUEZ, J. 2007. Corrosive wear failure analysis in a natural gas pipeline. Wear, 263, 567-571.
- HSE, Review of corrosion management for offshore oil and gas processing, HSE offshore technology report 2001/044, 2001, Available from: <http://www.hse.gov.uk/research/otopdf/2001/oto01044.pdf>. [22/12/14].
- HU, X., ALZAWAI, K., GNANA VELU, A., NEVILLE, A., WANG, C., CROSSLAND, A. & MARTIN, J. 2011a. Assessing the effect of corrosion inhibitor on erosion–corrosion of API-5L-X65 in multi-phase jet impingement conditions, Wear 271(9-10), 1432-1437.
- HU, X., BARKER, R. & NEVILLE, A. & GNANA VELU, A. 2011b. Case study on erosion-corrosion degradation of pipework located on an offshore oil and gas facility, Wear 271, 1295– 1301.
- MCMAHON, A. J. 1991. The mechanism of action of an oleic imidazoline based corrosion inhibitor for oilfield use, Colloids and Surfaces 59(0), 187-208.
- MCMAHON, A. J. & PAISLEY, D. M. E. 1997. Corrosion prediction modelling - A guide to the use of corrosion prediction models for risk assessment in oil and gas production and transportation facilities, Report No. ESR.96.ER.066, BP International, Sunbury, 1997
- MOHD, M. H. & PAIK, J. K. 2013. Investigation of the corrosion progress characteristics of offshore subsea oil well tubes. Corrosion Science, 67, 130-141.
- NACE 2005, NACE Standard RP0775, Preparation, installation, analysis, and interpretation of coupons in oilfield operations, 2005, Houston, TX
- NEŠIĆ, S. 2012. Effects of Multiphase Flow on Internal CO₂ Corrosion of Mild Steel Pipelines, Energy & Fuels 26 (7), 4098-4111.

- NEŠIĆ, S. 2007. Key issues related to modelling of internal corrosion of oil and gas pipelines – A review, *Corrosion Science*, 49, 4308-38.
- NEŠIĆ, S., CAI, J. & LEE, K.-L. J. 2005. A multiphase flow and internal corrosion prediction model for mild steel pipeline. Paper presented NACE CORROSION/05, Dallas, TX, paper, 5556.
- OSSAI, C. I. 2012. Advances in asset management techniques: an overview of corrosion mechanisms and mitigation strategies for oil and gas pipelines. *ISRN Corrosion*, 2012.
- OSSAI, C. I. 2013. Pipeline Corrosion Prediction and Reliability Analysis: A systematic approach with Monte Carlo simulation and degradation models. *International Journal of Scientific & Technology Research*, 2.
- OWEN, R., CHAUHAN, V., PIPET, D. & Morgan, G. 2003. Assessment of corrosion damage in pipelines with low toughness, In 14th Biennial joint technical meeting on pipeline research, Berlin.
- PAIK, J. K. & KIM, D. K. 2012. Advanced method for the development of an empirical model to predict time-dependent corrosion wastage, *Corrosion Science*, 63, 51-58.
- PANDEY, M., YUAN, X.-X. & VAN NOORTWIJK, J. 2009. The influence of temporal uncertainty of deterioration on life-cycle management of structures. *Structure and Infrastructure Engineering*, 5, 145-156.
- PAPAVINASAM, S. 2014. Modelling Internal Corrosion, In: *Corrosion control in the oil and gas industry*, edited by Sankara Papavinasam, Gulf Professional Publishing, Boston, USA (chapter 6).
- PAPAVINASAM, S., DOIRON, A. & REVIE, R. W. 2010. Model to predict internal pitting corrosion of oil and gas pipelines. *Corrosion*, 66, 035006-035006-11.
- PAPAVINASAM, S., DOIRON, A., PANNEERSELVAM, T. & Revie, R. W. 2007. Effect of hydrocarbons on the internal corrosion of oil and gas pipelines. *Corrosion*, 63(7),704-712.
- RACE, J. M. 2010. Management of corrosion of onshore pipelines, in: Editor-in-Chief: Tony J.A. Richardson, Editor(s)-in-Chief, Shreir's *Corrosion*, Elsevier, Oxford, ISBN 9780444527875, <http://dx.doi.org/10.1016/B978-044452787-5.00169-4>, 2010, (section 4.42).

- RENPU, W. 2011. Oil and gas well corrosion and corrosion prevention, in: advanced well completion engineering (Third Edition), Gulf professional publishing, Boston, ISBN 9780123858689, <http://dx.doi.org/10.1016/B978-0-12-385868-9.00018-X>, 2011 (Chapter 11).
- SONG, F. M. 2010. A comprehensive model for predicting CO₂ corrosion rate in oil and gas production and transportation systems. *Electrochimica Acta*, 55, 689-700.
- SONG, F., MCFARLAND, J., BICHON, B., HUYSE, L., KING, F., PERRY, L., & PIAZZA, M. 2011. New model predicts internal corrosion likelihood. *Oil & Gas Journal*, 109, 116-125.
- WANG, S., GEORGE, K. & NESIC, S. 2004. High pressure CO₂ corrosion electrochemistry and the effect of acetic acid, *Corrosion/2004*, paper no. 04375.
- WANG, B., DU, M., ZHANG, J. & GAO, C. J. 2011. Electrochemical and surface analysis studies on corrosion inhibition of Q235 steel by imidazoline derivative against CO₂ corrosion. *Corrosion Science*, 53, 353-361.
- XIAN, Y. & S. NESIC, S. 2005. A stochastic prediction model of localized CO₂ corrosion. Paper presented at NACE CORROSION/05, Dallas, TX, paper, 05057
- ZHANG, L., ZHONG, W., YANG, J., GU, T., XIAO, X. & LU, M. 2011. Effects of temperature and partial pressure on H₂S/CO₂ corrosion of pipeline steel in sour conditions. *CORROSION 2011*, 13-17 March, Houston, Texas, USA, paper 11079
- ZHANG, R., GOPAL, M. & JEPSON, W. 1997. Development of a mechanistic model for predicting corrosion rate in multiphase oil/water/gas flows. NACE International, Houston, TX (United States).
- ZHANG, S. & ZHOU, W. 2013. System reliability of corroding pipelines considering stochastic process-based models for defect growth and internal pressure. *International Journal of Pressure Vessels and Piping*, 111, 120-130.

Chapter 4 - Estimation of internal pit depth growth and reliability of aged oil and gas pipelines - A Monte Carlo simulation approach

4.0 Introduction

Corrosion estimate is fundamental to the health monitoring of pipelines since there is a tendency of pipelines decreasing in reliability with increase in age of operation especially when there is corrosion defect (Melchers 2008, Caleyó *et al.* 2009, Ossai 2013). This is because, as the corrosion wastage of the pipelines increase, the residual strength reduces due to the reducing pipe-wall thickness (ASME 2009, Owen *et al.* 2003) hence, increasing the likelihood of failure over time. Corrosion can also result in unscheduled downtime especially for pitting corrosion, crevice corrosion, stress corrosion cracking and fatigue corrosion since they occur without outward signs on the facilities (Engelhardt & Macdonald 1998). Reliability is a measure of the ability of an asset to perform its intended function within a stipulated time frame. The reliability of a pipeline is dependent on the corrosion wastage over time, hence, corrosion probability distribution is a vital tool for developing reliability and risk-based inspection models (Caleyó *et al.* 2009). Since future pit depth distribution can be estimated from previous pit depth distribution using Monte Carlo simulation (due to its ability to generate future data based on random walk principles (Soares & Garbatov 1999), it therefore follows that, proper application of Monte Carlo simulation technique is necessary for estimating the reliability of ageing pipelines.

Corrosion growth models are vital for the development of pipeline integrity management programs, which can include inspection, mitigation and repair activities (Valazquez *et al.* 2009, Valor *et al.* 2010, Zhang, Zhou & Qin 2013, Valor *et al.* 2013). Hence, time-dependent reliability of corroded high pressure offshore pipelines was established by researchers (Zhang & Zhou 2013) who utilized homogenous gamma process based corrosion growth model to determine the expected future corrosion wastage of the pipelines. These authors used the internal pressure, which was modelled with Poison Square Wave Model (PSWM) to calculate the corrosion growth rate and established the time of pipeline failure with respect to small leaks, large leaks and ruptures (Zhang & Zhou 2013). Again, the knowledge of pit depth transition probability was used by some researchers to develop a reliability model for managing

pitting corrosion of oil and gas pipelines (Rodriguez III & Provan 1989). This model will make it possible to design a mitigation program, which will enhance pipeline lifecycle through maintenance, inspection and repairs. Similarly, the use of historic data for calculating the reliability of corroded non-piggable upstream pipelines exposed to corrosion by statistical analyses was done by Valor *et al.* (2014). These researchers determined the corrosion distribution trend of the pit depths and correlated them to the failure pressure at a future time.

Different researchers have shown that pit depth growth process of pipelines is a time-dependent stochastic damage process that has exponential (Sheikh, Boah & Hansen 1990, Mohd & Paik 2013), logarithmic (Sheikh, Boah & Hansen 1990), lognormal (Bazan & Beck 2013, Mohd & Paik 2013), gamma (Katano *et al* 2003), Weibull (Katano *et al* 2003), normal (Sheikh, Boah & Hansen 1990, Mohd & Paik 2013) and generalized extreme value (Velazquez *et al.* 2009) growth patterns. However, long time exposure of pit depths has been shown to follow Fretchet distribution (Melchers 2008, Caleyó *et al.* 2009, Melchers 2010). Furthermore, pit depth growth can be determined using limited data via extreme value analysis, which depends on the maximum pit depth at an exposure time for extrapolating future pit depth distribution over a long time exposure (Laycock, Cottis & Scarf 1990).

Researchers such as Mohd & Paik (2013) investigated the relationship between internal pit depth growth and age of offshore pipelines statistically and showed the correlation between age of pipelines and Weibull scale and shape parameters. Although the work did not show the reliability of these pipelines at various ages, it is a good outlook for the progression of pit depth with time. Other researchers that have been pertinent about pit depth growth includes Alamilla & Sosa (2008) that used mathematical modelling to describe the propagation of cracks resulting from pitting corrosion defects. The authors showed that probability density function and propagation function of the pit depths are vital for characterizing the evolution of pit depth with time. Chookah *et al.* (2011) on the other hand utilized probabilistic physics-of-failure based mechanistic model to predict the growth trend of cracks on a pipeline associated with pitting corrosion. This work considered the amplitude and frequency of the mechanical stress initiated by the internal pressure and chemical corrosive species inside the pipeline in estimating the fatigue crack

growth. The authors used a Monte Carlo simulation approach, which incorporated the experimental findings of the physical parameters - applied stress, frequency and the concentration of the corrosive chemical agents as a function of the corrosion current in the modelling and subsequently in calculating the reliability of the pipelines. Soares & Garbatov (1999) on their part used a non-linear corrosion model based on exponential corrosion wastage to determine the reliability of a plate by quantifying the collapse strength against the compressive loading in the presence of corrosion. Hu *et al.* (2014) also predicted pipeline reliability using Monte Carlo simulation approach by determining the crack growth with time as a function of operating pressure, corrosion electric current and pipe wall thickness. Again, Bazan & Beck (2013) used Poisson Square Wave Model (PSWM) to determine the proportionality constant of pitting corrosion defect in a bid to establish a continuous growth of the corrosion defect with time. The authors concluded that a random linear growth model determined with PSWM conservatively predicted the long run corrosion growth of the selected field data but may not be optimal for the inspection intervals. Other authors such as Zhang and Zhou (2014) incorporated a second order polynomial dynamic linear model with Bayesian updating in a Monte Carlo simulation in order to estimate corrosion defect growth whereas Hasan, Khan & Kenny (2012) calculated failure probability of pipelines by characterizing corrosion defect based on geometry of the longitudinal section of the corrosion, growth rate and remaining mechanical hoop strength capacity.

The aim of this research is to complement the works reviewed above by determining the statistical characteristics of field data comprising of maximum pit depths and operating parameters – temperature, flow rate, pH, CO₂ partial pressure, sulphate ion concentration, chloride ion concentration, water cut and wall shear stress of onshore pipelines. This was done in a bid to establish the relationship between the maximum pit depth and the operating parameters whilst investing the internal maximum pit depth growth of the pipelines over time using Monte Carlo simulation. The maximum pit depths of the pipelines were classified as low, moderate, high and severe whereas the time lapse for pit depth growth was determined using PSWM, which estimated pitting time based on independent arrival rate of a Homogenous Poisson Process (HPP). The statistical best fit of the maximum

pit depth and operating parameters were used as input for the Monte Carlo simulation whereas the reliability of the pipeline as time elapsed were calculated using Weibull probability based on different distributions - Gamma, lognormal, exponential, generalized extreme value, Weibull and extreme value. A Magnetic Flux Leakage (MFL) in-line-inspection (ILI) data of an API X52 pipeline were used to test the proposed model.

The limitation of this research is the inability to consider the impacts of H₂S and O₂ in the pitting corrosion of the studied pipelines. This is because the H₂S concentrations of the studied fields are very small and hence will not enhance the pitting corrosion of the studied pipelines, which were predominantly under the influence of sweet corrosion. Seeing that H₂S concentration is minimal and the corrosion mechanism was dominated by sweet corrosion, it was not necessary to consider the effect of O₂ in the pitting process because O₂ have been shown to significantly enhance pitting corrosion in the presence of H₂S (Shoesmith *et al.* 1980). Furthermore, research has shown that limited concentration of H₂S and O₂ generally have small impact on the corrosion rates of carbon steel (Smith & Craig 2008) whereas H₂S results in pitting corrosion when the concentration is more than 100ppm (Dawson, Bruce & John 2001).

4.1 Experimental procedure

4.1.1 Field data acquisition

Internal pitting corrosion data of pipelines used for transmission of multiphase fluid from oil fields in Niger Delta region of Nigeria and the operating parameters of the pipelines – temperature, pH, CO₂ partial pressure, production rate, sulphate ion concentration, chloride ion concentration, water cut and operating pressure were obtained from the company's database. A total of six hundred sampled data of the maximum pit depths of the pipelines measured over a period of ten years were used for this study. The maximum pit depths were determined using pulse-echo Ultrasonic Thickness Measurement (UTM) technique whereas the operating parameters were measured as part of the routine quality assurance procedure in the organization. The linear flow rate of the fluid and the wall shear stress were determined using the production rate and operating pressures inside the pipelines

respectively. The maximum pit depths were categorized into four groups using NACE RP0775 standard (NACE 2005) shown in Table 4.1.

Table 4.1: Qualitative categorization of carbon steel corrosion rate for oil production systems.

Pitting categories	Maximum Pitting Rate (mmyr ⁻¹)
Low	<0.13
Moderate	0.13-0.20
High	0.21-0.38
Severe	>0.38

Based on this standard, a total of 80, 70, 150 and 300 samples of the maximum pit depths were classified as low, moderate, high and severe pitting rates respectively whilst a generic category, which involves all the collected data were referred to as all-data.

4.1.2 Maximum pit depth distribution

To estimate the best fit distribution for the maximum pit depths for the pitting corrosion and all-data categories, different probability density functions – Weibull, Gamma, generalized extreme value, extreme value, exponential and inverse Gaussian were tested on the data. The graphs of the statistical fitting of some of the distributions were plotted using MARLAB version R2014a whereas Maximum Likelihood Estimate (MLE) and Akaika Information Criterion (A_{IC}) were utilized to selected the best fit model by using the relationship shown in Equation (4.1) below.

$$A_{IC} = 2K - 2\text{Log}(L) \quad (4.1)$$

where K is the number of parameters and L is the maximum value of the likelihood function.

4.1.3 Regression analysis

To establish the relationship between the maximum pit depths and the operating parameters, a multivariate regression analysis was conducted using the average maximum pit depths of the pipelines and the average operating parameters for the

ten years collected data. The maximum pit depths can be expressed as function of the operating parameters according to Equation (4.2).

$$D_{max} = f(\theta, P, W, \tau, C, S, p_H, V) \quad (4.2)$$

where θ , P , W , τ , C , S , p_H and V represents temperature, CO₂ partial pressure (MPa), water cut (%), wall shear stress (Pa), chloride ion concentration (mg/l), sulphate ion concentration (mg/l), pH and flow rate (m/s) respectively. By determining the normal and slope coefficients of the maximum pit depths and the operating parameters, Equation (4.2) can be resolved using a matrix form shown in Equation (4.3).

$$\begin{bmatrix} n_v & \sum \theta & \sum P & \sum W & \sum \tau & \sum C & \sum S & \sum p_H & \sum V \\ \sum \theta & \sum \theta^2 & \sum \theta P & \sum \theta W & \sum \theta \tau & \sum \theta C & \sum \theta S & \sum \theta p_H & \sum \theta V \\ \sum P & \sum \theta P & \sum P^2 & \sum PW & \sum P\tau & \sum PC & \sum PS & \sum Pp_H & \sum PV \\ \sum W & \sum W\theta & \sum WP & \sum W^2 & \sum W\tau & \sum WC & \sum WS & \sum Wp_H & \sum WV \\ \sum \tau & \sum \tau\theta & \sum \tau P & \sum \tau W & \sum \tau^2 & \sum \tau C & \sum \tau S & \sum \tau p_H & \sum \tau V \\ \sum C & \sum C\theta & \sum CP & \sum CW & \sum C\tau & \sum C^2 & \sum CS & \sum Cp_H & \sum CV \\ \sum S & \sum S\theta & \sum SP & \sum SW & \sum S\tau & \sum SC & \sum S^2 & \sum Sp_H & \sum SV \\ \sum p_H & \sum p_H\theta & \sum p_HP & \sum p_HW & \sum p_H\tau & \sum p_HC & \sum p_HS & \sum p_H^2 & \sum p_HV \\ \sum V & \sum V\theta & \sum VP & \sum VW & \sum V\tau & \sum VC & \sum VS & \sum Vp_H & \sum V^2 \end{bmatrix} * \begin{bmatrix} \alpha \\ \beta_\theta \\ \beta_P \\ \beta_W \\ \beta_\tau \\ \beta_C \\ \beta_S \\ \beta_{p_H} \\ \beta_V \end{bmatrix} = \begin{bmatrix} \sum D_{max} \\ \sum D_{max} \theta \\ \sum D_{max} P \\ \sum D_{max} W \\ \sum D_{max} \tau \\ \sum D_{max} C \\ \sum D_{max} S \\ \sum D_{max} p_H \\ \sum D_{max} V \end{bmatrix} \quad (4.3)$$

where n_v , α , β_θ , β_P , β_W , β_τ , β_C , β_S , β_{p_H} , β_V represents the number of variables, intercept coefficient, temperature coefficient, CO₂ partial pressure coefficient, water cut coefficient, wall shear stress coefficient, Chloride ion concentration coefficient,

sulphate ion concentration coefficient, pH coefficient and flow rate coefficient respectively.

The summary of the maximum pit depths and the operating parameters is shown in Table 4.2.

Table 4.2: Description of the field measured data.

Descript. Variable	ED (yrs.)	D _{max} (mm/yr)	θ (°C)	P (MPa)	V (m/s)	P _H	W (%)	S (mg/l)	C (mg/l)	τ (Pa)	No of samples
Low pitting rate											
Min	10	0.032	24	0.01	0.07	6.21	1	2	117	8	80
Max		0.078	40	0.14	0.23	8.18	88	70	4431	45.9	
Mean		0.06	30.6	0.055	0.133	7.58	35	30.13	1291.34	19.4	
SD		0.017	5.9	0.04	0.049	0.75	38	22.38	1474.22	13.7	
Moderate pitting rate											
Min	10	0.079	21	0.01	0.04	6.78	6	6	66	4	70
Max		0.152	32	0.16	0.3	8.32	84	67	2729	150.3	
Mean		0.111	28	0.064	0.153	7.85	34	39.14	1273	36.8	
SD		0.028	3.5	0.046	0.093	0.54	30	23.81	841.73	51.1	
High pitting rate											
Min	10	0.121	27	0.02	0.05	6.21	3	7	404.6	5	150
Max		0.292	70	0.31	1.39	8.19	83	69	7621	134.2	
Mean		0.191	49.4	0.146	0.243	7.58	32	32.53	3513.73	44.7	
SD		0.042	17.2	0.095	0.336	0.67	29	20.79	2520.07	38.7	
Severe pitting rate											
Min	10	0.299	21	0.03	0.07	6.73	1	4	602.4	13.3	300
Max		0.695	74	0.61	2.01	8.57	90	66	7571.1	139.3	
Mean		0.506	50.7	0.192	0.413	7.66	42	36.33	4353.08	54.9	
SD		0.135	17	0.137	0.402	0.62	36	19.63	2285.35	37.8	
All data											
Min	10	0.032	21	0.01	0.04	6.21	1	2	66	4	600
Max		0.695	74	0.61	2.01	8.57	90	70	7621	150.3	
Mean		0.29	45.1	0.148	0.303	7.65	37	35.97	3482.07	45.5	
SD		0.19	17.4	0.122	0.348	0.63	33	19.93	2402.62	38.6	

SD: standard deviation, ED: exposure duration

4.1.4 Model prediction assumptions

To estimate the maximum pit depth growth of aged pipelines as a function of the operating parameters, the following key assumptions were made:

- The maximum pit depth growth follows a power law.

- The pitting initiation time is zero.
- Maximum pit depth is dependent on temperature, CO₂ partial pressure, pH, flow rate, sulphate ion concentration, chloride ion concentration, water cut and wall shear stress
- The operating conditions in the pipelines remains the same.
- The maximum pit depth results from accumulated stress initiated by the operating parameters and have a random growth rate over the time of exposure of the pipelines.
- Pit depth growth time interval and failure intensity are independently exponentially distributed with a Homogenous Poisson Process (HPP).
- The pipelines failed by leakage (after pitting corrosion caused 100% pipe-wall thickness loss) and not by burst or rupture.

4.2 Maximum pit depth growth estimation

Since degradation is a continuous process of wear and decay, it can be modelled as a stochastic process. The measured degradation path of i^{th} maximum pit depth from a total of n_v^{th} sample size ($i= 1, 2, \dots, S_v$) will consist of q_i measurements at time points t_{i1}, \dots, t_{iq_i} . If the pit depth is modelled as a form of degradation $\eta(t)$ plus measurement error(ϵ), then at time point q_i , the degradation measurement of the i^{th} maximum pit depth (D_{max_i}) is as follows:

$$D_{max_i} = \eta(t_{ij}) + \epsilon_{ij}, 1 \leq i \leq S_v, i \leq j \leq q_i \quad (4.4)$$

If a specific form is expressed for η , then Equation (4.4) can be expressed as

$$D_{ij} = \eta(t_{ij}, \omega, \rho_i) + \epsilon_{ij}, 1 \leq i \leq S, i \leq j \leq q_i; \rho_i = \rho_1, \rho_2, \dots, \rho_{S_v} \quad (4.5)$$

where ω represents an unknown common parameter across the pit depth whilst, ρ_i is the vector of the i^{th} maximum pit depth random effect parameter representing individual maximum pit depth characteristics. The degradation model used for predicting the maximum pit depth growth over time ($D_{max}(t)$) was assumed to follow a power model. The use of power model (Equation (4.6)) for pit depth growth have

been applied in prediction of pipelines reliability by different researchers (Sheikh, Boah & Hansen 1990, Katano *et al.* 2003, Caleyo *et al.* 2009, Velazquez *et al.* 2009).

$$\eta(t) = \gamma(t - t_{ini})^{\ell} \quad (4.6)$$

If γ represents the proportionality variable and ℓ represents the exponential variable and the pitting is assumed to start on a micro scale once the pipeline is in operation, then the time of initiation of pitting (t_{ini}) will be zero. If the distribution of the maximum pit depths is given by a g-gamma distribution, then Equation (4.6) can be expressed as follows:

$$D_{max}(t) = \eta \exp(\sigma z) \quad ; [\varepsilon = \sigma z] \quad (4.7)$$

where ε is error term.

If the pipeline is exposed to a series of stress shocks that occurs according to a Homogenous Poisson Process (HPP), then, the time interval t_1, t_2, \dots , of occurrence of the pitting corrosion process is independently exponentially distributed with the HPP rate. Assuming that the failure intensity of the HPP is λ and the pipeline wall leaks at shock stress k , the standardized error term z and the probability density function $f(\lambda)$ at λ can be expressed in terms of k and λ as shown in Equation (4.8) and (4.9) (Katano *et al.* 2003).

$$z = \sqrt{k} (\lambda - \log k) \quad (4.8)$$

$$f(\lambda) = \frac{\lambda}{\Gamma(k)} (\lambda)^{k-1} e^{-\lambda} \quad ; k > 0, \lambda > 0 \quad (4.9)$$

The values of k in Equation (4.9) indicates the specific form of the equation as follows:

- $K = \sigma = 1$, the equation is exponential
- $K = 1$, the equation is Weibull
- $K \rightarrow \infty$, the equation is lognormal.

If the natural log of Equation (4.7) is taken, the equation will be of the form shown in Equation (4.10):

$$\log D_{max} = \mu + \sigma z \quad (4.10)$$

where

$$\mu = \gamma_0 + \gamma_\theta \theta + \gamma_P P + \gamma_W W + Y_\tau \tau + Y_C C + Y_S S + Y_{pH} p_H + Y_V V + \ell \log t \quad (4.11)$$

and $\gamma_0, \gamma_\theta, \gamma_P, \gamma_W, Y_\tau, Y_C, Y_S, Y_{pH}, Y_V$ represents the intercept, temperature, CO₂ partial pressure, water cut, wall shear stress, chloride ion concentration, sulphate ion concentration, pH and flow rate coefficients of time variation of maximum pit depth growth respectively whereas ℓ represents the coefficient of the natural log of time.

Using Equations (4.8) and (4.10), the probability density function in Equation (4.9) can be recomputed according to Equation (4.12).

$$f(\lambda) = \left(\frac{\log D_{max} - \mu + \sigma \sqrt{k} \log k}{\sigma \sqrt{k} \Gamma(k)} \right) \left(\frac{\log D_{max} - \mu + \sigma \sqrt{k} \log k}{\sigma \sqrt{k}} \right)^{k-1} e_e \quad (4.12)$$

where

$$e_e = e^{-\left(\frac{\log D_{max} - \mu + \sigma \sqrt{k} \log k}{\sigma \sqrt{k}} \right)}$$

The estimates of the coefficients of the maximum pit depth and the operating parameters and the best fit distributions for each variable were determined using the maximum likelihood estimate and Akaike Information Criterion (AIC) shown in Equation (4.1).

4.3 Reliability analysis

To estimate the survivability of the pipelines with passage of time, a Weibull probability model was used. The least square estimation method was applied to determine the probability density function given by Equation (4.13).

$$f(t) = \frac{\varphi}{v} \left(\frac{t - \Phi}{v} \right)^{\varphi-1} e^{-\left(\frac{t - \Phi}{v} \right)^\varphi} \quad \varphi > 0, v > 0; t \geq \Phi \geq 0 \quad (4.13)$$

While the cumulative density function is given by Equation (4.14).

$$F(t) = 1 - e^{-\left(\frac{t - \Phi}{v} \right)^\varphi} \quad (4.14)$$

where φ is the shape parameter, v is the scale parameter and ϕ is the location parameter. In this work t represents time lapse of pit depth growth. If $\phi = 0$ and a double logarithmic transformation of the cumulative density function is taken, Equation (4.14) becomes:

$$\log \log \left[\frac{1}{1 - F(t)} \right] = \varphi \log v - \varphi \log t \quad (4.15)$$

In order to apply least square method for estimating the scale and shape parameters, the pipeline time of pitting failure will be ranked with Equation (4.16).

$$M_R = \frac{i - 0.3}{m + 0.4} \quad (4.16)$$

Where M_R is the median rank; m is the number of observed failures; i is ranked time lapse for pit depth growth of the pipeline.

Since Equation (4.15) is linear, the following relationship can be deduced:

$$\bar{x} = \frac{1}{m} \sum_{i=1}^n \log \left[\log \left(\frac{1}{1 - M_R} \right) \right] \quad (4.17)$$

$$\bar{y} = \frac{1}{m} \sum_{i=1}^m \log t_i \quad (4.18)$$

$$\varphi = \frac{\{m \sum_{i=1}^m (\log t_i) * \log(\log M_R)\} - \{\sum_{i=1}^m \log[\log M_R] * [\sum_{i=1}^m \log t_i]\}}{\{m \sum_{i=1}^m (\log t_i)^2 - (\sum_{i=1}^m (\log t_i))^2\}} \quad (4.19)$$

$$v = e^{\left(\bar{y} - \frac{\bar{x}}{\varphi}\right)} \quad (4.20)$$

The failure intensity can be calculated using the shape and scale parameters as shown in Equation (4.21):

$$\lambda(t) = \frac{\varphi}{v} \left(\frac{t}{v}\right)^{\varphi-1}, t > 0 \quad (4.21)$$

The survivor function ($R(t)$) is given as follows:

$$R(t) = e^{-(t/v)^\varphi} \quad (4.22)$$

Since Monte Carlo simulation have been successfully used for predicting maximum pit depth growth of pipelines and other structures by numerous authors (Ahammed & Melchers 1996, Caleyó *et al.* 2002, Li *et al.* 2009, Ossai 2013, Bazan & Beck 2013), the principle was adopted for estimating the time lapse for maximum pit depth growth based on Poisson Square Wave Model (PSWM) shown in Figure 4.1.

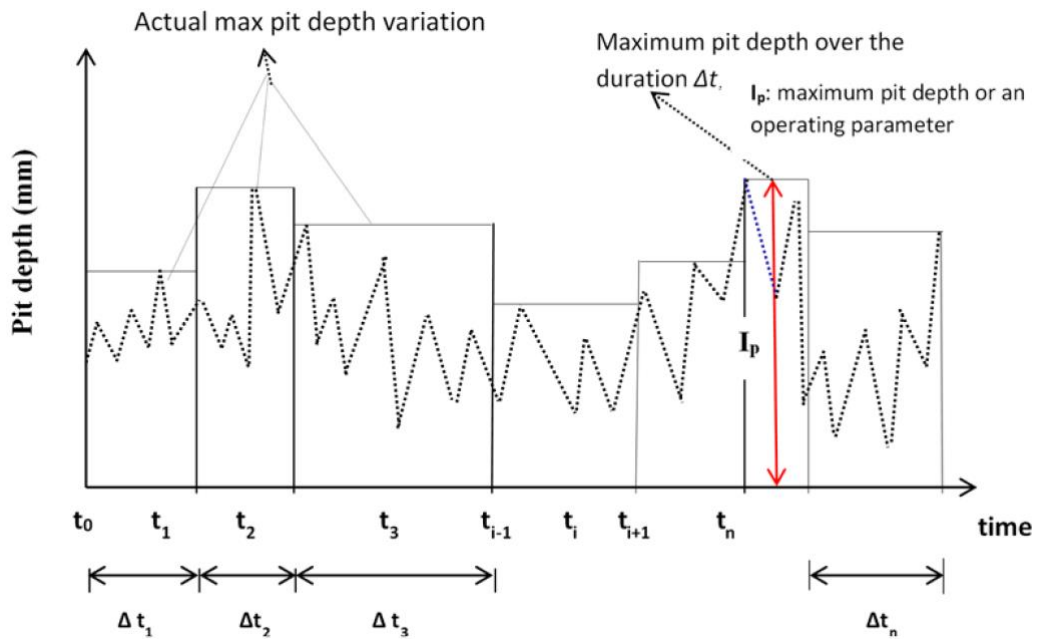


Figure 4.1: Poisson Square Wave Model (PSWM)

PSWM assumes a Homogeneous Poisson Process (HPP) (Dawotola *et al.* 2011) in which the failure intensity is independent and identically distributed according to an exponential distribution (Caleyó *et al.* 2009). PSWM have been used for modelling real life situations by researchers such as Bazan & Beck (2013), Pandey, Yuan & Van Noordwijk (2009) and Zheng & Zhou (2013) who used Gumbel and gamma distributions for modelling Poisson arrival process. However, any positive random distribution can be utilized for the modelling of the lapse time (Bazan & Beck 2013).

In this work, Generalized Extreme Value (GEV), Weibull, Gamma, Extreme Value (EV), lognormal and exponential distributions were used for estimating the survival probabilities of the studied pipelines. The statistical best fits of the operating

parameters and maximum pit depths were utilized to predict the simulated values of the maximum pit depths and operating parameters at different Poisson arrival times. The relationship between the maximum pit depth, the operating parameters and the time lapse for maximum pit depth growth were used for calculating the reliability trend of the pipelines.

4.4 Monte Carlo simulation framework

As a pragmatic tool for abstractions of reality, Monte Carlo simulation gives a robust approach for solving problems that may be extremely difficult to solve practically in consideration of cost and risk. The survivor functions of the pipelines were determined in consideration of time lapse of maximum pit depth growth by using the statistical best fit distributions and the model equations. The framework for the simulation process is shown in Figure 4.2.

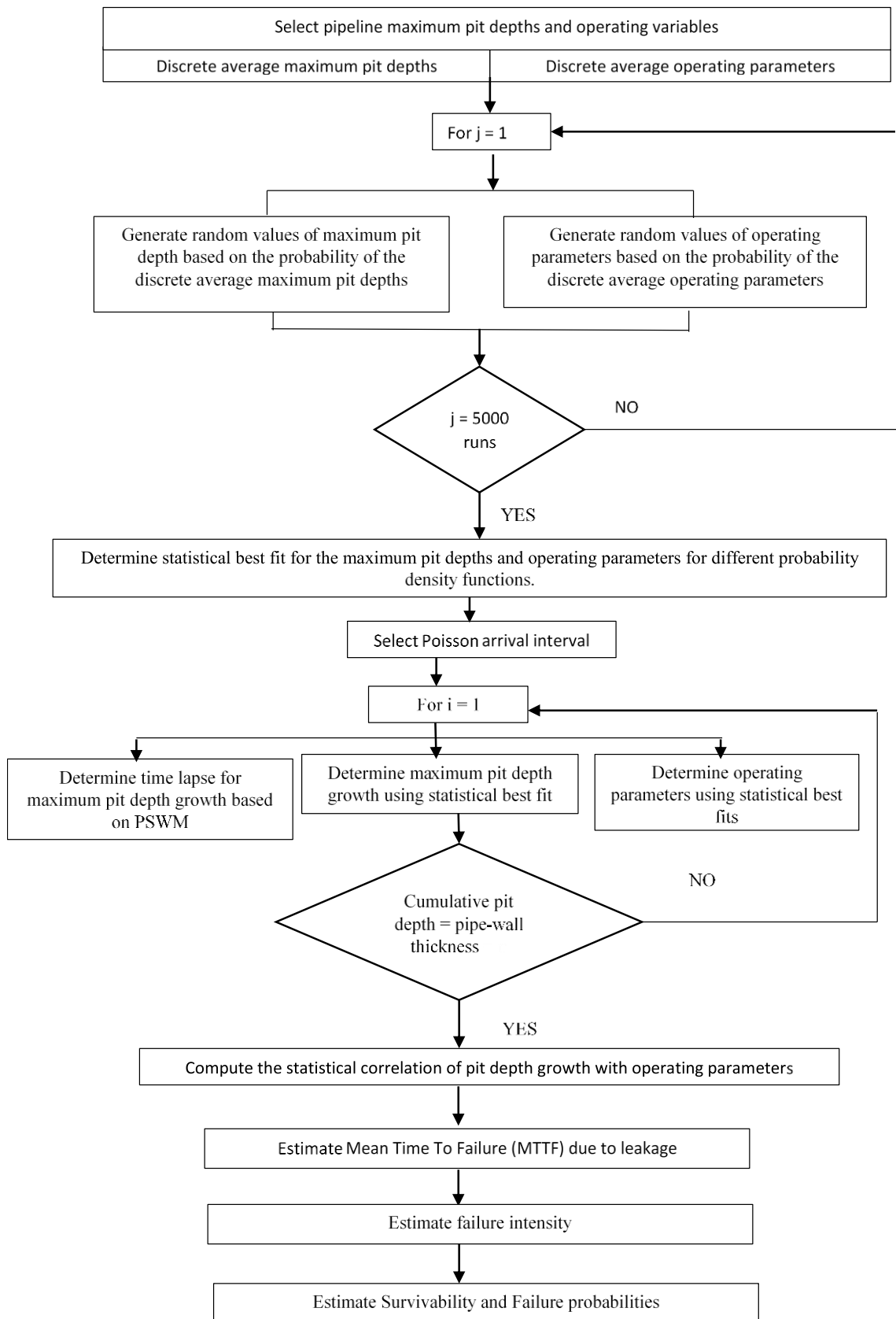


Figure 4.2: Monte Carlo simulation framework for reliability estimate of internal pit corroded pipeline

4.5 Results and discussion

4.5.1 Maximum pit depth distribution

The results of the maximum pit depth distribution for all the categories of pitting corrosion considered in this work are shown in Figures 4.3 – 4.7. These figures show the field data distribution and the fitting curves of some of the probability density function distributions tested.

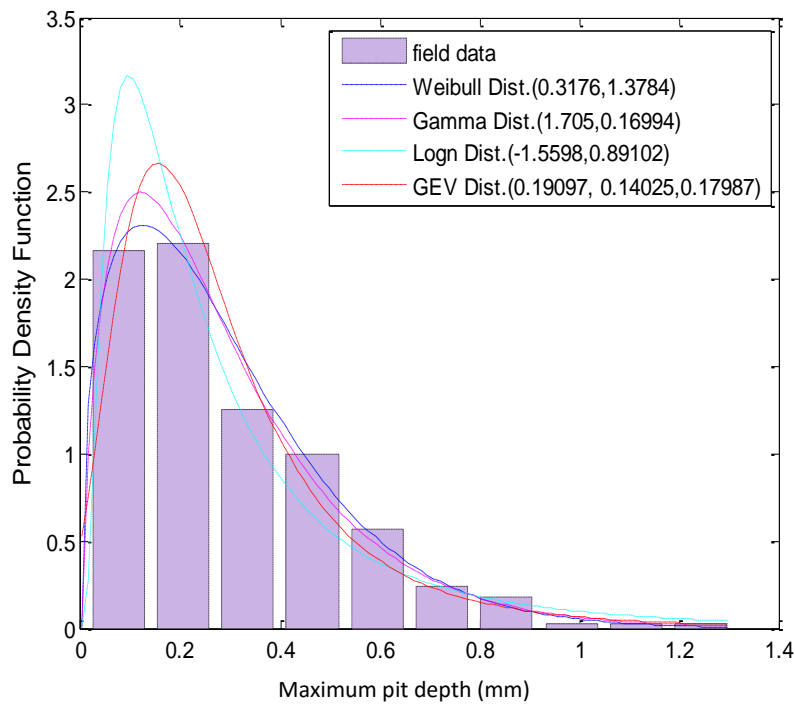


Figure 4.3: Field data and probability density functions of some of the considered distributions for all-data category

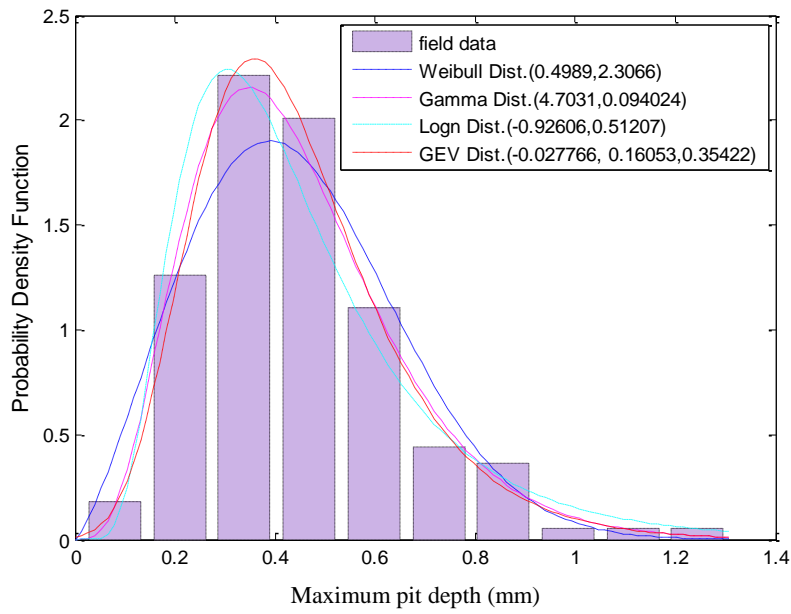


Figure 4.4: Field data and probability density functions of some of the considered distributions for severe pitting category

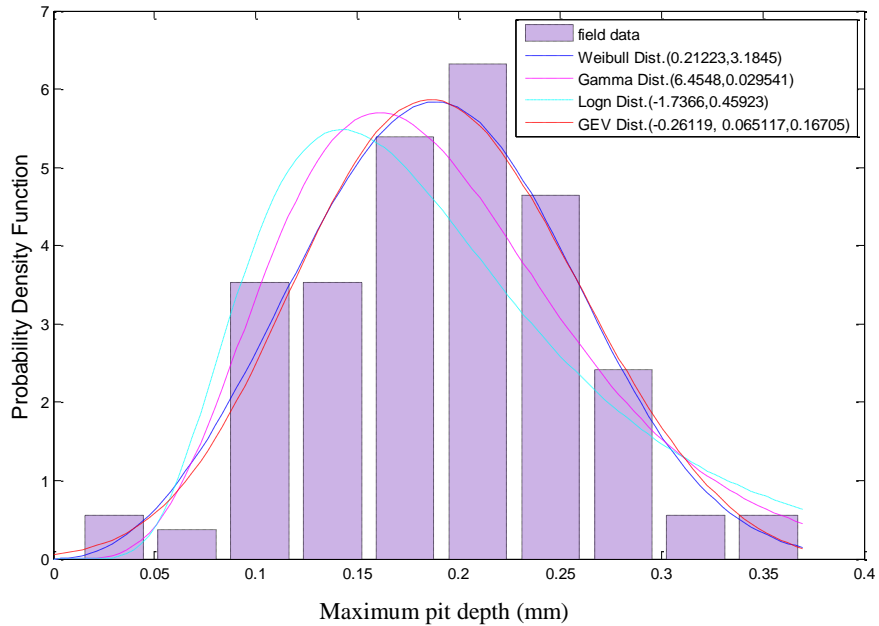


Figure 4.5: Field data and probability density functions of some of the considered distributions for high pitting category

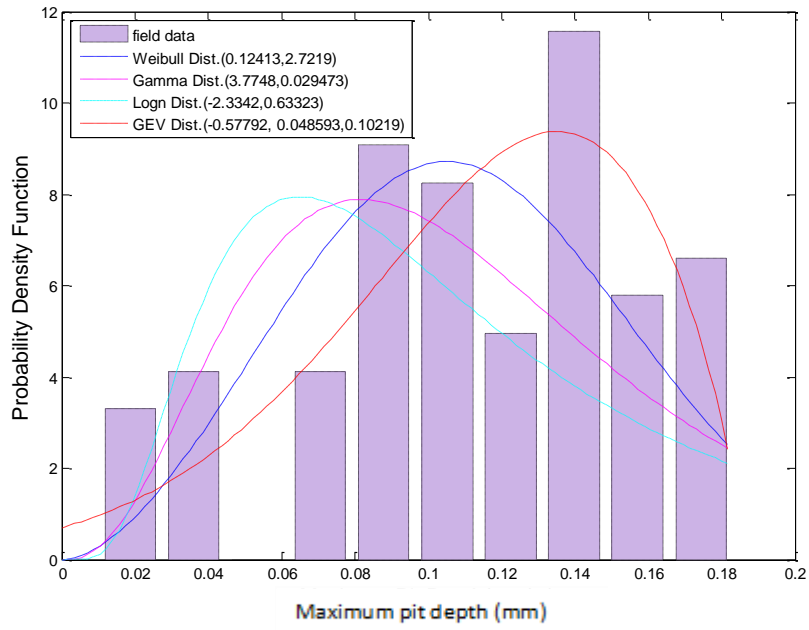


Figure 4.6: Field data and probability density functions of some of the considered distributions for moderate pitting category

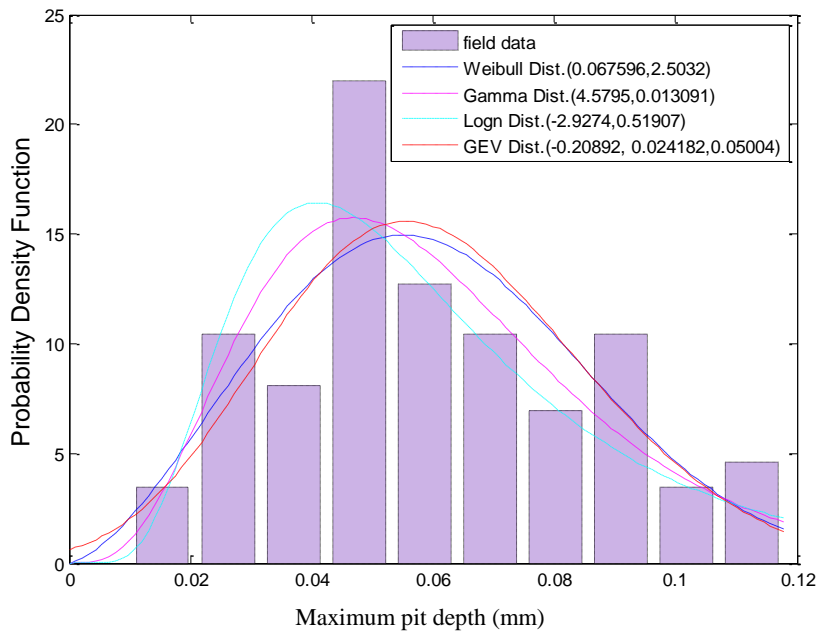


Figure 4.7: Field data and probability density functions of some of the considered distributions for low pitting category

The results of these fitted distributions for the pitting corrosion categories as calculated with Maximum Likelihood Estimates (MLEs) and Akaike Information Criterion (AIC) is shown in Table 4.3.

Table 4.3: Maximum Likelihood Estimates (MLEs) and Akaike Information Criterion (AIC) for maximum pit depth categories

Distribution	Low Pitting		Moderate pitting		High Pitting		Severe Pitting		All- data	
	No of samples:80		No of samples:70		No of samples:150		No of samples:300		No of samples:600	
	MLE	AIC	MLE	AIC	MLE	AIC	MLE	AIC	MLE	AIC
Weibull	2.5	158.16	2.72	138	3.18	297.68	2.31	598.33	1.38	1199.4
GEV	0.05	165.99	0.1	144.56	0.17	303.58	0.35	602.08	0.19	1203.3
lognormal	0.53	161.32	0.63	140.93	0.46	301.56	0.51	601.34	0.89	1200.2
Gamma	4.58	156.96	3.77	137.34	6.45	296.27	4.7	596.9	1.71	1198.9
Exponential	0.06	165.63	0.11	144.39	0.19	303.31	0.44	601.63	0.29	1202.5
Inverse Gaussian	0.19	163.31	0.21	143.16	0.67	300	1.2	599.64	0.29	1202.5
Extreme value	0.07	165.23	0.13	144.05	0.22	303	0.55	601.19	0.41	1201.8

Since the smallest AIC value is the best fit for a given distribution (Katano *et al.* 2003), gamma distribution is the best statistical distribution for all-data, low, moderate, high and severe pitting corrosion categories.

4.5.2 Correlation of maximum pit depth with operating parameters

The correlation of the maximum pit depth with the operating parameters involved a multivariate regression analysis and removal of outliers, which can be done by using boxplot, cook distant and Q-Q standardized residuals (Velazquez *et al.* 2009). For this work, a boxplot and Q-Q standardized residual analysis of all-data category is used to exemplify the result in Figures 4.8 – 4.9.

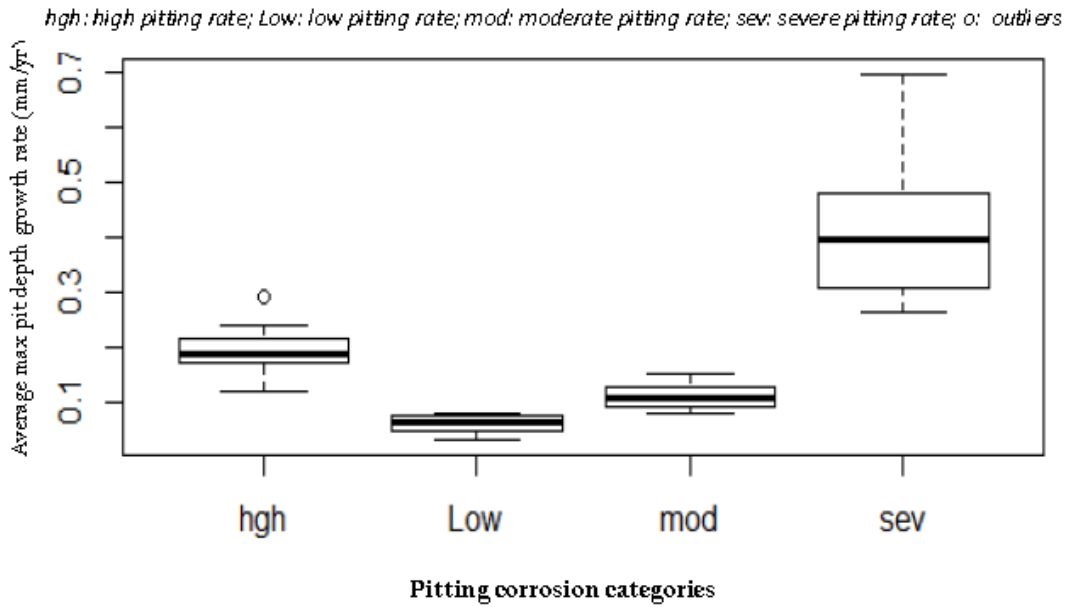


Figure 4.8: boxplot analysis of maximum pit depth of the pipelines according to pitting corrosion categories

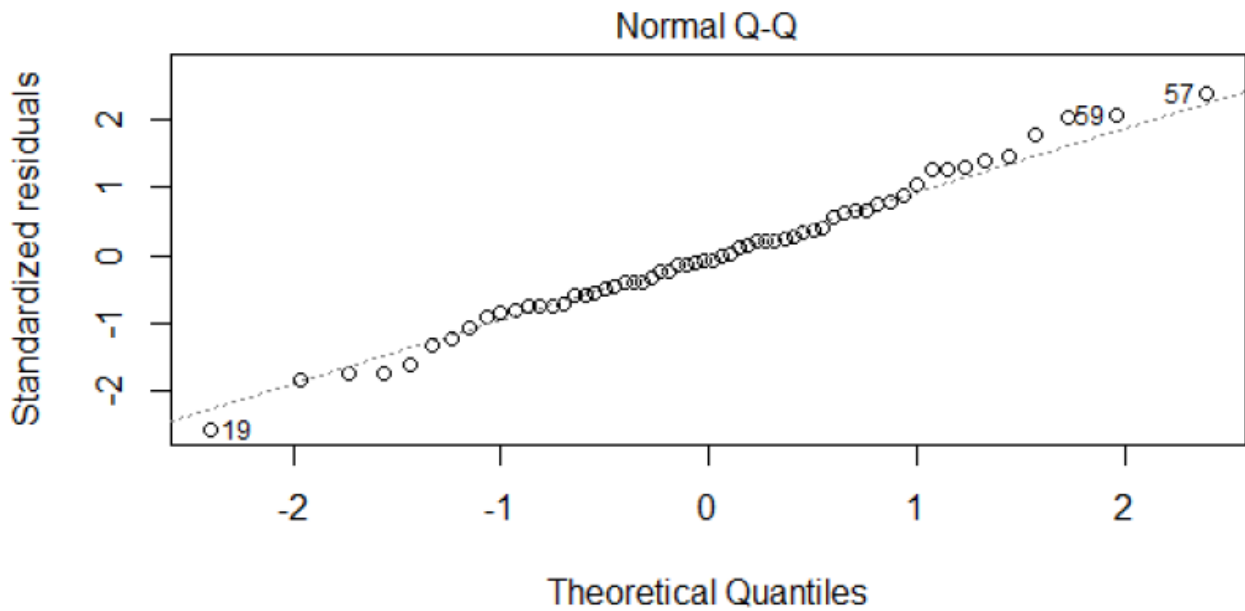


Figure 4.9: Q-Q plot analysis of maximum pit depth as a function of operating parameters for all-data category

The relationship between the maximum pit depth and the operating parameters for all-data category is shown in Table 4.4.

Table 4.4: Parameter estimate for regression analysis of average pitting rate and operation parameters for all-data category

variable	A: Prior to removing outliers				B: After removing outliers			
	Coefficient	S.E	t-value	Pr(> t)	Coefficient	S.E	t-value	Pr(> t)
α	-7.80E-02	2.30E-01	-0.338	0.737	-1.90E-01	2.00E-01	-0.96	0.342
β_θ	1.90E-05	1.30E-03	0.015	0.988	1.20E-03	1.10E-03	1.027	0.31
β_p	5.10E-01	1.90E-01	2.688	0.010 **	4.70E-01	1.70E-01	2.795	0.007 **
β_v	1.80E-01	5.70E-02	3.129	0.003 **	1.40E-01	5.00E-02	2.739	0.009**
β_c	2.10E-05	7.90E-06	2.695	0.010 **	2.00E-05	7.60E-06	2.62	0.012 *
β_s	-7.30E-04	8.90E-04	-0.82	0.416	-1.30E-04	8.10E-04	-0.16	0.873
β_{pH}	1.70E-02	2.80E-02	0.601	0.55	2.40E-02	2.40E-02	0.979	0.332
β_w	3.40E-02	5.60E-02	0.609	0.545	3.10E-02	4.80E-02	0.635	0.529
β_r	1.10E-03	5.30E-04	1.984	0.053 *+	1.40E-03	5.10E-04	2.802	0.007 **
R ² : 0.5817				R ² : 0.6846				
Adjusted R ² : 0.516				Adjusted R ² : 0.6309				
Residual Standard Error: 0.1322				Residual Standard Error: 0.1112				
p-value: 1.652e-07				p-value: 1.569e-09				
F-stat: 8.864				F-stat: 12.75				

****:Pr≤ 0.1%; ***:Pr≤1%; **:Pr≤5%; *+:Pr≤10%

The table shows that 58.17% of the maximum pit depths is attributable to the studied operating parameters prior to removing the 3 outliers shown on the Q-Q plot in Figure 4.9. However, after removing the outliers, the maximum pit depth can be explained by 68.46% of the operating parameters. This implies that 41.83% and 31.54% of the maximum pit depths of the pipelines with and without outliers (Table 4.4) respectively are caused by either errors in the measurement of the parameters or due to other variables, which were not considered in this research. Notable amongst the variables not considered in this work that may contribute substantially to pitting corrosion are microbiological organisms such as Sulphate Reducing Bacteria (SRB), which are credited with increasing pitting corrosion by different researchers (Melchers 2008, Chandrasatheesh *et al.* 2014, Chen *et al.* 2014). The table further showed that flow rate, chloride ion concentration and sulphate ion concentration are significant at 99.9% confidence interval whilst wall shear stress is significant at 90% confidence interval prior to removing the outliers. Again, Flow rate, chloride ion concentration and wall shear stress are significant at 99.9% confidence interval prior to the removal of outliers and sulphate ion concentration is significant at 95%

confidence interval after removing the outliers. Prior to removing the outliers, it can be deduced from the analysis according to Table 4.4 that if other operating parameters are kept constant, 1 °C increase in temperature will result in 0.000019 mm increase in maximum pit depth of the pipelines. Figure 4.10 shows the relative increase in pipeline maximum pit depth due to one-unit increase of an operating parameter as others are kept constant. This figure indicates that CO₂ partial pressure will result in the highest relative change in maximum pit depth amongst the considered variables followed by flow rate, water cut, pH, wall shear stress, chloride ion concentration and temperature. This result implies that except for sulphate ion concentration, the other variable contributed to maximum pit depth growth at varying degrees. This finding is in line with the results of other researchers (Jepson & Menezes 1995, Zhang, Gopal & Jepson 1997, Hassani *et al.* 2012) in this area. Sulphate ion concentration did not show significant impact on the relative maximum pit depth change probably due to the trace quantity of H₂S in the studied fields since, sulphate ion may actively impact pitting corrosion in the presence of H₂S (Papavinasam, Doiron & Revie 2010).

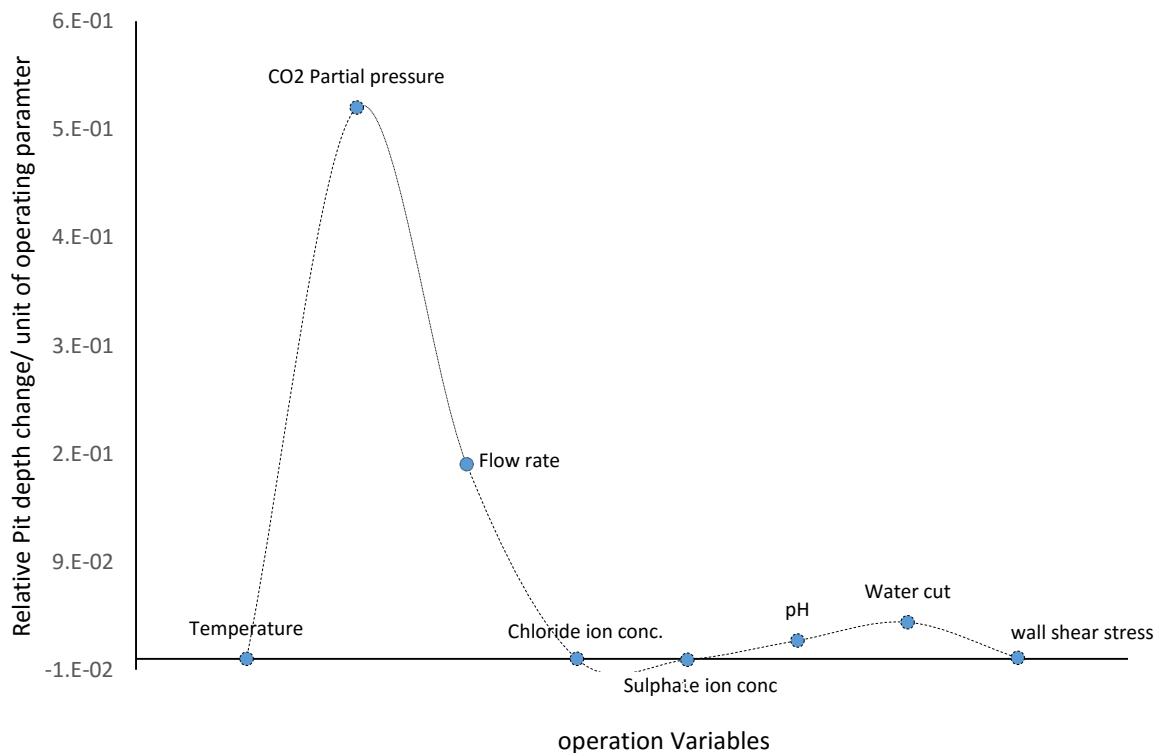


Figure 4.10: relative variation of pipeline pit depth due to unit increase of operating parameters

4.5.3 Time variation of pit depth growth

The statistical distribution of the maximum pit depths and the operating parameters for all-data category as obtained from the simulation was used for illustrating the results obtained in this session and is shown in Table 4.5.

Table 4.5: Statistical best fit for average operating parameters and average maximum pit depth for all-data category.

	Weibull		Exponential		Lognormal		Gamma	
	MLE	AIC	MLE	AIC	MLE	AIC	MLE	AIC
θ	50.77	112.15	45.05	112.38	3.73	117.37	6.87	116.15
P	1.28	119.51	0.15	123.83	0.91	120.19	1.56	119.11
V	1.09	119.82	0.3	122.39	0.85	120.33	1.39	119.35
pH	16.05	114.45	7.65	115.93	2.03	118.58	142.34	110.08
S	38.96	112.68	34.88	112.9	3.3	117.61	16.43	114.4
C	3613.8	103.62	3375.7	103.75	7.7	115.92	2555.6	104.31
W	0.89	120.23	0.37	121.96	1.46	119.25	0.81	120.43
τ	48.94	112.22	45.5	112.36	3.45	117.53	30.47	113.17
D_{max}	1.58	119.08	0.29	122.48	0.77	120.52	2.12	118.5

This table indicates that the statistical best fit for temperature, sulphate ion concentration, chloride ion concentration and wall shear stress is Weibull distribution whereas Gamma distribution is the statistical best fit for CO₂ partial pressure, flow rate, pH and maximum pit depth. The statistical best fit for water cut is lognormal distribution.

The parametric estimate of the time variation of pit depth growth for all-data category as estimated from Monte Carlo simulation is shown in Table 4.6. The time variation for the maximum pit depth growth and the cumulative pipe-wall thickness loss at different pipeline ages for all-data category was constructed based on Equation (4.6) and exponential and proportionality constants in Table 4.6. This time lapse for maximum pit depth growth and pipe-wall thickness loss is shown in Figure 4.11. This figure shows that the maximum pit depth growth is higher at the early part of the pipeline exposure and gradually reduces as the pitting rate becomes more stable. This finding is similar to the body of knowledge concerning pit depth nucleation, stabilization and growth trend over long period of exposure (Caleyo *et al* 2009).

Table 4.6: Parameter estimate for pit depth growth based on all data category

Variables	Coefficient	SE	t value	Pr(> t)
Υ_0	-1.11E+00	6.29E-01	-1.773	0.0868 *+
Υ_θ	3.58E-03	2.02E-03	1.776	0.0862 *+
Υ_p	3.41E-01	2.93E-01	1.162	0.2549
Υ_v	3.41E-02	1.24E-01	0.274	0.7861
Υ_c	2.26E-05	1.86E-05	1.218	0.2331
Υ_s	-5.13E-03	2.11E-03	-2.426	0.0217 *
Υ_{pH}	8.71E-02	8.51E-02	1.023	0.315
Υ_w	-1.67E-01	2.06E-01	-0.813	0.4228
Υ_τ	-3.46E-04	9.27E-04	-0.373	0.7121
$\ell \log t$	6.50E-01	3.20E-02	20.338	<2e-16 ***
Residual standard error	0.1985			
F-statistics	68.56			
p-value	< 2.2e-16			
R ²	0.9551			
Adjusted R ²	0.9412			
Proportionality variable	0.693			
Exponential variable	0.65			

****:Pr≤ 0.1%; ***:Pr≤1%; **:Pr≤5%; *+:Pr≤10%

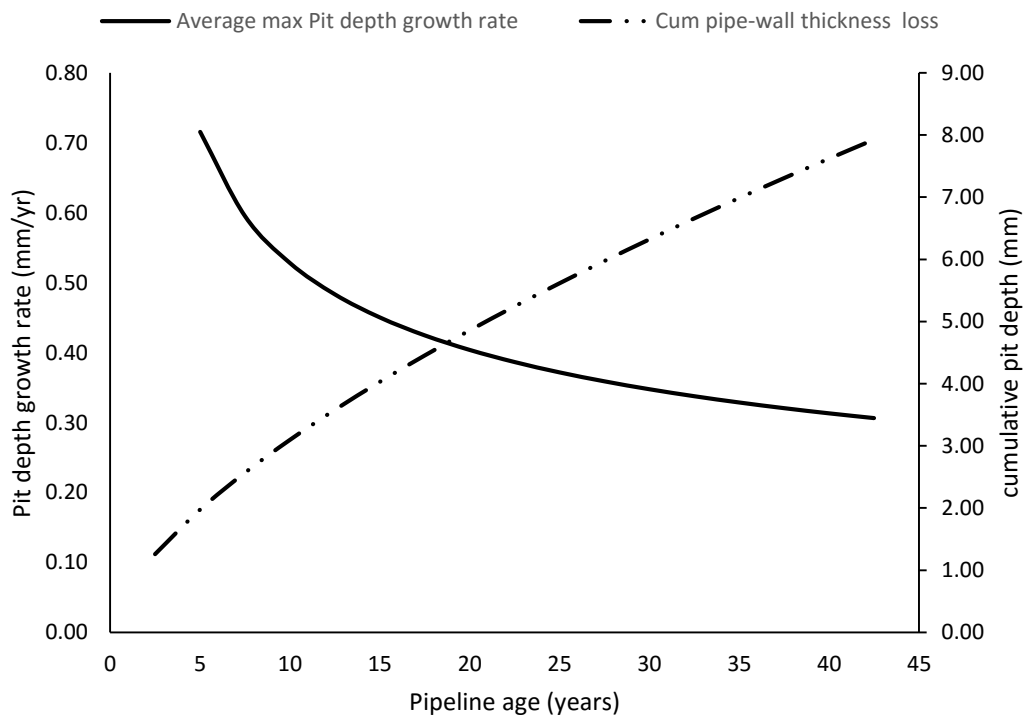


Figure 4.11: Time variation of average maximum pit depth growth and cumulative pipeline wall thickness loss

4.5.4 Reliability estimates

The shape and scale parameters of Weibull distribution probability and failure intensity of the pipelines for different probability distribution functions is shown in Table 4.7.

Table 4.7: Summary of Weibull probability scale and shape parameters and failure intensity of different distributions for all-data category

Distribution	Scale factor (ν)	Shape factor (φ)	Failure intensity (yr^{-1})
Gamma	15.57	0.7	0.040
Weibull	15.57	1.24	0.093
lognormal	14.81	1.25	0.097
Exponential	9.69	1.07	0.115
Extreme Value	9.57	1.22	0.143
Generalized Extreme Value	9.48	1.24	0.145

The goodness of fit test for all data category used for determining the Weibull probability scale and shape parameters for the various distributions considered is shown in Figures 4.12 - 4.17.

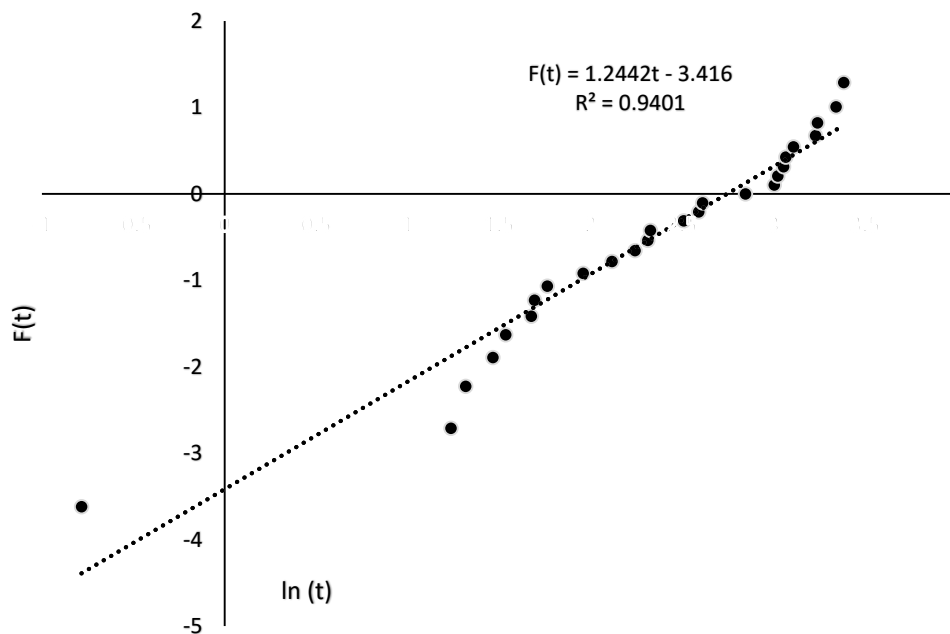


Figure 4.12: Goodness of fit test for Weibull probability plot based on Weibull distribution

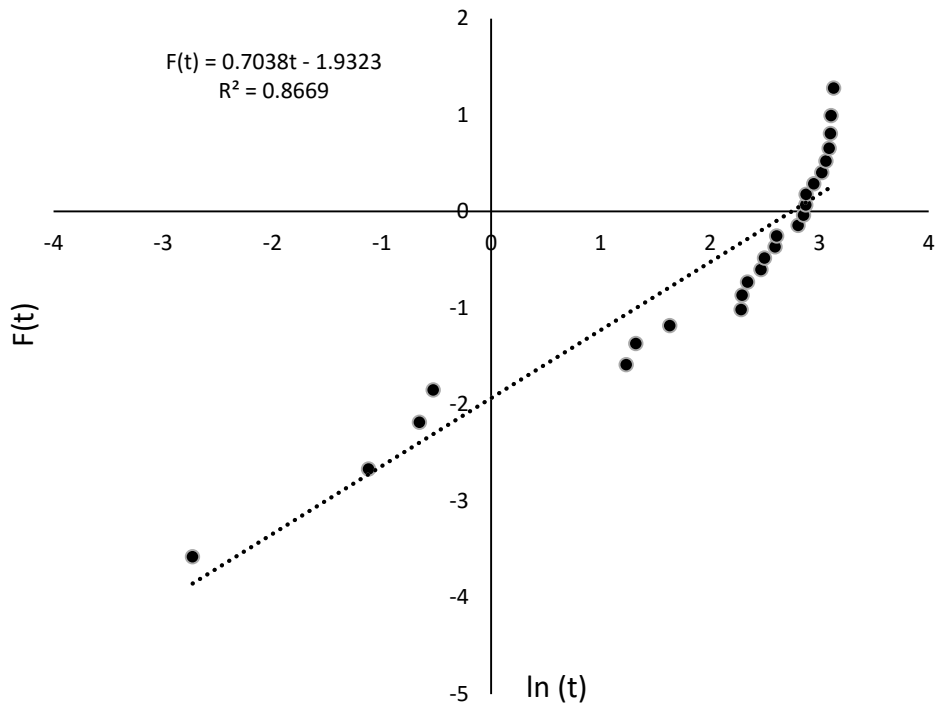


Figure 4.13: Goodness of fit test for Weibull probability plot based on Gamma distribution of pitting time

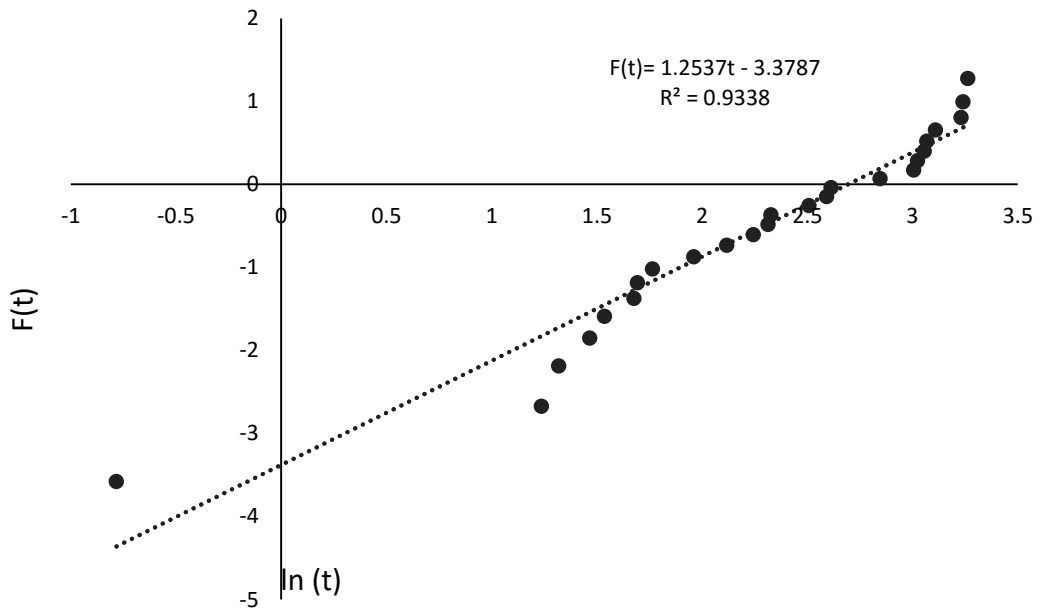


Figure 4.14: Goodness of fit test for Weibull probability plot based on lognormal distribution of pitting time

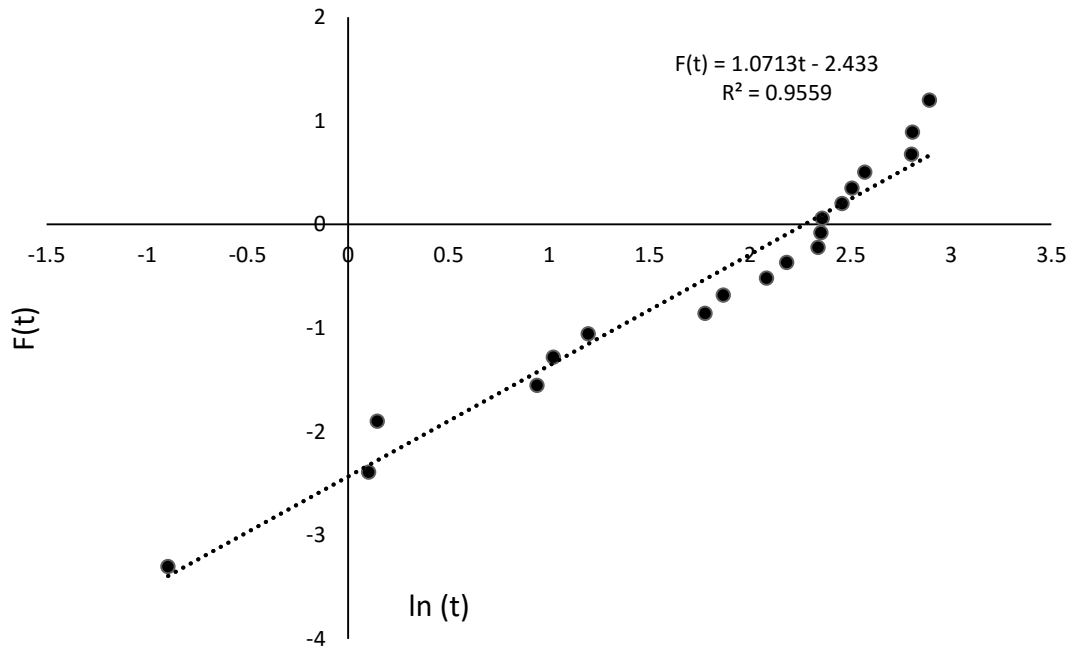


Figure 4.15: Goodness of fit test for Weibull probability plot based on exponential distribution of pitting time

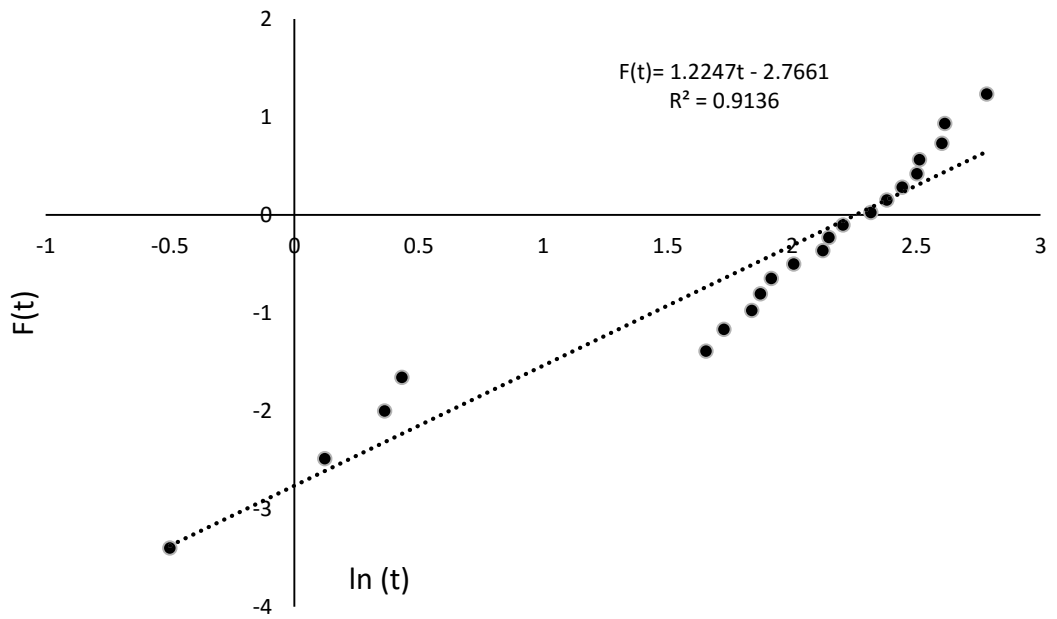


Figure 4.16: Goodness of fit test for Weibull probability plot based on extreme value distribution of pitting time

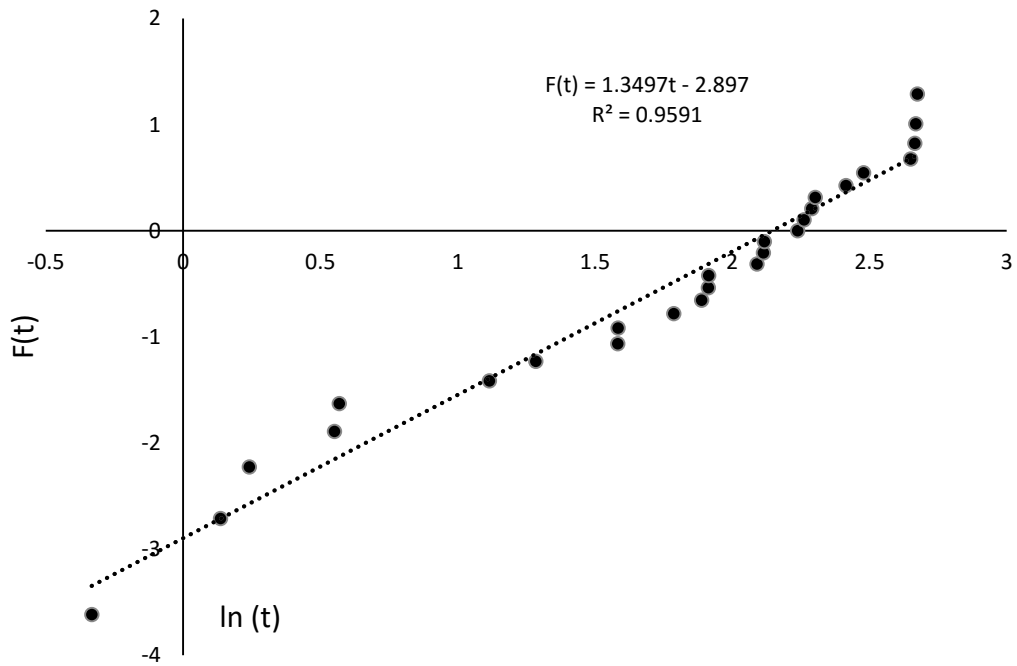


Figure 4.17: Goodness of fit test for Weibull probability plot based on generalized extreme value distribution of pitting time

The relationship between the scale and shape parameters of Weibull probability distribution with the service life of the pipelines is shown in Figures 4.18-4.19. The relationship is vital for estimating the survivability probability of the pipelines at any given time in service. The scale (ν) and shape (φ) parameters can be approximated with the continuous formula shown in Equation (4.23) and (4.24).

$$\varphi = -0.0256T_{years}^2 + 1.6076T_{years} - 9.3795 \quad (4.23)$$

$$\nu = 0.0069T_{years}^2 - 0.3024T_{years} + 4.234 \quad (4.24)$$

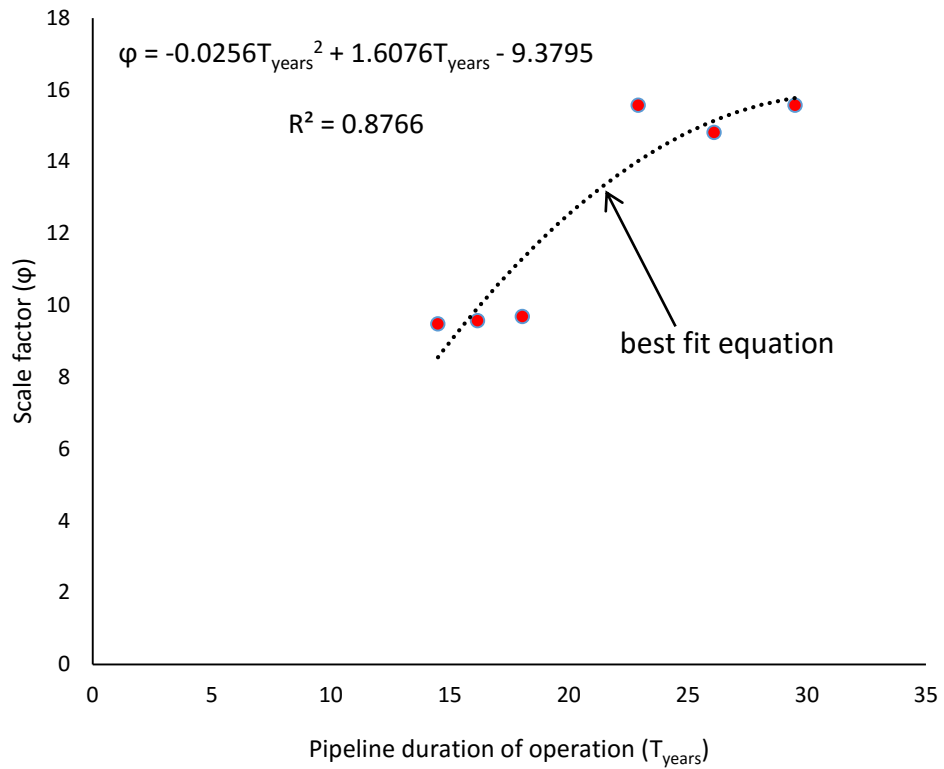


Figure 4.18: Variation of Weibull function scale parameter with estimated time of pipeline operation

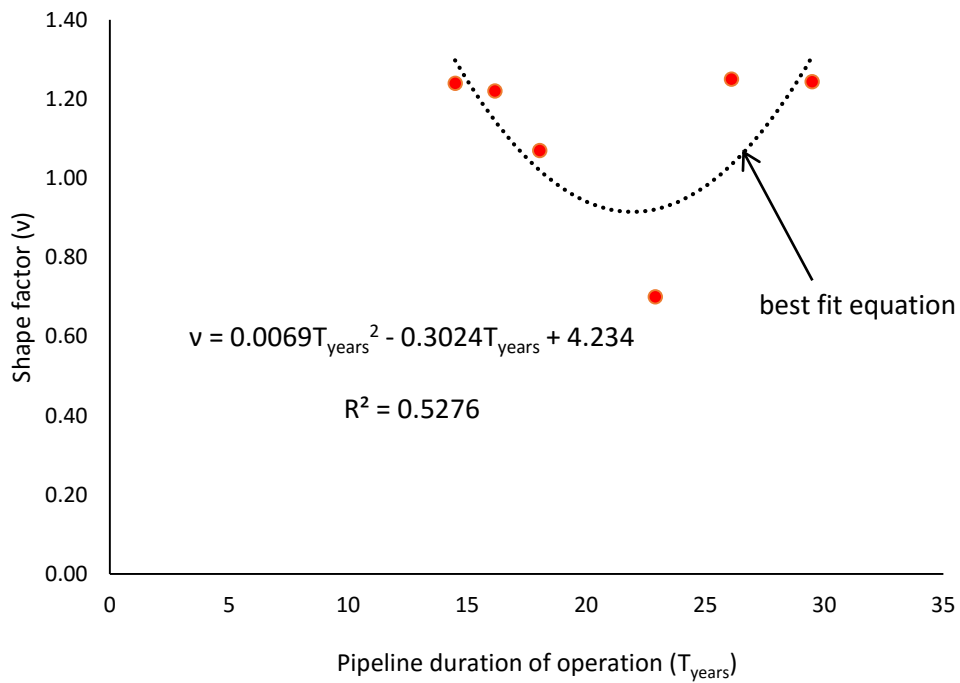


Figure 4.19: Variation of Weibull function shape parameter with estimated time of pipeline operation

The survivability and failure probabilities of the pipelines for different distributions are shown in Figure 4.20.

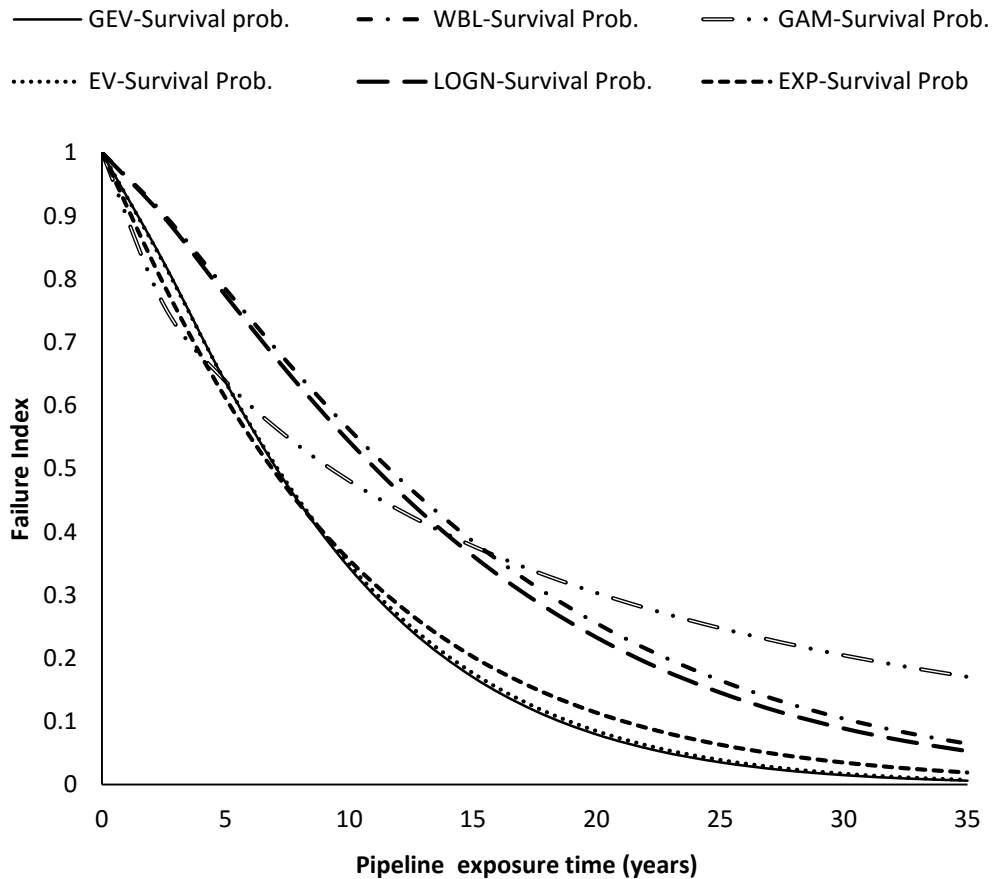


Figure 4.20: Survival probabilities classified according to distribution function types

Figure 20 indicates that 80% of the pipe wall thickness will be lost after 13.99 years based on generalized extreme value distribution whilst extreme value, exponential, lognormal, Weibull and Gamma distributions will have the same 80% loss of pipe wall thickness lost in 14.20 years, 15.09 years, 21.70 years, 22.80 years and 30.57 years respectively.

4.6 Application

The application of this model is on Magnetic Flux Leakage (MFL) in-line inspection (ILI) data of a 3700m long API X52 transmission pipeline having 8.7 mm nominal wall thickness and 203.2 mm external diameter. This pipeline was commissioned in December 1994 and was inspected in August 2012 with magnetic flux leakage in-line

inspection (ILI) technique. The inspection produced a total of 1037 pit depths samples that ranged from 10% to 60% of the nominal pipe-wall thickness of the pipeline.

To estimate the reliability of the pipeline, it was assumed that the data from this pipeline belong to all-data category whilst a discrete event simulation similar to the one described previously in this work was used to estimate the maximum pit depth data in order to ascertain the precision of the approach adopted in this work. The Root Mean Square Percentage Error (RMSPE) of the simulated data in comparison to the field measure MFL ILI data was determined to be 0.948. Figure 4.21 shows the field data measurement of the pipeline and Generalized Extreme Value Distribution (GEVD) of the field and simulated data.

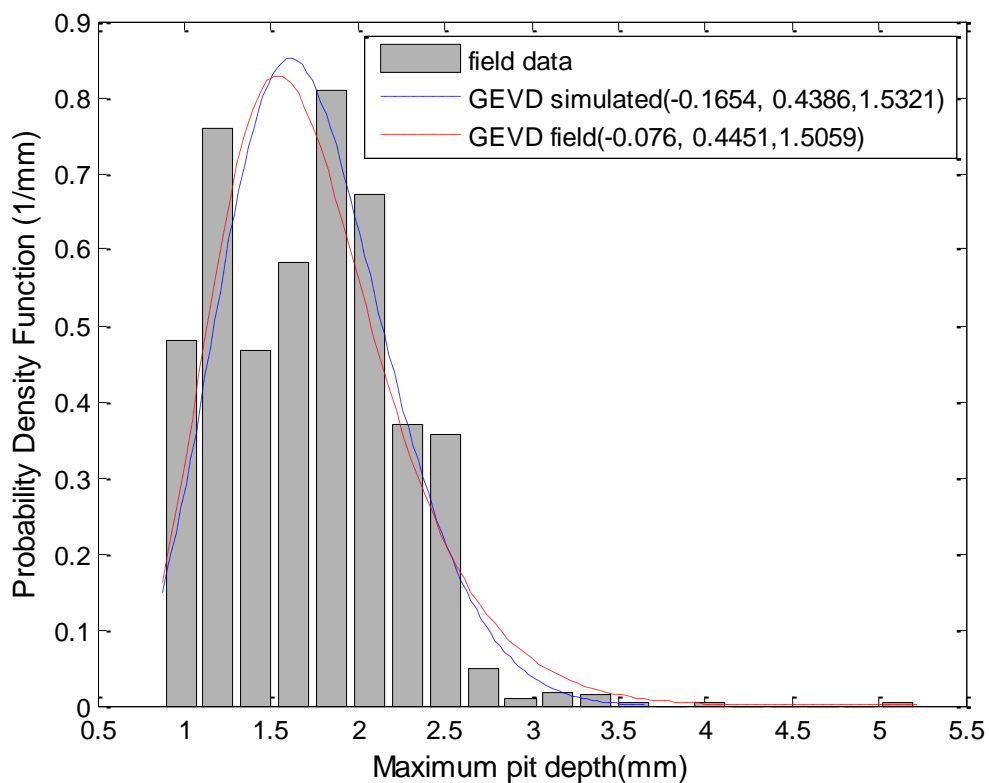


Figure 4.21: PDF of field measured pit depths, GEVD of field and simulated data of API X52 oil and gas transmission pipeline

In a bid to make some comparison, the pit depth distribution was assumed to follow a linear growth pattern according to Equation (4.25) and an exponential growth process shown in Equation (4.26) (Soares & Garbatov 1999).

$$D(t) = D(t_0) + \psi(t - t_0), \text{ for } t > t_0, \psi = \frac{D(t_0)}{t_0} \quad (4.25)$$

$$D(t_0) = D(t) \left(1 - e^{-\left(\frac{t_0 - t_{ini}}{t - t_0}\right)} \right) \quad (4.26)$$

where $D(t_0)$ represents pit depth measured at time of inspection t_0 , $D(t)$ represents future pit depth at time t , t_{ini} represents the time of pitting initiation, which has been assumed to be zero in this work and ψ represents the pitting rate which is determined as a function of the pit depth at time of inspection and age of the pipeline.

Figure 4.22 shows the future pit depth distribution of the pipeline ten years after MFL ILI in 2012. The simulated future pit depth was compared to linear and exponential prediction models shown in Equation (4.25) and (4.26).

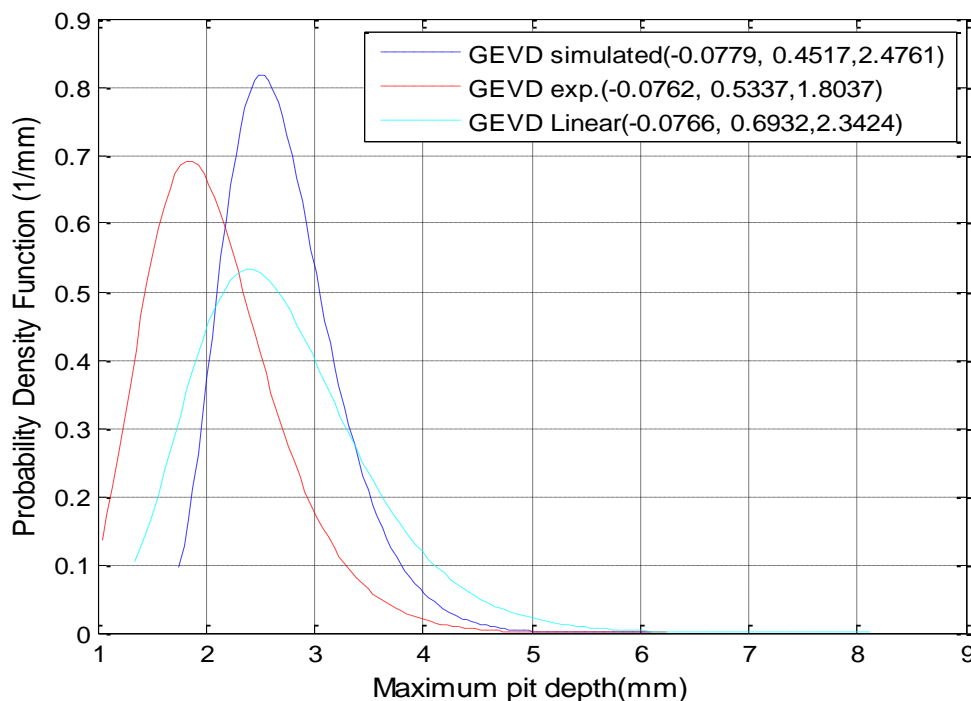


Figure 4.22: Comparison of initial pit depth distribution of MFL ILI-inspected API X52 transmission pipeline after 10 years of ILI-inspection

The figure indicates that after 10 years from the time of inspection in 2012, the pit depth will vary from 1.04 mm to 6.25 mm when exponential model was used for predicting future growth whilst linear model and simulation resulted in pit depth growth of 1.35 mm to 8.12mm and 1.75 mm to 6.1mm respectively. This information shows that the linear model shows more variation in comparison to the other two models. This highlights one of the limitations of using linear model for predicting pit depth growth seeing that the model does not consider the cessation and reduced rate of pit depth growth over a long time of exposure as was shown in different research works (Velazquez *et al.* 2009, Bazan & Beck 2013).

To estimate the reliability of this pipeline, it was assumed that the distribution of the pipeline pitting time follows a Weibull distribution. Figure 4.23 shows the survivability and failure probabilities of this pipeline ten years after the inspection done in 2012 whereas the failure rate per km-year is shown in Figure 4.24. It can be deduced from the figures that the failure rate predicted by the linear model is more than twice as much as that predicted using the exponential model and about three-quarter more than that predicted by Monte Carlo simulation.

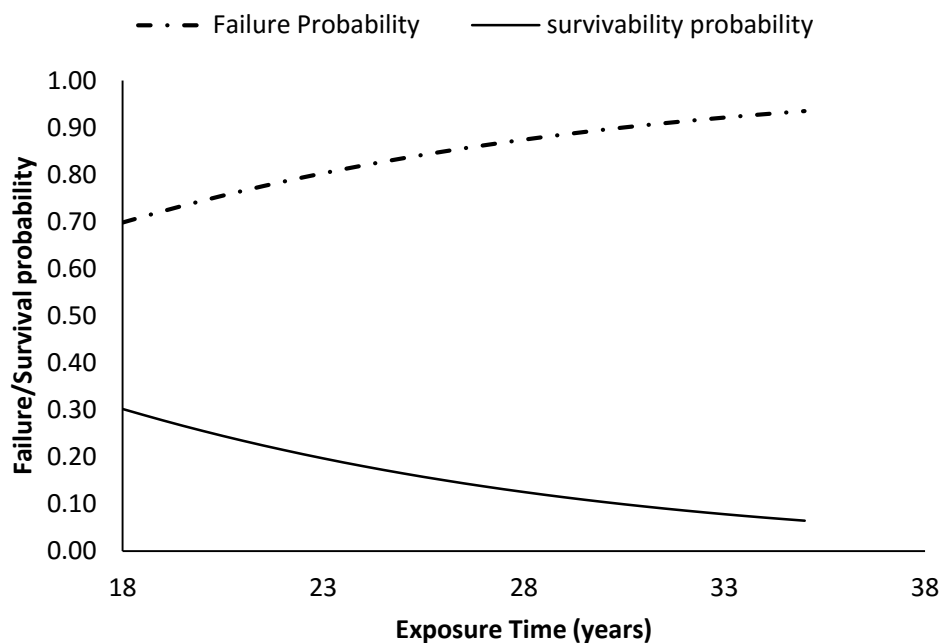


Figure 4.23: Failure and Survival probability of MFL ILI-inspected pipeline

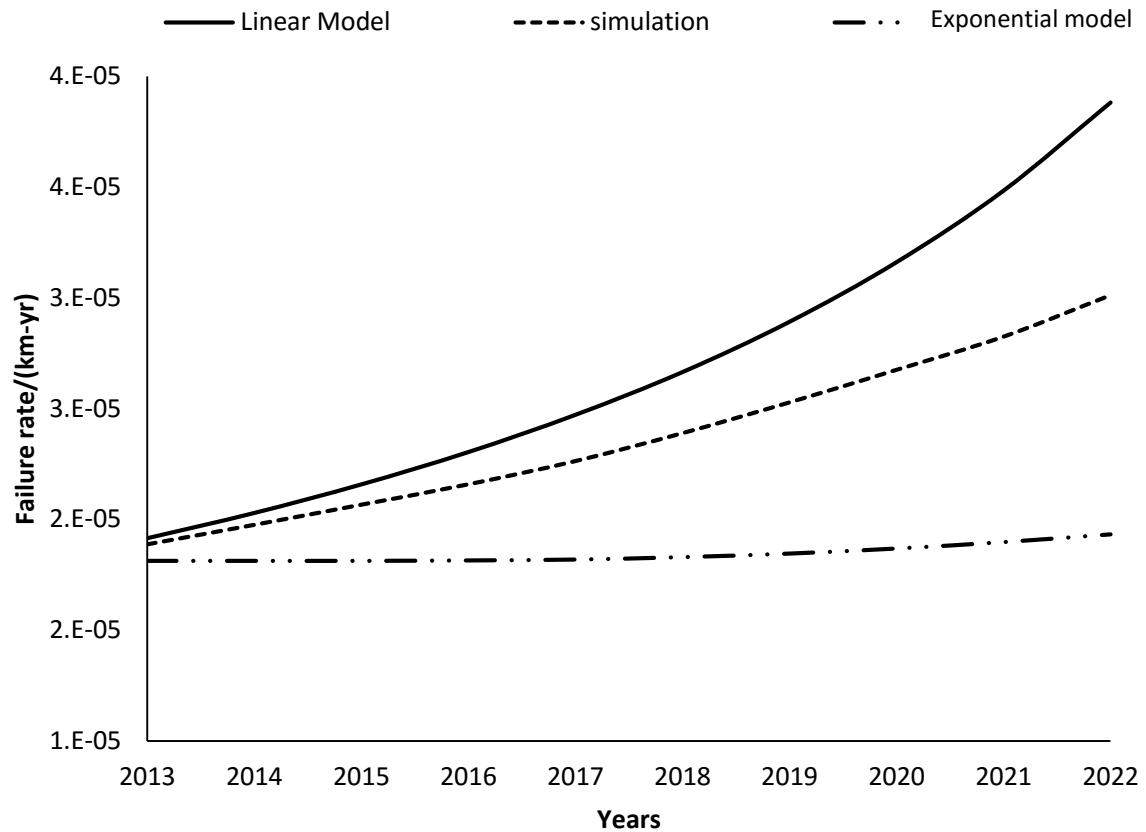


Figure 4.24: Estimation of the reliability trend of X52 pipeline ILI-inspected in 2012

4.7 Conclusions

Internal maximum pit depth growth of pipelines for transmission of crude oil was investigated in this work. The pit depths of the studied pipelines were classified as either low, moderate, high or severe based on NACE standard RP0775. Multivariate regression analysis of the maximum pit depth with operating parameters and the maximum pit depth growth rate was established using the field data and Monte Carlo simulated data. Poisson Square Wave Model (PSWM), which determined pitting time using a Homogenous Poisson Process (HPP) arrival interval was used for estimating the time lapse for the simulated pit depth growth.

The work showed that maximum pit depth growth was more at the initial time of exposure of the pipelines but reduced to almost a uniform growth rate after a long time of exposure of the pipelines. The reliability of the pipelines was also determined based on Weibull probability function using different distribution forms for the simulation of the maximum pit depth and operating parameters. The work was

tested on a 3700 km transmission pipeline by comparing the pit depth distribution measured with Magnetic Leakage Flux (MFL) in-line-inspection with that from Monte Carlo simulation, linear model and exponential model. It was inferred from the results that linear model could not conservatively predict the future pit depth growth and reliability of the pipeline when compared with that from Monte Carlo simulation and exponential models. The Root Mean Square Percentage Error (RMSPE) estimate of 0.948% was obtained when simulated maximum pit depth was compared with the field data. This is a further prove that Monte Carlo simulation is a vital tool for predicting maximum pit depth growth and estimating reliability of ageing oil and gas pipelines. The result obtained in this work is also showing that this method is useful for predicting future maximum pit depth distribution and reliability of ageing pipelines using only one inspection data. Experts can be able to plan inspection, repairs and maintenance of pipelines when results of future maximum pit depth growth are known however, it is recommended that more testing of this technique be carried out especially with pipelines affected by sour corrosion prior to a robust application.

References

- AHAMMED, M. 1998. Probabilistic estimation of remaining life of a pipeline in the presence of active corrosion defects. *International Journal of Pressure Vessels and Piping*, 75, 321-329.
- AHAMMED, M. & MELCHERS, R. 1996. Reliability estimation of pressurised pipelines subject to localised corrosion defects. *International Journal of Pressure Vessels and Piping*, 69, 267-272.
- ALAMILLA, J. & SOSA, E. 2008. Stochastic modelling of corrosion damage propagation in active sites from field inspection data. *Corrosion Science*, 50, 1811-1819.
- ASME, 2009, Manual for determining the remaining strength of corroded pipelines. American Society of Mechanical Engineers, B31G, New York.
- BAZÁN, F. A. V. & BECK, A. T. 2013. Stochastic process corrosion growth models for pipeline reliability. *Corrosion Science*, 74, 50-58.
- CALEYO, F., GONZALEZ, J. & HALLEN, J. 2002. A study on the reliability assessment methodology for pipelines with active corrosion defects. *International Journal of Pressure Vessels and Piping*, 79, 77-86.
- CALEYO, F., VELÁZQUEZ, J., VALOR, A. & HALLEN, J. 2009. Probability distribution of pitting corrosion depth and rate in underground pipelines: A Monte Carlo study. *Corrosion Science*, 51, 1925-1934.

- CHANDRASATHEESH, C., JAYAPRIYA, J., GEORGE, R. & MUDALI, U. K. 2014. Detection and analysis of microbiologically influenced corrosion of 316 L stainless steel with electrochemical noise technique. *Engineering Failure Analysis*, 42, 133-142.
- CHEN, Y., HOWDYSHELL, R., HOWDYSHELL, S. & JU, L.-K. 2014. Characterizing pitting corrosion caused by a long-term starving sulfate-reducing bacterium surviving on carbon steel and effects of surface roughness. *Corrosion*, 70, 767-780.
- CHOOKAH, M., NUHI, M. & MODARRES, M. 2011. A probabilistic physics-of-failure model for prognostic health management of structures subject to pitting and corrosion-fatigue. *Reliability Engineering & System Safety*, 96, 1601-1610.
- DAWOTOLA, A. W., VAN GELDER, P., CHARIMA, J. & VRIJLING, J. 2011. Estimation of failure rates of crude product pipelines. *Applications of Statistics and Probability in Civil Engineering—Faber, Köhler & Nishijima (eds) Taylor & Francis Group, London.*
- DAWSON, J., BRUCE, K. & JOHN, D. 2001. Corrosion risk assessment and safety management for offshore processment facilities.
- ENGELHARDT, G. & MACDONALD, D. 1998. Deterministic prediction of pit depth distribution. *Corrosion*, 54, 469-479.
- HASAN, S., KHAN, F. & KENNY, S. 2012. Probability assessment of burst limit state due to internal corrosion. *International Journal of Pressure Vessels and Piping*, 89, 48-58.
- HASSANI, S., ROBERTS, K., SHIRAZI, S., SHADLEY, J., RYBICKI, E. & JOIA, C. Flow loop study of chloride concentration effect on erosion, corrosion and erosion-corrosion of carbon steel in CO₂ saturated systems. *CORROSION 2011, 2011. NACE International.*
- HU, J., TIAN, Y., TENG, H., YU, L. & ZHENG, M. 2014. The probabilistic life time prediction model of oil pipeline due to local corrosion crack. *Theoretical and Applied Fracture Mechanics*, 70, 10-18.
- JEPSON, W. & MENEZES, R. 1995. The effects of oil viscosity on sweet corrosion in multiphase oil/water/gas horizontal pipelines. *NACE International, Houston, TX (United States).*
- KATANO, Y., MIYATA, K., SHIMIZU, H. & ISOGAI, T. 2003. Predictive model for pit growth on underground pipes. *Corrosion*, 59, 155-161.
- LAYCOCK, P., COTTIS, R. & SCARF, P. 1990. Extrapolation of extreme pit depths in space and time. *Journal of the Electrochemical Society*, 137, 64-69.
- LI, S.-X., YU, S.-R., ZENG, H.-L., LI, J.-H. & LIANG, R. 2009. Predicting corrosion remaining life of underground pipelines with a mechanically-based probabilistic model. *Journal of Petroleum Science and Engineering*, 65, 162-166.
- MELCHERS, R. 2010. Estimating uncertainty in maximum pit depth from limited observational data. *Corrosion Engineering, Science and Technology*, 45, 240-248.
- MELCHERS, R. E. 2008. Extreme value statistics and long-term marine pitting corrosion of steel. *Probabilistic Engineering Mechanics*, 23, 482-488.

- MOHD, M. H. & PAIK, J. K. 2013. Investigation of the corrosion progress characteristics of offshore subsea oil well tubes. *Corrosion Science*, 67, 130-141.
- NACE 2005, NACE Standard RP0775, Preparation, installation, analysis, and interpretation of coupons in oilfield operations, 2005, Houston, TX
- OSSAI, C. I. 2013. Pipeline corrosion prediction and reliability Analysis: A systematic approach with Monte Carlo simulation and degradation models. *International Journal of Scientific & Technology Research*, 2.
- OWEN, R., CHAUHAN, V., PIPET, D. & MORGAN, G. Assessment of corrosion damage in pipelines with low toughness. 14th Biennial joint technical meeting on pipeline research, Berlin, 2003.
- PANDEY, M., YUAN, X.-X. & VAN NOORTWIJK, J. 2009. The influence of temporal uncertainty of deterioration on life-cycle management of structures. *Structure and Infrastructure Engineering*, 5, 145-156.
- PAPAVINASAM, S., DOIRON, A. & REVIE, R. W. 2010. Model to predict internal pitting corrosion of oil and gas pipelines. *Corrosion*, 66, 035006-035006-11.
- RODRIGUEZ III, E. & PROVAN, J. 1989. Part II: development of a general failure control system for estimating the reliability of deteriorating structures. *Corrosion*, 45, 193-206.
- SHEIKH, A., BOAH, J. & HANSEN, D. 1990. Statistical modeling of pitting corrosion and pipeline reliability. *Corrosion*, 46, 190-197.
- SHOESMITH, D. W., TAYLOR, P., BAILEY, M. G. & OWEN, D. G. 1980. The formation of ferrous monosulfide polymorphs during the corrosion of iron by aqueous hydrogen sulfide at 21 C. *Journal of the Electrochemical Society*, 127, 1007-1015.
- SOARES, C. G. & GARBATOV, Y. 1999. Reliability of maintained, corrosion protected plates subjected to non-linear corrosion and compressive loads. *Marine Structures*, 12, 425-445.
- VALOR, A., CALEYO, F., ALFONSO, L., VIDAL, J. & HALLEN, J. M. 2014. Statistical analysis of pitting corrosion field data and their use for realistic reliability estimations in non-piggable pipeline systems. *Corrosion*, 70, 1090-1100.
- VALOR, A., CALEYO, F., HALLEN, J. M. & VELÁZQUEZ, J. C. 2013. Reliability assessment of buried pipelines based on different corrosion rate models. *Corrosion Science*, 66, 78-87.
- VALOR, A., CALEYO, F., RIVAS, D. & HALLEN, J. 2010. Stochastic approach to pitting-corrosion-extreme modelling in low-carbon steel. *Corrosion Science*, 52, 910-915.
- VELÁZQUEZ, J., CALEYO, F., VALOR, A. & HALLEN, J. 2009. Predictive model for pitting corrosion in buried oil and gas pipelines. *Corrosion*, 65, 332-342.
- VELAZQUEZ, J., VALOR, A., CALEYO, E., VENEGAS, V., ESPINA-HERNANDEZ, J., HALLEN, J. & LOPEZ, M. 2009. Pitting corrosion models improve integrity management, reliability. *Oil & Gas Journal*, 107, 56-56.

- ZHANG, R., GOPAL, M. & JEPSON, W. 1997. Development of a mechanistic model for predicting corrosion rate in multiphase oil/water/gas flows. NACE International, Houston, TX (United States).
- ZHANG, S. & ZHOU, W. 2013. System reliability of corroding pipelines considering stochastic process-based models for defect growth and internal pressure. *International Journal of Pressure Vessels and Piping*, 111, 120-130.
- ZHANG, S. & ZHOU, W. 2014. Bayesian dynamic linear model for growth of corrosion defects on energy pipelines. *Reliability Engineering & System Safety*, 128, 24-31.
- ZHANG, S., ZHOU, W. & QIN, H. 2013. Inverse Gaussian process-based corrosion growth model for energy pipelines considering the sizing error in inspection data. *Corrosion Science*, 73, 309-320.

Chapter 5 - Stochastic modelling of perfect inspection and repair actions for leak-failures prone internal corroded pipelines

5.0 Introduction

Utilization of pipelines for transportation of oil and gas from production fields to refineries and loading terminals has resulted in the deterioration of the pipelines over time. This deterioration, which is caused predominantly by corrosion (Nesic 2007, Fang, Brown & Nescaronicacute 2011, Singer *et al.* 2011), results in pipe-wall thinning and reduction in reliability (Ma *et al.* 2013, Ossai 2013). Although corrosion inhibitors and biocides have played a significant role in the reduction of the rate of pipe-wall thinning (Hu *et al.* 2011), the problem of pipeline corrosion, especially, internal ones, has impacted the operations and maintenance cost of oil and gas companies as it accounts for over 50% of the downtimes in the industry (HSE 2001, CAPP 2009, AER 2013).

The need to establish optimal inspection and repair policy is vital for risk quantification in operating oil and gas pipelines, hence, the reason why numerous researchers have worked on different aspects of risk optimization models for corroded pipelines (Ahammed 1997, Dawotola *et al.* 2011, Ossai 2013, Ma *et al.* 2013, Sahraoui, Khelif & Chateauneuf 2013, Hu *et al.* 2014). Gomes, Beck & Haukaas (2013) addressed inspection and maintenance optimization of corroded pipelines by using Monte Carlo simulation to sample and evaluate expected number of failures and repairs. These authors determined an optimal inspection and failure cost based on their model. The work of Wang & Zarghamee (2014) also focused on estimating the reliability of corroded pipelines using finite element analysis and Monte Carlo simulation. This research, which determined the retained strength of corroded pipelines at different defect sizes was aimed at establishing the fitness-for-service of corroded pipelines. And also establish the optimal inspection and maintenance schedules that will ensure the safety of operations. Hasan, Khan & Kenny (2012) also used Monte Carlo simulation and First Order Second Moment (FOSM) method to establish the failure probability of internal corroded oil and gas pipelines, after analysing the remaining mechanical hoop strength capacity of the corrosion defects. Sahraoui, Khelif & Chateauneuf (2013) on their part proposed an inspection and

maintenance policy, which was based on an imperfect inspection by considering the probability of corrosion defect detection and wrong assessment of defect sizes. These researchers had an ultimate aim of ensuring that the reliability of corroded pipelines is determined to a high degree of accuracy. Other researchers (Dawotola *et al.* 2011) approached corroded pipeline maintenance optimization for general corrosion, pitting corrosion and stress corrosion cracking from the point of failure frequency and the associated consequences of failure to health, safety and environment. They also optimized maintenance intervals in order to minimize cost. Again, Zhou (2010) evaluated the reliability of corroded pipelines under the influence of internal operating pressure. The author modelled the reliability with respect to corrosion induced failures as - small leakage, large leakage and rupture.

Since corrosion is a function of uncertainties associated with the operating environment of the pipelines, it is always necessary to monitor the variability of the environment, materials and technique used for acquiring the data used for predicting the growth of corrosion defects of Pipeline (Maes *et al.* 2009, Ossai, Boswell & Davies 2015a). To establish the deterioration arising from these external and internal constraints in a pipeline, a hierarchical Bayes framework, which used multi-level generalized least square was adopted for estimating corrosion defect growth while modelling the uncertainties in the operability of the material and environment (Maes, Faber & Dann 2009). Similarly, in order to optimize the service life of structures, a 2-stage inspection based maintenance management framework was used (Sheils *et al.* 2012). This technique, which considered deterioration defects and sizing error of detection of the defects, have the potentials of minimizing lifecycle cost of structures and optimizing the inspection intervals.

Optimal maintenance and repair planning involves the establishment of the acceptable failure probability level for the corroded pipelines, in consideration of cost. This also involves checking alternative inspection and repair policies, in order to establish the most appropriate for the expected pipeline reliability. Since the retained strength of corroded pipeline has direct link to the corrosion wastage at a given time, failure limit functions- leakage, burst and rupture have been established by different authors in consideration of stochastic corrosion growth rate (Ahammed 1997, Sahraoui, Khelif & Chateauneuf 2013, Hu *et al.* 2014). Hence, managing

corroded pipelines effectively entails, understanding the expected time of leakage, burst and rupture failures, as the corrosion wastage changes over time.

From the foregoing discussion, it can be seen that much has been done on reliability management of corroded pipelines. However, to the best of the knowledge of the authors, there have not been notable research on inspection and repairs optimization, in consideration of stochastic and probabilistic risk quantification. This situation motivated the authors to carry out such research using Markov modelling, Monte Carlo simulation and degradation modelling by focusing on the stochastic behaviour of corrosion defect depths. First order Markov chain modelling will be used in this paper for proposing the model, seeing that it has been used for establishing the effect of corrosion defect depth growth on corroded pipelines and other facilities by other researchers (Louis 2003 Sinha & Mckim 2007, Ana & Bauwens 2010, Zhang & Gao 2012, Valor *et al.* 2013). The successful use of first order Markov chain modelling in different research areas such as corrosion has also made it an established principle for solving real life problems that requires sequence modelling, control tasks, machine learning and stochastic modelling.

This paper, therefore, aims to utilize information about corrosion wastage times to estimate inspection and repair procedures for internally corroded pipelines, subjected to failure by leakage. As such, inspection and repair planning is expected to be done in consideration of the corrosion wastage times of the pipelines at the lifecycle transition phases – introduction-maturity, maturity-ageing, ageing-terminal, terminal-failure and failure-leakage. The objective of this research is to model stochastically, leak-prone pipeline failure by considering different inspection and repairs alternatives associated with the corroded pipeline and estimate the cost. Even though numerous research works have been carried out on different aspects of inspection and maintenance cost models for corroded pipelines, the consideration of the lifecycle phases of corroded pipelines in inspection and repairs cost determination that is considered in this research is novel. Although we have assumed a perfect inspection that results in a non-significant measurement error of corrosion defects, it is important to note that the model developed in this research has a higher potentials of cost savings for inspection and repairs actions requiring leak failure. This is because other researchers have considered the threshold defect depth that will

trigger inspection and repair of corroded pipelines as 50% (Gomes & Beck 2013) whereas this paper has taken this defect threshold as 80% in consideration of ASME standard (ASME 1991). Again, this research also considered the failure probability of the pipeline at different lifecycle phases in the determination of the survival probability, which is vital for estimating the inherent risk at any lifecycle phase of a corroded pipeline. It is also expected that the knowledge of the inspection and repair cost developed in this research will be useful for determining the future cost of pipeline integrity management as corrosion defect depths grow.

5.1 Markov modelling concept

A Markov Process is a stochastic system which has future events only depending on current ones without reference to previous events. This peculiarity makes a Markov Decision Process (MDP) to be memoryless since the impact of previous events on future occurrences are not recognized in predicting the future events (Cekyay & Ozekici 2012, White III & white 1989). The growth of corrosion defects of a pipeline has a typical memoryless system since the future corrosion defects growth rates and initiation locations on the pipeline does not depend on the previous corrosion defect sizes or spots. This is because the growth rates of existing corrosion defects and new corrosion defects initiation, depend on the characteristics of the operational parameters (Stephens & Nessim 2006, Nesic 2007, Papavinasam, Doiron & Revie 2010, Cole *et al.* 2011, Ossai, Boswell & Davies 2015) that fluctuate with time and location on a pipeline. The interaction of the operating parameters and the pipeline material and specific behaviours of the corrosion process - stable and meta-stable states of a localized corrosion such as pitting (Melchers 2008, Valor *et al.* 2013) also stochastically influence corrosion defects and contribute to the memoryless behaviour. The undependability of future corrosion defect depths on previous ones is the reason for the randomness of corrosion defects growth rates at different times for a given pipeline. This is why unique multi- corrosion defects growth rates and new defects initiation spots are identified during repeated in-line-inspection (ILI) as exemplified by different researchers (Nessim *et al.* 2008, Caleyó *et al.* 2009).

If a discrete time stochastic process X_t , $t=0, 1, 2, \dots$ is represented by a state space

S, such that $S = \{0, 1, 2, \dots, N_s-1\}$ or $\{1, 2, \dots, N_s\}$, then for all i and j in S , the relationship in Equation (5.1) holds for a time homogeneous process (Kulkarni 2011).

$$P\{(X_{t+1} = j | X_t = i, X_{t-1}, \dots, X_0) = P(X_{t+1} = j | X_t = i)\} \quad (5.1)$$

For a finite action set $A = \{a_1, a_2, \dots, a_n\}$ and discrete time points $t_0, t_1, t_2, t_i, t_{i+1}, \dots$, the future state of the stochastic process X_{t+1} is independent of the previous states X_0, X_1, \dots, X_{t-1} but depends only on X_t and can be written as shown in Equation (5.2) for a 1-steps stochastic processes (Kulkarni 2011).

$$P^{(1)}(j|i, a) = P(X_{t+1} = j | X_t = i, A_t = a)_{\forall i, j \in X_t, a \in A, t=1, 2, \dots} \quad (5.2)$$

where $P^{(1)}(j|i, a)$ is the probability of a 1-step Markov process that the next state is in j at time $t+1$ and the current state is in i and the action a is taken at time t .

For an m -step transition matrix with next state j' at a time $t+1$ and action a is taken at current state i' and time t (Equation (5.3)), to be a stochastic matrix, the relationship in Equation (5.4) will hold, since there will be no inherent negative values in the Markov processes (Feldman & Valdezffores 2010, Kulkarni 2011).

$$P_{i', j'}^m = \begin{bmatrix} P_{1,1}^m & P_{1,2}^m & \dots & P_{1,N_s}^m \\ P_{2,1}^m & P_{2,2}^m & \dots & P_{2,N_s}^m \\ \vdots & \vdots & \ddots & \vdots \\ P_{N_s,1}^m & P_{N_s,2}^m & \dots & P_{N_s,N_s}^m \end{bmatrix}_{\forall i', j' \in S, a \in A, t=1, 2, \dots} \quad (5.3)$$

$$\begin{cases} P^m(j'|i', a) \geq 0, & \text{for } 1 \leq i', j' \leq N_s \\ \sum_{j=1}^{N_s} P^m(j'|i', a) = 1, & \text{for } 1 \leq i' \leq N_s \end{cases} \quad (5.4)$$

In Markov decision process, a state space, $S' = \{S_1, S_2, S_3, \dots, S_t\}$ remains in a particular state for a given exponential length of time and then transits to another state as shown in Figure 5.1 (Feldman & Valdezffores 2010). If the time for the transition from one state to another is such that the condition in Equation (5.5) holds,

$$\begin{cases} t_{i+1} = \min\{t > t_i | X_t \neq X_{t_i}\} \\ S_t = X_{t_i} \end{cases} \quad (5.5)$$

Then, the sojourn time $\{t_{i+1}-t_i\}$ can be described using Markov's memoryless property according to Equation (5.6).

$$P\{(t_{i+1} - t_i) \leq t | S_0, \dots, S_{t_i}, t_0, \dots, t_i\} = P\{(t_{i+1} - t_i) \leq t | S_{t_i}\} \quad (5.6)$$

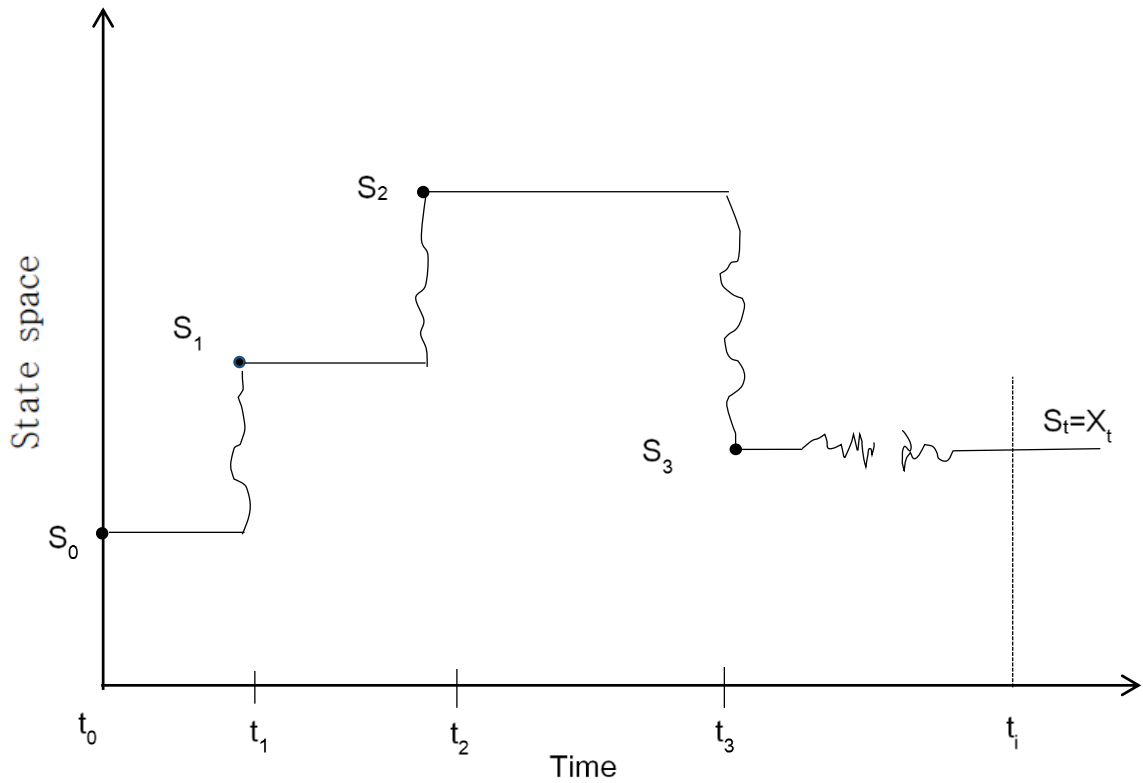


Figure 5.1: State transition & Sojourn time of a Markov Process

For a stochastic process, X_t under finite state space S' and transition times denoted as t_0, t_1, t_i, \dots , and space state denoted by S_0, S_1, \dots , there are scalar quantities $\mu(i)$ for $i \in S$ that describes the mean sojourn rates as shown in Equation (5.7) (Feldman & Valdezffores 2010).

$$P\{t_{i+1} - t_i \leq t | S_t = i\} = 1 - e^{-\mu(i)t} \quad (5.7)$$

If R is the policy resulting from a set of decision processes such that $R = \{\pi_1, \pi_2, \dots, \pi_t\}$ where π_t is the decision at time point t , the transition matrix ($P\pi_t$) and reward $r(\pi_t)$ at time t will be given as shown in Equations (5.8) and (5.9) (Kallenberg 2011).

$$P\pi_t = \sum_{a \in A} P^m(j|i, a) * \pi_t^m(i, a), \forall ij \in S, t=1, 2, \dots, \quad (5.8)$$

$$r(\pi_t)i = r_t^m(i) * \pi_t^m(i, a), \forall ij \in S, a \in A, t=1, 2, \dots, \quad (5.9)$$

For a finite planning horizon over a period N , a policy R and initial state $i \in S$, the expected total reward will be given by Equation (5.10).

$$V_i^N(R) = \sum_{t=1}^N \mathbb{E}_{i,R}\{r_t^m(A_t)\} = \sum_{t=1}^N \sum_{j,a} \mathbb{P}_{t,R}\{S_t = j, A_t = a\} * r_t^m(j, a), i \in S \quad (5.10)$$

Where $\mathbb{E}_{i,R}$ is the expectation operator with respect to the probability measure ($\mathbb{P}_{t,R}$) at time t and reward R .

Over an infinite horizon, the expected total reward can be expressed as a function of the discounted rate γ , according to the expression in Equation (5.11).

$$V_i^\gamma(R) = \sum_{t=1}^{\infty} \mathbb{E}_{i,R}\{\gamma^{t-1}, r_t^m(A_t)\} = \sum_{t=1}^{\infty} \gamma^{t-1} \sum_{j,a} \mathbb{P}_{t,R}\{S_t = j, A_t = a\} * r_t^m(j, a), i \in S \quad (5.11)$$

5.2 Characterizing pipeline lifecycle phases

Assets generally deteriorate with years in operation with a resultant increased failure probability. However, ageing assets are more susceptible to failure due to the degradation of the material components of the assets. Pipelines degradation are caused majorly by stress-driven damages, cracking and fracture resulting from metallurgical and environmentally induced conditions that normally result in pipe-wall thinning (Wintle *et al.* 2006, Horrocks *et al.* 2010). This pipe-wall thickness reduction have been reported by many researchers to emanate from corrosion and erosion mechanisms going on in the pipelines (Nesic 2007, Fang, Brown & Nescaronicacute 2011, Singer *et al.* 2011, Ossai 2012). In order to characterize the

lifecycle phases of the pipelines, the pipe-wall thickness (P_{WT}) loss was used as a measure of the fraction of the Remaining Useful Life (R_{UL}) by recognizing the maximum corrosion wastage $\{D_{max}(t)\}$ of the pipeline at a given time according to the expression in Equation (5.12). The lifecycle phases were later categorized into five stages (Wintle *et al.* 2006) in consideration of critical milestones in the pipeline wall thickness loss.

$$R_{UL}(t) = 1 - \frac{D_{max}(t)}{P_{WT}} \quad (5.12)$$

Equation (5.13) and Figure 5.2 shows the variation of the lifecycle phases of corroded pipelines with the fraction of the remaining useful life.

$$\left\{ \begin{array}{l} 0.9 \leq R_{UL} \leq 1 \text{ for } S_{IM} \\ 0.7 \leq R_{UL} < 0.9 \text{ for } S_{MA} \\ 0.4 \leq R_{UL} < 0.7 \text{ for } S_{AT} \\ 0.2 \leq R_{UL} < 0.4 \text{ for } S_{TF} \\ 0 \leq R_{UL} < 0.2 \text{ for } S_{FL} \end{array} \right. \quad (5.13)$$

where S_{IM} , S_{MA} , S_{AT} , S_{TF} and S_{FL} represents the transition of the pipeline lifecycle phases between introduction and maturity, maturity and ageing, aging and terminal and terminal and failure respectively.

At the introduction-maturity phase of the pipeline, the minimum retained pipe-wall thickness (PWT) is 90% and the pipeline is expected to perform as good as new seeing that the microstructural composition of the pipeline material is not significantly altered. However, when the retained PWT is 70% at maturity-ageing phase, some of the physical and chemical characteristics of the pipeline must have been lost as a result of corrosion. Despite the fact that the operators of the pipeline can establish the corrosion trend at this phase, the prevalence of localized corrosion can result in the reduced retained strength of the pipeline. At 40% retained PWT at ageing-terminal phase, the pipeline could start having more defects that could aid in the increased alteration of the physical and chemical characteristics of the pipeline material. When the retained PWT is 20% at terminal-failure phase, the pipeline could

fail, hence the recommendation to replace the pipeline (ASME 2001). However, if the pipeline gets to the failure state when the PWT is less than 20%, the pipeline can fail by bursting or rupture due to the significant loss of retained strength and the possible accumulation of other defects.

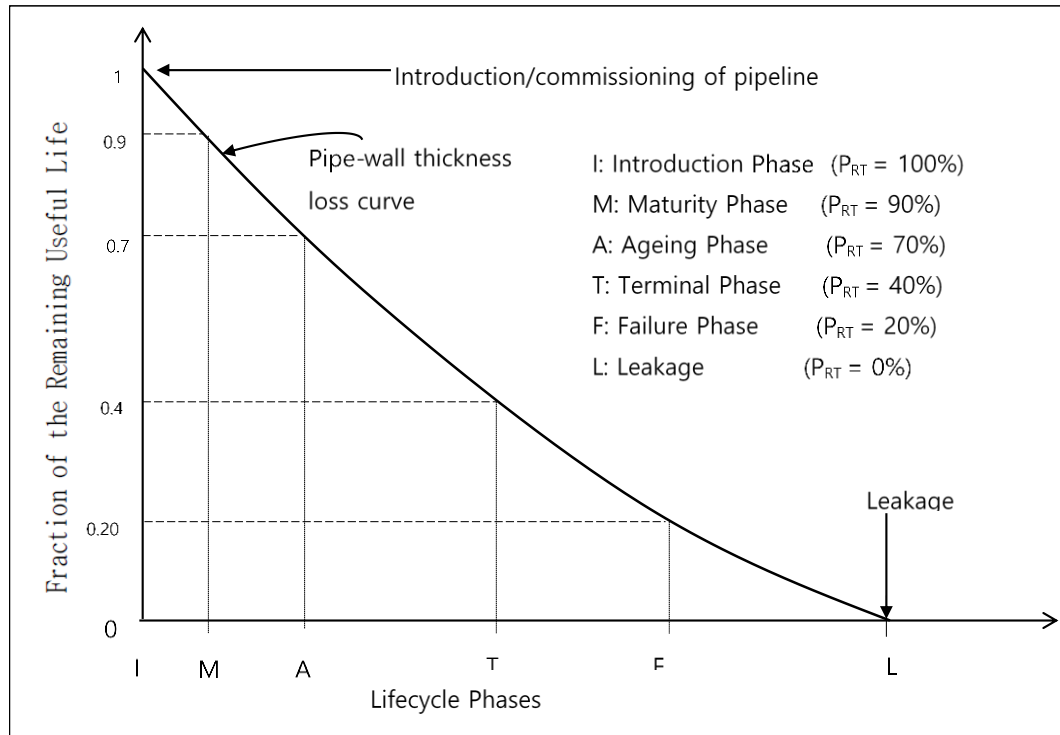


Figure 5.2: Variation of corroded pipeline lifecycle phases with the RUL

At the time of introduction/commissioning of a pipeline into operation, there is practically no significant corrosion process going on in it, since all necessary steps are taken to maintain the integrity of the pipes during construction of the pipeline. However, when the pipelines start transporting oil and gas, which could be in a multiphase flow regime after commissioning them into operation, the interaction of the corrosive species such as CO₂, H₂S, propionic acids, acetic acids, oxygen and chloride ion (Louis 2003, Nescic 2007, Papavinasam, Doiron & Revie 2010) with the carbon steel material of the pipeline results in a corrosion process (Cole *et al.* 2011, Ossai 2012). At the time of introducing the pipeline into operation, the pipe-wall thickness is intact as there is no corrosion process going on at this instant, hence, the retained pipe-wall thickness is 100%. As the pipeline commences operation, the passivity of the carbon steel material of the pipeline is destroyed over time due to

the electrochemical and mechanical actions associated with the corrosive species (Abdallah 2004, Valcarce & Vazquez 2009) and other subcutaneous materials such as sand coming from the production wells (Papavinasam, Doiron & Revie 2010, Biomorgi *et al.* 2012). This destruction of the passivation of the carbon steel material of the pipeline normally results in the start of corrosion process, which brings about pipe-wall thickness loss over the lifecycle phase of the pipeline.

The corrosion of pipeline can result in a uniform loss of pipe-wall thickness over time and localized loss of pipe-wall thickness at discrete random portions of the pipeline (Ossai 2012). The rate of the corrosion of the pipeline depends on some factors that includes the transport mechanism (flow rate), the characteristics of the pipeline material and the concentration of the corrosive species (Nesic 2007, Ossai, Boswell & Davies 2015). Corrosion generally affects the lifecycle phase of a pipelines, which depends on the amount of pipe-wall thickness loss over the duration of exposure to a corrosive environment. This implies that lower corrosion rates will result in longer time to loss the pipe-wall thickness, hence increased time to get to the lifecycle phases whereas higher rates of corrosion will result in the opposite effect.

The pipe-wall thickness loss due to corrosion results in distinctive lifecycle phases of the pipelines – Introduction, maturity, ageing, terminal, failure and leakage. The introduction phase of the pipeline lifecycle phase represents the time immediately after the pipeline is commissioned into operation with the pipe-wall thickness being intact. The maturity phase of the pipeline lifecycle phase follows immediately after the introduction phase of the pipeline. The maturity phase is reached when the retained pipe-wall thickness is 90%. The time between the commissioning of the pipeline and the time 10% of the pipe-wall thickness is loss to corrosion, helps experts to determine the corrosion wastage rate of the pipeline based on practical field data, obtained from different operational conditions. The corrosion rate information collected at this lifecycle phase of the pipeline is vital for planning Corrosion Risk Assessment (CRA) and In-Line Inspection (ILI) (HSE 2001, Venkatesh & Farinha 2006) while establishing whether or not the pipeline is corroding according to the design. Establishing the rate of corrosion of the pipeline at this lifecycle phase also guide the experts on the quantity and quality of corrosion

inhibitors (if required), that will be necessary for maintaining the integrity of the pipeline. The corrosion rate between the introduction and maturity lifecycle phases of the pipeline has been shown to be higher than the corrosion rate at other lifecycle phases based on power model. The ageing lifecycle phase of the pipeline is reached when the retained pipe-wall thickness of the pipeline is 70%. The transition between maturity and ageing phase is notable for stable corrosion wastage rate, due to the management practice applied to the pipeline. The corrosion rate at this phase is lower than that at the previous phase. At this phase, In-Line-Inspection (ILI) is also scheduled in order to determine the areas of the pipeline that is affected by localized corrosion since, the predicted future corrosion rate is always based on general corrosion, which is uniform. At the terminal lifecycle phase of the pipeline, the retained pipe-wall thickness is 40% and the corrosion wastage rate continuous to decrease at the transition between ageing and terminal phases. Due to the reduced retained pipe-wall thickness of the pipeline at this phase, it is easier for the pipeline to fail if the corrosion defect is accompanied by other defects such as cracking, dents and out-of-roundness. At this lifecycle phase, ILI is performed at a more frequent rate than the other lifecycle phases due to the increased risk of failure of the pipeline.

At the failure lifecycle phase, the retained pipe-wall thickness is 20%. Although the pipeline may not practically fail at this phase if there are no other corrosion defects, however, due to the increased risk of pipeline failure, the pipeline is monitored closely by experts. The rate of corrosion at this phase is lowest in comparison to the other phases (Caleyo *et al.* 2009). The pipeline is expected to leak when all the pipe-wall thickness is lost to corrosion at discrete defect spots, even for a pin-hole opening. However, it is never a practical option for operators of pipelines to allow the pipelines to leak but cost and operational constraints have repeatedly made it difficult to manage the pipeline integrity by repairs, maintenance and replacement (Wang & Zarghamee 2014).

5.2.1 Remaining Useful Life(RUL) and failure probability of corroded pipeline

The remaining Useful Life (RUL) is vital for estimating the retained strength of pipelines at a given time in consideration of corrosion defects (Ahammed 1997).

Hence, monitoring the remaining pipe-wall thickness using techniques that includes in-line inspection, on-line inspection, risk based inspection and process control (Hu *et al.* 2014) are vital for risk quantification and safety estimation during the service life of the pipeline. To forestall catastrophic failures and prevent pipeline leakages, different regulatory agencies for the oil and gas sector have set benchmarks for determining the strength of defective oil and gas pipelines such as those undergoing internal corrosion. These standards which guide experts in predicting the strength of the corroded sections of the pipelines have been based on the remaining pipe-wall thickness hence, the reason for choosing the remaining useful life for categorizing pipeline lifecycle phases.

Utilization of pipelines for oil and gas gathering results in deterioration, which is commonly caused by corrosion and erosion as was previously stated, however, inspection and repair actions have the ability to reduce the effect of the corrosion and erosion actions (Hu *et al.* 2011, Vega *et al.* 2008). Although worn-out pipe-wall thicknesses cannot grow back on its own, but repair actions such as attaching of new sleeves and replacement of sections of corroded pipelines will result in the safety at such spots due to the additional wall thickness of the sleeve/replaced section. This repair action results in reduced failure probability at such corrosion defect spots as shown in Figure 5.3.

According to Figure 5.3, it is expected that when a pipeline is commissioned into operation at point A, presumably, without corrosion defects, it systematically loses its wall thickness over time until point B, when repair takes place at time t_n . Despite the fact that the loss of pipe-wall thickness will generally vary with the category of corrosion, the only major difference will be that, it will take shorter time to loss the same pipe-wall thickness for severe corrosion rate ($>0.25 \text{ mmyr}^{-1}$) (NACE 2005) than low corrosion rate of ($<0.025 \text{ mmyr}^{-1}$) (NACE 2005). Since pipe-wall thickness loss due to corrosion can follow power law model (Ossai, Boswell & Davies 2015b), it is expected that pipe-wall loss at time t_{n+1} will be at point D, however, repair at point B resulted in the RUL of the pipeline at the defect spot being, at either C or E. It could be noted that point E could normally result from replacement of a section of the pipeline whereas point C could be as a result of localized repair using steel or composite sleeves. This repair action in point B will reduce the failure

probability of the pipeline at the corrosion defect spot B, to E' or C' instead of D' expected for the defect spot, if no repair was undertaken (see Figure 5.4).

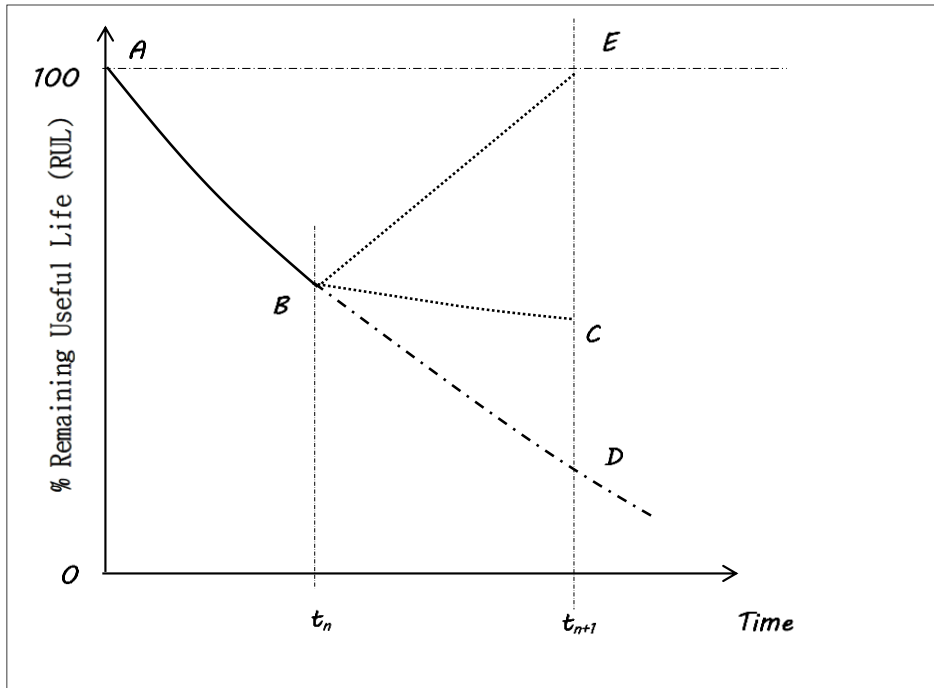


Figure 5.3: Effect of maintenance and repair on the remaining useful life of corrosion defect spots of corroded pipelines

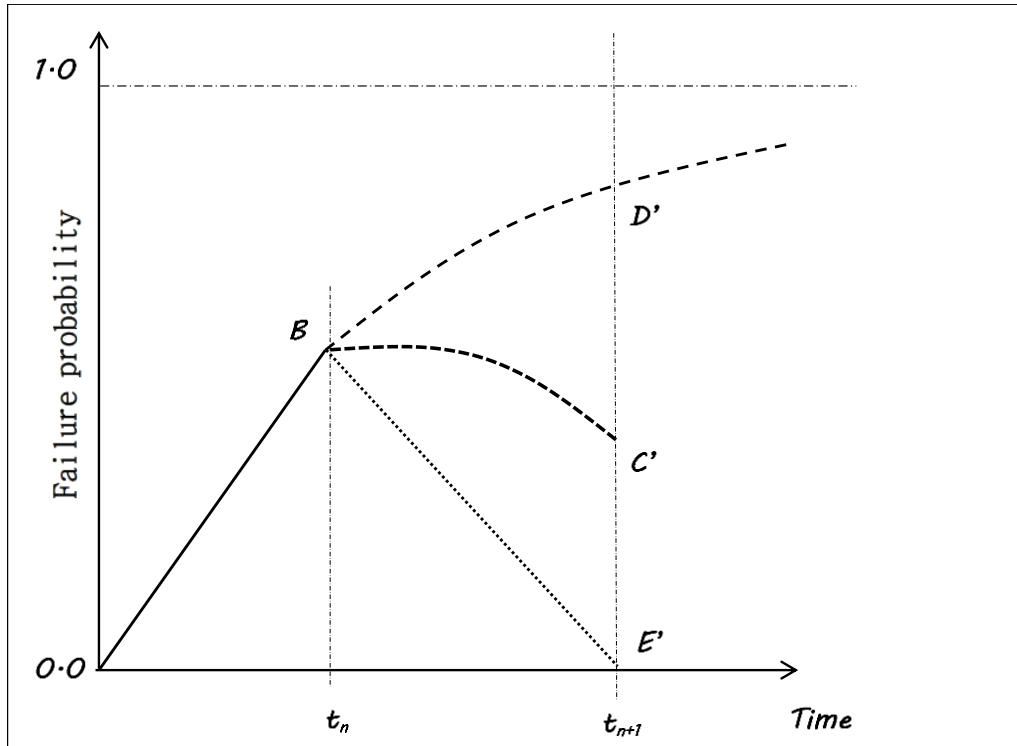


Figure 5.4: Impact of pipeline inspection and repairs on failure probability of a corroded defect spot

5.3 Modelling corroded pipeline inspection and repair actions

To effectively evaluate the effect of inspection and repairs on the lifecycle phases of pipelines, the pipe-wall thickness degradation rate with time of exposure of the pipeline to corrosion need to be considered. Since the RUL is a function of the remaining pipe-wall thickness after a given time of corrosion effect (HSE 2001), the state space S of the lifecycle phases of the corroded pipeline have therefore been described as a function of the transition between different lifecycle phases with $S = \{S_{IM}, S_{MA}, S_{AT}, S_{TF}, S_{FL}\}$. As already shown in Equation (5.13), S_{IM} , S_{MA} , S_{AT} , S_{TF} , S_{FL} represents the fraction of the remaining pipe-wall thickness at 90% or more, 70% or less than 90%, 40% or less than 70%, 20% or less than 40% and 0% or less than 20% respectively. Again S_{IM} is termed to be an excellent condition of the pipeline whereas S_{MA} , S_{AT} , S_{TF} and S_{FL} represent good, fair, poor and unacceptable conditions respectively.

Three repair actions $A = \{a_1, a_2, a_3\}$ are assumed to be predominant for managing the corrosion defect depths of the pipelines at different times of in-line

inspection. Repair actions a_1 , a_2 and a_3 , which represents major repair, minor repair and no repair actions respectively, may be undertaken after ILL inspection on a spot having corrosion defect depth (d_i) depending on the pipe-wall thickness loss.

5.4 Markovian modelling of inspection and repair of corroded pipeline

Research has shown that pipeline corrosion may not always be uniform throughout the lifespan of a pipeline. For pitting corrosion, pit initiation, stabilization and meta-stabilization states, results in differential corrosion wastage rates at different stages of the pipelines lifecycle duration (Melchers 2008, Valor *et al.* 2013). Corrosion defect depths show a stochastic behaviour (Rivas *et al.* 2008, Valor *et al.* 2013), which makes it useful for using Markov's modelling for analysing the transition probabilities based on corrosion wastage rates.

5.4.1 Transition probabilities of inspection and repair actions

To establish the transition probabilities of the corroded pipeline at the stipulated lifecycle phases considered in this research, the following procedures were taken:

- Determine the statistical best fit distribution of the corrosion defect depths of the pipeline measured in the field.
- Utilize Monte Carlo simulation to establish the time lapse for the loss of the pipe-wall thickness due to corrosion.
- Estimate the parameters for corrosion wastage using the time lapse for pipe-wall thickness loss.
- Calculate the transition probabilities for inspection and repair actions using the parameters determined in the previous step.

5.4.2 Best fit statistical distribution of corrosion defect depths

The statistical best fit distribution for the corrosion defect depths were determined by testing distribution functions such as exponential, normal, lognormal, Weibull, Gamma, inverse Gaussian and generalized extreme value distributions. These distribution functions have been predominantly used for establishing the distribution of corrosion defect depths by other researchers (Melchers 2008, Valor *et al.* 2013,

Ossai, Boswell & Davies 2015b). Akaike Information criterion (AIC), which have also been used to determine the statistical best fit of corrosion defect depths (Katano *et al.* 2003) was used to establish the best fit distributions.

5.4.3 Time lapse of corrosion wastage of the pipeline

In order to establish the time lapse for the corrosion defect depth growth, Monte Carlo simulation, which utilized Poisson Square Wave Process (PSWP) described by other researchers (Bazan & beck 2013, Zhang & Zhou 2013) was adopted. The procedure, which involved the utilization of the statistical best fit of the corrosion defect depths for estimating future corrosion wastage of the pipeline, assumed that the time of corrosion wastage is independently exponentially distributed (Dawotola *et al.* 2011, Bazan & beck 2013) and follows a Poisson arrival rate (λ_t). The cumulative corrosion wastage of the pipe-wall thickness and cumulative time for the wastage were collectively determined in the simulation process. However, the cumulative times for the corrosion defect depths growth generated by the simulation runs were utilized for establishing the parameters for determining the transition probabilities. The framework for the simulation process is shown in Figure 5.5.

5.4.4 Estimation of the parameters of corrosion wastage time

The corrosion wastage times estimated in the previous section were assumed to follow a Weibull probability distribution pattern shown in Equation (5.14) (Ossai, Boswell & Davies 2015c).

$$\begin{cases} f(t) = \alpha\lambda(\alpha t)^{\lambda-1}e^{-(\alpha t)^\lambda}, & t > 0, \lambda > 0, \alpha > 0 \\ F(t) = 1 - e^{-(t/\alpha)^\lambda}, & t > 0, \lambda > 0, \alpha > 0 \\ 0 & \text{otherwise} \end{cases} \quad (5.14)$$

where λ , α , $f(t)$, $F(t)$ are shape parameter, scale parameter, probability and cumulative density functions respectively. Based on Equation (5.14), the corrosivity time (C_T) at the lifecycle phases of the pipeline was calculated according to Equation (5.15).

$$C_T = \alpha(-\log(\kappa))^{\frac{1}{\lambda}} \quad (5.15)$$

where κ represents the fraction of retained pipe-wall thickness at the lifecycle phases.

5.4.5 Transition probability at the lifecycle phases

The failure intensity (η) shown in Equation (5.16), determined by the Weibull parameters was used to calculate the transition probability (T_P) according to Equation (5.17).

$$\eta = \frac{\lambda}{\alpha} \left(\frac{C_T}{\alpha} \right)^{\lambda-1} \quad (5.16)$$

$$T_P = e^{-\eta C_T} \quad (5.17)$$

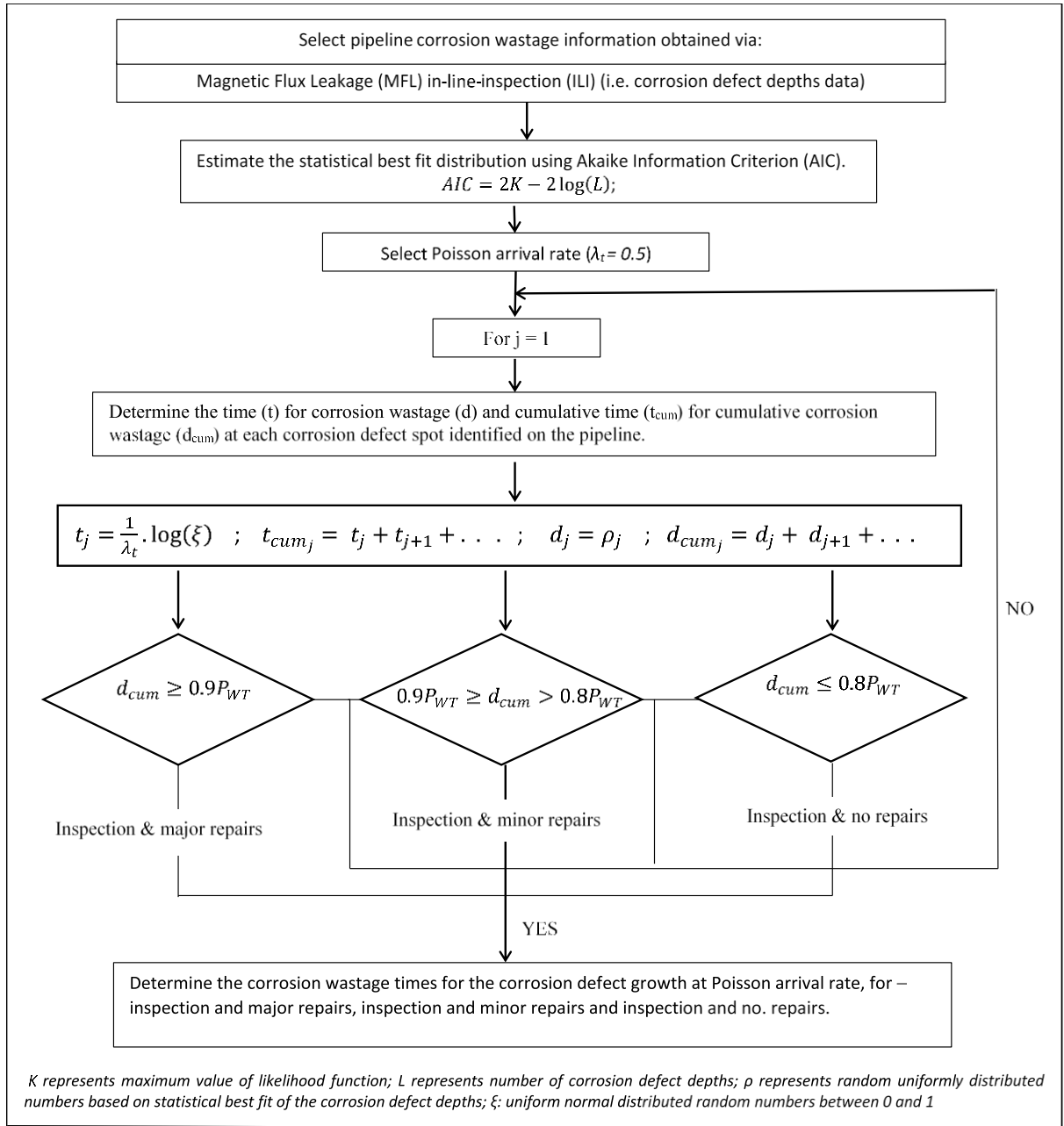


Figure 5.5: Framework for Monte Carlo simulation of corrosion wastage time of corrosion defect depth

5.5 Probability of failure distribution

The time for failure (t_{fail}) of the pipeline due to corrosion wastage can be determined using Equation (5.18) (Hokstad & Frovig 1996, Feldman & Valdezffores 2010) whereas the survivor function ($R_s(t)$) at time t is shown in Equation (5.19).

$$t_{fail} = \min(t_{IM}, t_{MA}, t_{AT}, t_{TF}, t_{FL}) \quad (5.18)$$

where t_{IM} , t_{MA} , t_{AT} , t_{TF} and t_{FL} represents the cumulative lifecycle durations of the pipeline at introduction-maturity, maturity-ageing, ageing-terminal, terminal-failure and failure-leakage lifecycle phases respectively.

$$R_S(t) = P(t_{fail} > t) = R_{IM}(t) \cdot R_{MA}(t) \cdot R_{AT}(t) \cdot R_{TF}(t) \cdot R_{FL}(t) \quad (5.19)$$

where R_{IM} , R_{MA} , R_{AT} , R_{TF} and R_{FL} represents the survivor function of the pipeline at introduction-maturity, maturity-ageing, ageing-terminal, terminal-failure and failure-leakage lifecycle phases respectively.

The survivor functions at the lifecycle phases of the pipeline are shown in Equation (5.20).

$$\begin{cases} R_{IM} = P(T_{IM} > t) = e^{-\eta_{IM} \cdot t} \\ R_{MA} = P(T_{MA} > t) = e^{-\eta_{MA} \cdot t} \\ R_{AT} = P(T_{AT} > t) = e^{-\eta_{AT} \cdot t} \\ R_{TF} = P(T_{TF} > t) = e^{-\eta_{TF} \cdot t} \\ R_{FL} = P(T_{FL} > t) = e^{-\eta_{FL} \cdot t} \end{cases} \quad (5.20)$$

where η_{IM} , η_{MA} , η_{AT} , η_{TF} and η_{FL} represents the failure intensity of the pipeline at introduction-maturity, maturity-ageing, ageing-terminal, terminal-failure and failure-leakage lifecycle phases respectively.

If the failure intensities at the lifecycle phase were random and independently occurring, the availability (A_{CR}) of the pipeline with respect to corrosion wastage at a future time (τ) can be expressed according to Equation (5.21) (Hokstad & Frovig 1996).

$$A_{CR} = \frac{1}{\tau} \int_0^{\tau} R_S(t) dt \quad (5.21)$$

Equation (5.21) can be further simplified to Equation (5.22) whilst the probability of failure (P_{fail}) can be expressed according to Equation (5.23).

$$A_{CR} = \left(\frac{1}{\tau(\eta_{IM} + \eta_{MA} + \eta_{AT} + \eta_{TF} + \eta_{FL})} \right) (1 - e^{-(\eta_{IM} + \eta_{MA} + \eta_{AT} + \eta_{TF} + \eta_{FL})\tau}) \quad (5.22)$$

$$P_{fail} = 1 - A_{CR} \quad (5.23)$$

5.6 Holding time over state-action pair

If the expected holding time for state action pair is given by $\psi(i,a)$ for a finite decision horizon and $\zeta(i,a)$ for an infinite decision horizon, then Equation (5.24) gives the holding time of different lifecycle transition phases over a finite time of exposure T_{finite} and infinite decision horizon (Kulkarni 2011).

$$\left\{ \begin{array}{l} \psi(i, a) = \sum_{t=1}^T P_{i,j}^{(t)}, \forall i, j \in S, a \in A, t = 1, 2, \dots, T_{finite} \quad , \text{for finite horizon} \\ \zeta(i, a) = \lim_{t \rightarrow \infty} \sum_{t \rightarrow \infty} P_{i,j}^{(t)}, \forall i, j \in S, a \in A, t = 1, 2, \dots \quad , \text{for infinite horizon} \end{array} \right. \quad (5.24)$$

5.7 Inspection and repair cost

The cost of inspection and repair is expected to vary at different times over a finite decision horizon (Hokstad & Frovig 1996), however at an infinite horizon, the long run cost will be steady (Kulkarni 2011). If the cost of a state-action pair is given by $c(i,a)$, then the cost of inspection and repairs over a finite ($g_c(i,a)$) and infinite ($L_c(i,a)$) decision horizons can be expressed as Equation (5.25) (Kulkarni 2011).

$$\left\{ \begin{array}{l} g_c(i, a) = \psi(i, a) * c(i, a), \quad \text{for finite horizon} \\ L_c(i, a) = \zeta(i, a) * c(i, a), \quad \text{for Infinite Horizon} \end{array} \right. \quad (5.25)$$

5.8 Pipeline inspection and repair policy

The internally corroded pipeline is subjected to failure by leakage at discrete points of the pipeline due to corrosion defect depth and a perfect inspection that results in non-significant measurement error existed. After Magnetic Flux Leakage (MFL) in-Line Inspection (ILI), the points on the pipeline that have gone beyond a certain threshold of the pipe-wall thickness is repaired based on the condition stated in Equation (5.26). For case 3, major repair action is undertaken whilst case 2 and case 1 results in minor repair and no repair actions respectively.

$$\begin{cases} \text{case 1: } 0 < d_i < 0.8P_{WT} & \text{for } a_3 \\ \text{case 2: } 0.8P_{WT} < d_i \leq 0.9P_{WT} & \text{for } a_2 \\ \text{case 3: } 0.9P_{WT} < d_i \leq 0.8 P_{WT} & \text{for } a_1 \end{cases} \quad (5.26)$$

It was assumed that the repairs on the defect depths are done independently of each other, hence a corrosion defect spot can be subjected to major, minor or no repair after an ILI. The pipeline is assumed to be under general corrosion, which results in pipe-wall thickness loss of varying quantities at different spots. It was also assumed that the pipeline has no other defects that could result in burst and rupture in operation. Although the cost of failure by leakage may be small compared to burst or rupture failure (Zhang & Zhou 2014), however, it is still pertinent to determine the expected cost of failure by leakage of the pipelines, as it also significantly contribute to operational expenditure of the company. The in-line inspection (ILI) is expected to be scheduled based on the expected pipe-wall thickness loss prediction, but the inspection should be done at most every 5 years (American Gas Association 2011). The ILI inspection will be scheduled before 5 years if the expected corrosion defect depth growth at corrosion defect spots are predicted to get to the threshold for repair (Equation (5.26)) prior to the 5 years of regular ILI. However, because of the cost associated with this process, if a defect spot is expected to get to any of the thresholds for minor or major repairs within 2 years from the time of ILI (based on modelling of the corrosion defect depths), it is repaired at that time of inspection. Again, it was assumed that any corrosion defect depth repaired by a minor or major repair will be as good as new. This is possible since, the replaced section of the pipeline in case of major repair or sleeve re-encirclement in case of minor repair will have available pipe-wall thickness that is equivalent or more than the original pipe-wall thickness. Based on this scenario, it is reasonable to assume that the quality of the repair job is good enough to support the pipeline for at least the entire duration of exposure of the pipeline prior to the repair. Hence, the assumption that after repair on a corrosion defect spot, it will not be repaired again until the pipeline is decommissioned. There is no inspection and repair required at the end of the service life of the pipeline.

5.9 Strategy for future inspection and repair cost evaluation

For an internally corroded pipeline subjected to periodic inspection and repair action, the cost of inspection and repair ($C_{IR}(t)$) at time t can be expressed according to Equation (5.27).

$$C_{IR}(t) = \left(C_{ILI} + C_{ma} \sum_{i=1}^{n_{ma}} d_m + C_{mi} \sum_{i=1}^{n_{mi}} d_n \right) (\gamma + 1)^t \quad (5.27)$$

where $C_{IR}(t)$, C_{ILI} , C_{ma} , n_{ma} , d_m , C_{mi} , n_{mi} , d_n represents cost of inspection and repairs, cost of in-line inspection, unit cost of a major defect repair, number of major repair spots in a pipeline, corrosion defect depth needing major repairs, cost of minor repair of a defect, number of minor repairs in a pipeline and corrosion defect depth needing minor repairs respectively at the time of inspection t . The cost of inspection and repairs is shown in Table 5.1. It is important to note that the cost shown in Table 5.1, which is based on the information from (American Gas Association 2011, Thompson 2011, Thompson no date) is about half of the current cost of Magnetic Flux Leakage (MFL) in-line-inspection for energy pipelines.

Table 5.1: Cost of Magnetic Flux Leakage In-Line Inspection of energy pipeline

Description of activity	cost (\$)	Remark
Major repairs	1,500	for a given defect spot
Minor repairs	800	
Inspection	2900	Per Km

Source: (American Gas Association 2011, Thompson 2011, Thompson no date)

The reward for inspection and repair action (R_{IR}) at any of the lifecycle phase transition will depend on the total cost of in-line-inspection (ILI) and repair cost associated with either major or minor repairs. To establish the reward at each lifecycle phase of the pipeline, the expected duration of the lifecycle phases of the pipeline, the predetermined interval of ILI inspection (ℓ) and the cost of inspection and repair (\$/Km-yr.) for the state-action pairs were used according to Equation (5.28).

$$R_{IR} = \frac{C_i}{\ell} * \begin{cases} t_{IM} , & \text{for } S_{IM} \\ t_{MA} - t_{IM} , & \text{for } S_{MA} \\ t_{TA} - t_{MA} , & \text{for } S_{AT} \\ t_{TF} - t_{TA} , & \text{for } S_{TF} \\ t_{FL} - t_{FT} , & \text{for } S_{FL} \end{cases} \quad (5.28)$$

To predict the future cost of inspection and repair for an in-line inspected pipeline undergoing internal corrosion, Monte Carlo simulation and degradation modelling were employed to predict the corrosion defect growth over a specified inspection duration. The procedure employed is as follows:

- Generate future corrosion defect depths over a stated period T_{future} , for $t_i, t_{i+1}, \dots \in T_{future}$. Where t_i represents the time of initial future inspection after ILI.
- Determine the time of next ILI by considering the predicted future corrosion defect depths generated by Monte Carlo simulation or degradation modelling. Hence for predicted corrosion defect depths $d_i, d_{i+1}, d_{i+2}, \dots, d_{i+n}$, at inspection time t_i , establish the appropriate inspection and repair strategy based on Equation (5.26).
- Calculate the number of corrosion defect depths that require major and minor repairs.
- Determine the cost of inspection and repair at inspection times t_i and repeat the steps for inspection times $t_{i+1}, t_{i+2}, \dots \in T_{future}$.
- Compute the cumulative cost of inspection and repair at future time T_{future} by adding up the inspection and repair costs at inspection times $t_i, t_{i+1}, \dots \in T_{future}$.

5.10 A case study of internal corroded X52 pipeline

This model was tested on a 219.1 mm, 8.7 mm thick and 3.7 km API X52 grade gathering pipeline that was internally inspected using Magnetic Flux Leakage (MFL) in-line-inspection (ILI) in 2012. This gathering pipeline delivers multiphase fluid from oil and gas fields in the Niger Delta region of Nigeria and has 1037 corrosion wastage points dictated during ILI. The minimum and maximum pipe-wall thickness loss of the pipeline recorded during the inspection are 10% and 60% respectively.

Table 5.2: Akaike Information Criterion (AIC) Values for different distributions pit depth

Distribution	AIC
Exponential	5270.30
Normal	3613.75
Gamma	3545.99*
Weibull	3642.98
Gaussian Inverse	3550.49
Generalized Extreme Value	3556.77
Lognormal	7689.28

*represents the statistical best-fit distribution

Table 5.2 shows the AIC values for the tested probability distribution functions. Since the lowest AIC value represents the best statistical fit (Katano *et al.* 2003), Gamma distribution with AIC value of 3545.99 represents the statistical best fit for the corrosion defect depths of the pipeline. Although research has previously shown that corrosion defect depth can be best fitted with Gamma distribution (Caleyo *et al.* 2009, Mohd & Paik 2013), however, lognormal distribution (Bazan & Beck 2013, Ossai, Boswell & Davies 2015b) and Weibull distribution (Mohd & Paik 2013) have been reported by other researchers as well. The probability density functions of the corrosion defect depths established with different probability distributions and the field data distribution of the corrosion defect depths are shown in Figure 5.6.

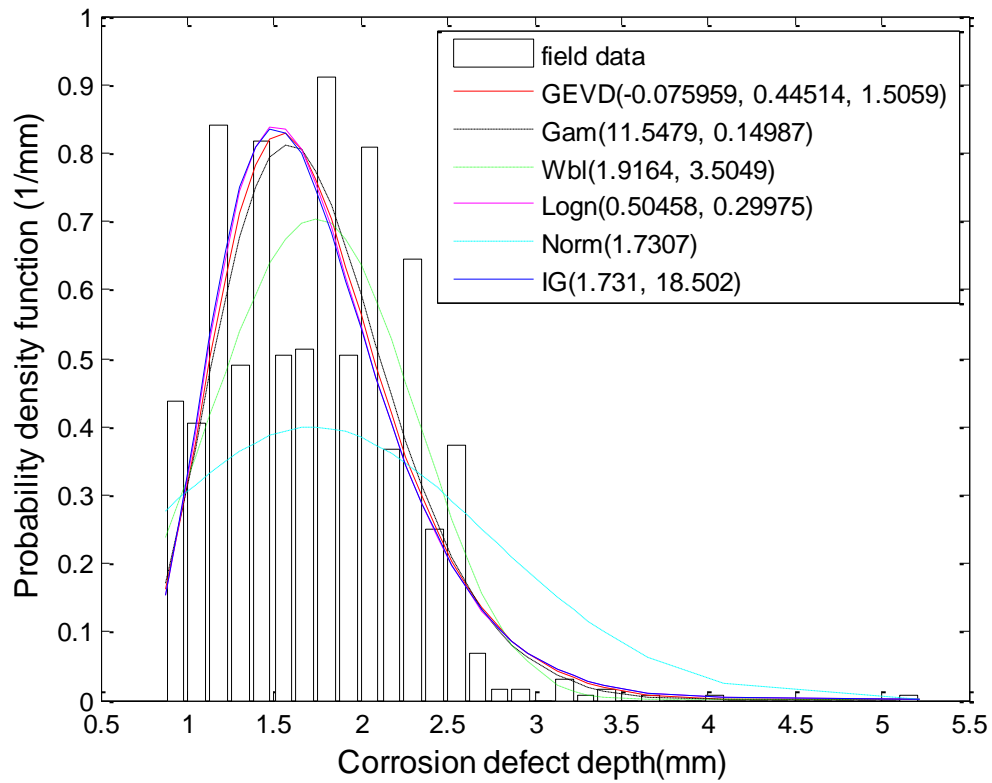


Figure 5.6: Field data and probability density distribution of the corrosion defect data for different probability density functions

5.11 Estimation of corrosion wastage parameters and transition probabilities

The Weibull parameters of the corrosion wastage time of defect depths for the various inspection and repair actions is shown in Table 5.3.

Table 5.3: Parameters of Weibull distribution

Inspection and repair action	Scale Parameter (α)	Shape Parameter (λ)
Inspection and major repairs	26.311	2.1863
Inspection and minor repairs	24.1053	2.2786
Inspection and no repair	22.277	2.554

The transition probabilities over a finite decision horizon computed for different inspection and repair actions using Equations (5.14) – (5.19) and information in Table 5.3 is shown in Table 5.4 whereas the steady state transition probabilities and failure intensities are shown in Table 5.5.

Table 5.4: Transition Probability Over a finite horizon

inspection and minor repair action					Inspection and major repair action					Inspection and no repair action				
S _{IM}	S _{MA}	S _{AT}	S _{TF}	S _{FL}	S _{IM}	S _{MA}	S _{AT}	S _{TF}	S _{FL}	S _{IM}	S _{MA}	S _{AT}	S _{TF}	S _{FL}
0.77	0.23	0.00	0.00	0.00	0.74	0.26	0.00	0.00	0.00	0.64	0.36	0.00	0.00	0.00
0.00	0.54	0.46	0.00	0.00	0.00	0.50	0.50	0.00	0.00	0.00	0.40	0.60	0.00	0.00
0.00	0.00	0.31	0.69	0.00	0.00	0.00	0.29	0.71	0.00	0.00	0.00	0.22	0.78	0.00
0.00	0.00	0.00	0.19	0.81	0.00	0.00	0.00	0.17	0.83	0.00	0.00	0.00	0.13	0.87
0.97	0.00	0.00	0.00	0.03	0.97	0.00	0.00	0.00	0.03	0.98	0.00	0.00	0.00	0.02

Table 5.5: Transition Probability (TP) and Failure Intensity (FI) of the state action pairs for the corroded pipeline

states	inspection and major repair action		inspection and minor repair action		inspection and no repair action	
	FI	TP	FI	TP	FI	TP
S _{IM}	0.0426	0.4258	0.0511	0.4037	0.0702	0.3507
S _{MA}	0.0558	0.2124	0.0655	0.2130	0.0856	0.2127
S _{AT}	0.0681	0.1418	0.0787	0.1478	0.0991	0.1619
S _{TF}	0.0766	0.1195	0.0877	0.1269	0.1080	0.1450
S _{FL}	0.0961	0.1005	0.1080	0.1087	0.1275	0.1297

Tables 5.5 indicates that the failure intensity of the pipeline increased with time of exposure to corrosion for all the inspection and repair actions. This is the trend expected from ageing assets, which have the survivability rates reduced with increasing age. Imperatively, the more a pipeline is exposed to corrosion, the more the probability of failure, despite the fact that the corrosion rates may be higher at initial exposure times and slower towards the terminal end of the corrosion wastage cycle of the pipeline (Caleyo *et al.* 2009, Ossai, Boswell & Davies 2015c).

5.12 Failure probability analysis

Figure 5.7 shows the failure probabilities of the pipeline with time lapse of exposure to the corrosive environment. The failure risk of the pipeline varied with the type of inspection and repair action that is undertaken at a given time. If the inspection and repair actions on the pipeline are predominately characterized by major repairs, the probability of failure is expected to be lower than that with minor repair action.

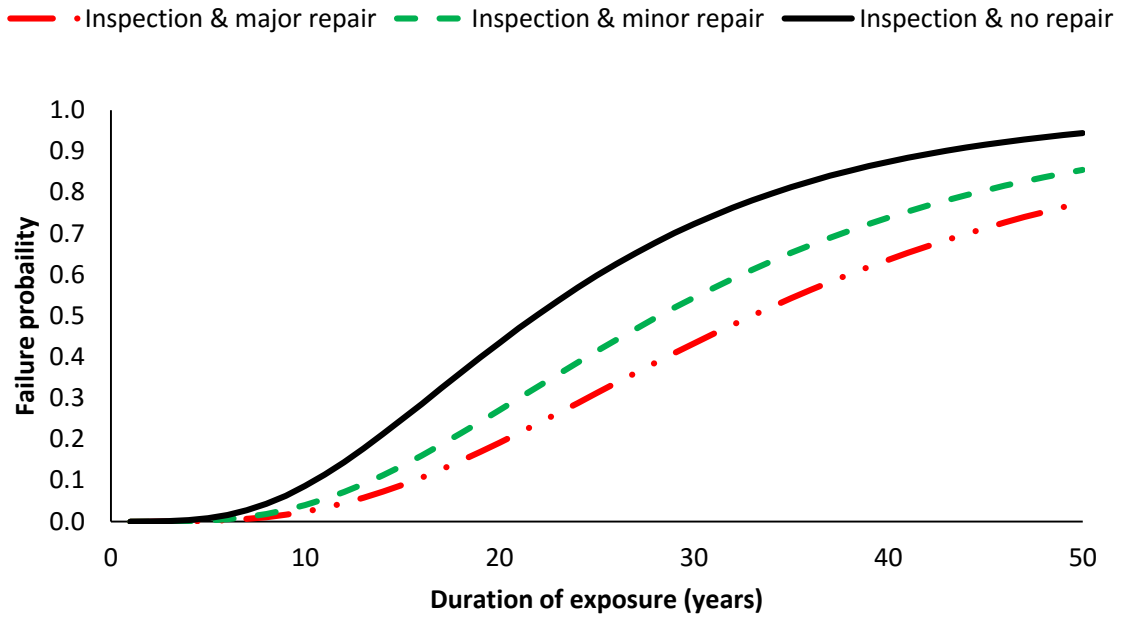


Figure 5.7: Failure probability of corroded pipeline managed with different inspection and repair options

Despite the lower failure probability expected with the inspection and major repair action, the cost of managing the pipeline integrity under this scenario is more than that for the other two options (see Figure 5.8).

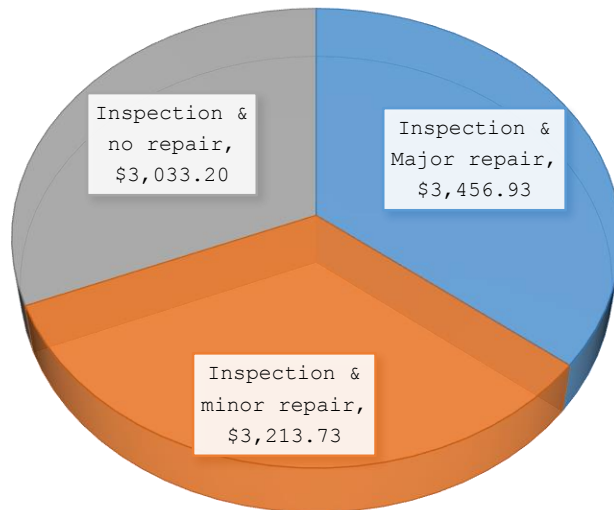


Figure 5.8: Long run inspection and repair cost (per km-yr.) for different inspection and repair options for maintaining a corroded pipeline

With increase in the number of defects on the pipelines, the cost of inspection and repair actions increases across the board for both major and minor repairs but not with spots that need no repair action after ILI inspection as shown in Figure 5.9. If the number of defect spots in a pipeline needing major or minor repairs increases, the cost of repairs increases as shown in the figure. Although there may be isolated cases of this sort of occurrence, however, the company could always make a decision to change a substantial section of a pipeline that has deteriorated due to corrosion, when it is no longer economical to repair.

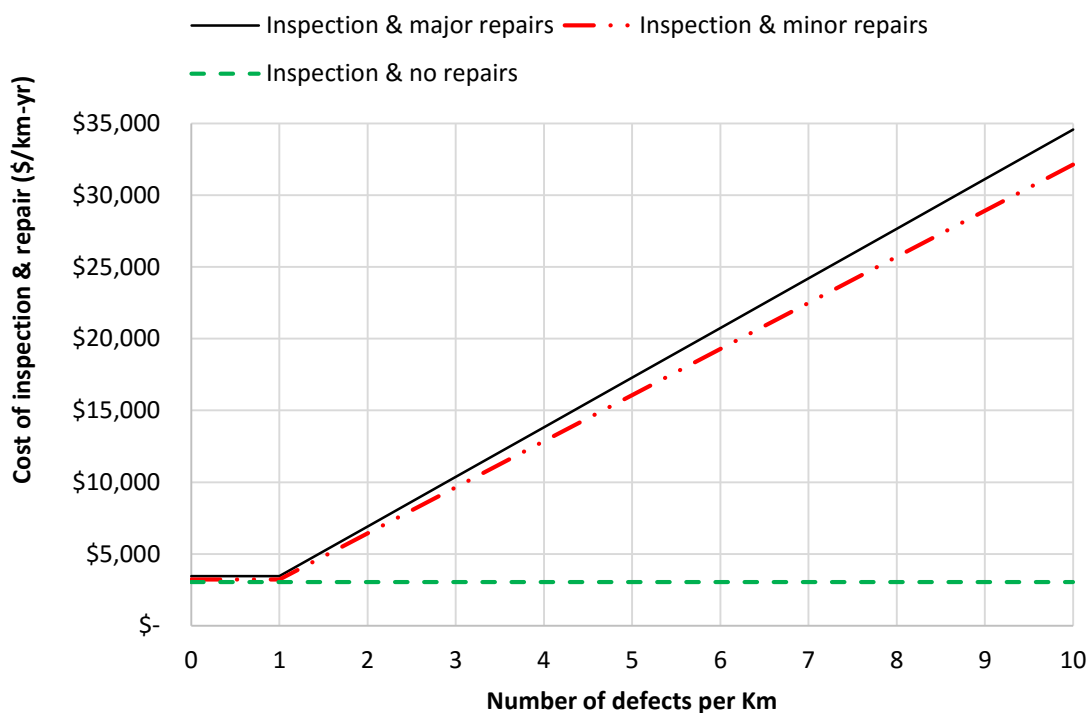


Figure 5.9: Variation of cost of inspection and repairs for number of corrosion defects per kilometre

Over a finite planning horizon, the inspection and repair cost per km of the corroded pipeline is also expected to have inspection and major repair having the highest value, inspection and minor repair having the second highest value whilst inspection and no repair will have the least value. This case is shown in Figure 5.10.

5.13 Future cost of inspection and repair

Managing the integrity of corroded pipelines based on only one of the inspection and repairs action stipulated in this research may not be most economical for stakeholders, since there is need to maintain both integrity and optimize cost at all

times. Hence, a future inspection and repair option for the corrosion defect depths involves the combination of the three inspections and repair options. This is extremely necessary for cost optimization and risk minimization given the fact that the defect rates at the defect spots of the pipelines are always varying. In order to apply the strategy described in section 5.6 to determine the optimal future cost of inspection and repair of the pipeline, it was assumed that-

- I. The corrosion defect depth was growing linearly and hence the future corrosion wastage was determined as a linear model in consideration of the previous corrosion wastage rate at each of the defect spots.
- II. The corrosion defect depths grew randomly but based on discrete corrosion wastage rates. This implies that the corrosion defect depths are expected to grow at random based on the prevalent corrosion wastage rates at the corrosion defect spots on the pipeline. Hence, a spot having small corrosion growth rate may grow more rapidly than those that grew rapidly prior to the ILL of the pipeline and vis-versa.

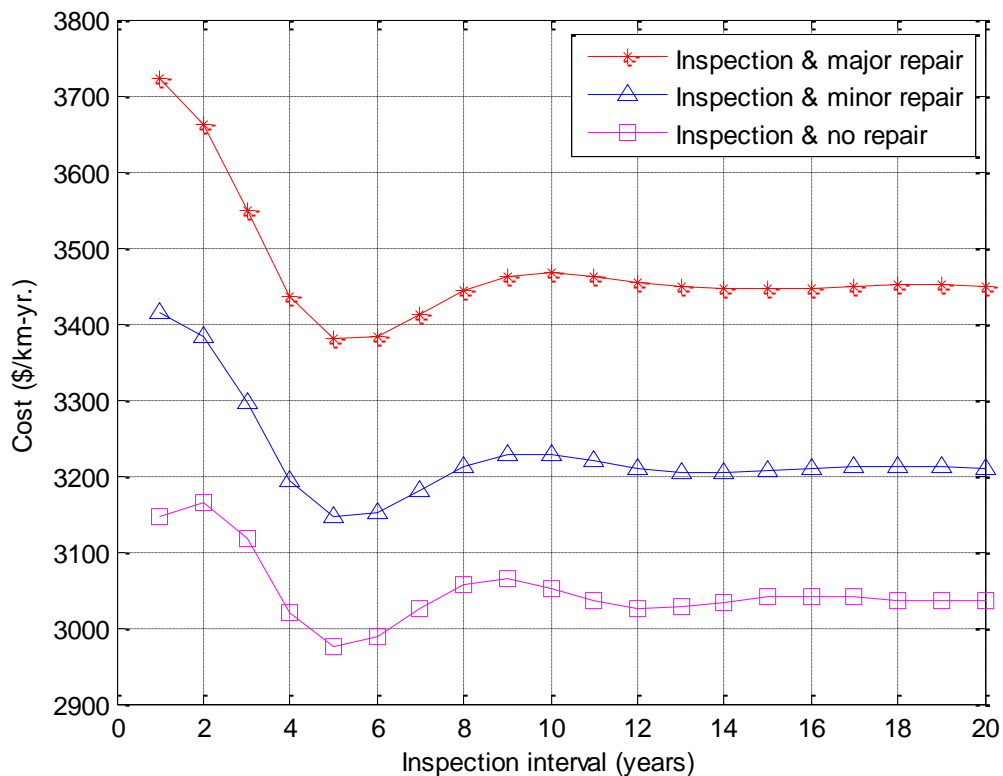


Figure 5.10: Variation of the cost of managing pipeline integrity based on the inspection and repair actions over a finite planning horizon.

The variation of the inspection and repair cost over a future inspection time of 25 years is shown in Figure 5.11. The cumulative cost of inspection and repair of the pipeline based on linear model and random corrosion defect depth growth using Monte Carlo simulation did not show much distinction after 25 years' inspection and repairs. The inspection and repair action that was based on random corrosion defect depth growth was approximately 2% higher than that determined on the basis of linear modelling. This implies that the linear modelling approach could be a potential cost saving approach in comparison to the random corrosion wastage growth. Despite this result, it will be appropriate to compare the future corrosion defect depths growth obtained with this process with that obtained from ILI prior to deciding on the appropriate repair actions.



Figure 5.11: Cost of inspection and repair for different linear predicted and random growth of corrosion defect depth

5.14 Conclusions

Managing of an internally corroded pipeline is a complicated task that involves the calculation of the Remaining Useful Life (RUL) of the pipeline based on the retained pipe-wall thickness at the time of inspection. The retained pipe-wall thickness of the pipeline as a measure of the RUL was used to classify pipeline lifecycle phases at

introduction, maturity, ageing, terminal, failure or leakage. The transition probabilities between these lifecycle phases based on five state Markov decision process were determined using the corrosion wastage rates.

The holding time of different inspection and repair actions over a finite planning horizon was determined for the corroded pipeline whereas the expected failure probability of the corroded pipeline over a given time of exposure of the pipeline to corrosion was determined for the inspection and repair actions considered. The research also described a technique for evaluating future inspection and repair cost of corroded pipelines by relying on the corrosion defect depth information of previous ILI.

The results obtained from this research proves that Markov modelling and Monte Carlo simulation can be utilized for modelling stochastic behaviour of corrosion defect depths. Hence, the ease of determining failure probability and types of repair that is appropriate at a given time in the lifecycle duration of a pipeline and the associated future cost of inspection and repairs. This means that the integrity of corroded pipelines can be maintained whilst optimizing the expected cost of future inspection and repairs of internally corroded pipelines.

References

- AHAMMED, M. 1997. Prediction of remaining strength of corroded pressurised pipelines. *International Journal of Pressure Vessels and Piping*, 71(3), 213-217.
- ALBERTA ENERGY REGULATOR (AER). 2013. Report 2013 - B: Pipeline performance in Alberta, 1990–2012. Available from: <<http://www.aer.ca/documents/reports/R2013-B.pdf>>. [17/09/13].
- AMERICAN GAS ASSOCIATION. 2011. Summary of costs and factors impacting, in-line inspection, direct assessment, pressure testing and pipeline replacements for natural gas transmission pipelines. Available from: <<http://www.aga.org/our-issues/safety/pipeline-safety/Technicalreports/Documents/ILI%20DA%20Hydro%20Replacement%20Cost%20and%20Factors%20Summary%20Final%2004-04-11.pdf>>. [2/12/14].
- BAZÁN, F. A. V. & BECK, A. T. 2013. Stochastic process corrosion growth models for pipeline reliability. *Corrosion Science*, 74, 50-58.
- CALEYO, F., VELÁZQUEZ, J. C., VALOR, A. & HALLEN, J. M. 2009. Markov chain modelling of pitting corrosion in underground pipelines. *Corrosion Science* 51, 2197–2207.

- CAPP.2009. Best Management Practices: Mitigation of internal corrosion in oil effluent pipeline systems, 2009, Calgary Canada. Available from: <<http://www.capp.ca/getdoc.aspx?DocId=155641&DT=PDF>>. [19/6/14].
- CEKYAY, B. & OZEKICI, S. 2012. Optimal maintenance of systems with markovian mission and deterioration, *European journal of Operation Research* 2012, 219, 123-133.
- DAWOTOLA, A. W., VAN GELDER, P., CHARIMA, J. & VRIJLING, J. 2011. Estimation of failure rates of crude product pipelines. *Applications of Statistics and Probability in Civil Engineering*—Faber, Köhler & Nishijima (eds) Taylor & Francis Group, London.
- FANG, H., BROWN, B. & NESCARONICACUTE, S. 2011. Effects of sodium chloride concentration on mild steel corrosion in slightly sour environments, *Corrosion*, 67(1), 015001-1.
- FELDMAN, R. M. & VALDEZ-FLORES, C. 2010. *Applied probability and stochastic processes*, Springer Science & Business Media.
- GOMES, W. J. S., BECK, A. T. & HAUKAAS, T. 2013. Optimal inspection planning for onshore pipelines subject to external corrosion. *Reliability Engineering & System Safety*, 118, 18-27.
- HASAN, S., KHAN, F. & KENNY, S. 2012. Probability assessment of burst limit state due to internal corrosion, *International Journal of Pressure Vessels and Piping*, 89, 48-58.
- HOKSTAD, P. & FROVIG, A.T. 1996. The modelling of degraded and critical failures for components with dormant Failures. *Reliability Engineering and System Safety*, 51, 189–199.
- HORROCKS, P., MANSFIELD, D., PARKER, K., THOMSON, J., ATKINSON, T., WORSLEY, J., ... & PARK, B. 2010. *Managing ageing plant*. Health and Safety Executive, UK: Norwich.
- HSE. 2001. Review of corrosion management for offshore oil and gas processing, HSE offshore technology report 2001/044. Available from: <<http://www.hse.gov.uk/research/otopdf/2001/oto01044.pdf>>. [22/6/14].
- HU, J., TIAN, Y., TENG, H., YU, L. & ZHENG, M. 2014. The probabilistic life time prediction model of oil pipeline due to local corrosion crack. *Theoretical and Applied Fracture Mechanics*, 70, 10-18.
- HU, X., BARKER, R., NEVILLE, A. & GNANAVELU, A. 2011. Case study on erosion–corrosion degradation of pipework located on an offshore oil and gas Facility. *Wear* 271, 1295– 1301.
- KALLENBERG, L. 2011. Markov decision processes. Available from: <<http://www.math.leidenuniv.nl/~kallenberg/Lecture-notes-MDP.pdf>>. [2/12/2014].
- KATANO, Y., MIYATA, K., SHIMIZU, H. & ISOGAI, T. 2003. Predictive model for pit growth on underground pipes. *Corrosion*, 59, 155-161.
- KULKARNI, V. G. 2011. *Introduction to modeling and analysis of stochastic systems*, Springer Texts in Statistics, 2011, DOI 10.1007/978-1-4419-1772-0 2.

- MA, B., SHUAI, J., LIU, D. & XU, K. 2013. Assessment on failure pressure of high strength pipeline with corrosion defects, *Engineering Failure Analysis*, 32, 209-19.
- MAES, M. A., FABER, M. H & DANN, M. R. 2009. Hierarchical modeling of pipeline defect growth subject to ILI uncertainty. ASME 2009 28th International Conference on Ocean, Offshore and Arctic Engineering. American Society of Mechanical Engineers, 2009.
- MELCHERS, R.E. 2008. Extreme value statistics and long-term marine pitting corrosion of steel, *Probabilistic Engineering Mechanics*, 23(4), 482-488.
- MOHD, M.H. & PAIK, J.K. 2013. Investigation of the corrosion progress characteristics of offshore subsea oil well tubes, *Corrosion Science*, 67, 130-141.
- NACE 2005, NACE Standard RP0775, Preparation, installation, analysis, and interpretation of coupons in oilfield operations, 2005, Houston, TX
- NESIC, S. 2007. Key issues related to modelling of internal corrosion of oil and gas pipelines – a review, *Corrosion Science*, 49, 4308-38.
- OSSAI, C.I. 2012. Advances in asset management techniques: An overview of corrosion mechanisms and mitigation strategies for oil and gas pipelines, *ISRN Corrosion*, vol. 2012. <http://dx.doi.org/10.5402/2012/570143>, Article ID 570143.
- OSSAI, C.I. 2013. Pipeline Corrosion prediction and reliability analysis: A systematic approach with Monte Carlo simulation and degradation models. *International Journal of Scientific & Technology Research* 2013, 2(3)
- OSSAI, C.I., BOSWELL, B. & DAVIES, I.J. 2015a. Pipeline failures in corrosive environments – A conceptual analysis of trends and effects. *Engineering Failure Analysis*, 53, 36-58, ISSN 1350-6307
- OSSAI, C.I., BOSWELL, B. & DAVIES, I.J. 2015b. Predictive modelling of internal pitting corrosion of aged non-piggable pipelines. *J. Electrochem. Soc.*, 162(6): C251-C259, doi: 10.1149/2.0701506jes
- OSSAI, C.I., BOSWELL, B. & DAVIES, I.J. 2015c. Estimation of internal pit depth growth and reliability of aged oil and gas pipelines - A Monte Carlo simulation Approach, *Corrosion*, 71(8), 977-99.
- RIVAS, D., CALEYO, F., VALOR, A. & HALLEN, J. 2008. Extreme value analysis applied to pitting corrosion experiments in low carbon steel: Comparison of block maxima and peak over threshold approaches. *Corrosion Science*, 50, 3193-3204.
- SAHRAOUI, Y., KHELIF, R. & CHATEAUNEUF, A. 2013. Maintenance planning under imperfect inspections of corroded pipelines. *International journal of pressure vessels and piping* 104, 76-82.
- SHEILS, E., O'CONNOR, A., SCHOEFS, F. & BREYSSE, D. 2012. Investigation of the effect of the quality of inspection techniques on the optimal inspection interval for structures. *Structure and Infrastructure Engineering: Maintenance, Management, Life-Cycle Design and performance*, 8(6), 557-568.

- SINGER, M., BROWN, B., CAMACHO, A. & NESIC, S. 2011. Combined effect of carbon dioxide, hydrogen sulfide, and acetic acid on bottom-of-the-line corrosion, *Corrosion*, 67(1), 015004-1.
- THOMPSON, N. G. 2011. Gas and Liquid Transmission Pipelines. Corrosion Cost and Preventive Strategies in the United States. Available from: <http://www.dnvusa.com/Binaries/gasliquid_tcm153-378807.pdf>. [2/6/15].
- THOMPSON, N. G. Appendix J- Gas distribution, Available from: <http://www.dnvusa.com/Binaries/gas_tcm153-339949.pdf>. [16/6/15].
- VALOR, A., CALEYO, F., ALFONSO, L., VELÁZQUEZ, J. & HALLEN, J. 2013. Markov chain models for the stochastic modeling of pitting corrosion. *Mathematical Problems in Engineering*, 2013.
- VEGA, O. E., HALLEN, J. M., VILLAGOMEZ, A. & CONTRERAS, A. 2008. Effect of multiple repairs in girth welds of pipelines on the mechanical properties, *Materials Characterization*, 59, 1498-507.
- WANG, N. & ZARGHAMEE, M. 2014. Evaluating fitness-for-service of corroded metal pipelines: Structural Reliability Bases, *Journal of Pipeline Systems Engineering and Practice*, 5, 04013012.
- WHITE, C. C. III & WHITE, D. J. 1989. Markov decision process, *European Journal of Operational Research*, 39, 1-16.
- WINTLE, J., MOORE, P., HENRY, N., SMALLEY, S., & AMPHLETT, G. 2006. Plant ageing: Management of equipment containing hazardous fluids or pressure. *Health and Safety Executive, UK: Norwich*.
- ZHANG, S. & ZHOU, W. 2013. System reliability of corroding pipelines considering stochastic process-based models for defect growth and internal pressure. *International Journal of Pressure Vessels and Piping*, 111, 120-130.
- ZHANG, S. & ZHOU, W. 2014. Cost-based optimal maintenance decisions for corroding natural gas pipelines based on stochastic degradation models, *Engineering Structures*, 74, 74-85.
- ZHOU, W. 2010. System reliability of corroding pipelines. *International Journal of Pressure Vessels and Piping*, 87, 587-595.

Chapter 6 - Markov chain modelling for time evolution of internal pitting corrosion distribution of oil and gas pipelines

6.0 Introduction

Pitting process can be metastable in nature - a situation in which a pitting process starts and stops after a while or immediately (Melchers 2008, Varlor *et al.* 2013) or it can be a stable pitting that nucleates and grows indefinitely. Stable pits generally show stochastic behaviour (Rivas *et al.* 2008, Varlor *et al.* 2013,) and are the focus of many researches. Pitting corrosion is initiated due to:

- i. Electrochemical reactions of the carbon steel surfaces with the environment resulting in formation of surface layers.
- ii. Discontinuity of the carbon steel material as a result of inclusions.
- iii. Removal of already formed surface layer due to erosion (Papavinasam, Doiron & Revie 2010).

Forecasting of pitting corrosion rate has been done by modelling, extrapolation or using expert judgement (Tarantseva 2010). Modelling technique can follow either probabilistic, deterministic or both approaches and has widespread application as exemplified by numerous publications (Sheikh, Boah & Hansen 1990, Valor *et al.* 2010, Valor *et al.* 2013, Yusof, Noor & Yahaya 2014,). Yusof, Noor & Yahaya (2014) studied pitting corrosion of offshore pipelines with Markov chain model and discovered that the prediction was not conservative due to the assumption that the model is linear. The data for the analysis was from repeated in-line inspection (ILI) of internally corroded offshore pipelines. The authors assumed the time of initiation of internal pitting corrosion as 2.9 years (after Velazquez *et al.* 2009a), which is time of initiation of underground pipeline external pitting corrosion. This assumption may invalidate the result of these authors since the environmental condition of the soil is definitely different from that inside the pipeline. Although the future predicted pit depth distribution in this work was based on the exponential parameter (V_p) of power law being 1, the authors proposed Equation (6.1) for predicting the value of V_p for future pit depth distribution. Hence, if the initial pit depth (P_{d_1}), initial time (t_1),

future pit depth (P_{d_2}) and future time (t_2) are known with the pitting initiation time (t_{int}), then:

$$V_p = \frac{\log\left(\frac{P_{d_2}}{P_{d_1}}\right)}{\log\left(\frac{t_2 - t_{int}}{t_1 - t_{int}}\right)} \quad (6.1)$$

The work of Valor *et al.* (2013) focused on pitting corrosion of underground pipelines and corrosion coupons. The authors used discrete pit depths in non-homogenous, continuous time Markov chain modelling to determine the transition probability function by correlating the stochastic mean pit depth with the empirical deterministic pit depth. They used Weibull process for simulation of the pitting induction time. Other researchers such as Caleyó *et al.* (2009) and Rodriguez & Provan (1989) also applied non-homogenous, continuous time pure birth Markov chain modelling to estimate the pit depth distribution of pipelines by using a closed form of Kolmogorov forward equation for the computation of the transition probability function whilst assuming that the pit depth follows a stochastic process. Similarly, Camacho *et al.* (2012) applied Fokker-Planck equation for transition probability function estimate of pitting corrosion of underground pipelines based on a continuous time, non-homogenous pit depth evolution. And Hong (1999) worked on pit initiation and growth processes by modelling pit initiation as a homogenous Poisson process whilst estimating the pit growth with time as a non-homogenous, continuous time Markov process.

Corrosion can result in unscheduled downtime especially for pitting corrosion, crevice corrosion, stress corrosion cracking and fatigue corrosion since they occur without outward signs on the facilities (Engelhardt & Macdonald 1998). Hence, corrosion modelling is used for integrity management via prediction of expected time of pipeline failure so that mitigation actions that could include inspection and repairs will be initiated (Zhang, Zhou & Qin 2013, Valor *et al.* 2010, Valor *et al.* 2013, Velazquez *et al.* 2009a). To establish the time dependent reliability of corroded high pressure offshore pipelines, Zhang & Zhou (2013) determined the expected future internal corrosion wastage distribution due to internal pressure using Poisson square wave process. The authors established the time of pipeline

failure with respect to small leak, large leak and rupture by using in-line inspection data after modelling stochastic pit depth growth with homogenous gamma distribution according to Equation (6.2):

$$f_G(P_d(t)|\alpha(t - t_{int}), \beta) = \frac{\beta^\alpha (t - t_{int}) * P_d(t)^{\alpha(t-t_0)-1} * e^{-P_d(t)^\beta} * I(t)}{\Gamma(\alpha(t - t_{int}))} \quad (6.2)$$

where $f_G(P_d(t)|\alpha(t - t_0), \beta)$ is the probability density function of the pit depth at time t , $\alpha(t - t_0)$ is the time dependent shape parameter, $\Gamma(\cdot)$ is the gamma function, $I(t)$ is an indicator function with values given in Equation (6.3).

$$I(t) = \begin{cases} 1 & \text{if } t > t_{int} \\ 0 & \text{if } 0 \leq t \leq t_{int} \end{cases} \quad (6.3)$$

Bazan & Beck (2013) also used Poisson square wave process to model external pitting corrosion of underground pipelines and concluded that power model gave a more conservative estimate of the future corrosion wastage than random linear model after comparing the results with field inspection data. Similarly, Valor *et al.* (2014) used historic data to determine the reliability of corroded non-piggable upstream pipelines exposed to external corrosion by statistically analysing the acquired data, determining the corrosion distribution at a future time and correlating the results with the designed pipeline failure pressure. The goal of these researchers was to establish a mitigation program aimed at enhancing the lifecycle of the pipelines (Valor *et al.* 2014). The work of Rodriguez III & Provan (1989b) was also aimed at mitigation and control of pitting corrosion by applying Markov chain modelling to determine the future pit depth whilst predicting the remaining useful life of the pipeline at future times based on the pit depth distribution. Other pitting corrosion related researches that are noteworthy includes the work of Valor *et al.* (2014) that used Monte Carlo reliability framework to model different corrosion distributions that included linear growth model, time dependent and time independent models, Markov model and single value distribution model. They utilized both synthetic and field data in evaluating these models whilst considering defect sizes, age and depth of corrosion with time. They concluded that Markov chain predictive model was the

best for describing the corrosion distributions (Valor *et al.* 2013). Caleyó *et al.* (2009b) also used Monte Carlo simulation to model pit depth growth of underground pipelines in different soil conditions and fitted the three maximal extreme value distributions - Weibull, Fretchet and Gumbel to the resulting best fit models of the studied soils, however, Fretchet distribution was best for describing the best fit model over a long-time exposure as was already stated in this work. Again, another work on experimental determination of internal pitting rate of pipelines concluded that increases in pitting rate occurs due to increased chloride concentration, temperature, subcutaneous substances (such as sand) and flow rate whereas decrease in pitting rate was observed with increase in bicarbonate, CO₂ and H₂S partial pressures and operating pressure (Papavinasam, Doiron & Revie 2010). However, the results in this research were validated with limited field data. Pitting corrosion rate has also been modelled by researchers using damage function analysis by considering pit nucleation, growth rate and re-passivation of carbon steel in chloride solution (Engelhardt & Macdonald 1998). The pitting rate for underground pipelines was also predicted with lognormal linear model in consideration of environmental variables (Katano *et al.* 2003) and the time of initiation of pitting has also been predicted for different soil categories using Monte Carlo simulation of field observed soil conditions (Velazquez *et al.* 2009a).

The above reviewed literatures show that limited work has been done on Markov modelling of internal pitting corrosion of oil and gas pipelines and the few works are either flawed due to limited field validation data or are not based on pure birth non-homogenous Markov modelling, hence, the need for a holistic field data analysis of pitting rate distribution using a continuous time non-homogenous linear growth pure birth Markov model. Since effective corrosion modelling requires a combination of electrochemical activities relating to water and oxides transport within the metal surface, macro-environment (such as temperature, pH, humidity, salinity, porosity) and external environment (such as rainfall, seasonal rainfall and temperature fluctuations) (Cole & Marney 2012), it is possible to model internal pitting corrosion of oil and gas pipelines by considering the operating conditions of the pipelines and the pit depths at different ages. The present work is aimed at determining the future distribution of pit depths of internally corroded oil and gas

pipelines by using non-homogenous, continuous time linear growth pure birth Markov process. A multivariate regression analysis of field data was used in a Monte Carlo simulation framework to estimate the time of initiation of the pitting for different categories of pitting rates based on NACE classification. The work used initial knowledge of pit depth distribution to determine the transition probability function of pit depth growth in future time based on the closed form of negative binomial distribution solution of Kolmogorov's forward equation.

6.1 Finite Markov chain modelling of internal pitting corrosion of pipelines

A Markov process has no memory because future events are independent of past ones but dependent on the present event (White III & White 1989) hence, if the pit depth of oil and gas pipeline at time t is represented by (P_d) , then the probability at such a time can be written as Equation (6.3):

$$P\{P_d(t) = i\} = P_i(t), i = 1, 2, \dots, N \quad (6.3)$$

where N represents the number of states the pipeline wall is divided, $P_i(t)$ is the probability that the pit depth is at i^{th} state at time t and can be determined by measuring the pit depth distribution at such a time or by expert knowledge (Varlor *et al.* 2010, Valor *et al.* 2013).

If Figure 6.1 represents a portion of pipeline with wall thickness (w), the time of pit depth distribution shown as a state space variable is represented with Equation (6.4):

$$\{P_d(t), t \in T\} \quad (6.4)$$

It should be noted that the pit depth at any time t is an integral part of the pipeline wall thickness whilst T is the time set for the observation of the pit depth. If a small change in the pipeline wall thickness (δw) results in a pit depth at i^{th} state represented by (P_{d_i}) , then

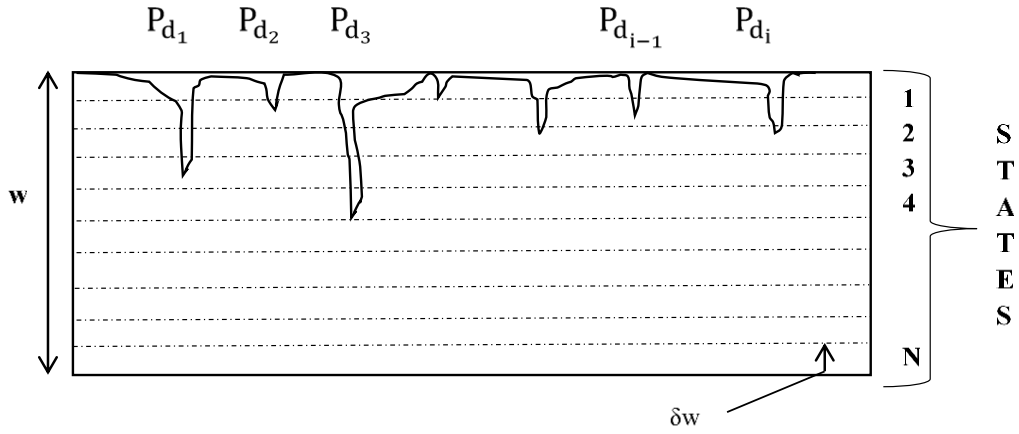


Figure 6.1: Model of pipeline pitting corrosion

$$\begin{cases} P_d(t) \leq P_{d_i} + \delta w \\ P_d(t) > P_{d_i} \\ \text{for } i = 1, 2, \dots, N \end{cases} \quad (6.5)$$

Assuming P_{d_i} is uniformly distributed with δw corresponding to individual states in the pipeline wall thickness such that the sum of each limit of observable pit depth P_{d_i} is given by $S_{(Pd)_i}$ then

$$P\{P_{d_i}(t) \in S_{(Pd)_i}\} = \begin{cases} P\{P_{d_i}(t) > P_{d_i}\} \\ P\{P_d(t) \leq P_{d_i} + \delta w\} \end{cases} \quad (6.6)$$

It follows therefore that the probability of observed corrosion pit depth at any increase in pipeline wall thickness at time t will satisfy the condition in Equation (6.7) as shown in literature (Rodriguez & Provan 1989a).

$$\begin{cases} 0 \leq P\{S_{(Pd)_i}\} \leq 1 \\ P\{w\} = 1 \\ P\{\sum_{i=1}^N S_{(Pd)_i}\} = \sum_{i=1}^N P\{S_{(Pd)_i}\} \end{cases} \quad (6.7)$$

For any finite collection of time t_1, t_2, \dots, t_n and pit depth, $P_d(t_1), P_d(t_2), \dots, P_d(t_n)$, the time variation of pit depth growth shown in Equation(6.4) is a stochastic process if the condition in Equation(6.8) is met.

$$\begin{aligned} P\{P_d(t_{n+1}) = j | P_d(t_n) = i, P_d(t_{n-1}) = i_{n-1}, \dots, P_d(t_0) = i_0\} \\ = P\{P_d(t_{n+1}) = j | P_d(t_n) = i\}_{i,j \in N} \end{aligned} \quad (6.8)$$

where i and j are variables showing the various state of the pit depth at different times.

6.2 Time evolution of pit depth

For transition of the pit depth from state i to j in time interval $(t, t+\delta t)$,

$$P\left\{\{P_d(t + \delta t) = j | P_d(\delta t) = i\} = P_{i,j}(\delta t, t)\right\}_{0 \leq \delta t < t} \quad (6.9)$$

For the transition probability in Equation (6.9) to satisfy a Markov process, the condition in Equation (6.10) will hold.

$$\left\{ \begin{array}{l} 0 \leq P_{ij}(t + \delta t) \leq 1, \quad \text{for } i, j, \delta t, t \geq 0 \\ \sum_{j=1}^N P_{ij}(t + \delta t) = 1, \quad \text{for } i, \delta t, t \geq 0 \\ P_{ij}(0,0) = \begin{cases} 1, & \text{for } i = j \\ 0, & \text{for } i \neq j \end{cases} \end{array} \right. \quad (6.10)$$

It is expected that the pit depth in state i at a given time δt will remain in the state until a later time (Feldman & Valdezffores 2010). However, it can move to another state j by passing through an arbitrary state h in s time (see Figure 6.2) whilst obeying the time-dependent probability condition of Chapman-Kolmogorov equation shown in Equation (6.11) (Feldman & Valdezffores 2010):

$$P_{ij}(\delta t, t) = \sum_{h=1}^N P_{ih}(\delta t, s) * P_{hj}(s, t), \quad \text{for } \delta t < s < t; s \in (\delta t, t); i, j, h \in N \quad (6.11)$$

Assuming that for this small increase in time δt , the probability of transition of the pit depth from state i to j at time $t+\delta t$ is given by the expression in Equation (6.12).

$$P_{ij}(t, t + \delta t) = \lambda_{ij}(t)\delta t + O(\delta t) \quad (6.12)$$

where λ is the intensity of the Markov process and can be represented by Equation (6.13) (Feldman & Valdezffores 2010, Valor *et al.* 2010).

$$\lambda_i(t) = i\lambda(t) \quad (6.13)$$

Since $O(\delta t)$ is a limiting state and tends to zero, if a continuous function is assumed such that $\lambda_i(t) \geq 0$, then

$$\begin{cases} \lambda_i(t) = \lim_{\delta t \rightarrow 0} \left(\frac{1 - P_{ii}(t, t + \delta t)}{\delta t} \right) , i = 1, 2, \dots, N \\ \lambda_{ij}(t) = \lim_{\delta t \rightarrow 0} \left(\frac{P_{ij}(t, t + \delta t)}{\delta t} \right) , i, j = 0, 1, 2, \dots, N; i \neq j \end{cases} \quad (6.14)$$

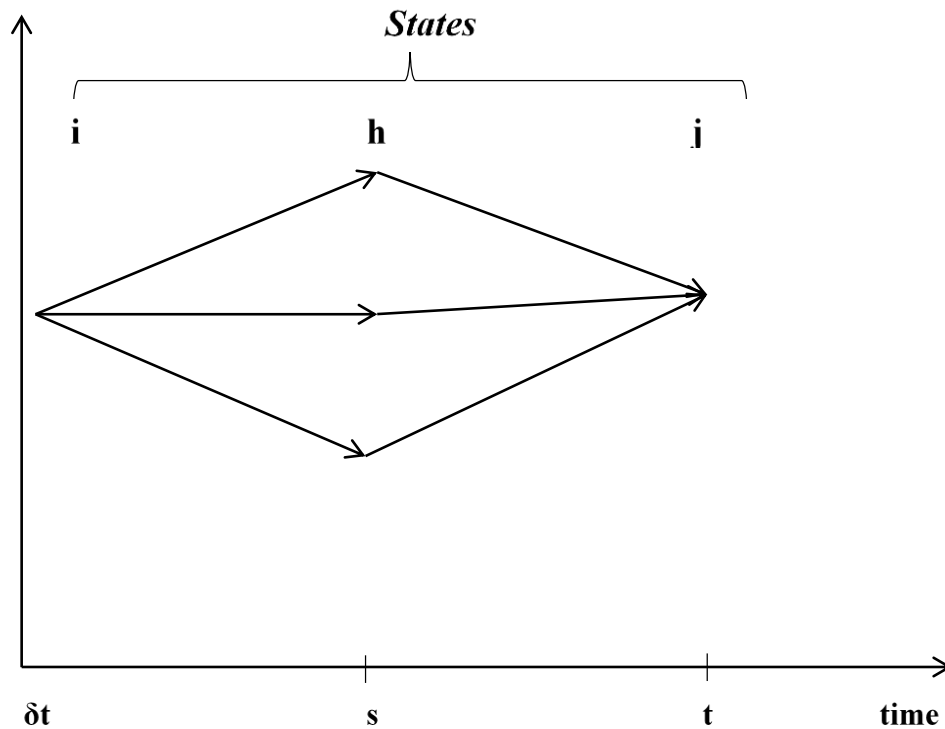


Figure 6.2: Graphical representation of Chapman-Kolmogorov equation of three stage Markov process - adapted from (Feldman & Valdezffores 2010)

Manipulating Equation (6.14) will give the Kolmogorov forward and backward equations, however, for a continuous time non-homogenous linear growth Markov process, which the pit depth is assumed to follow in this research, the probability

that a process at state i will be in state j for $j \geq i$ at a later time follows Kolmogorov forward equation shown in Equation (6.15) (Rodriguez & Provan 1989a, Valor *et al.* 2010, Valor *et al.* 2013).

$$\frac{dP_{ij}(t)}{dt} = \begin{cases} \lambda_{j-1}(t)P_{i,j-1}(t) - \lambda_j(t)P_{i,j}(t), & \text{for } j \geq i + 1 \\ -\lambda_i(t)P_{i,i}(t) \end{cases} \quad (6.15)$$

The transition probability function of the pit depth defined by Kolmogorov forward equation can be solved with a negative binomial distribution function (Rodriguez & Provan 1989a, Valor *et al.* 2010, Valor *et al.* 2013, Yusof, Noor & Yahaya 2014) hence the conditional probability (P_{n,n_0}) of moving from state n_0 to n ($n \geq n_0$) in time interval (t_0, t) can be represented with the relationship in Equation (6.16).

$$P_{n,n_0} = P\{P_d(t) = n | P_d(t_0) = n_0\} \quad (6.16)$$

Parzen (1999) showed that Equation (6.16) can be represented in a closed form of negative binomial distribution (Equation (6.17)) for the distribution of pit depths with initial state n_0 and n being the probability density of the smallest and deepest pit depths respectively of the pipeline at time t_0 .

$$P_{n,n_0} = \binom{n-1}{n-n_0} * e^{-(\gamma(t)-\gamma(t_0))n_0} * (1 - e^{-(\gamma(t)-\gamma(t_0))})^{n-n_0} \quad (6.17)$$

where,

$$\gamma(t_0, t) = \int_{t_0}^t \lambda(t) dt \quad (6.18)$$

The time-dependent pit depth growth can be expressed as a function of the intensity of the Markov process and change in time Δt (Taylor & Karlin 1998) as shown in Equation (6.19):

$$P_d(t + \Delta t) = P_d(t) + P_d(t) * \lambda \Delta t \quad (6.19)$$

Since

$$\frac{d(P_d(t))}{dt} = \lim_{\Delta t \rightarrow 0} \frac{P_d(t + \Delta t) - P_d(t)}{\Delta t} \quad (6.20)$$

Solving Equation (6.19) and (6.20) will yield the non-probabilistic pit depth (Equation (6.21)) at any change in the time interval ($\Delta t = t - t_0$) assuming that the pit depth at time t_0 is in the initial state n_0 .

$$P_d(t) = n_0 e^{\lambda \Delta t} \quad (6.21)$$

The time dependent stochastic mean pit depth growth ($M(t)$) is equivalent to the non-probabilistic pit depth and can be expressed as follows:

$$M(t) = n_0 e^{\lambda(t-t_0)} \quad (6.22)$$

If the deterministic corroded pit growth in this work is assumed to follow a linear random model, which have been used by researchers to model different kinds of physical systems including pipelines deterioration (Ahammed 1996, Ahammed 1998, Caley *et al.* 2002, Li *et al.* 2009, Bazan & Beck 2013), then the progression of the deterministic pit depth ($P_{da}(t)$) will be of the form shown in Equation (6.23).

$$P_{da}(t) = \beta_d(t - t_{int}) \quad (6.23)$$

where β_d represents the deterministic pitting rate, t_{int} is the time of initiation of the pitting process (this is explained later in this work). The time of pitting initiation on the pipeline depends on the physical and chemical characteristics of the environment exposed to the pipeline (Velazquez *et al.* 2009b, Cole & Marney 2012) and the corrosion resistance ability of the pipeline material. The rate of change of the deterministic pit depth ($\Delta P_{da}(t)$) can be expressed in terms of the deterministic intensity (λ_d) and the change in the time interval as follows:

$$\Delta P_{da}(t) = \lambda_d(t) P_{da}(t) \Delta t \quad (6.24)$$

According to Cox and Miller (1965) (as cited by Valor *et al.* 2013), the stochastic corroded pit growth rate is assumed to be equal to the deterministic pit growth rate. Then solving Equations (6.18), (6.22) and (6.24) and simplifying will yield the following relationships:

$$\gamma(t) = \ln(\beta_d(t - t_{int})) \quad (6.25)$$

$$\lambda(t) = \frac{1}{t - t_{int}} \quad (6.26)$$

$$\gamma_s = \frac{t_0 - t_{int}}{t - t_{int}}, t \geq t_0 \geq t_{int} \quad (6.27)$$

where $\gamma(t)$ represents the pitting corrosion damage with time while γ_s represents the probability of pitting evolution with time.

6.3 Estimation of the probability distribution of the corroded pitting depth

Caleyo *et al.* (2009a) has shown that the probability distribution ($FD(\pi)$) over the time interval (t, t_0) at state n_0 can be related to the probability density function ($f(\pi)$) according to Equation (6.28):

$$FD(\pi) = \int_{t_0}^t f(\pi), t > 0 \quad (6.28)$$

If the pitting corrosion rate (π) is continuously distributed with $f(\pi)$, $FD(\pi)$ and Δt , then Equation (6.28) can be expressed below after taking the limiting states and simplifying:

$$P\{\pi(t) < T \leq \pi(t) + \pi(\Delta t)\} \cong f(\pi) * \Delta t \quad (6.29)$$

$$f(\pi, n_0, t_0, t) = P_{n_0}(t_0) * P_{n_0, n_0 + \pi \Delta t}(t_0, t) * \Delta t \quad (6.30)$$

For an oil and gas pipeline with a measured total pitting population, the pitting distribution for the entire pitting states (N) of the pit depths can be expressed as Equation (6.31):

$$f(\pi, t_0, t) = \sum_{n_0=1}^N f(\pi, n_0, t_0, t) \quad (6.31)$$

Different researchers have shown that if the initial probability distribution of the pit depth at time t_0 is known, the future probability distribution of the pit depth can be estimated (Caleyo *et al.* 2009a, Valor *et al.* 2010, Valor *et al.* 2013, Yusof, Noor & Yahaya 2014) and reliability of the pipeline established. Equation (6.32) is used to compute the future distribution of the pit depth ($P_n(t)$) (Caleyo *et al.* 2009a).

$$P_n(t) = \sum_{n_0}^n P_{n_0}(t_0) * P_{n_0,n}(t_0, t) \quad (6.32)$$

Combining Equations (6.17), (6.25), (6.26) and (6.32) will give a general equation for determining the future pit depth distribution.

$$P_{n_0,n}(t_0, t) = \frac{(n-1)!}{(n_0-1)!(n-n_0)!} * \left(\frac{t_0 - t_{int}}{t - t_{int}}\right)^{n_0} * \left(\frac{t - t_0}{t - t_{int}}\right)^{n-n_0} \quad (6.33)$$

6.4 Prediction of the model parameters

To predict the transition probabilities for the deterministic pit depth requires the estimation of the deterministic pitting rate and the time of initiation of the pitting in Equation (6.23). To estimate these parameters, pit depths and operating parameters (pH, temperature, flow rate and CO₂ partial pressure) measurements of oil transmission pipelines obtained from a producing company in the Nigerian Niger Delta region were used for numerical analysis and determination of the multivariate coefficients following the Monte Carlo framework shown in Figure 6.3.

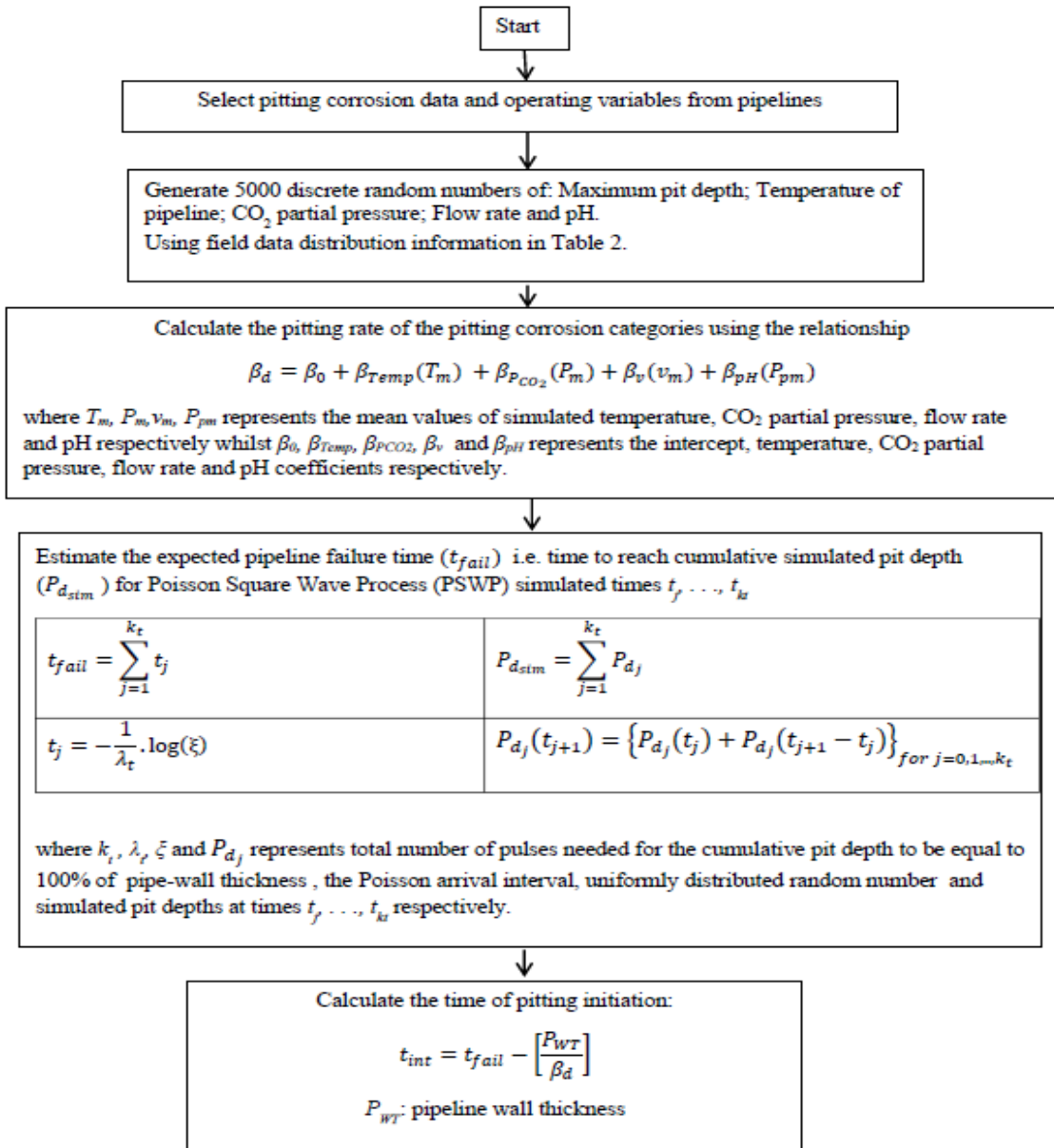


Figure 6.3: Framework for Monte Carlo simulation of pitting initiation time

The pitting rates in the pipelines were classified into four categories using NACE pitting corrosion guideline shown in Table 6.1 (NACE 2005).

Table 6.1: Qualitative categorization of carbon steel corrosion rate for oil production systems

	Average Corrosion Rate	Maximum Pitting Rate
	mm/yr	mm/yr
Low	<0.025	<0.13
Moderate	0.025-0.12	0.13-0.20
High	0.13-0.25	0.21-0.38
Severe	>0.25	>0.38

The pit depths of the pipelines were determined according to the relationship in Equation (6.34) - (6.36):

$$P_{d_{max}} = \left\{ \left(\beta_0 + \sum_{i=1}^m \beta_i x_i \right) (t_i - t_{int}) \right\}_{i=1,2,\dots,m} \quad (6.34)$$

Where

$$\beta_d = \left\{ \beta_0 + \sum_{i=1}^m \beta_i x_i \right\}_{i=1,2,\dots,m} \quad (6.35)$$

$$\beta_d = \beta_0 + \beta_{Temp}(T_m) + \beta_{P_{CO_2}}(P_m) + \beta_v(v_m) + \beta_{pH}(P_{pm}) \quad (6.36)$$

$P_{d_{max}}$ represents the maximum pit depth, which is equivalent to the deterministic pit depth ($P_{d_d}(t)$), β_i represents the coefficients of the operating variables of the pipelines and x_i is used to represent the operating variables while m is the number of operating variables.

To ensure that the random walk nature of the pit depth growth rate is maintained, a Poisson Square Wave Process (PSWP) was used to predict the time lapse for the pitting process. Although any positive random distribution can be used for realizing the pulse heights (Bazan & Beck 2013), Gamma distribution (Bazan & Beck 2013) as well as Gumbel distribution (Zhang & Zhou 2013) have been used for estimating variables in PSWP by other authors. However, lognormal distribution is employed in this work because the best fitting distribution of the field data followed a lognormal distribution. In order to estimate the time of pitting initiation process

(t_{int}) using the procedure shown in Figure 6.3, a 5000 run random numbers simulation was carried out using the minimum and maximum values of the operating variables and the maximum pit depths for the corrosion categories shown in Table 6.2 as boundary conditions. By assuming that the maximum pit depth and operating parameters follow a lognormal distribution as earlier stated, the best fit distributions were obtained from the simulated data. Poisson Square Wave Process (PSWP) shown in Figure 6.4 was used to calculate the pit depth growth with time using the relationship shown in Equation (6.37) (Bazan & Beck 2013).

$$P_{d_j}(t_{j+1}) = \left\{ P_{d_j}(t_j) + P_{d_j}(t_{j+1} - t_j) \right\}_{for\ j=0,1,\dots,k_t} \quad (6.37)$$

where P_{d_j} represents the simulated pit depth at time t_j and k_t represents the expected number of time pulses needed for the cumulative pit depth to be 100% of the pipe-wall thickness. A multivariate regression analysis of the simulated data was used to obtain the regression coefficients of the operating variables and the intercept whereas the mean values of the operating parameters computed from the simulation result were used for the computation of the pitting rates of the corrosion categories according to Equation (6.36).

To estimate the expected pipeline failure time (t_{fail}), Poisson arrival rate (λ_t) was assumed to be 0.5 and the statistical best fit parameters of the lognormal distribution estimated from the 5000 simulation runs were used to predict pit depth for random times calculated for each Poisson arrival. Since the magnitude and duration of the generated pulses from the PSWP follow a Poisson distribution with the duration of individual pulses being independently exponentially distributed (Bazan & beck 2013, Zhang & Zhou 2013), the expected pipeline failure time (t_{fail}) can be computed as the cumulative simulated times for which the cumulative simulated pit depth ($P_{d_{sim}}$) is equivalent to 100% of the pipe-wall thickness of the pipeline.

As the deterministic pit depth at the expected time of pipeline failure (t_{fail}) is assumed to be equivalent to 100% of the pipe-wall thickness (P_{WT}) loss, then Equation (6.23) can be represented as shown in Equation (6.38) if $t \approx t_{fail}$.

$$P_{WT}(t_{fail}) = \beta_d(t_{fail} - t_{int}) \quad (6.38)$$

Hence the pitting initiation time can be simplified from Equation (6.38) to give the relationship expressed in Equation (6.39) at the time of failure of the pipeline.

$$t_{int} = t_{fail} - \left[\frac{P_{WT}}{\beta_d} \right] \quad (6.39)$$

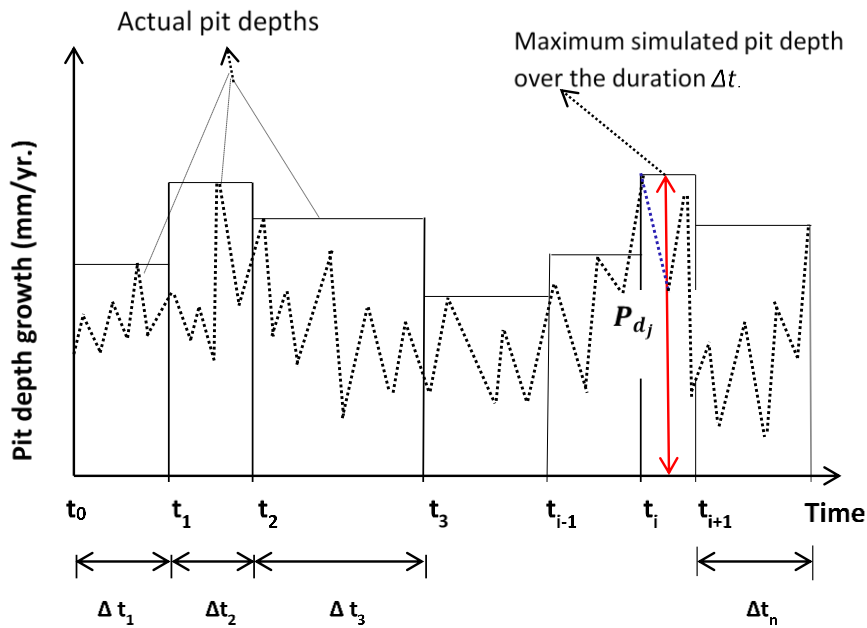


Figure 6.4: Poisson Square Wave Process (PSWP) for estimating pitting initiation time

The summary of the field data for the pitting corrosion categories, the coefficients of regression for the linear regression model and Monte Carlo simulation predicted values of time for pitting initiation is shown in Table 6.2. In the table, “all data” category represents the total number of collected data whereas low, moderate, high and severe pitting rate categories were determined according to the number of all the sampled data that fell into the classifications shown in Table 6.1. After the simulation and estimation of the relevant variables in Equation (6.34), the transition probability function given in Equation (6.33) can be calculated for the pitting corrosion categories.

Table 6.2: Variables and coefficients of the predictive for the pitting corrosion

Variables	Description	Pitting corrosion category					
		Low	Moderate	High	Severe	All data	
$P_{d_{max}}$	min	Maximum pitting depth	0.049	0.132	0.204	0.396	0.049
	max	(mm)	0.118	0.183	0.371	1.309	1.309
ϑ	min	Temperature (°C)	24	21	27	21	21
	max		40	32	70	74	74
P_{CO_2}	min	CO ₂ partial pressure	0.01	0.01	0.02	0.03	0.01
	max	(MPa)	0.14	0.16	0.31	0.61	0.61
V	min	Flow rate(ms ⁻¹)	0.07	0.04	0.05	0.07	0.04
	max		0.23	0.3	1.39	2.01	2.01
p_H	min	pH of fluid	6.21	6.78	6.21	6.73	6.21
	max		8.18	8.32	8.19	8.57	8.57
No of sampled pipelines			8	7	15	30	60
No of sampled pit depths			80	70	150	300	600
Coefficient of parameters							
β_0	Constant pitting rate		0.0836	0.1574	0.2859	0.8235	0.7303
	Standard error		0.0029	0.00278	0.0064	0.037	0.042
	Coefficient of temperature		-0.0001	-0.0001	-0.0001	-0.0002	-0.0002
β_{Temp}	Standard error		4.24e-05	4.24e-05	3.82e-05	0.0002	0.0002
	Coefficient of CO ₂ partial pressure		-0.003	-0.0019	-0.0033	0.0133	-0.0279
	Standard error		0.0053	0.0034	0.0057	0.0157	0.021
β_V	Coefficient of flow rate		0.0002	-0.0001	-0.0001	-0.0026	0.0038
	Standard error		0.0042	0.0019	0.0012	0.0047	0.006
	Coefficient of pH		0.0003	0.0003	0.0007	0.0046	-0.0049
β_{pH}	Standard error		0.0003	0.0003	0.0008	0.0049	0.005
	Estimated pitting parameters						
β_d	Pitting rate (mmyr ⁻¹)		0.0824	0.1568	0.2855	0.8506	0.6801
t_{int}	pit initiation time(years)		1.56	0.58	1.03	1.89	3.60

6.5 Results and discussion

The minimum and maximum observed pit depths of each of the 60 pipelines were used as boundary conditions for a Monte Carlo simulation experiment aimed at predicting the variation of the pit depth growth with time of exposure of the pipelines for different categories of pitting rate shown in Table 6.1. This simulation executed in MATLAB was used to obtain results for 1 year to 40 years' exposure of the studied pipelines. The cumulative simulated pit depths for each of the simulated exposure years (5, 10, 15, 20, 25, 30, 35 and 40 years) for the 60 pipelines were ranked in increasing order and the pit depth of each pipeline plotted against the ranked position. The distribution of the simulated pit depths for all the field data and the best fit equations for the exposure times are shown in Figure 6.5.

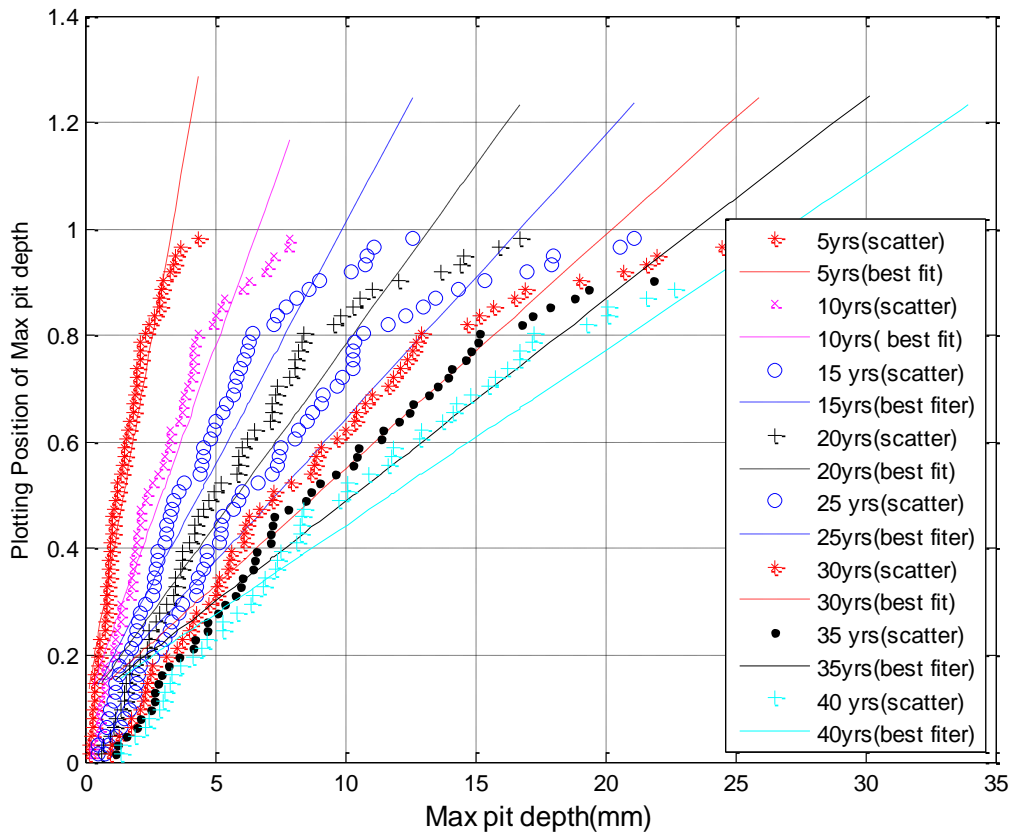


Figure 6.5: Maximum pit depth plot for Monte Carlo simulated maximum pit depths for studied pipelines

Figure 6.5 shows that the distributions were shifting towards the right in a clockwise direction as the values increased, which is an indication of experiment under control (Rodriguez & Provan 1989b). The trend shown in Figure 6.5 is similar to those of the simulated pit depth growth of the pitting corrosion categories not shown in this paper.

The simulated pit depths and the exposure times for the pitting corrosion categories were fitted to the generalized extreme value (GEV) distribution shown in Equation (6.40).

$$f(x) = \text{Exp} \left[- \left(1 + \sigma \frac{x - \varphi}{\alpha} \right)^{-\frac{1}{\sigma}} \right] \text{ for } \left(1 + \sigma \frac{x - \varphi}{\alpha} \right) > 0 \quad (6.40)$$

where $f(x)$ represents the GEV distribution, σ is the shape parameter, φ is the location parameter, α is the scale parameter.

Figure 6.6a shows the GEV distribution of the simulated data for the entire field data used in this research. The pitting depth states were obtained by dividing the pipeline wall thickness into 100 states of 0.0841 mm-thick with each state representing a damage penetration of the pipeline wall in the discretization process. The figure indicates that the variance and the mean of the pitting rate distribution decrease with the increase in time of exposure.

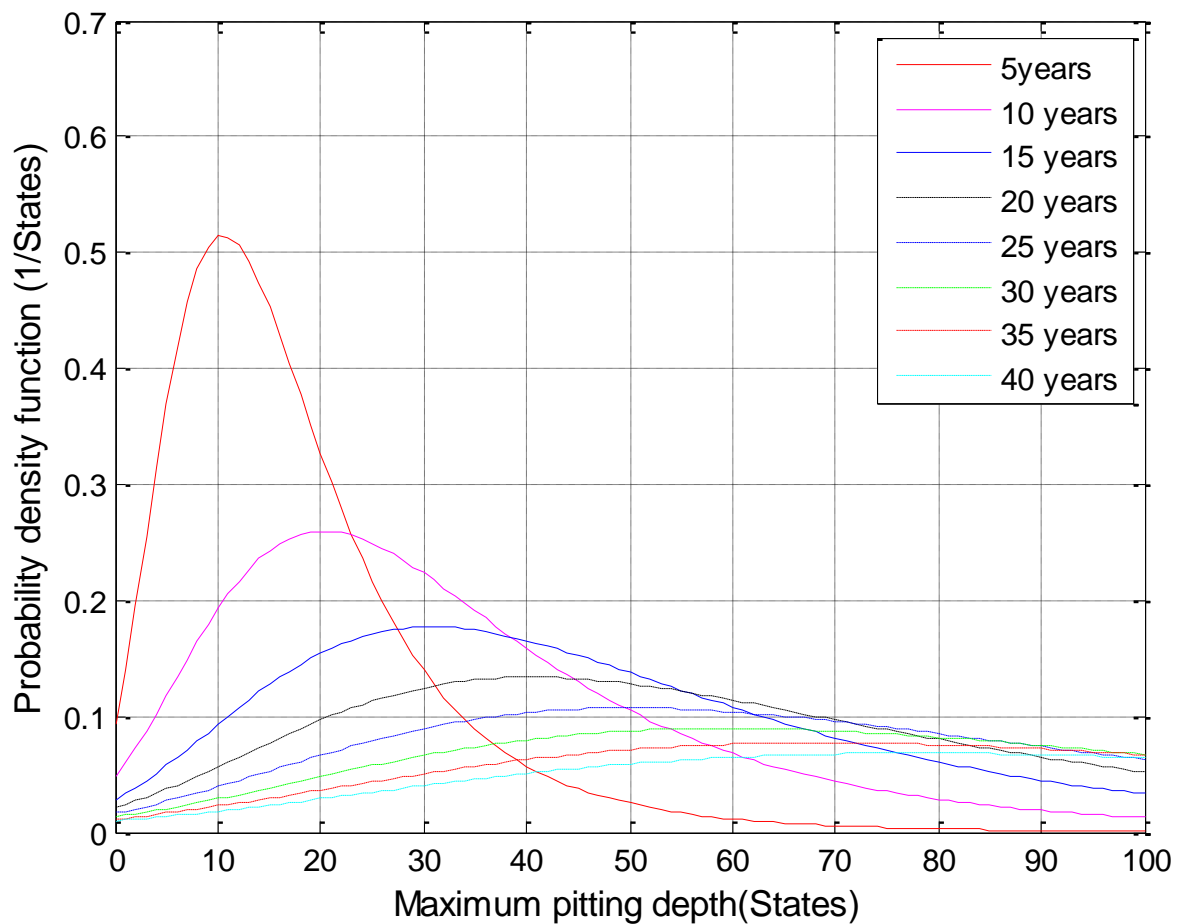


Figure 6.6a: GEV distribution of Monte Carlo simulated pit depth for all pitting corrosion data

The stochastic internal pit depth growth was illustrated in Figure 6.6b using Monte Carlo simulated pit depth growth shown in Figure 6. 6a. The pit depth distribution at 5 years was used for constructing the future pit depth distribution at 10 years, 15 years and 20 years as the pipeline wall thickness was divided into 100 states of 0.0841 mm-thick per state. The constructed pit depth distribution shown in Figure 6.6b indicated that the pitting rate distribution decreased with the increase in time of

exposure as was concluded by other researchers (Valor *et al.* 2013, Caleyó *et al.* 2009a).

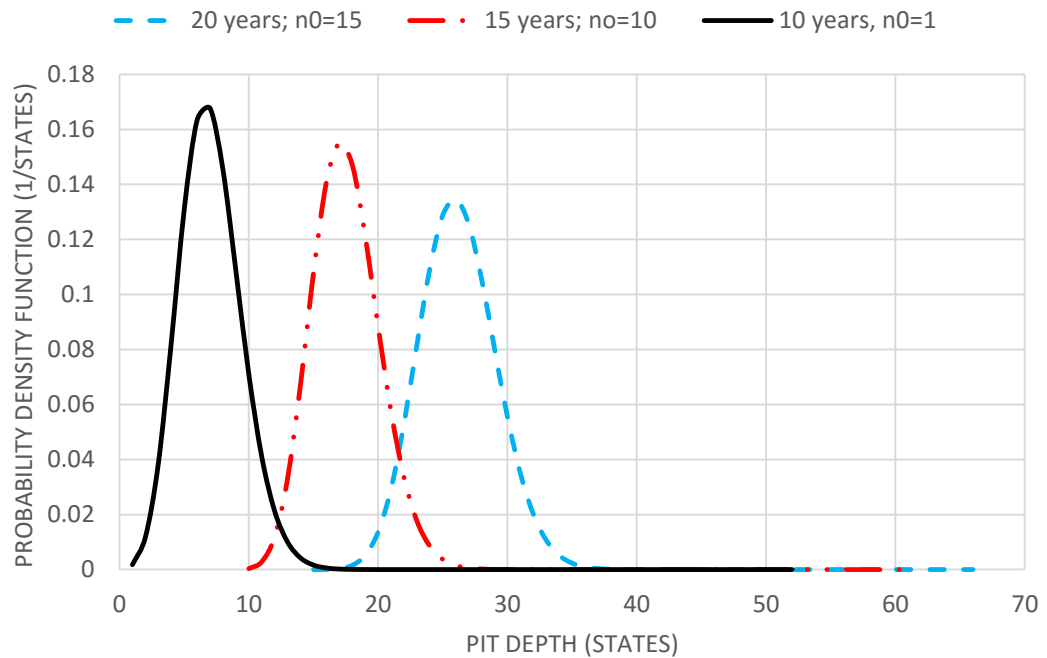


Figure 6.6b: Variation of pitting depth distribution with pipeline exposure time (years)

Figures 6.7a and 6.7b represent the mean and variance of the simulated pit depths over different times of exposure. The figures indicate an increase in mean and variance of the pitting corrosion categories as the time of exposure increased. It could also be seen that severe pitting and ‘all data’ categories have higher values and showed more scatter than low, moderate and high pitting corrosion classes. This implies that the increase in pit depths resulted in higher mean and variance for pipelines with the same duration of exposure.

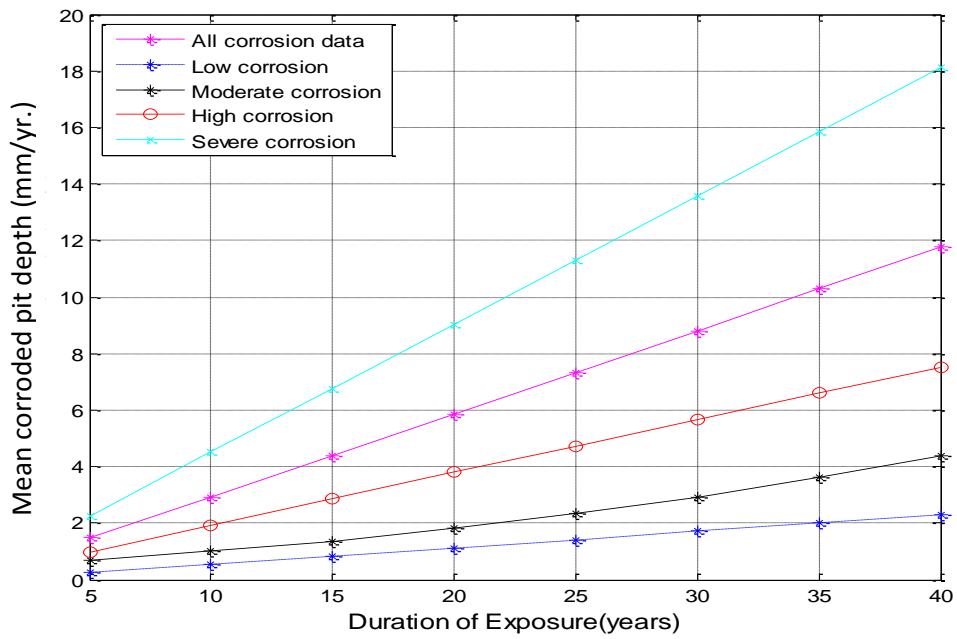


Figure 6.7a: Time evolution of the best fit mean of Monte Carlo simulated pit depth

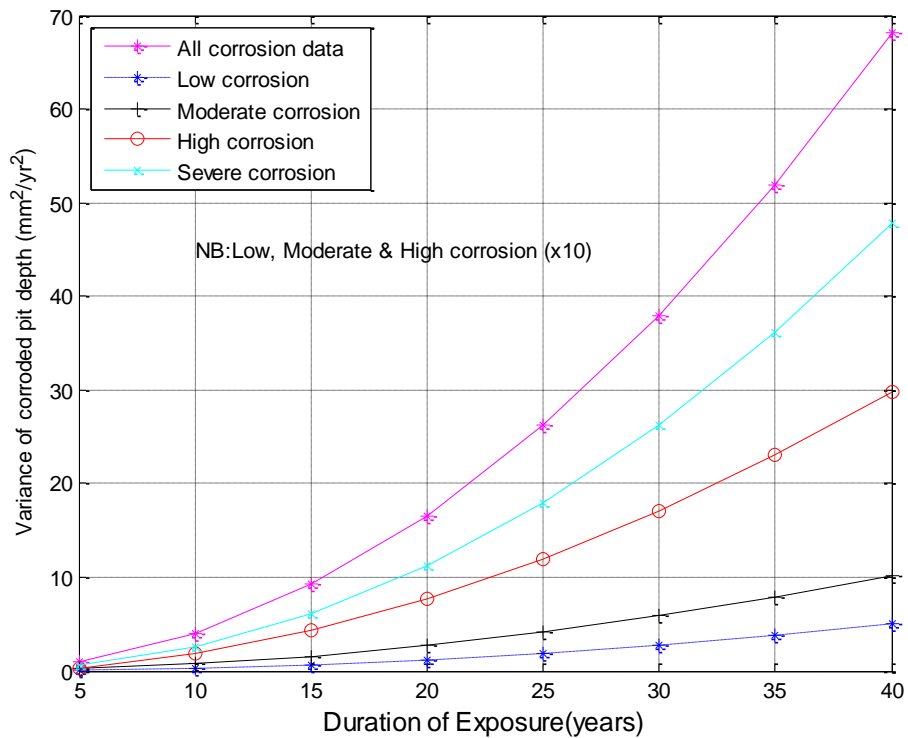


Figure 6.7b: Time evolution of the best fit variance of Monte Carlo simulated pit depth

Figures 6.8a, 6.8b and 6.8c represent the variation of the shape, scale and location parameters of the pitting corrosion categories for the simulated data. As expected, there is increase in these variables with increased duration of exposure with low, moderate and high categories giving lower values of the scale and location parameters whilst shape parameters showed slight changes for high, severe and all data.

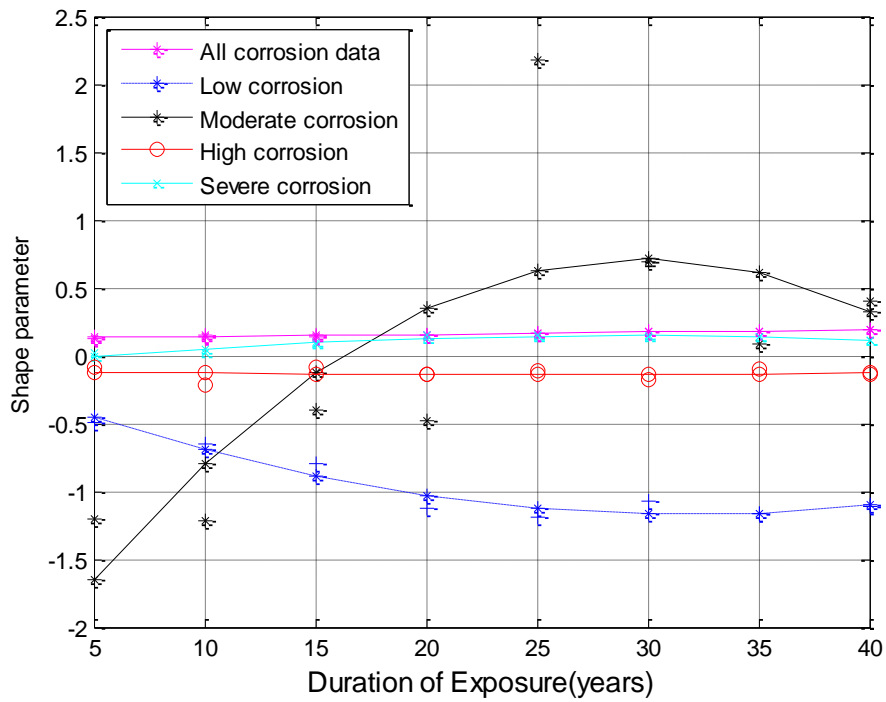


Figure 6.8a: Time evolution of the best fit shape parameter of GEV distribution of the pit depth

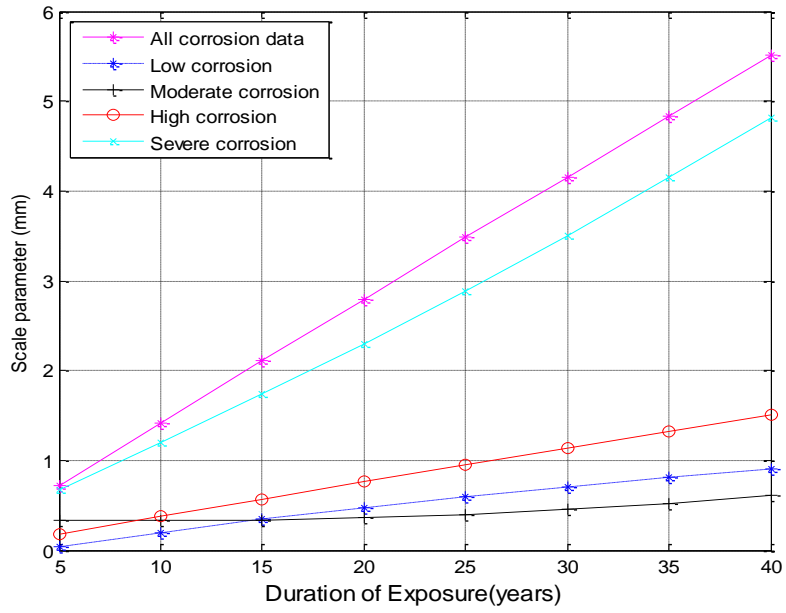


Figure 6.8b: Time evolution of the best fit scale parameter of GEV distribution of the pit depth

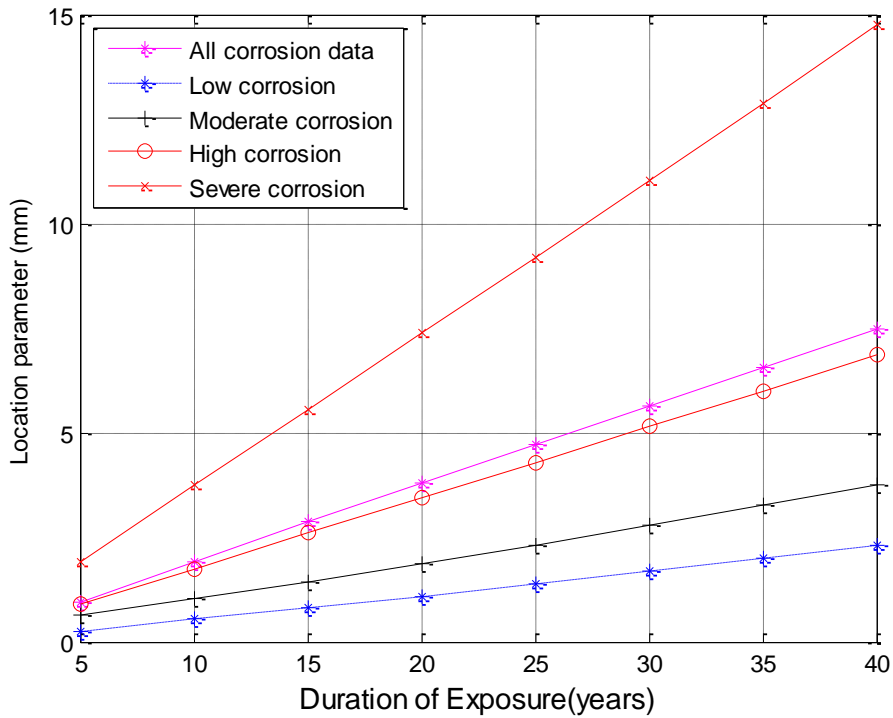


Figure 6.8c: Time evolution of the best fit location parameter of GEV distribution of the pit depth

The variation of the pitting damage ($\gamma(t)$) and the probability parameter (γ_s) with time is also shown in Figures 6.9a and 6.9b respectively whereas Figure 6.9c shows the maximum pit depth growth with time as computed from the simulation result. The estimation of these parameters is vital for the computation of the transition

probability function. The pitting corrosion damage increased with time as expected, with the least increase observed in low pitting corrosion category whereas severe pitting corrosion category accounted for the highest increase as was concluded by other researchers (Melchers 2005, Melchers 2010, Valor *et al.* 2013). Since higher pit depths resulted in lower probability parameter (Figure 6.9b), it follows that the reliability of the pipeline reduces with an increased risk of failure as exemplified by other authors in literature (Sheikh, Boah & Hansen 1990, Valor *et al.* 2014).

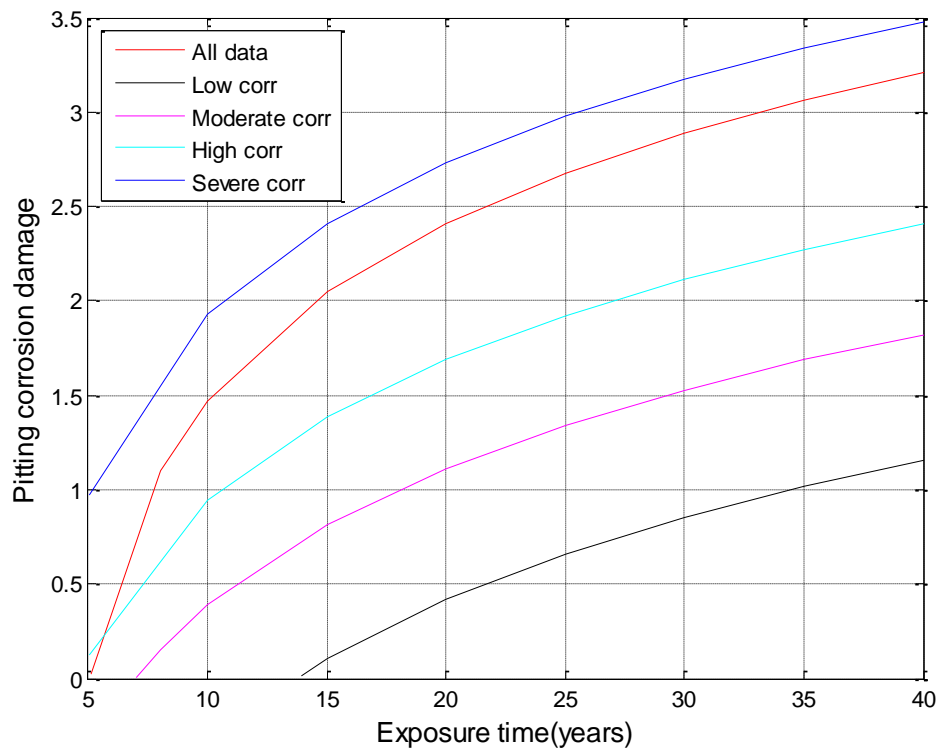


Figure 6.9a: Time evolution of the pitting corrosion damage ($Y(t)$) for GEV distribution of Monte Carlo simulated pit depth for different categories of pitting corrosion

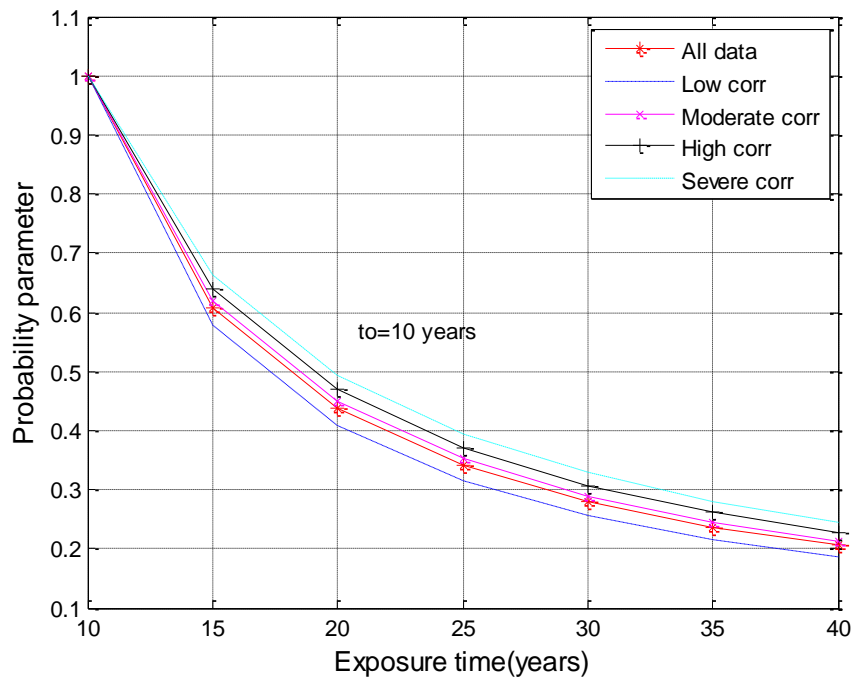


Figure 6.9b: Time evolution of probability parameter (Y_s) for GEV distribution of Monte Carlo simulated pit depth for different categories of pitting corrosion

Figure 6.9c indicates that the cumulative rate of growth of the pit depth is maximum for severe corrosion rate as expected whereas low corrosion category showed the least cumulative pit growth with time of pipeline exposure. Hence, to manage pipelines with these corrosion severities involves the application of varying quantities of corrosion inhibitors, however, if the maximum uninhibited corrosion rate is less than 0.4mm/yr., there may not be any need for corrosion inhibitor seeing that this level of pipe-wall thickness loss is accommodated in corrosion allowance during pipeline design (McMahon & Paisley 1997). Although the pipelines studied in this work were treated with imidazoline-based corrosion inhibitor, however, to reduce the risk of pipeline failure due to corrosion rates greater than 0.4mm/yr., varying quantities of corrosion inhibitors are injected to the pipelines in accordance to the rate of corrosion. For instance, when the total uninhibited corrosion rate on a carbon steel pipeline is 0.7mm/yr., the maximum required inhibitor availability will be 50% (McMahon & Paisley 1997). Again, the concentration of the inhibitor is also vital in achieving the expected corrosion reduction seeing that at certain concentrations, corrosion is enhanced. This is evident in X52 grade pipeline, which showed perfect corrosion reduction at 50ppm of amine type inhibitor but increased corrosion rate at

100 ppm under static condition (Martínez *et al.* 2009). This inhibitor application can be periodically reviewed after inspection of the pipelines to determine whether or not the quantity is sufficient or in excess. Imperatively, the quantity of corrosion inhibitor to be applied to the pipelines studied in this research will increase from low corrosion to moderate, high and severe corrosion categories in that order of listing. Again, the pipelines with higher pit depth growth rates are expected to continue growing at a higher pace than those with lower pitting rates hence, the failure risk expected for severe corroded pipelines are much higher than the risk inherent in low corroded pipeline.

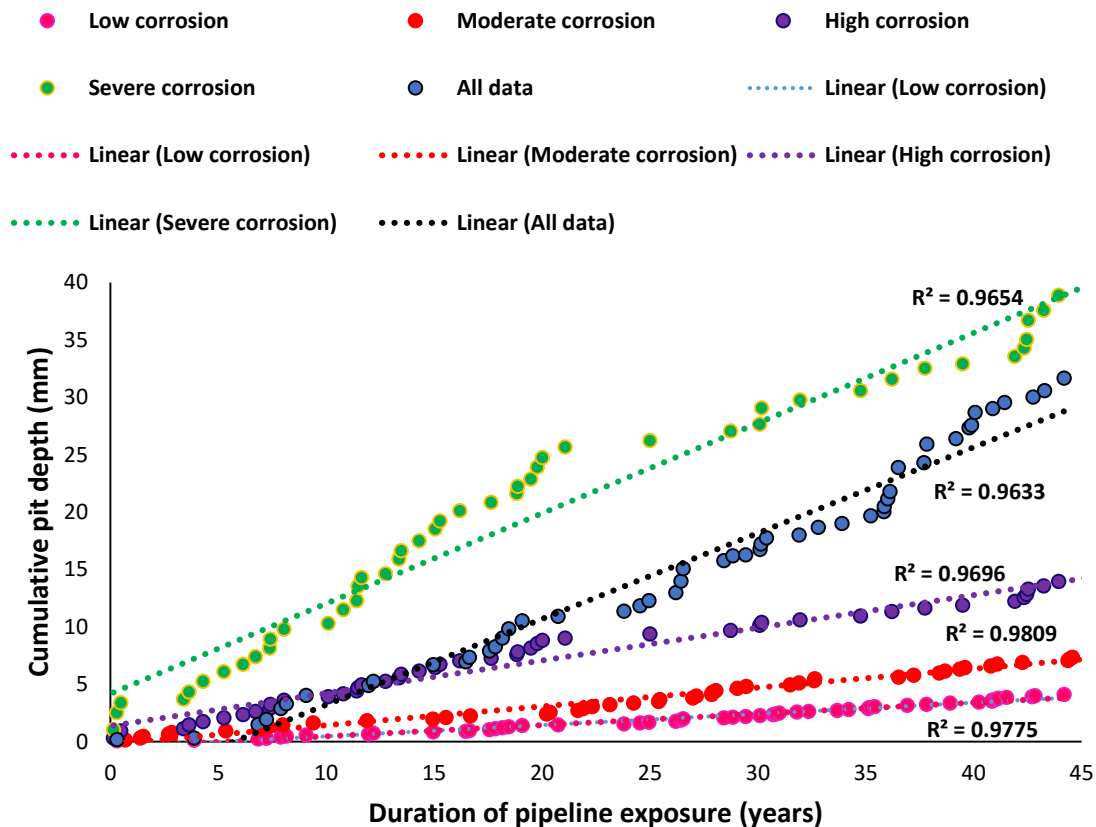


Figure 6.9c: Simulated maximum pit depth growth and pipeline exposure time for different corrosion categories.

6.6 Applications of the pitting prediction model

The Markov prediction model was tested on two sets of in-line inspection data of pit depth of offshore well tubing and onshore transmission pipelines.

6.6.1 Predicting future pitting corrosion distribution of well tubing

The proposed Markov model was used to predict the future pitting corrosion distribution of well tubes used for offshore production. The pit depths of these tubes were measured with Multi-Finger Imaging Tool (MIT). The summary of the pit depths, the ages and the frequency of occurrences of the field measured data can be found in reference (Mohd & Paik 2014). The pit depth frequency of occurrence was used to determine the transition probability function of the pit depths that were divided into 100 states of 0.0645 mm-thick per state. To apply the Markov prediction model, the pit depths were assumed to belong to all data category (see Table 6.2) with pitting initiation time of 3.6 years.

For L-80 grade steel well tubing, the initial probability distribution function was taken as the pit depth distribution at age 5.1 years whilst the future pit depth distribution was calculated for 5.8 years and the result compared with the field measured pit depth distribution at 5.8 years. The result of the field measured and Markov predicted pit depth distribution is shown in Figure 6.10. The field and Markov predicted pit depth distributions were subjected to two-sample Kolmogorov Smirnov (K-S) test to prove the hypothesis that Markov predicted distributions of L-80 grade carbon steel's pit depth is similar to the future field measured pit depth distribution in offshore location. The resulting p-value of 0.4496 from the K-S test shows that this hypothesis cannot be rejected.

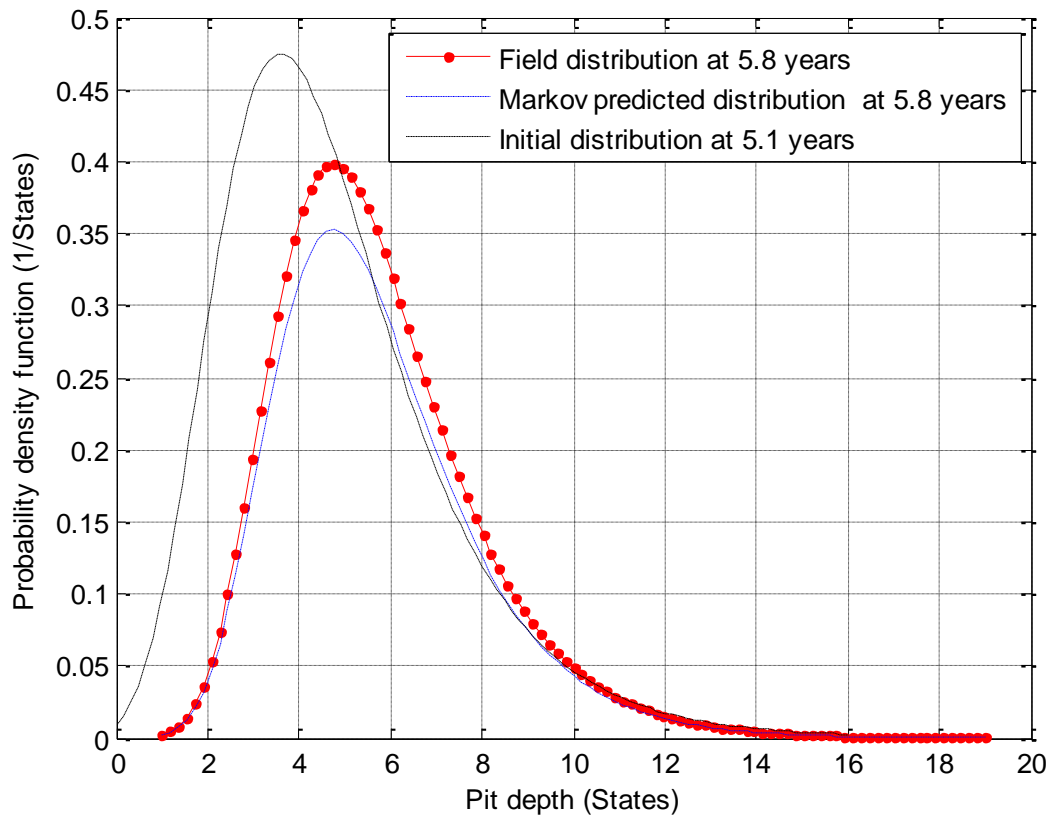


Figure 6.10: Comparison of Markov model prediction and field measured pit depths distribution for L-80 grade well tubing at 5.8 years from initial field distribution at 5.1 years

Similarly, for the N-80 grade carbon steel well tubing, the initial pit depth at the age of 9.1 years was used as the initial transition probability function distribution for calculating the future pit depth distribution at 15.3 years, 18.2 years and 22.8 years. The results of the Markov predicted and field measured pit depth distribution is shown in Figures 6.11a, 6.11b and 6.11c. Again, a two-sample K-S test of the Markov and field measured pit depth were conducted to test the hypothesis that Markov predicted distributions of N-80 grade carbon steel's pit depth is similar to the future field measured pit depth distribution in offshore location. The p-values of 0.1976, 0.1438 and 0.1024 for 15.3 years, 18.2 years and 22.8 years respectively were enough not to reject the hypothesis.

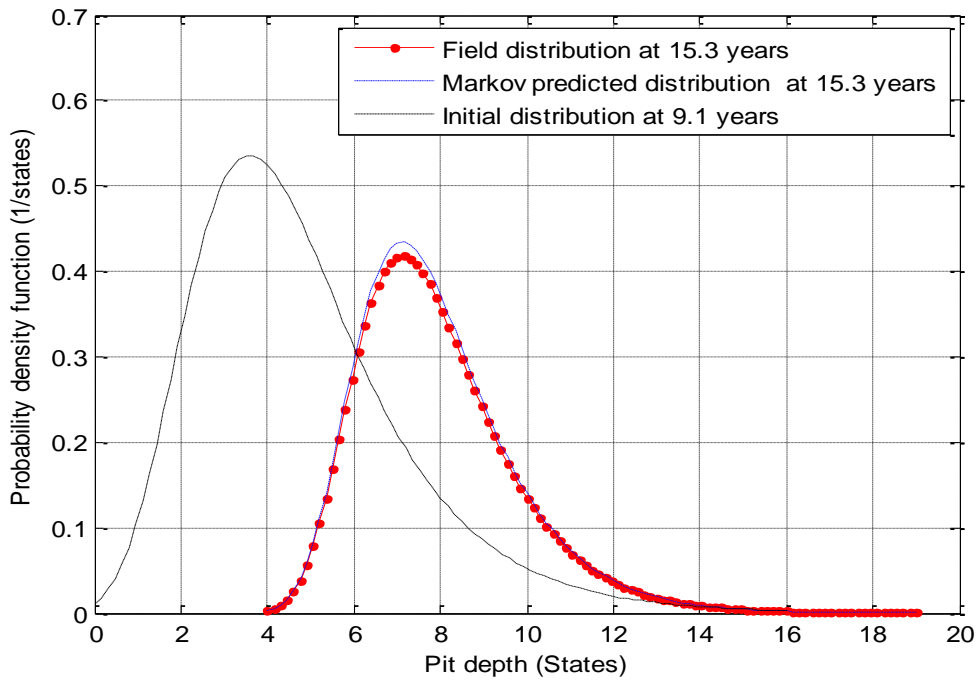


Figure 6.11a: Comparison of Markov model prediction and field measured pit depths distribution for N-80 grade well tubing at 15.3 years from initial field distribution at 9.1 years

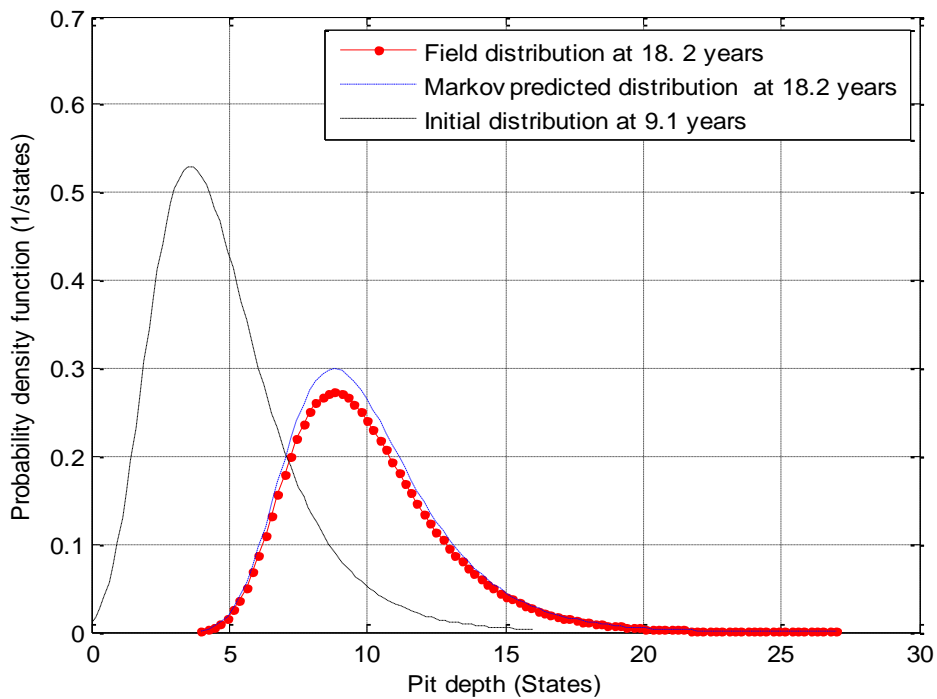


Figure 6.11b: Comparison of Markov model prediction and field measured pit depths distribution for N-80 grade well tubing at 18.2 years from initial field distribution at 9.1 years

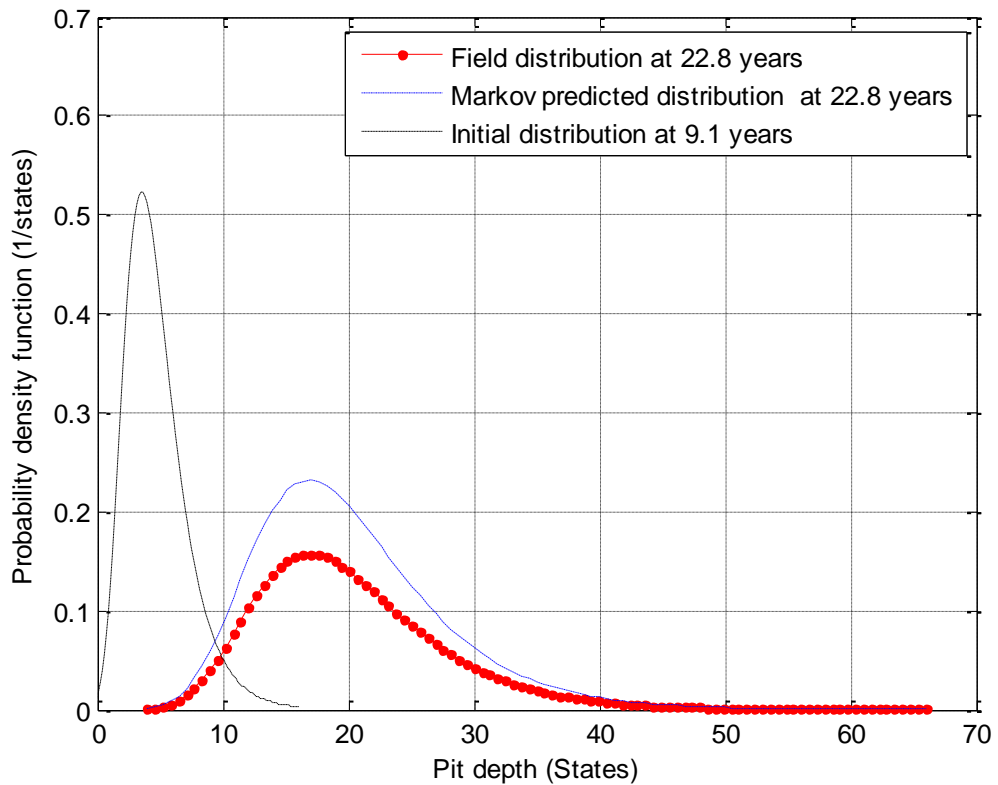


Figure 6.11c: Comparison of Markov model prediction and field measured pit depths distribution for N-80 grade well tubing at 22.8 years from initial field distribution at 9.1 years

6.6.2 Modelling pitting distribution of in-line inspected transmission pipeline

The prediction model developed in this research was further validated with magnetic flux leakage in-line inspection data of a 3.7 km X52 grade oil transmission pipeline inspected in August 2012. The inspection on this 203 mm external diameter and 8.7 mm thick pipeline commissioned in 1994 was carried out according to ASME BG31G standards (ASME 2009). A total of 1037 pit depths that ranged from 10% to 60% of the pipeline wall thickness were observed. The pipeline wall thickness was divided into 100 states of 0.087 mm-thick each and the transition probability distribution of the pit depth in 2012 was used as the initial distribution for predicting the future pit depth distribution, hence $t_0=18$ years, for the pit depth distribution in 2022, $\Delta t=10$, $t_{int}=3.6$ years since the distribution was assumed to fall into all data pitting category as explained previously. To determine the future distribution of the pit depth in 2022,

a Monte Carlo simulation framework shown in Figure 6.12 was utilized to predict the pit depth growth.

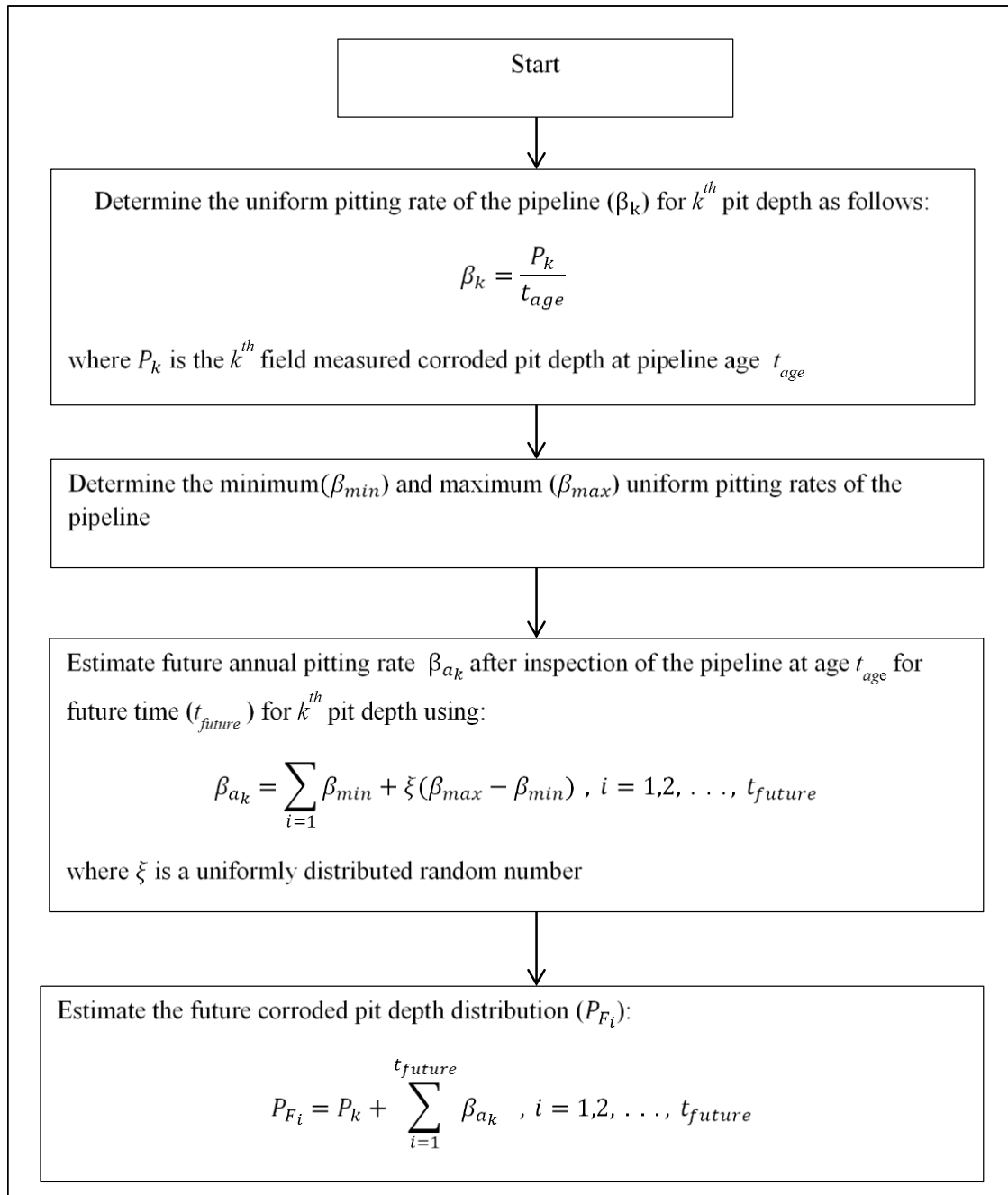


Figure 6.12: Monte Carlo simulation framework for estimation of future corroded pit depth distribution of a single in-line inspection

Figure 6.13 shows the pit depths distribution for the field measured in-line inspection data of the pipeline in 2012, Markov predicted and Monte Carlo simulated pit depth distribution in 2022. The goodness of fit test with two-sample K-S test showed that a p-value of 0.6828 made it possible to accept the hypothesis that

Markov predicted pit depth distribution came from similar distribution with Monte Carlo simulated distribution of the transmission pipeline.

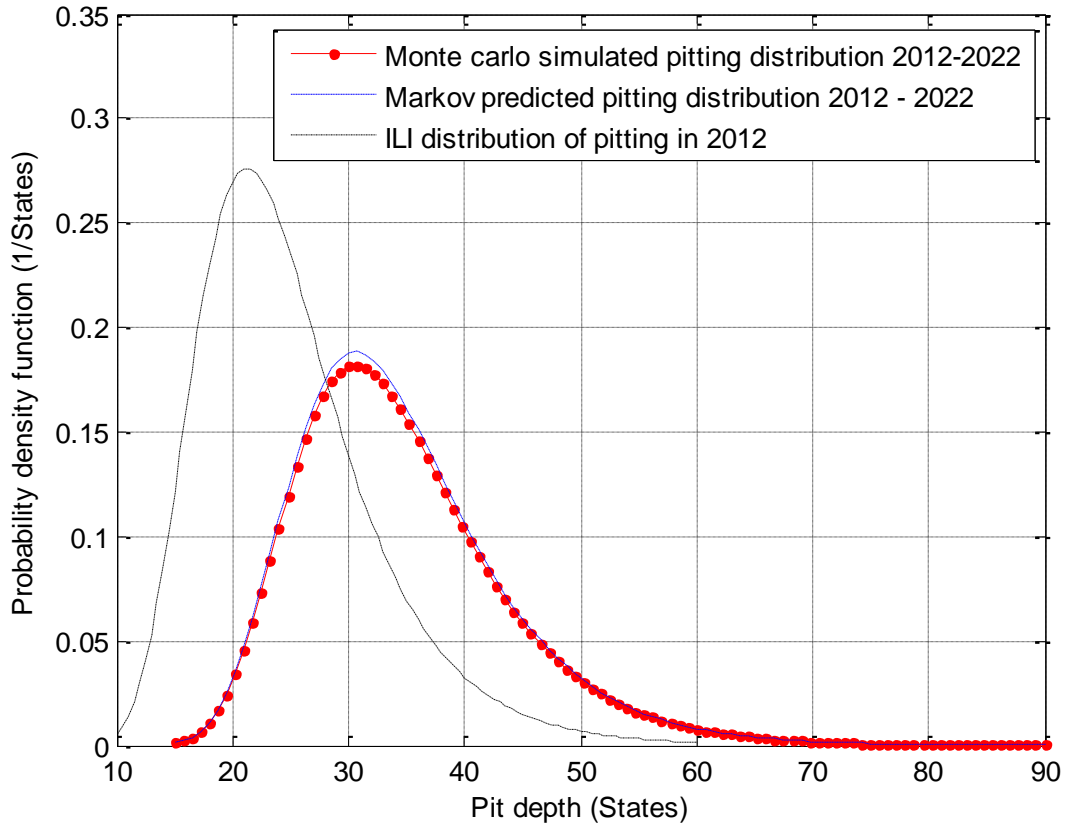


Figure 6.13: Comparison of Markov predicted and Monte Carlo simulated pit depth distribution in 2022 from initial pitting distribution in 2012

6.7 Validation of the Monte Carlo simulated pit depths

To validate the pit depth data generated by Monte Carlo simulation, the probability density distributions of the field observed data and the Monte Carlo simulated data were compared using the techniques described by other researchers for predicting pit depth growth of pipelines (Mohd *et al.* 2014, Paik & Kim 2012). The field observed maximum pit depths were tested with Kolmogorov Smirnov goodness of fit test for different distributions – Generalized Extreme Value (GEV), Weibull and lognormal and lognormal distribution was found to be the best fitting distribution (see Figure 6.14). Other researchers have also shown that lognormal distribution was the best fit distribution for studied pit depths (Bazan & Beck 2013, Mohd & Paik 2013). The comparison of the lognormal distributions of the field and simulated pit depths is

shown in Figure 6.15. A two-sample Kolmogorov Smirnov goodness of fit test shows that a p-value of 0.995 is enough to accept the hypothesis that both simulated and field observed distributions are similar whereas a root mean square error of 0.0012 indicates that Monte Carlo simulated pit data has not varied much when compared with the field observed data.

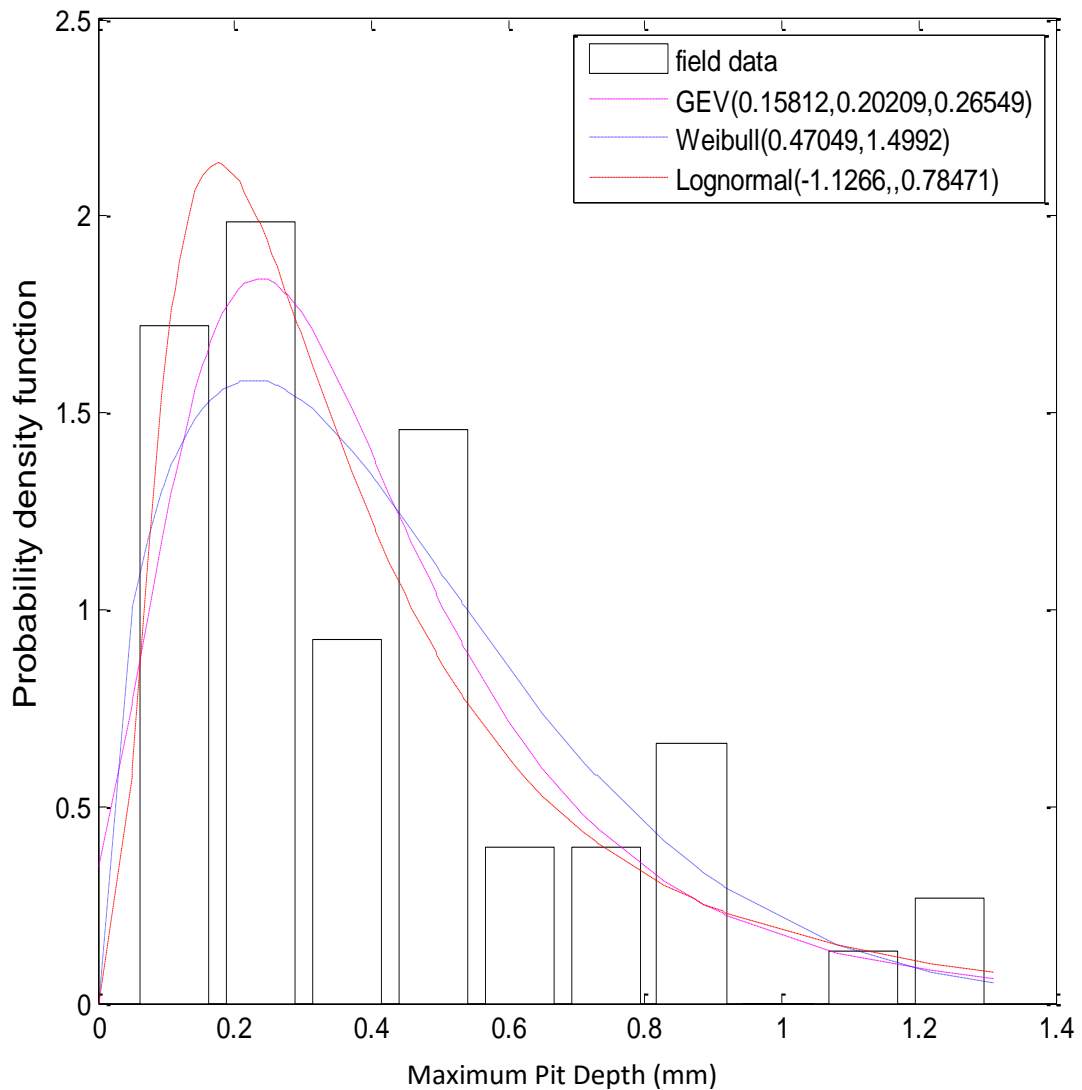


Figure 6.14: Probability density function distribution of field measured data

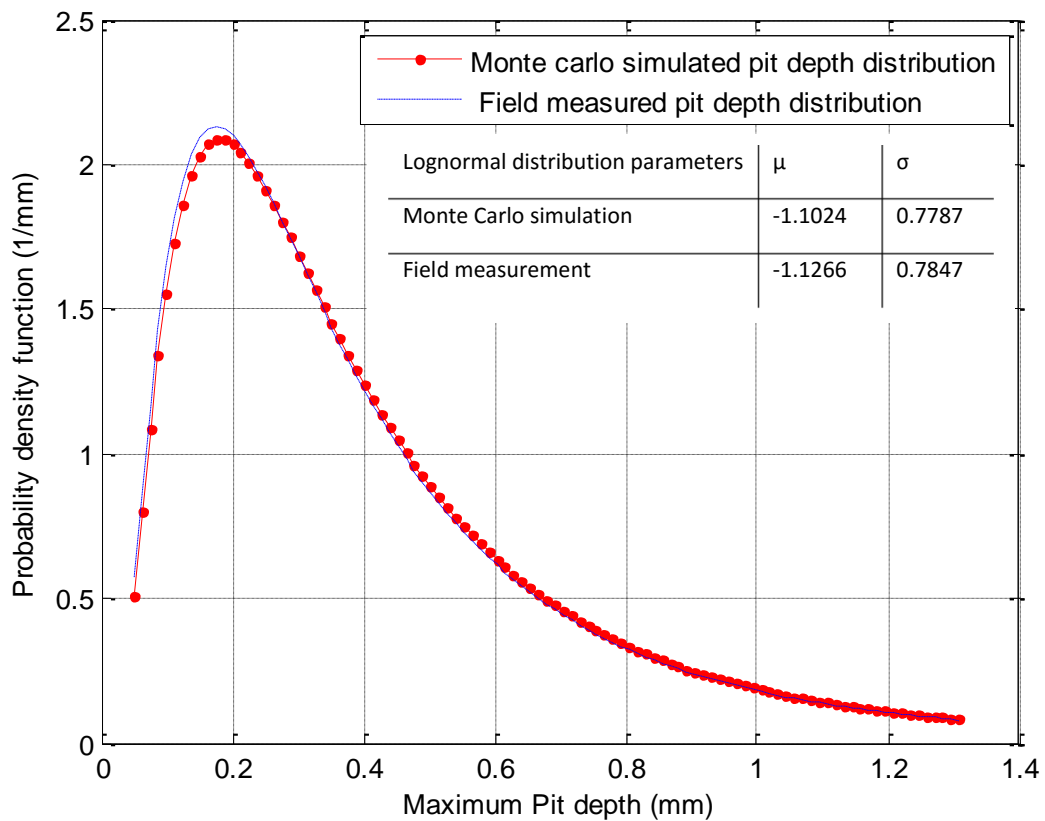


Figure 6.15: Comparison of pit depth distribution for field and Monte Carlo simulated data

6.8 Validation of the Markov prediction model

Root Mean Square Error (RMSE) was also used to validate the field observed pit depth data and Markov predicted data. The summary of the RMSE for the tested field data are shown in Table 6.3.

Table 6.3: Summary of the RMSE of the tested field data

L-80 Grade Well Tubing		
Age (years)		RMSE
5.8		0.0368
N-80 Grade Well Tubing		
Age (years)		RMSE
15.3		0.0616
18.2		0.0724
22.2		0.0869
X52 Transmission Pipeline		
Year		RMSE
2022		0.0154

Table 6.3 indicates that the error in Markov estimation of the future pit depth of the tested field data is between 1.54% and 8.69%. This result implies that Markov model prediction of future pit depth distribution is over 90% accurate.

6.9 Conclusions

To estimate the future pit depth distribution of oil and gas pipelines, a non-homogenous, continuous time pure birth Markov process was used. The work focused on internal pitting corrosion of oil and gas pipelines by considering the effects of some operating parameters – temperature, CO₂ partial pressure, pH and flow rate on the pit depth growth at different pitting categories stipulated by NACE. The pipeline wall thickness was divided into a number of states and the pit depths categorized into the states whilst the transition probability functions estimated by using a closed form of negative binomial distribution was used to estimate the future pit depths distribution.

By analysing the operational parameters and pit depths of the pipelines, the pitting initiation times were estimated for different categories of pitting corrosion rates. The Markov predicted model was tested with field data from L-80 and N-80 grades of well tubing used in offshore oil and gas production and the results agrees well. Onshore oil and gas transmission pipeline inspection data for X52 grade pipe was also tested with the Markov prediction model and the result showed a good agreement with future pit depth distribution modelled with discrete events Monte Carlo simulation.

The field data was also compared with data obtained from the Monte Carlo simulation experiment and the error in the prediction was less than 1%. The comparison of the Markov predicted model and the field data indicated an accuracy of 91.3%~ 98.5%. Since this model has predicted successfully the future pit depth distribution for similar materials in different oil and gas producing wells, it will be a vital tool for pipelines reliability management.

References

- AHAMMED, M. 1998. Probabilistic estimation of remaining life of a pipeline in the presence of active corrosion defects. *International Journal of Pressure Vessels and Piping*, 75, 321-329.
- AHAMMED, M. & MELCHERS, R. E. 1996. Reliability estimation of pressurised pipelines subject to localised corrosion defects. *International Journal of Pressure Vessels and Piping*, 69, 267-272.
- ASME, 2009, Manual for determining the remaining strength of corroded pipelines. American Society of Mechanical Engineers, B31G, New York.
- BAZÁN, F. A. V. & BECK, A. T. 2013. Stochastic process corrosion growth models for pipeline reliability. *Corrosion Science*, 74, 50-58.
- CALEYO, F., GONZÁLEZ, J. L. & HALLEN, J. M. 2002. A study on the reliability assessment methodology for pipelines with active corrosion defects. *International Journal of Pressure Vessels and Piping*, 79, 77-86.
- CALEYO, F., VELÁZQUEZ, J. C., VALOR, A. & HALLEN, J. M. 2009. Markov chain modelling of pitting corrosion in underground pipelines. *Corrosion Science*, 51, 2197-2207.
- CALEYO, F., VELÁZQUEZ, J. C., VALOR, A. & HALLEN, J. M. 2009a. Probability distribution of pitting corrosion depth and rate in underground pipelines: A Monte Carlo study. *Corrosion Science*, 51, 1925-1934.
- CALEYO, F., VELÁZQUEZ, J. C., VALOR, A., & HALLEN, J. M. 2009b. Probability distribution of pitting corrosion depth and rate in underground pipelines: A Monte Carlo study. *Corrosion Science*, 51(9), 1925-1934.
- CAMACHO, E. N., FRUTUOSO, E., MELO, P. F., SALDANHA, P. L. C., & DA SILVA, E. P. 2012. A fokker-planck model of pitting corrosion in underground pipelines to support risk-informed decision making. Paper presented at the Advances in Safety, Reliability and Risk Management - Proceedings of the European Safety and Reliability Conference, ESREL, (2012), 2993-2999.
- COLE, I. S. & MARNEY, D. 2012. The science of pipe corrosion: A review of the literature on the corrosion of ferrous metals in soils, *Corrosion Science* 56, 5-16

- ENGELHARDT, G. & MACDONALD, D. 1998. Deterministic prediction of pit depth distribution. *Corrosion*, 54, 469-479.
- FELDMAN, R. M. & VALDEZ-FLORES, C. 2010. Applied probability and stochastic processes, Springer Science & Business Media.
- HONG, H. P. 1999. Inspection and maintenance planning of pipeline under external corrosion considering generation of new defects. *Structural Safety*, 21, 203-222.
- KATANO, Y., MIYATA, K., SHIMIZU, H. & ISOGAI, T. 2003. Predictive model for pit growth on underground pipes. *Corrosion*, 59, 155-161.
- LAYCOCK, P., COTTIS, R. & SCARF, P. 1990. Extrapolation of extreme pit depths in space and time. *Journal of the Electrochemical Society*, 137, 64-69.
- LI, S.-X., YU, S.-R., ZENG, H.-L., LI, J.-H. & LIANG, R. 2009. Predicting corrosion remaining life of underground pipelines with a mechanically-based probabilistic model. *Journal of Petroleum Science and Engineering*, 65, 162-166.
- MARTÍNEZ, D., GONZALEZ, R., MONTEMAYOR, K., JUAREZ-HERNANDEZ, A., FAJARDO, G. & HERNANDEZ-RODRIGUEZ, M. A. L. 2009. Amine type inhibitor effect on corrosion–Erosion wear in oil gas pipes, *Wear*, 267, 255-58.
- MCMAHON, A. J. & PAISLEY, D. M. E. 1997. Corrosion Prediction Modelling - A guide to the use of corrosion prediction models for risk assessment in oil and gas production and transportation facilities, Report No. ESR.96.ER.066, BP International, Sunbury.
- MELCHERS, R. E. 2005. Representation of uncertainty in maximum depth of marine corrosion pits. *Structural safety*, 27(4), 322-334.
- MELCHERS, R. E. 2008. Extreme value statistics and long-term marine pitting corrosion of steel. *Probabilistic Engineering Mechanics*, 23, 482-488.
- MELCHERS, R. E. 2010. Estimating uncertainty in maximum pit depth from limited observational data. *Corrosion Engineering, Science and Technology*, 45(3), 240-248.
- MOHD, M. H. & PAIK, J. K. 2013. Investigation of the corrosion progress characteristics of offshore subsea oil well tubes. *Corrosion Science*, 67, 130-141.

- NACE 2005, NACE Standard RP0775, Preparation, Installation, analysis, and interpretation of coupons in oilfield operations, 2005, Houston, TX
- PAIK, J. K. & KIM, D. K. 2012. Advanced method for the development of an empirical model to predict time-dependent corrosion wastage, *Corrosion science* 63, 51-58.
- PAPAVINASAM, S., DOIRON, A. & REVIE, R. W. 2010. Model to predict internal pitting corrosion of oil and gas pipelines. *Corrosion*, 66, 035006-035006-11.
- PARZEN, E. 1999. Stochastic processes, classics in applied mathematics, Society for Industrial and Applied Mathematics (SIAM), PA.
- RIVAS, D., CALEYO, F., VALOR, A. & HALLEN, J. M. 2008. Extreme value analysis applied to pitting corrosion experiments in low carbon steel: Comparison of block maxima and peak over threshold approaches. *Corrosion Science*, 50, 3193-3204.
- RODRIGUEZ III, E. & PROVAN, J. 1989a. Part II: development of a general failure control system for estimating the reliability of deteriorating structures. *Corrosion*, 45, 193-206.
- RODRIGUEZ III, E. & PROVAN, J. 1989b. Part I: Development of a general failure control system for estimating the reliability of deteriorating structures. *Corrosion*, 45(3), 178-192.
- SHEIKH, A., BOAH, J. & HANSEN, D. 1990. Statistical modeling of pitting corrosion and pipeline reliability. *Corrosion*, 46, 190-197.
- TARANTSEVA, K. R. 2010. Models and methods of forecasting pitting corrosion. *Protection of metals and physical chemistry of surfaces*, 46(1), 139-147.
- TAYLOR, H. M. & KARLIN, S. 1998. An introduction to stochastic modelling 3rd edition. Academic press San Diego, California USA, 1998, ISBN-13:978-0-12-684887-8.
- VALOR, A., CALEYO, F., ALFONSO, L., VELÁZQUEZ, J. & HALLEN, J. 2013. Markov chain models for the stochastic modeling of pitting corrosion. *Mathematical Problems in Engineering*, 2013.
- VALOR, A., CALEYO, F., RIVAS, D., & HALLEN, J. M. 2010. Stochastic approach to pitting-corrosion-extreme modelling in low-carbon steel. *Corrosion Science*, 52(3), 910-915.

- VALOR, A., CALEYO, F., ALFONSO, L., RIVAS, D. & HALLEN, J. M. 2007. Stochastic modeling of pitting corrosion: A new model for initiation and growth of multiple corrosion pits. *Corrosion Science*, 49, 559-579.
- VALOR, A., CALEYO, F., HALLEN, J. M. & VELÁZQUEZ, J. C. 2013. Reliability assessment of buried pipelines based on different corrosion rate models. *Corrosion Science*, 66, 78-87.
- VALOR, A., CALEYO, F., ALFONSO, L., VIDAL, J., & HALLEN, J. M. 2014. Statistical analysis of pitting corrosion field data and their use for realistic reliability estimations in non-piggable pipeline systems. *Corrosion*, 70(11), 1090-1100.
- VELÁZQUEZ, J. C., CALEYO, F., VALOR, A., & HALLEN, J. M. 2009a. Predictive model for pitting corrosion in buried oil and gas pipelines. *Corrosion*, 65(5), 332-342.
- VELAZQUEZ, J. C., VALOR, A., CALEYO, E., VENEGAS, V., ESPINA-HERNANDEZ, J. H., HALLEN, J. M., & LOPEZ, M. R. 2009b. Pitting corrosion models improve integrity management, reliability. *Oil & Gas Journal*, 107(28), 56-62.
- WHITE, C. C. III & WHITE, D. J. 1989. Markov decision process, *European Journal of Operational Research*, 39, 1-16.
- YUSOF, S., NOOR, N. M., YAHAYA, N., & RASHID, A. S. A. 2014. Markov chain model for predicting pitting corrosion damage in offshore pipeline. *Asian Journal of Scientific Research*, 7(2), 208-216.
- ZHANG, S. & ZHOU, W. 2013. System reliability of corroding pipelines considering stochastic process-based models for defect growth and internal pressure. *International Journal of Pressure Vessels and Piping*, 111, 120-130.
- ZHANG, S., ZHOU, W., & QIN, H. 2013. Inverse Gaussian process-based corrosion growth model for energy pipelines considering the sizing error in inspection data. *Corrosion Science*, 73, 309-320.

Chapter 7 - Conclusions and recommendations

To safely operate oil and gas pipelines requires the mitigation of fatigue stress that is caused by the corrosion defects that originated from the operating environment. The corrosion defects have been associated with electrochemical reaction of water and iron content of the pipeline material in the presence of CO₂ (sweet corrosion), H₂S (sour corrosion) and/or microorganisms (microbiologically induced corrosion) such as bacteria. Corrosion has contributed enormously to pipeline failures in the oil and gas industry as the initiation of localized corrosion defect on pipelines have resulted in fatigue due to the cyclic load induced by the internal operating pressure of the pipeline. The electrochemical and mechanical effects of subcutaneous substances in the pipeline also contribute to the fatigue stress of this asset as the pipe-wall thick reduces.

Despite the difficulty associated with pipeline corrosion mitigation, it is imperative that optimal performance of pipelines is achieved based on integrity assurance cycle by embarking on core activities that includes strategic policy initiation, policy implementation, information analysis and reviews and implementation actions. In order to achieve this, corrosion controls, monitoring and inspections strategies are carried out to ensure that the fatigue failures of operational pipelines are minimized via fitness-for-service testing at design, manufacture, installation and operation. It is also important that enhanced manufacturing practices are used for the production of pipes in the industry, since it will help to reduce defects such as cracks, dents, buckles, bulges and out-of-roundness, which increase the stress load on corroded pipelines.

This research had utilized different techniques that included a non-homogenous, continuous time pure birth Markov process, degradation models, multivariate regression analysis and Monte Carlo simulation to estimate the remaining useful life, corrosion defect growth and reliability of internally corroded oil and gas pipelines. By estimating the future corrosion defect depth distribution in consideration of the operational parameters – CO₂ partial pressure, temperature, flow rate, pH, sulphate ion concentration, chloride ion concentration, wall shear stress and water cut at different corrosion categories, it was possible to determine

the remaining useful life of the pipeline. This involved dividing the pipe-wall thickness of the pipelines into a number of states and the corrosion defect depths categorized into these states while the transition probability functions estimated by using a closed form of negative binomial distribution was used to predict the future pit depths distribution. The variability of the operational parameters was used in establishing the pitting initiation time for pipelines undergoing – low, moderate, high and severe corrosion while establishing the growth rate of the corrosion defect depths over the lifespan of the pipeline.

The lifecycle phases - introduction, maturity, ageing, terminal, failure/leakage of the corroded pipelines were also classified by the retained pipe-wall thickness whereas transition probabilities between the phases were used for establishing the corrosion wastage rates. The holding time of different inspection and repair actions was also determined for the corroded pipeline whereas the expected failure probability over a given time of exposure of the pipeline to corrosion was estimated for different inspection and repair actions. This research also described a technique for evaluating inspection and repair cost of corroded pipelines by exemplifying with the corrosion defect depth information of data from In-Line Inspection (ILI) measurement of X52 grade pipeline.

After analysing the operational parameters and corrosion defect depths of the pipelines, the predicted models for corrosion defect growth, pitting initiation and reliability of the pipelines were tested with field data and the results showed a good agreement. The error margin obtained from the predicted models and the field data for X52, L-80 and N-80 grade pipelines ranged between 1% to 8.7%. Other results obtained from the models also indicated that the developed models in this research is viable for estimating the reliability of aged corroded pipelines.

This research has not considered the impacts of measurement errors on the predicted future pit depth growth and reliability of aged corroded pipelines because the measurement errors were not obtained during the corrosion defect measurement. Given the fact that the presence of inspection errors can bring about the differentiation in the predicted values of corrosion defect depths, which will in turn affect the retained strength and the reliability of the pipelines, it is

recommended that future research will focus on the effects of measurement errors on the remaining useful life of corroded pipelines. Other possible future areas of research include –

- Optimal inspection planning for imperfect monitoring of corroded aged pipelines
- Pipeline reliability prediction in consideration of stress corrosion cracking since the present techniques for monitoring this pipeline defect has not adequately provided enough help for reasonably estimating the burst failure of pipelines.
- The influence of pipeline manufacturing processes on corrosion and reliability over the service life of this asset need more investigation, especially, in the area of safe testing pressure that may not increase the risk of fatigue stress on pipelines.
- There is need for more experimental analysis on the correlation of pipeline burst pressure and toughness of ageing pipelines.
- The role of microorganisms in pipeline corrosion also need further investigation in a bid to establish the link between them and corrosion fatigue failure of pipelines.

Appendix

Statement of contribution

To Whom It May Concern,

I, **Chinedu Ishiodu Ossai**, is the principal author of the papers entitled:

- Pipeline fatigue failures in corrosive environments – A conceptual analysis of trends and effects, Engineering failure analysis 53 (2015) 36–58.
<http://dx.doi.org/10.1016/j.engfailanal.2015.03.004>
- Predictive modelling of internal pitting corrosion of aged non-piggable Pipelines, J. Electrochem. Soc. 2015, 162(6): C251-C259; doi: 10.1149/2.0701506jes
- Estimation of internal pit depth growth and reliability of aged oil and gas pipelines - A Monte Carlo simulation approach, Corrosion: August 2015, Vol. 71, No. 8, pp. 977-99, doi: <http://dx.doi.org/10.5006/1543>
- Stochastic modelling of perfect inspection and repair actions for leak–failure prone internal corroded pipelines. Engineering Failure Analysis, 2016, 60, 40-56. DOI: 10.1016/j.engfailanal.2015.11.030
- Markov chain modelling for time evolution of internal pitting corrosion distribution of oil and gas pipelines. Engineering Failure Analysis (2016), pp. 209-228, DOI: 10.1016/j.engfailanal.2015.11.052



Signature

I, as a Co-Author, endorse that this level of contribution by the candidate indicated above is appropriate.

Dr. Brian Boswell



Signature

Dr. Ian J. Davies



Signature

Abstracts of published paper that are not part of the thesis

Paper1: Reliability Analysis and Performance Predictions of Aged Pipelines Subjected to Internal Corrosion - A Markov Modelling Technique

Abstract

To maintain the integrity of corroded oil and gas pipelines, the reliability at times of exposure over the lifecycle duration need to be understood. This paper describes the procedures for predicting the performance of internally corroded oil and gas pipelines using a probabilistic-based Markovian process. The Pipeline Corrosivity Index (PCI), which is expressed as a function of the retained pipe-wall thickness was used to describe the condition of the corroded pipelines at exposure durations for low, moderate, high and severe corrosion rates. The time variation of the predicted Pipeline Corrosivity Index (PCI) was compared with field measured Pipeline Corrosivity Indexes (PCIs) of corroded API X52 grade pipelines and the results indicate that the model developed in this research is viable for integrated management of aged corroded pipelines and remaining useful life predictions.

Keywords: Pipe-wall thickness; Markov process; Internal corrosion; Monte Carlo Simulation; Corrosion wastage

Paper 2: Modelling the effects of production rates and physico-chemical parameters on pitting rate and pit depth growth of onshore oil and gas pipelines.

Abstract

To estimate the pitting rate of internally corroded oil and gas gathering pipelines, a multivariate regression modelling was carried out, using pitting rates and operating parameters. These operating parameters, which included - temperature, pH, CO₂ partial pressure, water cut, wall shear stress, chloride ion concentration, sulphate ion concentration, operating pressure, oil production rate, gas production rate and water production rate, were obtained from routine monitoring of the pipelines, whereas, the pitting rates (mean pit depths over time) were determined by Ultrasonic Thickness measurement (UTM) technique. It was observed that a unit CO₂ partial pressure increase, contributed most, to the pitting rate increase whilst a unit increase in sulphate ion concentration, contributed most, to pitting rate decrease. The

operating parameters and pitting rates were also used to estimate the pit depth growth of the pipelines using Monte Carlo simulation, and field data was used to test the developed models. The results obtained indicated that, the pipelines under severe pitting corrosion rate were, more conservatively predicted than those under low, moderate and high pitting corrosion rates.

Keywords: pitting corrosion; pit depth growth; oil and gas pipeline; CO₂ partial pressure; power law; multivariate regression modelling

Copyright permissions

Department of Mechanical Engineering
Curtin University, GPO Box U1987,
Perth, WA 6845, Australia
7th September 2015

Permissions Request
The Electrochemical Society (ECS)
65 South Main Street
Pennington, NJ 08534, USA

Dear Copyright Owner,

I am writing to obtain permission from you to enable me to reproduce the article entitled: **Predictive Modelling of Internal Pitting Corrosion of Aged Non-Piggable Pipelines** authored by Chinedu I. Ossai, Brian Boswell and Ian J. Davies of the Department of Mechanical Engineering, Curtin University Perth Australia in my doctoral thesis. This article appeared on The Journal of Electrochemical Society, volume 162, issue 6, pages C251-C259, 2015, doi: 10.1149/2.0701506jes.

This thesis, which I am carrying out in my own right and have no association with any commercial organisation or sponsor is titled: **Predictive Modelling and Reliability Analysis of Aged, Corroded Pipelines**, will be made available in online form via Curtin University's Institutional Repository [espace@Curtin \(http://espace.library.curtin.edu.au\)](http://espace.library.curtin.edu.au) and will be strictly used for educational purposes and on a non-commercial basis.

I would be most grateful for your consent to the copying and communication of the work as proposed.

I look forward to hearing from you and thank you in advance for your consideration of my request.

Yours sincerely

Chinedu Ishiodu Ossai

Permission is granted to include the above-referenced paper in your thesis, provided that you obtain permission of the other individual authors. In the thesis, please acknowledge the authors and the citation given above, and include the words: "Reproduced by permission of ECS — The Electrochemical Society."

Sept. 10, 2015

Date

Ann F. Goedkoop

Ann F. Goedkoop, Publications Production Director

RIGHTS & ACCESS

Elsevier Ltd

Article: Stochastic modelling of perfect inspection and repair actions for leak-failure prone internal corroded pipelines
Corresponding author: Mr. Chinedu I. Ossai
E-mail address: ossaici@yahoo.com
Journal: Engineering Failure Analysis
Our reference: EFA2755
PII: S1350-6307(15)30149-7
DOI: 10.1016/j.engfailanal.2015.11.030

YOUR STATUS

» I am one author signing on behalf of all co-authors of the manuscript

DATA PROTECTION & PRIVACY

» I do wish to receive news, promotions and special offers about products and services from Elsevier Ltd and its affiliated companies

ASSIGNMENT OF COPYRIGHT

I hereby assign to Elsevier Ltd the copyright in the manuscript identified above (where Crown Copyright is claimed, authors agree to grant an exclusive publishing and distribution license) and any tables, illustrations or other material submitted for publication as part of the manuscript (the "Article") in all forms and media (whether now known or later developed), throughout the world, in all languages, for the full term of copyright, effective when the Article is accepted for publication.

SUPPLEMENTAL MATERIALS

With respect to Supplemental Materials that I wish to make accessible either through a link in the Article or on a site or through a service of Elsevier Ltd, Elsevier Ltd shall be entitled to publish, post, reformat, index, archive, make available and link to such Supplemental Materials on a non-exclusive basis in all forms and media (whether now known or later developed) and to permit others to do so. "Supplemental Materials" shall mean additional materials that are not an intrinsic part of the Article, including but not limited to experimental data, e-components, encodings and software, and enhanced graphical, illustrative, video and audio material.

REVERSION OF RIGHTS

Articles may sometimes be accepted for publication but later rejected in the publication process, even in some cases after public posting in "Articles in Press" form, in which case all rights will revert to the author (see <http://www.elsevier.com/locate/withdrawalpolicy>).

REVISIONS AND ADDENDA

I understand that no revisions, additional terms or addenda to this Journal Publishing Agreement can be accepted without Elsevier Ltd's express written consent. I understand that this Journal Publishing Agreement supersedes any previous agreements I have entered into with Elsevier Ltd in relation to the Article from the date hereof.

RETENTION OF RIGHTS FOR SCHOLARLY PURPOSES.

I understand that I retain or am hereby granted (without the need to obtain further permission) the Retained Rights (see description below), and that no rights in patents, trademarks or other intellectual property rights are transferred to Elsevier Ltd.

The Retained Rights include the right to use the [Preprint](#), [Accepted Manuscript](#) and the [Published Journal Article](#) for [Personal Use](#), [Internal Institutional Use](#) and for [Scholarly Sharing](#).

In the case of the Accepted Manuscript and the Published Journal Article the Retained Rights exclude Commercial Use (unless expressly agreed in writing by Elsevier Ltd), other than use by the author in a subsequent compilation of the author's works or to extend the Article to book length form or re-use by the author of portions or excerpts in other works (with full acknowledgment of the original publication of the Article).

AUTHOR REPRESENTATIONS / ETHICS AND DISCLOSURE

I affirm the Author Representations noted below, and confirm that I have reviewed and complied with the relevant Instructions to Authors, Ethics in Publishing policy, and Conflicts of Interest disclosure. Please note that some journals may require that all co-authors sign and submit Conflicts of Interest disclosure forms. I am also aware of the publisher's policies with respect to retractions and withdrawal (<http://www.elsevier.com/locate/withdrawalpolicy>). For further information see the publishing ethics page at <http://www.elsevier.com/publishingethics> and the journal home page.

Author representations

- » The Article I have submitted to the journal for review is original, has been written by the stated authors and has not been published elsewhere
- » The Article was not submitted for review to another journal while under review by this journal and will not be submitted to any other journal



NACE International
15835 Park Ten Place
Houston, TX 77084
Tel: 281-228-6200
Fax: 281-228-6300

Permission to Reproduce Figures, Photos, and Tables from Copyrighted Works

Date: 11/09/2015

Name: Chinedu Ishiodu Ossai Title: Mr

Company ("Publisher"): Corrosion Journal

Address: Unit 4/99-103 Armstrong Road, Wilson, WA 6107, Australia

Tel: +61404581441 Fax: _____

Email: chinedu.ossai@postgrad.curtin.edu.au; ossaic@gmail.com

Material to be Reproduced ("Work"): Please provide a complete description of the material involved. Include the following elements where applicable: publication name, issue date, page number, figure/photo/table number, paper number, conference name, etc.

Estimation of Internal Pit depth Growth and Reliability of Aged Oil and Gas Pipelines -

A Monte Carlo simulation Approach. Corrosion: August 2015, Vol. 71, No. 8, pp. 977-99,

doi: <http://dx.doi.org/10.5006/1543>

Reproduction Method ("Publication Media"): Please provide a complete description of how and where the Work will be used. Include the following elements as applicable: publication name, issue, circulation, print run, web site address, conference name, presentation time and place, etc.

Doctoral Thesis - Department of Mechanical Engineering, Curtin University, Perth, Australia

Thesis Topic: Predictive Modelling and Reliability Analysis of Aged, Corroded Pipelines

Thesis Publication: espace@Curtin (<http://espace.library.curtin.edu.au>)

NACE International ("NACE") hereby grants to "Publisher" the right to publish the Work utilizing the Publication Media described above. The publication right granted herein is limited to the specific Publication Media described above. To the extent the publication of the Work is to occur by an above-specified date, such as in a particular periodical or at a particular conference, the right granted herein shall automatically terminate upon the date of such occurrence, whether or not the Work is actually published. To the extent the Publication Media is a web site, the publication right is limited to publication at the specific web site URL identified above. Any right granted herein is a limited, non-transferable, non-exclusive right. No other rights in the Work are granted herein.

Publisher shall not edit or modify the Work except to meet the style and graphic requirements of the individual media involved.

The Publisher shall include the following notation with any publication of the Work:*

A. Conference Paper

Reproduced with permission from NACE International, Houston, TX. All rights reserved. Author(s), Paper NUMBER presented at CORROSION/YEAR, City, State. © NACE International FIRST YEAR OF PUBLICATION.

B. Journal Article

Reproduced with permission from NACE International, Houston, TX. All rights reserved. Author(s) name, Article title, Journal title, Vol. no., Issue no., and publication year. © NACE International FIRST YEAR OF PUBLICATION.

C. Magazine Article

Reproduced with permission from NACE International, Houston, TX. All rights reserved. Author(s) name, Article title, Magazine title, Vol. no., Issue no., and publication year. © NACE International FIRST YEAR OF PUBLICATION.

D. Standards

STANDARDS/TECHNICAL COMMITTEE REPORT NAME. © NACE International YEAR. All rights reserved by NACE. Reprinted with permission. NACE standards are revised periodically. Users are cautioned to obtain the latest edition; information in an outdated version of the standard may not be accurate.

* Modifications to Notations: Other reference wording can be used, but must be approved by NACE in writing *in advance*.

- » The Article and the Supplemental Materials contain no libellous or other unlawful statements and do not contain any materials that proprietary rights of any other person or entity.
- » I have obtained written permission from copyright owners for any excerpts from copyrighted works that are included and have created Article or the Supplemental Materials.
- » Except as expressly set out in this Journal Publishing Agreement, the Article is not subject to any prior rights or licenses and, if my authors' institution has a policy that might restrict my ability to grant exclusive rights under this Journal Publishing Agreement, a written policy has been obtained.
- » If I am using any personal details or images of patients, research subjects or other individuals, I have obtained all consents required and complied with the publisher's policies relating to the use of such images or personal information. See <http://www.elsevier.com> for further information.
- » Any software contained in the Supplemental Materials is free from viruses, contaminants or worms.
- » If the Article or any of the Supplemental Materials were prepared jointly with other authors, I have informed the co-author(s) of the Journal Publishing Agreement and that I am signing on their behalf as their agent, and I am authorized to do so.

For information on the publisher's copyright and access policies, please see <http://www.elsevier.com/copyright>.
[For more information about the definitions relating to this agreement click here.](#)

I have read and agree to the terms of the Journal Publishing Agreement.

17th November 2015

T-copyright-v20/2015



NACE International
15835 Park Ten Place
Houston, TX 77064
Tel: 281-226-6200
Fax: 281-228-6300

Permission to Reproduce Figures, Photos, and Tables from Copyrighted Works

Date: 11/09/2015
Name: Chinedu Ishiodu Ossai Title: Mr
Company ("Publisher"): Corrosion Journal
Address: Unit 4/99-103 Armstrong Road, Wilson, WA 6107, Australia
Tel: +61404581441 Fax: _____
Email: chinedu.ossai@postgrad.curtin.edu.au; ossaic@gmail.com

Material to be Reproduced ("Work"): Please provide a complete description of the material involved. Include the following elements where applicable: publication name, issue date, page number, figure/photo/table number, paper number, conference name, etc.

Estimation of Internal Pitting Growth and Reliability of Aged Oil and Gas Pipelines -
A Monte Carlo simulation Approach. Corrosion: August 2015, Vol. 71, No. 8, pp. 977-98,
doi: <http://dx.doi.org/10.5006/1543>

Reproduction Method ("Publication Media"): Please provide a complete description of how and where the Work will be used. Include the following elements as applicable: publication name, issue, circulation, print run, web site address, conference name, presentation time and place, etc.

Doctoral Thesis - Department of Mechanical Engineering, Curtin University, Perth, Australia
Thesis Topic: Predictive Modeling and Reliability Analysis of Aged, Corroded Pipelines
Thesis Publication: espac@Curtin (<http://espace.library.curtin.edu.au/>)

NACE International ("NACE") hereby grants to "Publisher" the right to publish the Work utilizing the Publication Media described above. The publication right granted herein is limited to the specific Publication Media described above. To the extent the publication of the Work is to occur by an above-specified date, such as in a particular periodical or at a particular conference, the right granted herein shall automatically terminate upon the date of such occurrence, whether or not the Work is actually published. To the extent the Publication Media is a web site, the publication right is limited to publication at the specific web site URL identified above. Any right granted herein is a limited, non-transferable, non-exclusive right. No other rights in the Work are granted herein.

Publisher shall not edit or modify the Work except to meet the style and graphic requirements of the individual media involved.

The Publisher shall include the following notation with any publication of the Work:

A. Conference Paper

Reproduced with permission from NACE International, Houston, TX. All rights reserved. Author(s), Paper NUMBER presented at CORROSION YEAR, City, State. © NACE International FIRST YEAR OF PUBLICATION.

B. Journal Article

Reproduced with permission from NACE International, Houston, TX. All rights reserved. Author(s) name, Article title, Journal title, Vol. no., issue no., and publication year. © NACE International FIRST YEAR OF PUBLICATION.

C. Magazine Article

Reproduced with permission from NACE International, Houston, TX. All rights reserved. Author(s) name, Article title, Magazine title, Vol. no., issue no., and publication year. © NACE International FIRST YEAR OF PUBLICATION.

D. Standards

STANDARDS/TECHNICAL COMMITTEE REPORT NAME. © NACE International YEAR. All rights reserved by NACE. Reprinted with permission. NACE standards are revised periodically. Users are cautioned to obtain the latest edition; information in an outdated version of the standard may not be accurate.

* Modifications to Notations: Other reference wording can be used, but must be approved by NACE in writing in advance.

The Publisher shall include full bibliographic citations of or references to the original NACE source, where applicable.

Publisher shall obtain a copy of the original Work directly from NACE International and shall not utilize copies of the Work from other sources, including the author(s).

To the extent the Work is published on a web site as authorized herein, the Work shall be posted in a file format that does not allow the content of the Work to be easily copied from the Web Site or changed.

As between NACE and Publisher, Publisher acknowledges that NACE owns all rights in the Works.

Publisher shall not be entitled to any compensation for its efforts in promoting the Work.

THE WORK IS PROVIDED "AS IS." ALL EXPRESS OR IMPLIED COVENANTS, CONDITIONS, REPRESENTATIONS OR WARRANTIES, INCLUDING ANY IMPLIED WARRANTY OF MERCHANTABILITY OR FITNESS FOR A PARTICULAR PURPOSE OR CONDITIONS OF ACCURACY, COMPLETENESS OR QUALITY AND THOSE ARISING BY STATUTE OR OTHERWISE IN LAW, ARE HEREBY DISCLAIMED.

IN NO EVENT WILL NACE BE LIABLE FOR ANY DIRECT, INDIRECT, PUNITIVE, SPECIAL, INCIDENTAL OR CONSEQUENTIAL DAMAGES IN CONNECTION WITH OR RELATED TO THIS AGREEMENT (INCLUDING LOSS OF PROFITS, USE, DATA, OR OTHER ECONOMIC ADVANTAGE), HOWSOEVER ARISING.

This Agreement and the rights granted herein may be terminated immediately by NACE upon breach of this Agreement by Publisher. Unless earlier terminated, this Agreement and the rights granted herein will automatically terminate 6 months from the Date set forth above. If the Work has not been published within that time period, a new Agreement must be obtained.

Publisher may not, directly or indirectly, sell, assign, sublicense, lease, rent, distribute, or otherwise transfer this Agreement or any rights granted herein, without the prior written consent of NACE.

If any provision of this Agreement is found to be unenforceable, then this Agreement shall be deemed to be amended by modifying such provision to the extent necessary to make it legal and enforceable while preserving its intent. The remainder of this Agreement shall not be affected by such modification.

This Agreement does not create, and shall not be construed to create, any employer-employee, joint venture or partnership relationship between the parties. No officer, employee, agent, servant or independent contractor of either party shall at any time be deemed to be an employee, servant, agent or contractor of any other party for any purpose whatsoever.

This Agreement shall be governed by, and construed and enforced in accordance with, the laws of the State of Texas, without regard to the choice of law provisions of that State.

This Agreement shall only be effective if signed by authorized representatives of both parties. This Agreement constitutes the entire Agreement between the parties with respect to the subject matter of this Agreement. Any change, modification or waiver hereto must be in writing and signed by authorized representatives of both parties.

Other Terms & Conditions: _____

Publisher hereby requests permission to publish the Work described above and agrees to comply with all Terms and Conditions listed above.

Request submitted by:
Chinadu Ishiodu Ossai
Printed Name
Mr
Title
Signature
Date 11/09/2015

Request approved by NACE:
Daniela Freeman
Printed Name
Audience Development Manager
Title
Signature
Date Sept 11, 2015

Request agreed to by:
Chinadu Ishiodu Ossai
Lead Author Printed Name
Mr
Lead Author Title
Lead Author Signature
Date 11/09/2015

Third parties requesting permission to use NACE logos/labels
FM_PUB_06
Revised 07/20/2015

RIGHTS & ACCESS

Elsevier Ltd

Article: Markov chain modelling for time evolution of internal pitting corrosion distribution of oil and gas pipelines
Corresponding author: Mr. Chinedu I. Ossaici
E-mail address: ossaici@yahoo.com
Journal: Engineering Failure Analysis
Our reference: EF A2777
PII: S1350-6307(15)30174-6
DOI: 10.1016/j.engfailanal.2015.11.052

YOUR STATUS

» I am one author signing on behalf of all co-authors of the manuscript

DATA PROTECTION & PRIVACY

» I do wish to receive news, promotions and special offers about products and services from Elsevier Ltd and its affiliated companies

ASSIGNMENT OF COPYRIGHT

I hereby assign to Elsevier Ltd the copyright in the manuscript identified above (where Crown Copyright is claimed, authors agree to grant an exclusive publishing and distribution license) and any tables, illustrations or other material submitted for publication as part of the manuscript (the "Article") in all forms and media (whether now known or later developed), throughout the world, in all languages, for the full term of copyright, effective when the Article is accepted for publication.

SUPPLEMENTAL MATERIALS

With respect to Supplemental Materials that I wish to make accessible either through a link in the Article or on a site or through a service of Elsevier Ltd, Elsevier Ltd shall be entitled to publish, post, reformat, index, archive, make available and link to such Supplemental Materials on a non-exclusive basis in all forms and media (whether now known or later developed) and to permit others to do so. "Supplemental Materials" shall mean additional materials that are not an intrinsic part of the Article, including but not limited to experimental data, e-components, encodings and software, and enhanced graphical, illustrative, video and audio material.

REVERSION OF RIGHTS

Articles may sometimes be accepted for publication but later rejected in the publication process, even in some cases after public posting in "Articles in Press" form, in which case all rights will revert to the author (see <http://www.elsevier.com/locate/withdrawalpolicy>).

REVISIONS AND ADDENDA

I understand that no revisions, additional terms or addenda to this Journal Publishing Agreement can be accepted without Elsevier Ltd's express written consent. I understand that this Journal Publishing Agreement supersedes any previous agreements I have entered into with Elsevier Ltd in relation to the Article from the date hereof.

RETENTION OF RIGHTS FOR SCHOLARLY PURPOSES.

I understand that I retain or am hereby granted (without the need to obtain further permission) the Retained Rights (see description below), and that no rights in patents, trademarks or other intellectual property rights are transferred to Elsevier Ltd.

The Retained Rights include the right to use the [Preprint](#), [Accepted Manuscript](#) and the [Published Journal Article](#) for [Personal Use](#), [Internal Institutional Use](#) and for [Scholarly Sharing](#).

In the case of the Accepted Manuscript and the Published Journal Article the Retained Rights exclude Commercial Use (unless expressly agreed in writing by Elsevier Ltd), other than use by the author in a subsequent compilation of the author's works or to extend the Article to book length form or re-use by the author of portions or excerpts in other works (with full acknowledgment of the original publication of the Article).

AUTHOR REPRESENTATIONS / ETHICS AND DISCLOSURE

I affirm the Author Representations noted below, and confirm that I have reviewed and complied with the relevant Instructions to Authors, Ethics in Publishing policy, and Conflicts of Interest disclosure. Please note that some journals may require that all co-authors sign and submit Conflicts of Interest disclosure forms. I am also aware of the publisher's policies with respect to retractions and withdrawal (<http://www.elsevier.com/locate/withdrawalpolicy>).

For further information see the publishing ethics page at <http://www.elsevier.com/publishingethics> and the journal home page.

Author representations

- » The Article I have submitted to the journal for review is original, has been written by the stated authors and has not been published
- » The Article was not submitted for review to another journal while under review by this journal and will not be submitted to any other journal
- » The Article and the Supplemental Materials contain no libellous or other unlawful statements and do not contain any materials that infringe the proprietary rights of any other person or entity.
- » I have obtained written permission from copyright owners for any excerpts from copyrighted works that are included and have credited the source in the Article or the Supplemental Materials.
- » Except as expressly set out in this Journal Publishing Agreement, the Article is not subject to any prior rights or licenses and, if my institution has a policy that might restrict my ability to grant exclusive rights under this Journal Publishing Agreement, a written policy has been obtained.

- » If I am using any personal details or images of patients, research subjects or other individuals, I have obtained all consents required, complied with the publisher's policies relating to the use of such images or personal information. See <http://www.elsevier.com/patients> for further information.
- » Any software contained in the Supplemental Materials is free from viruses, contaminants or worms.
- » If the Article or any of the Supplemental Materials were prepared jointly with other authors, I have informed the co-author(s) of the Publishing Agreement and that I am signing on their behalf as their agent, and I am authorized to do so.

For information on the publisher's copyright and access policies, please see <http://www.elsevier.com/copyright>.
[For more information about the definitions relating to this agreement click here.](#)

I have read and agree to the terms of the Journal Publishing Agreement

20th November 2015

T-copyright-v20/2015

RIGHTS & ACCESS

Elsevier Ltd

Article: Pipeline Failures in Corrosive Environments – A Conceptual Analysis of Trends and Effects
Corresponding author: Mr. Chinedu I. Ossai
E-mail address: ossai@yahoo.com; ossaic@gmail.com
Journal: Engineering Failure Analysis
Our reference: EFA2527
PII: S1350-6307(15)00083-7
DOI: 10.1016/j.engfailanal.2015.03.004

YOUR STATUS

» I am one author signing on behalf of all co-authors of the manuscript

DATA PROTECTION & PRIVACY

» I do wish to receive news, promotions and special offers about products and services from Elsevier Ltd and its affiliated companies

ASSIGNMENT OF COPYRIGHT

I hereby assign to Elsevier Ltd the copyright in the manuscript identified above (where Crown Copyright is claimed, authors agree to grant an exclusive publishing and distribution license) and any tables, illustrations or other material submitted for publication as part of the manuscript (the "Article") in all forms and media (whether now known or later developed), throughout the world, in all languages, for the full term of copyright, effective when the Article is accepted for publication.

SUPPLEMENTAL MATERIALS

With respect to Supplemental Materials that I wish to make accessible through a link in the Article or through a service of Elsevier Ltd, Elsevier Ltd shall be entitled to publish, post, reformat, index, archive, make available and link to such Supplemental Materials on a non-exclusive basis in all forms and media (whether now known or hereafter developed) and to permit others to do so. "Supplemental Materials" shall mean additional materials that are not an intrinsic part of the Article, including but not limited to experimental data, e-components, encodings and software, and enhanced graphical, illustrative, video and audio material.

REVERSION OF RIGHTS

Articles may sometimes be accepted for publication but later rejected in the publication process, even in some cases after public posting in "Articles in Press" form, in which case all rights will revert to the author (see <http://www.elsevier.com/locate/withdrawalpolicy>).

REVISIONS AND ADDENDA

I understand that no revisions, additional terms or addenda to this Journal Publishing Agreement can be accepted without Elsevier Ltd's express written consent. I understand that this Journal Publishing Agreement supersedes any previous agreements I have entered into with Elsevier Ltd in relation to the Article from the date hereof.

RETENTION OF RIGHTS FOR SCHOLARLY PURPOSES

I understand that I retain or am hereby granted (without the need to obtain further permission) the Retained Rights (see description below), and that no rights in patents, trademarks or other intellectual property rights are transferred to Elsevier Ltd.

The Retained Rights include:

- » the right to use the [Preprint](#) or [Accepted Author Manuscript](#) for [Personal Use](#), [Internal Institutional Use](#) and for [Permitted Scholarly Published Journal Article](#) for [Personal Use](#); and [Internal Institutional Use](#).

but in each case as noted in the Definitions' clause excluding [Commercial Use](#) or [Systematic Distribution](#) (unless expressly agreed in writing by Elsevier Ltd).

AUTHOR REPRESENTATIONS / ETHICS AND DISCLOSURE

I affirm the Author Representations noted below, and confirm that I have reviewed and complied with the relevant Instructions to Authors, Ethics in Publishing policy, and Conflicts of Interest disclosure. Please note that some journals may require that all co-authors sign and submit Conflicts of Interest disclosure forms. I am also aware of the publisher's policies with respect to retractions and withdrawal (<http://www.elsevier.com/locate/withdrawalpolicy>).

For further information see the publishing ethics page at <http://www.elsevier.com/publishingethics> and the journal home page.

Author representations

- » The Article I have submitted to the journal for review is original, has been written by the stated authors and has not been published elsewhere.
- » The Article was not submitted for review to another journal while under review by this journal and will not be submitted to any other journal.
- » The Article and the Supplemental Materials contain no libellous or other unlawful statements and do not contain any materials that infringe the proprietary rights of any other person or entity.

- » I have obtained written permission from copyright owners for any excerpts from copyrighted works that are included and have created the Article or the Supplemental Materials.
- » Except as expressly set out in this Journal Publishing Agreement, the Article is not subject to any prior rights or licenses and, if my authors' institution has a policy that might restrict my ability to grant exclusive rights under this Journal Publishing Agreement, a written policy has been obtained.
- » If I am using any personal details or images of patients, research subjects or other individuals, I have obtained all consents required and complied with the publisher's policies relating to the use of such images or personal information. See <http://www.elsevier.com> for further information.
- » Any software contained in the Supplemental Materials is free from viruses, contaminants or worms.
- » If the Article or any of the Supplemental Materials were prepared jointly with other authors, I have informed the co-author(s) of this Journal Publishing Agreement and that I am signing on their behalf as their agent, and I am authorized to do so.

For information on the publisher's copyright and access policies, please see <http://www.elsevier.com/copyright>.
[For more information about the definitions relating to this agreement click here.](#)

I have read and agree to the terms of the Journal Publishing Agreement.

19th March 2015

T-copyright-v19/2014

Bibliography

- ABEDI, S. S., ABDOLMALEKI, A. & ADIBI, N. 2007. Failure analysis of SCC and SRB induced cracking of a transmission oil products pipeline. *Engineering Failure Analysis*, 14, 250-261.
- ADIB, R., SCHMITT, C. & PLUVINAGE, G. 2006. Application of volumetric method to the assessment of damage induced by action of foreign object on gas pipes. *Strength of Materials*, 38, 409-416.
- ADIB-RAMEZANI, H., JEONG, J. & PLUVINAGE, G. 2006. Structural integrity evaluation of X52 gas pipes subjected to external corrosion defects using the SINTAP procedure. *International Journal of Pressure Vessels and Piping*, 83, 420-432.
- AHMED, F., ALI, L., IQBAL, J. & HASAN, F. 2008. Failure of pipe joints during hydrostatic testing. *Engineering Failure Analysis*, 15, 766-773.
- AHMED, T. M., LAMBERT, S. B., SUTHERBY, R., & PLUMTREE, A. 1997. Cyclic crack growth rates of X-60 pipeline steel in a neutral dilute solution. *Corrosion*, 53 (7), 581-590.
- AHAMMED, M. 1997. Prediction of remaining strength of corroded pressurised pipelines. *International Journal of Pressure Vessels and Piping*, 71(3), 213-217.
- AHAMMED, M. 1998. Probabilistic estimation of remaining life of a pipeline in the presence of active corrosion defects. *International Journal of Pressure Vessels and Piping*, 75, 321-329.
- AHAMMED, M. & MELCHERS, R. 1996. Reliability estimation of pressurised pipelines subject to localised corrosion defects. *International Journal of Pressure Vessels and Piping*, 69, 267-272.
- ALAMILLA, J. & SOSA, E. 2008. Stochastic modelling of corrosion damage propagation in active sites from field inspection data. *Corrosion Science*, 50, 1811-1819.
- ALBERTA ENERGY REGULATOR (AER). 2013. Report 2013 - B: Pipeline performance in Alberta, 1990–2012. Available from: <<http://www.aer.ca/documents/reports/R2013-B.pdf>>. [17/09/13].

- ALIZADEH, A.H., KHISHVAND, M., IOANNIDIS, M.A. & PIRI, M. 2014. Multi-scale experimental study of carbonated water injection: An effective process for mobilization and recovery of trapped oil, *Fuel* 132, 219–235.
- AMERICAN GAS ASSOCIATION. 2011. Summary of costs and factors impacting, in-line inspection, direct assessment, pressure testing and pipeline replacements for natural gas transmission pipelines. Available from: <<http://www.aga.org/our-issues/safety/pipeline-safety/Technicalreports/Documents/ILI%20DA%20Hydro%20Replacement%20Cost%20and%20Factors%20Summary%20Final%2004-04-11.pdf>>. [2/12/14].
- AMERICAN PETROLEUM INSTITUTE (API). 2000. Fitness-for-service, API Recommended Practice 579. API Publication 579, USA.
- AMERICAN SOCIETY OF MECHANICAL ENGINEERS, ASME B31.8S. 2004. Managing system integrity of gas pipelines, American Society of Mechanical engineers, New York, USA.
- AMERICAN SOCIETY OF MECHANICAL ENGINEERS, ASME, 2009. Manual for determining the remaining strength of corroded pipelines. American Society of Mechanical Engineers, B31G, New York.
- AMIRAT, A., MOHAMED-CHATEAUNEUF, A. & CHAOUI, K. 2006. Reliability assessment of underground pipelines under the combined effect of active corrosion and residual stress. *International Journal of Pressure Vessels and Piping*, 83, 107-117.
- AZEVEDO, C. R. F. 2007. Failure analysis of a crude oil pipeline, *Engineering Failure Analysis*, 14, 978-94.
- AZEVEDO, C. R. F. & SINATORA, A. 2004. Failure analysis of a gas pipeline, *Engineering Failure Analysis*, 11, 387-400.
- BAZÁN, F. A. V. & BECK, A. T. 2013. Stochastic process corrosion growth models for pipeline reliability. *Corrosion Science*, 74, 50-58.
- BBC. 2014. Taiwan gas blasts in Kaohsiung kill at least 25. Available from: <<http://www.bbc.com/news/world-asia-28594693>>. [7/2/15].

- BEDAIRI, B., CRONIN, D., HOSSEINI, A. & PLUMTREE, A. 2012. Failure prediction for Crack-in-Corrosion defects in natural gas transmission pipelines. *International Journal of Pressure Vessels and Piping*, 96–97, 90-99.
- BEIDOKHTI, B., DOLATI, A. & KOUKABI, A. H. 2009. Effects of alloying elements and microstructure on the susceptibility of the welded HSLA steel to hydrogen-induced cracking and sulfide stress cracking, *Materials Science and Engineering: A*, 507, 167-73.
- BESEL, M., ZIMMERMANN, S., KALWA, C., KÖPPE, T., & LIESSEM, A. 2010. Corrosion assessment method validation for high-grade line pipe. In 2010 8th International Pipeline Conference (pp. 385-394). American Society of Mechanical Engineers.
- BHANDARI, J., KHAN, F., ABBASSI, R., GARANIYA, V. & OJEDA, R. 2015. Modelling of pitting corrosion in marine and offshore steel structures – A technical review. *Journal of Loss Prevention in the Process Industries*, 37, 39-62.
- BHASKARAN, R., PALANISWAMY, N., RENGASWAMY, N.S. & JAYACHANDRAN, M. 2005. Global cost of corrosion—A historical review, *ASM Handbook, Volume 13B: Corrosion: Materials*, S.D. Cramer, B.S. Covino, Jr., editors, 2005, p621-628, DOI: 10.1361/asmhba0003968.
- BISAGGIO, H. D. C. & NETTO, T. A. 2015. Predictive analyses of the integrity of corroded pipelines based on concepts of structural reliability and Bayesian inference. *Marine Structures*, 41, 180-199.
- BIOMORGI, J., HERNÁNDEZ, S., MARÍN, J., RODRIGUEZ, E., LARA, M. & VILORIA, A. 2012. Internal corrosion studies in hydrocarbons production pipelines located at Venezuelan Northeastern. *Chemical Engineering Research and Design*, 90, 1159-1167.
- BLIN, F., KOUTSOUKOS, P., KLEPETSANIS, P. & FORSYTH, M. 2007. The corrosion inhibition mechanism of new rare earth cinnamate compounds — Electrochemical studies, *Electrochimica Acta*, 52, 6212-20.
- BRITISH STANDARDS INSTITUTION (BSI). 2005. Guide on methods for assessing the acceptability of flaws in fusion welded structures BS 7910. London (UK), 2005.

- BROWN, G. K. 2014. Appendix - Internal corrosion monitoring techniques for pipeline systems, in Pipeline integrity handbook, ed. by Ramesh Singh (Boston: Gulf Professional Publishing, 2014), pp. 255-92.
- BRETON, T., SANCHEZ-GHENO, J. C., ALAMILLAC, J.L. & ALVAREZ-RAMIREZ, J. 2010. Identification of failure type in corroded pipelines: A Bayesian probabilistic approach, *Journal of hazardous materials* 179, 628–634.
- CALEYO, F., GONZÁLEZ, J.L. & HALLEN, J.M. 2002. A study on the reliability assessment methodology for pipelines with active corrosion defects, *International Journal of Pressure Vessels and Piping*, 79(1), 77-86.
- CALEYO, F., VELÁZQUEZ, J. C., VALOR, A. & HALLEN, J. M. 2009. Markov chain modelling of pitting corrosion in underground pipelines. *Corrosion Science* 51, 2197–2207.
- CAMACHO, E. N., FRUTUOSO, E., MELO, P. F., SALDANHA, P. L. C., & DA SILVA, E. P. 2012. A fokker-planck model of pitting corrosion in underground pipelines to support risk-informed decision making. Paper presented at the Advances in Safety, Reliability and Risk Management - Proceedings of the European Safety and Reliability Conference, ESREL, (2012), 2993-2999.
- CAPELLE, J., GILGERT, J., DMYTRAKH, I., & PLUVINAGE, G. 2008. Sensitivity of pipelines with steel API X52 to hydrogen embrittlement. *International journal of hydrogen energy*, 33(24), 7630-7641.
- CAPP.2009. Best Management Practices: Mitigation of internal corrosion in oil effluent pipeline systems, 2009, Calgary Canada. Available from: <<http://www.capp.ca/getdoc.aspx?DocId=155641&DT=PDF>>. [19/6/14].
- CASE, R. Assessment of CO₂ corrosion damage distribution in oilwells by deterministic and stochastic modelling. *CORROSION* 2008, 2008. NACE International.
- CAYARD, M.S. & KANE, R. D. 1997. Large-scale wet hydrogen sulphide cracking performance: evaluation of metallurgical, mechanical, and welding variables. *Corrosion* 53, 227–230.
- CEKYAY, B. & OZEKICI, S. 2012. Optimal maintenance of systems with Markovian mission and deterioration, *European journal of Operation Research* 2012, 219, 123-133.

- CERNY, I. & LINHART, V. 2004. An Evaluation of the resistance of pipeline steels to initiation and early growth of stress corrosion cracks, *Engineering Fracture Mechanics*, 71, 913-21.
- CALEYO, F., GONZALEZ, J. & HALLEN, J. 2002. A study on the reliability assessment methodology for pipelines with active corrosion defects. *International Journal of Pressure Vessels and Piping*, 79, 77-86.
- CALEYO, F., VELÁZQUEZ, J., VALOR, A. & HALLEN, J. 2009. Probability distribution of pitting corrosion depth and rate in underground pipelines: A Monte Carlo study. *Corrosion Science*, 51, 1925-1934.
- CALEYO, F., VELÁZQUEZ, J. C., VALOR, A. & HALLEN, J. M. 2009. Markov chain modelling of pitting corrosion in underground pipelines. *Corrosion Science* 51, 2197–2207
- CHANDRASATHEESH, C., JAYAPRIYA, J., GEORGE, R. P., & MUDALI, U. K. 2014. Detection and analysis of microbiologically influenced corrosion of 316 L stainless steel with electrochemical noise technique. *Engineering Failure Analysis*, 42, 133-142.
- CHAVES, I. A. & MELCHERS, R. E. 2011. Pitting corrosion in pipeline steel welds zones, *Corrosion Science* 53, 4026-4032
- CHEN, Y., HOWDYSHELL, R., HOWDYSHELL, S. & JU, L. 2014. Characterizing pitting corrosion caused by a long-term starving sulfate-reducing bacterium surviving on carbon steel and effects of surface roughness, *Corrosion*, 70 (8), 767-780.
- CHEXAL, B., HOROWITZ, J. & DOOLEY, B. 1998. Flow-accelerated corrosion in power plants. Revision 1. Electric Power Research Inst., Palo Alto, CA (United States).
- CHIODO, M. S. G. & RUGGIERI, C. 2009. Failure assessments of corroded pipelines with axial defects using stress-based criteria: Numerical studies and verification analyses, *International Journal of Pressure Vessels and Piping*, 86, 164-76.
- CHOI, H. J. & AL-AJWAD, H. 2008. Flow-Dependency of sweet and sour corrosion of carbon steel downhole production tubing in Khuff-gas wells. *CORROSION 2008*, 2008. NACE International.
- CHOI, H.S. & BOMBA, J.G. 2003. Acceptance criteria of defects in undersea pipeline using internal inspection. *Ocean engineering*, 30, 1613–1624.

- CHOI, J. B., GOO, B. K., KIM, J. C., KIM, Y. J., & KIM, W. S. 2003. Development of limit load solutions for corroded gas pipelines. *International Journal of Pressure Vessels and Piping*, 80(2), 121-128.
- CHOOKAH, M., NUHI, M. & MODARRES, M. 2011. A probabilistic physics-of-failure model for prognostic health management of structures subject to pitting and corrosion-fatigue. *Reliability Engineering & System Safety*, 96, 1601-1610.
- CHOKSHI, K., SUN, W. & NESIC, S. 2005. Iron carbonate scale growth and the effect of inhibition in CO₂ corrosion of mild steel. *Corrosion/2005*, paper no 05285.
- COLE, I. S., CORRIGAN, P., SIM, S., & BIRBILIS, N. 2011. Corrosion of pipelines used for CO₂ transport in CCS: Is it a real problem? *International Journal of Greenhouse Gas Control*, 5(4), 749-756.
- COLE, I. S. & MARNEY, D. 2012. The science of pipe corrosion: A review of the literature on the corrosion of ferrous metals in soils, *Corrosion Science* 56, 5–16
- COSHAM, A., HOPKINS, P. & MACDONALD, K.A. 2007. Best practice for the assessment of defects in pipelines–Corrosion. *Engineering Failure Analysis*, 14 (7), 1245-1265.
- CONTRERAS, A., ALBITER, A., SALAZAR, M. & PÉREZ, R. 2005. Slow strain rate corrosion and fracture characteristics of x-52 and x-70 pipeline steels, *Materials Science and Engineering: A*, 407, 45-52.
- CRAVERO, S. & RUGGIERI, C. 2006. Structural integrity analysis of axially cracked pipelines using conventional and constraint-modified failure assessment diagrams, *International Journal of Pressure Vessels and Piping*, 83, 607-17.
- CUMBER, P. S. 2001. Predicting Outflow from High Pressure Vessels, *Process Safety and Environmental Protection*, 79, 13-22.
- DAVOODI, A., PAKSHIR, M., BABAIEE, M. & EBRAHIMI, G.R. 2011. A comparative H₂S corrosion study of 304L and 316L stainless steels in acidic media, *Corrosion Sci.*, 53(1), 399-408.
- DAWOTOLA, A. W., VAN GELDER, P., CHARIMA, J. & VRIJLING, J. 2011. Estimation of failure rates of crude product pipelines. *Applications of Statistics and Probability in Civil Engineering–Faber, Köhler & Nishijima (eds) Taylor & Francis Group, London.*

- DAWSON, J., BRUCE, K. & JOHN, D. 2001. Corrosion risk assessment and safety management for offshore processing facilities. HSE Books UK, 2001
- DE LEON, D. & MACÍAS, O. F. 2005. Effect of spatial correlation on the failure probability of pipelines under corrosion. *International journal of pressure vessels and piping*, 82, 123-128.
- DEMOZ, A., PAPA VINASAM, S., OMOTOSO, O., MICHAELIAN, K., & REVIE, R. W. 2009. Effect of field operational variables on internal pitting corrosion of oil and gas pipelines, *Corrosion*, 65(11), 741-747.
- DET NORSKE VERITAS (DNV). 2010. Recommended Practice - RP-F101 Corroded Pipelines.
- DE WAARD, C., LOTZ, U. & MILLIAMS, D. 1991. Predictive model for CO₂ corrosion engineering in wet natural gas pipelines. *Corrosion*, 47, 976-985.
- DE WAARD, C., LOTZ, U. & MILLIAMS, D. 1975. Carbonic acid Corrosion of Steel. *Corrosion*, 31, 131
- DUGSTAD, A., GULBRANDSEN, E., SEIERSTEN, M., KVAREKVAL, J. & NYBORG, R. Corrosion testing in multiphase flow, challenges and limitations. *CORROSION 2006*, 2006. NACE International.
- DUGSTAD, A., LUNDE, L. & NESIC, S. Control of internal corrosion in multi-phase oil and gas pipelines. *Proceedings of the conference Prevention of Pipeline Corrosion*, Gulf Publishing Co, 1994.
- ELIAZ, N., SHACHAR, A., TAL, B., & ELIEZER, D. 2002. Characteristics of hydrogen embrittlement, stress corrosion cracking and tempered martensite embrittlement in high-strength steels. *Engineering Failure Analysis*, 9(2), 167-184.
- ELLIOTT, P. 2013. Corrosion-When you see the signs, which way do you go, *Materials performance*, NACE International 52(6), 30-34.
- ENGELHARDT, G. & MACDONALD, D. 1998. Deterministic prediction of pit depth distribution. *Corrosion*, 54, 469-479.
- FAJARDO, V., CANTO, C., BROWN, B. & NESIC, S. 2007. Effect of organic acids in CO₂ corrosion. In *proceedings of the NACE international conference and exposition Corrosion/2007*, paper no. 07319,

- FAZZINI, P. G. & OTEGUI, J. L. 2007. Experimental determination of stress corrosion crack rates and service lives in a buried ERW pipeline, *International Journal of Pressure Vessels and Piping*, 84, 739-48.
- FAZZINI, P. G. & OTEGUI, J.L. 2006. Influence of old rectangular repair patches on the burst pressure of a gas pipeline, *International Journal of Pressure Vessels and Piping*, 83, 27-34.
- FEKETE, G. & VARGA, L. 2012. The effect of the width to length ratios of corrosion defects on the burst pressures of transmission pipelines, *Engineering Failure Analysis*, 21, 21-30.
- FELDMAN, R. M. & VALDEZ-FLORES, C. 2010. *Applied probability and stochastic processes*, Springer Science & Business Media.
- FANG, H., BROWN, B. & NESCARONICACUTE, S. 2011. Effects of sodium chloride concentration on mild steel corrosion in slightly sour environments, *Corrosion*, 67(1), 015001-1.
- FERRIS, F. G., JACK, T. R. & BRAMHILL, B. J. 1992. Corrosion products associated with attached bacteria at an oil field water injection plant, *Canadian Journal of Microbiology*, 38, 1320-24.
- GAMBOA, E., LINTON, V. & LAW, M. 2008. Fatigue of stress corrosion cracks in X65 pipeline steels, *International Journal of Fatigue*, 30, 850-60.
- GARTLAND, P. O., JOHNSEN, R. & OVSTETUN, I. Application of internal corrosion modeling in the risk assessment of pipelines. *CORROSION 2003*, 2003. NACE International.
- GEARY, W. & HOBBS, J. 2013. Catastrophic failure of a carbon steel storage tank due to internal corrosion, *Case Studies in Engineering Failure Analysis*, 1, 257-64.
- GIEG, L. M., JACK, T. R. & FOGHT, J. M. 2011. Biological souring and mitigation in oil reservoirs. *Applied Microbiology and Biotechnology*, 92(2), 263-82.
doi:<http://dx.doi.org/10.1007/s00253-011-3542-6>.
- GOMES, W. J. S., BECK, A. T. & HAUKAAS, T. 2013. Optimal inspection planning for onshore pipelines subject to external corrosion. *Reliability Engineering & System Safety*, 118, 18-27.

- GONZALEZ, J. L. & MORALES, A. 2008. Analysis of laminations in X52 steel pipes by nonlinear by finite element, *Journal of Pressure Vessel Technology*, 130, 021706-06.
- GUO, B., SONG, S., GHALAMBOR, A. & LIN, T.R. 2014. Chapter 10 - Introduction to flexible pipelines. *Offshore pipelines (Second Edition)*. Gulf professional publishing, Boston, 2014, Pages 125-132, *Offshore Pipelines (Second Edition)*. ISBN 9780123979490. <http://dx.doi.org/10.1016/B978-0-12-397949-0.00010-8>.
- HAN, Z. Y. & WENG, W. G. 2010. An integrated quantitative risk analysis method for natural gas pipeline network, *Journal of Loss Prevention in the Process Industries*, 23, 428-36.
- HASAN, S., KHAN, F. & KENNY, S. 2012. Probability Assessment of Burst Limit State Due to Internal Corrosion, *International Journal of Pressure Vessels and Piping*, 89, 48-58.
- HASAN, F. & IQBAL, J. 2006. Consequential rupture of gas pipeline, *Engineering Failure Analysis*, 13, 127-35.
- HASAN, F., IQBAL, J. & AHMED, F. 2007. Stress Corrosion Failure of High-Pressure Gas Pipeline, *Engineering Failure Analysis*, 14, 801-09.
- HASSANI, S., ROBERTS, K., SHIRAZI, S., SHADLEY, J., RYBICKI, E. & JOIA, C. Flow loop study of chloride concentration effect on erosion, corrosion and erosion-corrosion of carbon steel in CO₂ saturated systems. *CORROSION 2011*, 2011. NACE International.
- HAYS, G. F. 2010. Now is the time. Available from: <<http://corrosion.org/wp-content/themes/twentyten/images/nowisthetime.pdf>>. [30/6/14].
- HERNANDEZ-RODRIGUEZ, M., MARTINEZ-DELGADO, D., GONZALEZ, R., UNZUETA, A. P., MERCADO-SOLIS, R. & RODRIGUEZ, J. 2007. Corrosive wear failure analysis in a natural gas pipeline. *Wear*, 263, 567-571.
- HIInt Dossier. 2005. Gas Pipeline Explosion at Ghislenghien, Belgium. Available from: <<http://www.iab-atex.nl/publicaties/database/Ghislenghien%20Dossier.pdf>>. [7/2/15].

- HOKSTAD, P. & FROVIG, A.T. 1996. The modelling of degraded and critical failures for components with dormant Failures. *Reliability Engineering and System Safety*, 51, 189–199.
- HONG, H.P. 1999. Inspection and maintenance planning of pipeline under external corrosion considering generation of new defects, *Structural safety* 21, 203-222.
- HORROCKS, P., MANSFIELD, D., PARKER, K., THOMSON, J., ATKINSON, T., WORSLEY, J., ... & PARK, B. 2010. *Managing ageing plant*. Health and Safety Executive, UK: Norwich.
- HSE. 2001. Review of corrosion management for offshore oil and gas processing, HSE offshore technology report 2001/044. Available from: <<http://www.hse.gov.uk/research/otopdf/2001/oto01044.pdf>>. [22/6/14].
- HU, J., TIAN, Y., TENG, H., YU, L. & ZHENG, M. 2014. The probabilistic life time prediction model of oil pipeline due to local corrosion crack. *Theoretical and Applied Fracture Mechanics*, 70, 10-18.
- HU, X., ALZAWAI, K., GNANAVELU, A., NEVILLE, A., WANG, C., CROSSLAND, A. & MARTIN, J. 2011a. Assessing the effect of corrosion inhibitor on erosion–corrosion of API-5L-X65 in multi-phase jet impingement conditions, *Wear* 271(9-10), 1432-1437.
- HU, X., BARKER, R. & NEVILLE, A. & GNANAVELU, A. 2011b. Case study on erosion-corrosion degradation of pipework located on an offshore oil and gas facility, *Wear* 271, 1295– 1301.
- HUANG, Y. & JI, D. 2008. Experimental study on seawater-pipeline internal corrosion monitoring system, sensors and actuators B: *Chemical*, 135, 375-80.
- ILMAN, M. N. & KUSMONO 2014. Analysis of internal corrosion in subsea oil pipeline. *Case Studies in Engineering Failure Analysis*, 2, 1-8.
- JAVAHERDASHTI, R. 2011. Impact of sulphate-reducing bacteria on the performance of engineering materials. *Applied Microbiology and Biotechnology*., 91(6), 1507-1517.
- JEPSON, W. & MENEZES, R. 1995. *The effects of oil viscosity on sweet corrosion in multiphase oil/water/gas horizontal pipelines*. NACE International, Houston, TX (United States).

- JIANG, X. C., & STAEHLE, R. W. 1997. Effects of stress and temperature on stress corrosion cracking of austenitic stainless steels in concentrated magnesium chloride solutions. *Corrosion*, 53(6), 448-466.
- JO, Y. & CROWL, D. A. 2008. Individual risk analysis of high-pressure natural gas pipelines, *Journal of Loss Prevention in the Process Industries* 21, 589-95.
- KALLENBERG, L. 2011. Markov decision processes. Available from: <http://www.math.leidenuniv.nl/~kallenberg/Lecture-notes-MDP.pdf>. [2/12/2014].
- KAPUSTA, S. 2008. Managing corrosion in sour gas system: testing, design, implementation and field experience, *CORROSION/2008*, paper no. 08641.
- KATANO, Y., MIYATA, K., SHIMIZU, H. & ISOGAI, T. 2003. Predictive model for pit growth on underground pipes. *Corrosion*, 59, 155-161.
- KENTISH, P. 2007. Stress corrosion cracking of gas pipelines – Effect of surface roughness, orientations and flattening, *Corrosion Science*, 49, 2521-33.
- KHAJOTIA, B., SORMAZ, D. & NESIC, S. Case-based reasoning model of CO₂ corrosion based on field data. *NACE International Conference Sereis, CORROSION, 2007*.
- KHAKSARFARD, R., PARASCHIVOIU, M., ZHU, Z., TAJALLIPOUR, N. & TEEVENS, P. J. 2013. CFD Based Analysis of Multiphase Flows in Bends of Large Diameter Pipelines, *CORROSION/2013*.
- KISHAWY, H. A. & GABBAR, H. A. 2010. Review of pipeline integrity management practices, *International Journal of Pressure Vessels and Piping*, 87, 373-80.
- KLEVER, F.J. & STEWARD, G. 1995. New developments in burst strength prediction for locally corroded pipes, *Shell Int. Research*.
- KLEVER, F. J., STEWART, G., & VAN DER VALK, C. A. 1995. New developments in burst strength predictions for locally corroded pipelines (No. CONF-950695--). American Society of Mechanical Engineers, New York, NY (United States).
- KULKARNI, V. G. 2011. Introduction to modeling and analysis of stochastic systems, *Springer Texts in Statistics*, 2011, DOI 10.1007/978-1-4419-1772-0 2.
- KUMAR, M. S., SUJATA, M., VENKATASWAMY, M. A., & BHAUMIK, S. K. 2008. Failure analysis of a stainless steel pipeline. *Engineering Failure Analysis*, 15(5), 497-504.

- LAYCOCK, P., COTTIS, R. & SCARF, P. 1990. Extrapolation of extreme pit depths in space and time. *Journal of the Electrochemical Society*, 137, 64-69.
- LECCHI, M. 2011. Evaluation of predictive assessment reliability on corroded transmission pipelines. *Journal of Natural Gas Science and Engineering*, 3, 633-641.
- LEE, H., CHOI, J., LEE, B. & KIM, T. 2007. Failure analysis of stress corrosion cracking in aircraft bolts, *Engineering Failure Analysis*, 14, 209-17.
- LEIS, N. & STEPHENS, D.R. 1997. Proceedings of the 7th International Offshore and Polar Engineering Conference, Part I, Honolulu, USA, 1997, ASME International, New York, 624-641.
- LI, D., ZHANG, L., YANG, J., LU, M., DING, J. & LIU, M. 2014. Effect of H₂S concentration on the corrosion behavior of pipeline steel under the coexistence of H₂S and CO₂, *International Journal of Minerals, Metallurgy, and Materials*, 21, 388-94.
- LI, S.-X., YU, S.-R., ZENG, H.-L., LI, J.-H. & LIANG, R. 2009. Predicting corrosion remaining life of underground pipelines with a mechanically-based probabilistic model. *Journal of Petroleum Science and Engineering*, 65, 162-166.
- LIANG, P., LI, X., DU, C., & CHEN, X. 2009. Stress corrosion cracking of X80 pipeline steel in simulated alkaline soil solution. *Materials & Design*, 30(5), 1712-1717.
- LIESER, M. J. & XU, J. 2002. Composites and the Future of Society: Preventing a legacy of costly corrosion with modern materials. Available from: <http://www.ocvreinforcements.com/pdf/library/CSB_Corrosion_White_Paper_Sept_10_10_English.pdf>. [1/7/14].
- LU, G., & KAXIRAS, E. 2005. Hydrogen embrittlement of aluminium: the crucial role of vacancies. *Physical review letters*, 94(15), 155501.
- LYNCH, S. 2012. Hydrogen embrittlement phenomena and mechanisms, *Corrosion Reviews* 30(3-4), 105-123.
- MACHUCA, L. L., MURRAY, L., GUBNER, R. & BAILEY, S. I. 2014. Evaluation of the effects of seawater ingress into 316L lined pipes on corrosion performance. *Material Corrosion* 65(2014)8–17.

- MA, B., SHUAI, J., LIU, D. & XU, K. 2013. Assessment on failure pressure of high strength pipeline with corrosion defects, *Engineering Failure Analysis*, 32, 209-19.
- MAES, M. A., FABER, M. H. & DANN, M. R. 2009. Hierarchical modeling of pipeline defect growth subject to ILI uncertainty. ASME 2009 28th International Conference on Ocean, Offshore and Arctic Engineering. American Society of Mechanical Engineers, 2009.
- MAJID, Z. A., MOHSIN, R., YAACOB, Z., & HASSAN, Z. 2010. Failure analysis of natural gas pipes. *Engineering failure analysis*, 17(4), 818-837.
- MARTÍNEZ, D., GONZALEZ, R., MONTEMAYOR, K., JUAREZ-HERNANDEZ, A., FAJARDO, G. & HERNANDEZ-RODRIGUEZ, M. A. L. 2009. Amine type inhibitor effect on corrosion–erosion wear in oil gas pipes, *Wear*, 267, 255-58.
- MARUTHAMUTHU, S., MUTHUKUMAR, N., NATESAN, M., & PALANISWAMY, N. 2008. Role of air microbes on atmospheric corrosion. *Current Science*, 94(3), 359-363.
- MAZUMDER, Q. H., SHIRAZI, S. A. & MCLAURY, B. 2008. Experimental investigation of the location of maximum erosive wear damage in elbows. *Journal of Pressure Vessel Technology*, 130, 011303-011303.
- MCMAHON, A. J. 1991. The mechanism of action of an oleic imidazoline based corrosion inhibitor for oilfield use, *Colloids and Surfaces* 59(0), 187-208.
- MCMAHON, A. J. & PAISLEY, D. M. E. 1997. Corrosion prediction modelling - A guide to the use of corrosion prediction models for risk assessment in oil and gas production and transportation facilities, Report No. ESR.96.ER.066, BP International, Sunbury, 1997
- MELCHERS, R.E. 2008. Extreme value statistics and long-term marine pitting corrosion of steel, *Probabilistic Engineering Mechanics*, 23(4), 482-488.
- MELIANI, M. H., MATVIENKO, Y. G., & PLUVINAGE, G. 2011. Corrosion defect assessment on pipes using limit analysis and notch fracture mechanics. *Engineering Failure Analysis*, 18(1), 271-283.
- MELCHERS, R. 2010. Estimating uncertainty in maximum pit depth from limited observational data. *Corrosion Engineering, Science and Technology*, 45, 240-248.

- MELCHERS, R. E. 2008. Extreme value statistics and long-term marine pitting corrosion of steel. *Probabilistic Engineering Mechanics*, 23, 482-488.
- MELCHERS, R. E. 2005. Representation of uncertainty in maximum depth of marine corrosion pits. *Structural safety*, 27(4), 322-334.
- MELCHERS, R. E. 2010. Estimating uncertainty in maximum pit depth from limited observational data. *Corrosion Engineering Science and Technology*, 45(3), 240-248.
- MENG, W., P. OGEA & KING, M. 2011. Changes of operating procedures and chemical application of a mature deepwater tie-back - Aspen field case study, *Offshore Technology Conference, Proceedings*, 2, 881-892
- MERESHT, E. S., FARAHANI, T. S. & NESHATI, J. 2011. Failure analysis of stress corrosion cracking occurred in a gas transmission steel pipeline, *Engineering Failure Analysis*, 18, 963-70.
- MILLER, R. 2013. Why pipes matter: The importance of clad pipes in the oil and gas industry. Available from: <<http://breakingenergy.com/2013/03/15/why-pipes-matter-the-importance-of-clad-pipe-in-the-oil-and-gas/>>. [1/7/14].
- MOHD, M. H. & PAIK, J. K. 2013. Investigation of the corrosion progress characteristics of offshore subsea oil well tubes. *Corrosion Science*, 67, 130-141.
- MOUSSA, W. A. 1998. Risk-based reliability evaluation of multi-site damage in pipelines. *Computers & industrial engineering*, 35, 595-598.
- MUTHUKUMAR, N., RAJASEKAR, A., PONMARIAPPAN, S., MOHANAN, S., MARUTHAMUTHU, S., MURALIDHARAN, S., ... & RAGHAVAN, M. 2003. Microbiologically influenced corrosion in petroleum product pipelines-a review. *Indian journal of experimental biology*, 41(9), 1012-1022.
- NACE 2005, NACE Standard RP0775, Preparation, installation, analysis, and interpretation of coupons in oilfield operations, 2005, Houston, TX
- NATIVIDAD, C., SALAZAR, M., ESPINOSA-MEDINA, M. A., & PÉREZ, R. 2007. A comparative study of the SSC resistance of a novel welding process IEA with SAW and MIG. *Materials characterization*, 58(8), 786-793.
- NAYAK, C. 2014. Fault Detection in Fluid Flowing Pipes Using Acoustic Method, *International Journal of Applied Engineering Research*, 9 (1), 23-28.

- NESIC, S. 2007. Key issues related to modelling of internal corrosion of oil and gas pipelines – A review, *Corrosion Science*, 49, 4308-38.
- NESIC, S. 2012. Effects of Multiphase Flow on Internal CO₂ Corrosion of Mild Steel Pipelines, *Energy & Fuels* 26 (7), 4098-4111.
- NESIC, S., CAI, J. & LEE, K. J. 2005. A multiphase flow and internal corrosion prediction model for mild steel pipelines. *Corrosion/2005*. Paper no 05556.
- NEŠIĆ, S. & LEE, K.-L. 2003. A mechanistic model for carbon dioxide corrosion of mild steel in the presence of protective iron carbonate films-Part 3: Film growth model. *Corrosion*, 59, 616-628.
- NICHOLSON, R., FEBLOWITZ, J., MADDEN, C., & BIGLIANI, R. 2010. The role of predictive analytics in asset optimization for the oil and gas industry. IDC Energy Insights, White Paper. Available from: <http://tessella.com/documents/role-predictive-analytics-asset-optimization-oil-gas-industry/>. [29/6/14].
- NIU, L. & CHENG, Y. F. 2007. Corrosion Behaviour of X-70 Pipe Steel in near-Neutral pH Solution, *Applied Surface Science*, 253, 8626-31.
- NORDSVEEN, M., NESIC, S., NYBORG, R. & STANGELAND, A. 2003. A mechanistic model for carbon dioxide corrosion of mild steel in the presence of protective iron carbonate films-Part 1: Theory and verification. *Corrosion*, 59, 443-456.
- OMWEG, G. M., FRANKEL, G. S., BRUCE, W. A., RAMIREZ, J. E., & KOCH, G. 2003. Performance of welded high-strength low-alloy steels in sour environments. *Corrosion*, 59(7), 640-653.
- OSSAI, C.I. 2012a. Advances in asset management techniques: An overview of corrosion mechanisms and mitigation strategies for oil and gas pipelines, *ISRN Corrosion*, vol. 2012. <http://dx.doi.org/10.5402/2012/570143>, Article ID 570143.
- OSSAI, C. I. 2012b. Predictive modelling of wellhead corrosion due to operating conditions: A field data approach, *ISRN Corrosion*, vol. 2012, Article ID 237025, 2012. doi:10.5402/2012/237025.

- OSSAI, C. I. 2013. Pipeline Corrosion Prediction and Reliability Analysis: A systematic approach with Monte Carlo simulation and degradation models. *International Journal of Scientific & Technology Research*, 2.
- OSSAI, C. I., BOSWELL, B. & DAVIES, I. J. 2015. Pipeline failures in corrosive environments—A conceptual analysis of trends and effects. *Engineering Failure Analysis*, 53, 36-58.
- OSSAI, C.I., BOSWELL, B. & DAVIES, I.J. 2015b. Predictive modelling of internal pitting corrosion of aged non-piggable pipelines. *J. Electrochem. Soc.*, 162(6): C251-C259, doi: 10.1149/2.0701506jes
- OSSAI, C.I., BOSWELL, B. & DAVIES, I.J. 2015c. Estimation of internal pit depth growth and reliability of aged oil and gas pipelines - A Monte Carlo simulation approach, *Corrosion*, 71(8), 977-99.
- OWEN, R., CHAUHAN, V., PIPET, D. & Morgan, G. 2003. Assessment of corrosion damage in pipelines with low toughness, In 14th Biennial joint technical meeting on pipeline research, Berlin.
- PAIK, J. K. & KIM, D. K. 2012. Advanced method for the development of an empirical model to predict time-dependent corrosion wastage. *Corrosion Science*, 63, 51-58.
- PANDEY, M.D. 1998. Probabilistic models for condition assessment of oil and gas pipelines, *NDT&E International*, 31(5), 349-358.
- PANDEY, M., YUAN, X.-X. & VAN NOORTWIJK, J. 2009. The influence of temporal uncertainty of deterioration on life-cycle management of structures. *Structure and Infrastructure Engineering*, 5, 145-156.
- PAPAVINASAM, S. 2014a. Chapter 6 - Modelling – Internal Corrosion, in *Corrosion control in the oil and gas industry*, ed. by Sankara Papavinasam (Boston: Gulf Professional Publishing, 2014), pp. 301-60.
- PAPAVINASAM, S. 2014b. Chapter 7 - Mitigation – Internal corrosion', in *Corrosion Control in the Oil and Gas Industry*, ed. by Sankara Papavinasam (Boston: Gulf Professional Publishing, 2014), pp. 361-424.
- PAPAVINASAM, S., DOIRON, A. & REVIE, R. W. 2010. Model to predict internal pitting corrosion of oil and gas pipelines. *Corrosion*, 66(3), 035006-035006-11.

- PAPAVINASAM, S., DOIRON, A., PANNEERSELVAM, T. & Revie, R. W. 2007. Effect of hydrocarbons on the internal corrosion of oil and gas pipelines. *Corrosion*, 63(7), 704-712.
- PARK, G. T., KOH, S. U., JUNG, H. G., & KIM, K. Y. 2008. Effect of microstructure on the hydrogen trapping efficiency and hydrogen induced cracking of linepipe steel. *Corrosion science*, 50(7), 1865-1871.
- PARK, N. G., MORELLO, L., WONG, J. E., & MAKSOUD, S. A. 2007. The effect of oxygenated methanol on corrosion of carbon steel in sour wet gas environments. In *CORROSION 2007*. NACE International.
- PARZEN, E. 1999. *Stochastic Processes, Classics in Applied Mathematics*, Society for Industrial and Applied Mathematics (SIAM), PA.
- PATEL, R. & RUDLIN, J. Analysis of corrosion/erosion incidents in offshore process plant and implications for non-destructive testing. *British Institute of Non-Destructive Testing, NDT'99 and UK Corrosion'99 Conference Proceedings (UK)*, 1999. 5-10.
- PILKEY, A.K., LAMBERT, S. B. & PLUMTREE, A. 1995. Stress corrosion cracking of X-60 line pipe steel in a carbonate-bicarbonate solution, *Corrosion Science* 51(2), 91–96.
- POPOOLA, L. T., GREMA, A. S., LATINWO, G. K., GUTTI, B., & BALOGUN, A. S. 2013. Corrosion problems during oil and gas production and its mitigation. *International Journal of Industrial Chemistry*, 4(1), 1-15.
- QIAN, X., LI, Y. & OU, Z. 2013. Ductile tearing assessment of high-strength steel x-joints under in-plane bending, *Engineering Failure Analysis*, 28, 176-91.
- RACE, J. M. 2010. 4.42 - Management of corrosion of onshore pipelines, In: Editor-in-Chief: Tony J.A. Richardson, Editor(s)-in-Chief, Shreir's *Corrosion*, Elsevier, Oxford, 2010, Pages 3270-3306, ISBN 9780444527875, <http://dx.doi.org/10.1016/B978-044452787-5.00169-4>.
- RAMAN, R. K. S., AVAHERDASHTI, R., PANTER, J. C. & PERELOMA, E. V. 2005. Hydrogen embrittlement of a low carbon steel during slow strain testing in chloride solutions containing sulphate reducing bacteria, *Materials Science and Technology* 21(9), 1094-1098.

- RENPU, W. 2011. Oil and gas well corrosion and corrosion prevention, in: advanced well completion engineering (Third Edition), Gulf professional publishing, Boston, ISBN 9780123858689, <http://dx.doi.org/10.1016/B978-0-12-385868-9.00018-X>, 2011 (Chapter 11).
- RIMKEVICIUS, S., KALIATKA, A., VALINCIUS, M., DUNDULIS, G., JANULIONIS, R., GRYBENAS, A. & ZUTAUTAITE, I. 2012. Development of approach for reliability assessment of pipeline network systems. *Applied energy*, 94, 22-33.
- RIVAS, D., CALEYO, F., VALOR, A. & HALLEN, J. 2008. Extreme value analysis applied to pitting corrosion experiments in low carbon steel: Comparison of block maxima and peak over threshold approaches. *Corrosion Science*, 50, 3193-3204.
- RODRIGUEZ III, E. & PROVAN, J. 1989. Part II: Development of a general failure control system for estimating the reliability of deteriorating structures. *Corrosion*, 45, 193-206.
- RODRIGUEZ III, E. & PROVAN, J. 1989b. Part I: Development of a general failure control system for estimating the reliability of deteriorating structures. *Corrosion*, 45(3), 178-192.
- SAHRAOUI, Y., KHELIF, R. & CHATEAUNEUF, A. 2013. Maintenance planning under imperfect inspections of corroded pipelines. *International journal of pressure vessels and piping* 104, 76-82.
- SANA, N. O., NAZIRB, H., DONMEZC, G. 2012. Microbiologically influenced corrosion failure analysis of nickel–copper alloy coatings by *Aeromonas salmonicida* and *Delftia acidovorans* bacterium isolated from pipe system. *Engineering Failure Analysis* 25, 63–70.
- SEDRIS, A. J. 1990. Stress corrosion cracking test methods. National Association of Corrosion Engineers.
- SHEIKH, A., BOAH, J. & HANSEN, D. 1990. Statistical modeling of pitting corrosion and pipeline reliability. *Corrosion*, 46, 190-197.
- SHEILS, E., O'CONNOR, A., SCHOEFS, F. & BREYSSE, D. 2012. Investigation of the effect of the quality of inspection techniques on the optimal inspection interval for structures. *Structure and Infrastructure Engineering*:

- Maintenance, Management, Life-Cycle Design and performance, 8(6), 557-568.
- SHOESMITH, D. W., TAYLOR, P., BAILEY, M. G. & OWEN, D. G. 1980. The formation of ferrous monosulfide polymorphs during the corrosion of iron by aqueous hydrogen sulfide at 21 C. *Journal of the Electrochemical Society*, 127, 1007-1015.
- SINGH, M. & MARKESET, T. 2014. Simultaneous handling of variability and uncertainty in probabilistic and possibilistic failure analysis of corroded pipes, *International Journal of System Assurance Engineering and Management*, 5, 43-54.
- SINGER, M., BROWN, B., CAMACHO, A. & NESIC, S. 2011. Combined effect of carbon dioxide, hydrogen sulfide, and acetic acid on bottom-of-the-line corrosion, *Corrosion*, 67(1), 015004-1.
- SINHA, S.K. & MCKIM, R. A. 2007. Probabilistic based integrated pipeline management system, *Tunnelling and underground space technology* 22, 543-552.
- SMITH, L. AND CRAIG, B., 2008. Corrosion mechanisms and material performance in environments containing hydrogen sulfide and elemental sulfur. In SACNUC Workshop, October (pp. 22-23).
- SOARES, C. G. & GARBATOV, Y. 1999. Reliability of maintained, corrosion protected plates subjected to non-linear corrosion and compressive loads. *Marine Structures*, 12, 425-445.
- SONG, F. M. 2010. A comprehensive model for predicting CO₂ corrosion rate in oil and gas production and transportation systems. *Electrochimica Acta*, 55, 689-700.
- SONG, F., MCFARLAND, J., BICHON, B., HUYSE, L., KING, F., PERRY, L., & PIAZZA, M. 2011. New model predicts internal corrosion likelihood. *Oil & Gas Journal*, 109, 116-125.
- SONG, Y., PALENCŚÁR, A., SVENNINGSEN, G., KVAREKVÅL, J., & HEMMINGSEN, T. 2012. Effect of O₂ and temperature on sour corrosion. *Corrosion*, 68(7), 662-671.

- STRUCTURAL INTEGRITY ASSESSMENT PROCEDURE (SINTAP). 1999. Final report E-U project BE95-1462. Brite Euram Programme Brussels. Available from: <http://www.eurofitnet.org/sintap_Procedure_version_1a.pdf>. [19/6/14].
- SUN, W. & NESIC, S. 2007. A mechanistic model of H₂S corrosion of mild steel. Paper No 07655. Corrosion 2007.
- SUN, Y., MA, L. & MORRIS, J. 2009. A practical approach for reliability prediction of pipeline systems. European Journal of Operational Research, 198, 210-214.
- TARANTSEVA, K. R. 2010. Models and methods of forecasting pitting corrosion. Protection of metals and physical chemistry of surfaces, 46(1), 139-147.
- TAYLOR, H. M. & KARLIN, S. 1998. An introduction to stochastic modelling 3rd edition. Academic press San Diego, California USA, 1998, ISBN-13:978-0-12-684887-8.
- TEIXEIRA, A. P., GUEDES SOARES, C., NETTO, T. A. & ESTEFEN, S. F. 2008. Reliability of pipelines with corrosion defects, International Journal of Pressure Vessels and Piping, 85, 228-37.
- THOMPSON, N. G. 2011. Gas and liquid transmission pipelines. Corrosion cost and preventive strategies in the United States. Available from: <http://www.dnvusa.com/Binaries/gasliquid_tcm153-378807.pdf>. [2/6/15].
- THOMPSON, N. G. Appendix J- Gas distribution, Available from: <http://www.dnvusa.com/Binaries/gas_tcm153-339949.pdf>. [16/6/15].
- United States Department of Transport, US DOT. 2014. Pipeline and Hazardous Materials Safety Administration. Available from: <<https://hip.phmsa.dot.gov/analyticsSOAP/saw.dll?Portalpages>>. [7/02/15].
- VALOR, A., CALEYO, F., ALFONSO, L., VIDAL, J. & HALLEN, J. M. 2014. Statistical analysis of pitting corrosion field data and their use for realistic reliability estimations in non-piggable pipeline systems. Corrosion, 70, 1090-1100.
- VALOR, A., CALEYO, F., HALLEN, J. M. & VELÁZQUEZ, J. C. 2013. Reliability assessment of buried pipelines based on different corrosion rate models. Corrosion Science, 66, 78-87.

- VALOR, A., CALEYO, F., RIVAS, D. & HALLEN, J. 2010. Stochastic approach to pitting-corrosion-extreme modelling in low-carbon steel. *Corrosion Science*, 52, 910-915.
- VALOR, A., CALEYO, F., ALFONSO, L., VELÁZQUEZ, J. & HALLEN, J. 2013. Markov chain models for the stochastic modeling of pitting corrosion. *Mathematical Problems in Engineering*, 2013.
- VALOR, A., CALEYO, F., ALFONSO, L., RIVAS, D. & HALLEN, J. M. 2007. Stochastic modeling of pitting corrosion: A new model for initiation and growth of multiple corrosion pits. *Corrosion Science*, 49, 559-579.
- VEGA, O. E., HALLEN, J. M., VILLAGOMEZ, A. & CONTRERAS, A. 2008. Effect of multiple repairs in girth welds of pipelines on the mechanical properties, *Materials Characterization*, 59, 1498-507.
- VELAZQUEZ, J. C., VALOR, A. CALEYO, F., VENEGAS, V., ESPINA-HERNANDEZ, J. H., HALLEN J. M., & LOPEZ, M. R. Pitting corrosion models improve integrity management, reliability, *Oil and Gas Journal*, 107(28), 56-62.
- VELÁZQUEZ, J., CALEYO, F., VALOR, A. & HALLEN, J. 2009. Predictive model for pitting corrosion in buried oil and gas pipelines. *Corrosion*, 65, 332-342.
- VENKATESH, C. D. & FARINHA, P. A. 2006. Corrosion Risk Assessment (CRA) in the oil and gas industry-An overview and its holistic approach. Available from: <<http://members.iinet.net.au/~extrin/ConferencePapers/CAP04~Paper06.pdf>>. [18/10/13].
- WAANDERS, F. B. & VORSTER, S. W. 2002. Corrosion products formed on mild steel samples submerged in various aqueous solution, *Hyperfine Interactions* 139,239–244.
- WANG, B., DU, M., ZHANG, J. & GAO, C. J. 2011. Electrochemical and surface analysis studies on corrosion inhibition of Q235 steel by imidazoline derivative against CO₂ corrosion. *Corrosion Science*, 53, 353-361.
- WANG, H., JEPSON, P.W., CAI, J.Y. & GOPAL, M. 2000. Effect of bubbles on mass transfer in multiphase flow, In: *NACE Int. Conference series, Corrosion/2000*, paper no. 00050.

- WANG, J. & LI, X. 2014. A phenomenological model for fatigue crack growth rate of x70 pipeline steel in h₂s corrosive environment, *Journal of Pressure Vessel Technology*, 136, 041703-03.
- WANG, N. & ZARGHAMEE, M. 2014. Evaluating fitness-for-service of corroded metal pipelines: structural reliability bases, *Journal of Pipeline Systems Engineering and Practice*, 5, 04013012.
- WANG, S., GEORGE, K. & NESIC, S. 2004. High pressure CO₂ corrosion electrochemistry and the effect of acetic acid, *Corrosion/2004*, paper no. 04375.
- WANG, W., SMITH, M. Q., POPELAR, C. H., & MAPLE, J. A. 1998. New rupture prediction model for corroded pipelines under combined loadings. In *The 1998 International Pipeline Conference, IPC. Part 1(of 2)* (pp. 563-572).
- WANG, X. & REINHARDT, W. 2003. On the Assessment of through-wall circumferential cracks in steam generator tubes with tube supports, *Journal of Pressure Vessel Technology* 125, 85-90.
- WEN, J., GU, T. & NESIC, S. 2007. Investigation of the effects of fluid flow on SRB biofilm, In: *NACE Int. Conference series, Corrosion/2007*, paper no. 07516.
- WHITE, C. C. III & WHITE, D. J. 1989. Markov decision process, *European Journal of Operational Research*, 39, 1-16.
- WINTLE, J., MOORE, P., HENRY, N., SMALLEY, S., & AMPHLETT, G. 2006. *Plant ageing: Management of equipment containing hazardous fluids or pressure*. Health and Safety Executive, UK: Norwich.
- WOODTLI J. & ROLF, K. 2000. Damage due to hydrogen embrittlement and stress corrosion cracking, *Engineering Failure Analysis* 7.6, 427-450.
- XIAO, Y. & NEŠIĆ, S. 2005. A stochastic prediction model of localized CO₂ corrosion Paper No. 05507. *CORROSION 2005*.
- XIAN, Y. & S. NESIC, S. 2005. A stochastic prediction model of localized CO₂ corrosion. Paper presented at *NACE CORROSION/05*, Dallas, TX, paper, 05057
- XU, L. Y. & CHENG, Y. F. 2012. Reliability and failure pressure prediction of various grades of pipeline steel in the presence of corrosion defects and pre-strain, *International Journal of Pressure Vessels and Piping*, 89, 75-84.

- YARDENI, E., JOHNSON, D. & QUINTANA, M. 2014. Global economic briefing: Global inflation, Available from: <http://www.yardeni.com/pub/infltrglb_bb.pdf>. [1/7/14].
- YIN, Z.F., ZHAO, W.Z. BAI, Z.Q., FENG, Y.R. & ZHOU, W.J. 2008. Corrosion behaviour of SM 80SS tube steel in stimulant solution containing H₂S and CO₂, *Electrochim. Acta*, 53(10), 3690.
- YUSOF, S., NOOR, N. M., YAHAYA, N., & RASHID, A. S. A. 2014. Markov chain model for predicting pitting corrosion damage in offshore pipeline. *Asian Journal of Scientific Research*, 7(2), 208-216.
- ZHANG, C., ZHANG, Q., CHEN, W., LIU, D., OU, T., HUANG, X., ... & CHEN, C. 2013. Assessment of corrosion and mechanical properties degradation of pipeline steel after long term service in high sour gas-Field environments. In *IPTC 2013: International Petroleum Technology Conference*.
- ZHANG, L., ZHONG, W., YANG, J., GU, T., XIAO, X. & LU, M. 2011. Effects of temperature and partial pressure on H₂S/CO₂ corrosion of pipeline steel in sour conditions. *CORROSION 2011*, 13-17 March, Houston, Texas, USA, paper 11079
- ZHANG, R., GOPAL, M. & JEPSON, W. 1997. Development of a mechanistic model for predicting corrosion rate in multiphase oil/water/gas flows. *NACE International*, Houston, TX (United States).
- ZHANG, S. & ZHOU, W. 2013. System reliability of corroding pipelines considering stochastic process-based models for defect growth and internal pressure. *International Journal of Pressure Vessels and Piping*, 111, 120-130.
- ZHANG, S. & ZHOU, W. 2014. Bayesian dynamic linear model for growth of corrosion defects on energy pipelines. *Reliability Engineering & System Safety*, 128, 24-31.
- ZHANG, S. & ZHOU, W. 2014. Cost-based optimal maintenance decisions for corroding natural gas pipelines based on stochastic degradation models, *Engineering Structures*, 74, 74-85.
- ZHANG, S., ZHOU, W. & QIN, H. 2013. Inverse Gaussian process-based corrosion growth model for energy pipelines considering the sizing error in inspection data. *Corrosion Science*, 73, 309-320.

- ZHANG, T., YANG, Y., SHAO, Y., MENG, G. & WANG, F. 2009. A stochastic analysis of the effect of hydrostatic pressure on the pit corrosion of Fe–20Cr alloy. *Electrochimica Acta*, 54, 3915-3922.
- ZHOU, W. 2010. System reliability of corroding pipelines. *International Journal of Pressure Vessels and Piping*, 87, 587-595.
- ZHU, X. & LEIS, B. N. 2006. Average shear stress yield criterion and its application to plastic collapse analysis of pipelines. *International Journal of Pressure Vessels Piping*, 83, 663–71.
- ZHU, X. & LEIS, B. N. 2007. Theoretical and numerical predictions of burst pressure of pipelines, *Journal of Pressure Vessel Technology*, 129, 644-52.

Every reasonable effort has been made to acknowledge the owners of copyright materials. I would be pleased to hear from any copyright owner who has been omitted or incorrectly acknowledged.